From Rubble to Resilience

A parametric approach to seismic assessment and resource-aware retrofit design for reinforced concrete frame residential buildings in Türkiye

Building Technology Graduation Studio
MSc Architecture, Urbanism & Building Sciences

Author:
Thys van Hoogdalem – 6257798
[15-06-2026]

Supervisors:
Dr. Simona Bianchi – Structural design & mechanics, TU Delft
Dr.ir. Olga Ioannou – Facade & product design, TU Delft

Acknowledgements

"The torch that the Turkish nation holds in her hand and in her mind, while marching on the road of progress and civilisation, is positive sciences." - Mustafa Kemal Atatürk.

These words, spoken nearly a century ago, feel as urgent today as they did then. When the earth shook beneath Kahramanmaraş in February 2023, it not only collapsed buildings; it also shattered the illusion that seismic resilience could wait. This thesis argues that advancing seismic safety through science is not just academic, it is a social and ethical necessity. It is grounded in the conviction that millions of people deserve buildings designed to protect them, and that Atatürk's legacy of reason and knowledge demands science be put in service to society. It is in that spirit, of science in service of people, that this research was conducted.

This work would not have been possible without the guidance of those who generously shared their knowledge and patience along the way.

First and foremost, I want to thank Simona Bianchi, whose expertise in structural engineering and earthquake design shaped the structural backbone of this research. Starting this project as someone unfamiliar with earthquake engineering, her patient explanations and clear thinking helped me find my footing in a field that is both very complex and consequential in this discipline. Her guidance transformed uncertainty into understanding.

I equally want to thank Olga Ioannou, whose critical thinking continuously sharpened the framing of the material design track and helped forge the connection between the circular economy narrative and the structural application that gives this research its coherence. Her ability to challenge my assumptions at the right moments prevented the work from losing its direction. The balance of intellectual precision and human attentiveness made all the difference.

Beyond the academic, I want to thank my family for their support throughout this journey; their encouragement has always helped me sustain myself through the long stretches of my academic career.

Lastly, I want to thank Ekin Sarıbaş. Her support and knowledge have helped me throughout this process far beyond what words can properly capture. Her exceptional eye for storytelling and her dedication to the layout of this report gave these ideas the form they deserved.

Abstract

Türkiye faces a dual challenge: high seismic vulnerability and large-scale construction and demolition waste. In cities such as Istanbul, ageing reinforced concrete residential buildings remain exposed to significant seismic risk. While ongoing urban transformation continues to generate large quantities of concrete and brick rubble. Seismic assessment and retrofit procedures are typically carried out building-by-building, making this process time-intensive and difficult to scale across the many vulnerable structures. Additionally, construction and demolition waste is still mostly directed to landfills, despite its potential as a material resource for structural strengthening.

This thesis develops a design framework in which seismic retrofitting is approached as both a structural assessment problem and a material supply problem. This framework is positioned behind the logic that the vulnerable building stock is assessed as the target of seismic strengthening, while demolition waste from the same urban transformation context is investigated as a potential resource for producing the retrofit components. In this way, the retrofit demand is defined by the structural workflow, while the material workflow explores how this demand could be supplied through locally available recycled concrete and brick aggregates, making this vulnerable building stock part of the material cycle that can support renewed seismic resilience

The research focuses on a representative Turkish building typology: mid-rise reinforced concrete moment-resisting frame apartment buildings. A survey-based workflow is proposed in which on-site building data is collected through a structured assessment form and translated into a parametric Grasshopper model. This model generates a simplified building geometry, calculates seismic loads using an equivalent static approach, and supports structural evaluation through Karamba3D analysis combined with analytical capacity checks in accordance with the relevant Turkish and European structural codes. These checks identify key vulnerability parameters, including excessive inter-storey drift and insufficient member capacity.

The identified vulnerabilities guide the choice of retrofit intervention, which is supported through a designer-led selection of suitable strategies, such as column jacketing or shear wall interventions. These types of interventions create the link between the two research tracks: the structural workflow defines the retrofit need while the material workflow explores how this need could be met through modular components made from recycled construction and demolition waste.

For this purpose, concrete and brick aggregates are processed into recycled aggregate inputs for modular retrofit components for column jacketing and shear wall interventions. Supported by a designed recycling process aimed at reducing impurities in the waste stream. The material investigation therefore supports the structural workflow by translating the selected retrofit strategies into a more resource-efficient and accessible supply system.

The result is a design-driven proof of concept for a faster, typology-based, and resource-aware retrofit workflow. In which the structural parametric workflow generates a retrofit demand by identifying what fails, where, by how much, directly informing which interventions are needed where to prevent collapse, while the material track designs the whole system of supplying locally sourced retrofit elements derived from demolition waste.

Glossary

Acronym	*Term*
ADS	Air drum separator
BRB	Buckling restrained bracing
C&D	Construction and demolition
CDDD	Construction and demolition diversion deposit
DASK	Tr: Doğal afet sigortaları kurumu - En: Natural disaster insurance institution
EBR	Externally bonded reinforcement
EERI	Earthquake Engineering Research Institute
ESM	Equivalent static method
FPS	Friction pendulum system
FRP	Fibre reinforced polymer
IAEE	International Association for Earthquake Engineering
IBB	Tr: İstanbul Büyükşehir Belediyesi - En: Istanbul metropolitan municipality
ITZ	Interfacial transition zone
KL	Knowledge level
MSW	Municipal solid waste
Mw	Moment magnitude scale for measuring earthquakes
NMS	Near-surface mounted system
RBA	Recycled brick aggregate(s)
RC	Reinforced concrete
RCA	Recycled concrete aggregate(s)
SCC	Self-consolidating concrete
TBDY	Tr: Türkiye bina deprem yönetmeliği - En: Turkish building earthquake code
TSC	Turkish seismic code
URCA	Untreated recycled concrete aggregate(s)

Academic integrity

In preparation of this thesis, AI tools were used for the following purposes: generative image creation for visualisation purposes, as a discussion partner for exploring and clarifying technical concepts, and for language editing of written sections. All technical calculations, design decisions, analysis results and conclusions are the author's own work. AI-generated content was always reviewed, questioned, verified and adapted before inclusion, in accordance with the academic integrity standards and the code of conduct of TU Delft.

Contents

Thesis structure

This thesis is organised into seven chapters. Chapter 1 introduces the research by establishing the problem context and sets out the research objective, question, methodology, scope, and expected output.

Chapter 2 establishes the case study context: the seismic landscape of Istanbul's Avcılar district, the prevailing residential building stock, and the selection of a representative reinforced concrete frame building. The following chapter develops the theoretical framework, tracing the full process from construction and demolition waste composition and recycling processes through the material treatment strategies, mechanical property benchmarks, and the seismic behaviour and retrofit classification of reinforced concrete frame buildings, providing the technical foundation for both research tracks. Chapter 4 examines the feasibility of implementing a C&D waste recycling system at the urban scale, assessing local conditions specific to Istanbul and the economic viability of the recycling chain. The subsequent chapter presents the typology-based parametric workflow: from the identification and classification of the target building typology to data acquisition, geometric modelling, seismic analysis, and the swift generation of retrofit design outputs and capacity checks. The following chapter illustrates the integration between the two research tracks in a full case study, progressing from a stand-alone seismic assessment of the unretrofitted building to the integration of precast recycled-aggregate retrofit elements. After this retrofit integration, a final evaluation is done to show how these interventions improve the building's overall seismic performance. Chapter 7 concludes this thesis, reflecting on the results, acknowledging limitations, and identifying directions for future research.

1. Introduction

On 6 February 2023, a magnitude 7.7 earthquake struck the Kahramanmaraş region of Türkiye, followed several hours later by a second event of magnitude 7.5. Together, these earthquakes caused the collapse of over 160,000 buildings, resulted in more than 50,000 fatalities, and displaced millions (Akın et al., 2024). Türkiye is situated along some of the world's most active fault lines, and its cities, particularly Istanbul, contain large concentrations of ageing reinforced concrete buildings that were not properly designed to withstand significant seismic forces (Erberik, 2008). The occurrence of another major earthquake in Istanbul is considered a statistical certainty rather than speculation. This risk has been emphasized by professor Celal Şengör, a leading Turkish geologist and expert in structural geology and plate tectonics, who stated: "The great Istanbul earthquake is at hand... we are under the threat of an average earthquake with a magnitude of 7.2 until 2030." (Habertürk, 2017). With approximately 6.7 million residential buildings across Türkiye still requiring structural evaluation (World Bank, 2021), the gap between the scale of seismic risk and the pace of intervention has never been more urgent to address.

Seismic resilience in this context represents both an engineering and an ethical challenge. Communities most exposed to earthquake risk frequently have the least access to retrofitting resources and often reside in the most vulnerable parts of the city. Creating pathways toward safer buildings requires solutions that are not only structurally sound but also faster, more scalable, and more resource-efficient than those currently implemented.

1.1 Problem statement

Although natural hazards occur worldwide, their impacts are distributed unevenly, showing major inequalities in disaster vulnerability between countries and regions. These disparities are unmistakably clear when looking at earthquakes. In some regions, earthquakes recur over generations, repeatedly displacing families, disrupting lives and destroying communities. In contrast, societies in safer geographic areas can benefit from stronger institutions and greater economic stability, and are therefore better positioned to prepare for and recover from such events. This imbalance raises a fundamental question of justice: Can we ensure a future where resilience is accessible, circular and fair for everyone?

For these reasons, seismic resilience does not only become an engineering challenge but also an ethical responsibility that requires careful consideration. Enhancing communities' capacity to withstand earthquakes is essential for an equitable chance at development, particularly in regions where such risks cannot be avoided.

In Türkiye, where major fault lines cross densely populated regions, the threats of seismic vulnerability are particularly high. Within cities, certain neighbourhoods consistently face higher risks of vulnerability due to ageing building typologies and limited access to retrofitting options. During urban regeneration and post-disaster recovery, these same locations also generate significant amounts of construction and demolition waste. Materials that are typically undervalued and treated as waste rather than as potential resources for new structural elements that could be employed for strategic seismic retrofitting.

Therefore, this thesis positions itself at the intersection of these challenges: the need for faster, more scalable seismic assessment methods, the urgency of retrofitting vulnerable building stock, and the potential for reusing locally available demolition materials. By developing a parametric workflow for seismic evaluation and retrofit design, this research aims to reduce the time and effort required for structural assessment while exploring how such approaches can support more accessible, resource-efficient retrofitting for everyone, creating a more equitable pathway toward seismic resilience.

1.2 Research objective

The objective of this thesis is to develop a parametric design framework that accelerates the early-stage seismic assessment and retrofit design process for existing buildings. This framework will also explore ways to use converted C&D waste as part of the retrofitting elements. The goal is to reduce the time and effort required by conventional building-by-building assessment methods. This is done by translating survey-based input data into automated geometric modelling, structural analysis, and capacity verification. The framework also enables fast and easy integration of retrofitting strategies into the workflow.

The proposed approach uses building typology-driven logic. Buildings with similar structural characteristics are represented by a parametric model. This enables rapid evaluation and iterative testing of retrofit strategies. In addition, the framework considers using C&D waste as input for retrofit elements. This could lead to more resource-efficient and accessible strengthening solutions.

1.3 Research question

The main research question that guides the thesis is:

"How can a system design strategy be developed to accelerate the seismic assessment and by extension retrofit design of mid-rise reinforced concrete frame buildings in Türkiye, while enabling the integration of recycled construction and demolition materials?"

Given the broad, multidisciplinary nature of this question, it is crucial to structure the approach by starting with a literature review and a set of categorised sub-questions that focus on the key aspects of research for this thesis. While the theoretical framework helps to establish the contextual, structural and material conditions of this thesis, the sub-questions guide the design-based investigation and directly contribute to answering the main research question.

1. Theoretical framework
The theoretical framework is organised into a series of categorised domains and serves as the basis for each research domain. These domains collect existing knowledge on construction and demolition waste, structural vulnerability, and current seismic retrofitting approaches in the built environment. Together, they provide a solid conceptual foundation for the subsequent material, structural, and system design phases of the research, which are shown in the corresponding chapter of this report.

2. Material design
The material design phase focuses on translating demolition waste streams into usable material inputs for retrofit applications. The following sub-questions guide this phase:

2.1 Which construction and demolition waste fractions can be most effectively reused in structural retrofit applications?

2.2 What processing steps are required to transform selected construction and demolition waste fractions into standardized and design-ready material inputs for retrofit applications?

2.3 How can recycled construction and demolition waste be utilised in the development of structural retrofitting elements for seismic strengthening?

3. Structural design
The structural design phase investigates how recycled materials can be integrated into retrofit solutions that address identified seismic vulnerabilities. This phase is guided by the following sub-questions:

3.1 What types of retrofitting strategies can be conceptualised using recycled construction waste as a primary material input?

3.2 How can seismic assessment parameters be used to inform retrofit strategy selection within this parametric modelling workflow?

3.3 How can seismic retrofitting strategies be integrated into a parametric model to enable rapid evaluation and iteration of design scenarios?

4. System design
The last design phase, the system design, investigates how to combine the separate material supply and demand entities into a developed, ready-to-use framework. This phase is guided by the following sub-questions:

4.1 How can the proposed workflow be evaluated as a rapid decision-support framework for seismic assessment and retrofit strategy testing?

4.2 How can such a system be standardised and applied across different building cases with similar structural characteristics?

1.4 Methodology

The methodology forms the backbone of this research and outlines the analytical and design workflow. It is structured as a dual-track approach, starting with structural and material/product design as separate research streams, but eventually bridging them within a unified framework. The methodology focuses on demonstrating how these domains can be integrated through a workflow that links structural assessment with material-informed retrofit design. An overview of the overall methodology is shown in Figure 1.1. A more detailed step-by-step explanation of the methodology, including the parametric structural model workflow and the material process from aggregate recovery to retrofit product development, is provided in Appendix A.

Material design

The material design trajectory begins with a theoretical framework that examines the current state of C&D waste in Istanbul and Türkiye, identifies key material streams, and highlights existing gaps in reuse practices. This is followed by a waste stream analysis to determine which materials are most suitable for structural reuse. Based on these insights, a material processing pathway is proposed to transform the selected waste fractions into reliable inputs for retrofit applications. These are subsequently translated into the development of retrofit products that are designed for efficient production and practical on-site application.

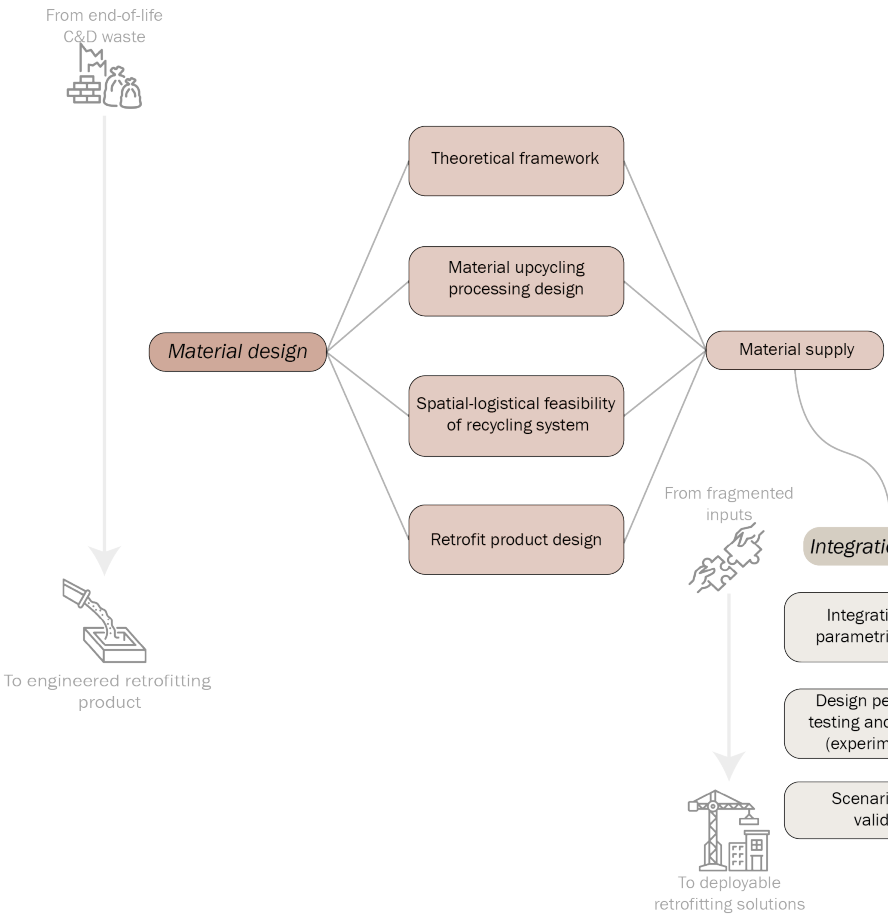

Figure 1.1: The research methodology utilised in this research

Structural design

On the other hand, the structural design trajectory begins with a theoretical framework that examines seismic damage mechanisms and existing retrofitting strategies. This is followed by the definition of the study context through typology-based parametrisation, enabling buildings with similar structural characteristics to be represented within a parametric model. Then, a software-based structural analysis is performed to quickly and conveniently identify key vulnerabilities. Based on these insights, targeted retrofitting strategies can be developed and integrated into the model, enabling quick, iterative design and easy verification of their structural performance, resulting in a streamlined process.

Integration design

At the centre of the methodology, the integration design connects the structural and material design tracks into one unified workflow. This phase focuses on translating the structural retrofit demand into more resource-aware retrofit solutions. The vulnerabilities identified through the parametric assessment, such as excessive drift or insufficient member capacity, are used to define where and what type of seismic strengthening intervention is required. These interventions are then linked to the material workflow, in which recycled concrete and brick aggregates are processed into retrofit components. By bringing both tracks together, the integration design illustrates how locally recovered construction and demolition waste can be aligned with the specific strengthening needs of vulnerable buildings.

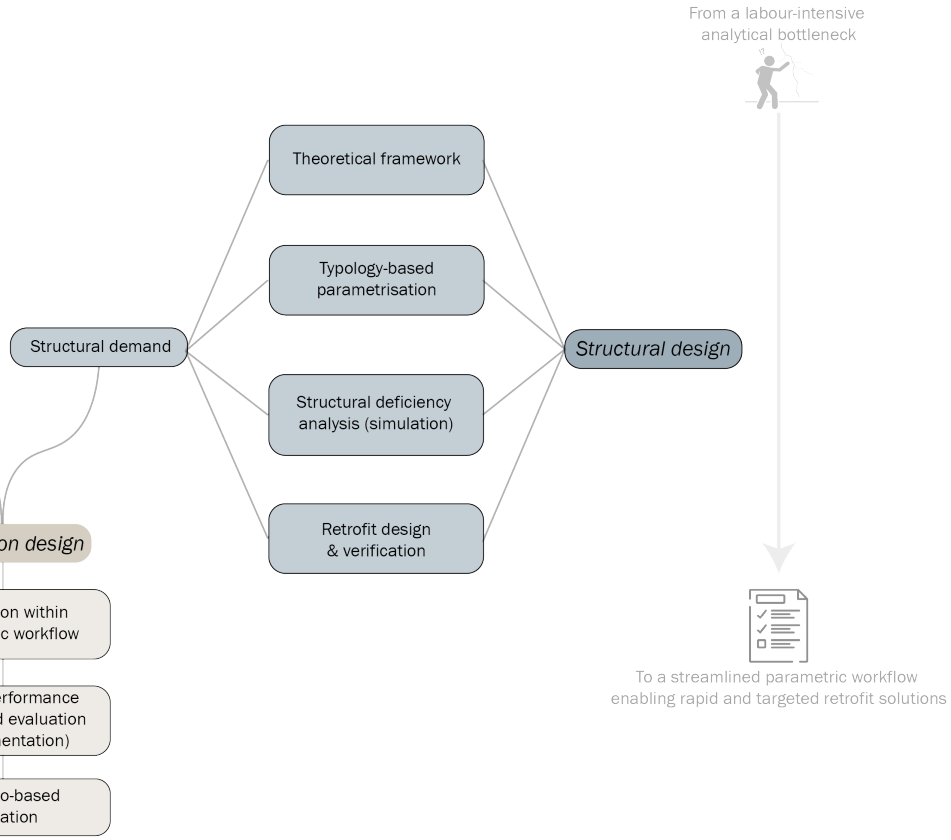

1.5 Research scope

This study examines the potential of a parametric workflow to facilitate seismic assessment and retrofit design for buildings with a common structural typology in Istanbul, Türkiye. By integrating typology-based structural analysis with the use of recycled construction and demolition retrofit products, the research demonstrates that strategic, targeted retrofit solutions can be developed more efficiently compared to conventional building-by-building methods.

Türkiye is selected as the study context due to its distinctive combination of high seismic hazard, evolving seismic regulations, construction practices, and government policies. These factors significantly affect building vulnerability, retrofit feasibility, and C&D waste management pathways. Focusing on Türkiye allows for the specification of constraints and opportunities addressed in this research. The city of Istanbul is chosen for its dense and complex urban fabric, high concentration of seismically vulnerable buildings, and the imminent threat of a major seismic event. As Professor Celal Sengör (2017) notes, "The great Istanbul earthquake is at hand... Although an exact date cannot be given, we are under the threat of an average earthquake with a magnitude of 7.2 until 2030." Consequently, Istanbul represents a critical and urgent case for evaluating retrofitting strategies and their associated material and waste implications.

This research is presented as a design-driven proof of concept centered on a single representative building typology. By developing a parametric workflow, the study illustrates how seismic assessment and retrofit design processes can be structured more efficiently. This approach establishes a foundation that can be adapted to additional structural typologies and a wider array of retrofit solutions, thereby enhancing flexibility and applicability over time.

1.6 Research impact

This research contributes to improving seismic resilience in Türkiye by addressing two key limitations in current practice: the limited scalability of building-by-building assessment methods and the time- and resource-intensive nature of conventional retrofitting. These constraints create a bottleneck that restricts how many buildings can be evaluated and strengthened within a meaningful timeframe, often leaving vulnerable communities at continued risk.

The proposed tool is intended as an early-stage decision-support workflow for structural engineers, engineering consultancies, and retrofit-oriented construction companies involved in the assessment and strengthening of vulnerable residential buildings. By translating survey-based input into a parametric assessment and retrofit workflow, it enables faster preliminary decision-making before detailed building-specific verification. It does not replace the role of the engineer, but assists in identifying likely weaknesses, comparing targeted retrofit strategies, and prioritising interventions more efficiently.

At a broader scale, the workflow may also support municipalities, public authorities, and governmental organisations responsible for seismic risk reduction and urban transformation. By organising buildings into comparable typologies, the tool helps shift assessment from isolated building-by-building decisions to more strategic, scalable retrofit planning.

1.7 Research output

The primary contribution of this research is a parametric, typology-based workflow designed for the seismic assessment and retrofit design of existing buildings. This workflow translates survey-based input data into a rule-based geometric model, facilitating automated structural modelling, seismic analysis, and capacity verification within a unified process.

Structuring buildings into typologies based on shared geometric and structural characteristics enables the generation and efficient analysis of multiple building configurations. This approach transitions from traditional building-by-building assessment to a scalable parametric system capable of evaluating groups of similar buildings.

The workflow integrates parametric modelling (Rhino and Grasshopper), seismic analysis (using Karamba3D), and capacity verification calculations to identify critical structural vulnerabilities, including excessive drift, insufficient member capacity, and global effects such as soft-storey behaviour. Targeted retrofit strategies can then be rapidly tested, iterated, and verified within the same framework, supporting more informed and efficient retrofit decision-making.

In addition to structural optimisation, this research introduces a material-oriented dimension to the retrofit workflow by examining the integration of recycled construction and demolition (C&D) waste into seismic strengthening strategies and outlining the necessary implementation steps. The study identifies concrete and brick rubble as the predominant waste streams in Türkiye, highlighting their significant but underutilised potential for reuse as secondary material inputs in structural applications.

Material integration is embedded within the parametric framework rather than treated as a separate process. By aligning material availability with typology-based retrofit demand, the workflow demonstrates how recycled materials can be systematically incorporated into standardised retrofit solutions, such as shear wall additions. This approach advocates a transition from a slow, linear retrofit process to a rapid, resource-conscious methodology that simultaneously addresses structural performance improvement and material reuse.

2. Seismic risk context and case study location

Summary
This chapter establishes the contextual anchor for this research by introducing Avcılar, a district in Istanbul, as the study area and by defining a representative case study building to demonstrate the parametric workflow.

The first section situates the research within Istanbul's broader seismic risk map. The city lies adjacent to the North Anatolian fault line and faces a significant probability of a major seismic event before 2030 (Habertürk, 2017). Within this context, Avcılar is selected as the study district because it concentrates several critical vulnerability factors: soft soils that amplify ground motion and a building stock that is dominated by low- and mid-rise reinforced concrete frame buildings built before 2000. The last section introduces the specific case study building selected to demonstrate the necessary information to start the seismic assessment workflow.

2.1 Case study context

Istanbul is a metropolis facing high seismic risks as it is situated adjacent to the North Anatolian fault line, which for instance caused the 1999 Izmit earthquake. Researchers have estimated that the probability of strong shaking near Istanbul is 62 ± 15% within 30 years after the 1999 Izmit earthquake (Parsons et al., 2000). However, as Kalkan and Gülkan (2023) state, Istanbul's western shorelines (where the district of Avcılar is located) face higher seismic risk. These areas are more prone to significant ground-shaking amplification, potentially up to 2.5 times greater than that experienced on hard-rock sites (as is illustrated in Figure 2.2 and 2.3 on the following page. Therefore, it is evident that seismic risk is not uniform across this city. Even between districts, vulnerability can differ substantially depending on two primary factors: proximity to active fault segments, and local soil conditions (Tezcan et al., 2002). Soft, alluvial, or coastal soils amplify ground motion more than rocky substrates do.

This spatial inequality is well illustrated by comparing Avcılar, on the western European coast of Istanbul, with Ataşehir, a more modern district on Istanbul's Asian side. Using damage estimates from the 7.5-magnitude (Mw) earthquake scenario studies conducted by the Municipality of Istanbul (IBB, 2020a; 2020b), a striking contrast emerges despite both districts having comparable numbers of analysed buildings. In Ataşehir, approximately 63% of the building stock is expected to remain undamaged, with 24% sustaining light damage, 10% moderate damage, 2% heavy damage, and 1% very heavy damage. This means that roughly 12% of the buildings (around 3.350 structures) would be classified as moderately damaged or worse (IBB, 2020b). In Avcılar, on the other hand, only 39% of the buildings are expected to remain undamaged, while 34% would sustain light damage, 21% moderate damage, 5% heavy damage, and 1% very heavy damage (IBB, 2020a). This places approximately 27% of the building stock, or around 7.039 structures, in the moderately damaged or worse category. This difference in damage distribution is also illustrated in the graph in Figure 2.1 below.

This elevated risk is not coincidental. Avcılar is situated on soft alluvial and partially reclaimed coastal soils, which amplify seismic ground motion significantly. This was demonstrated during the 1999 Kocaeli earthquake, when Avcılar sustained disproportionate damage despite being approximately 120 km from the epicentre, a consequence partly attributed to local soil amplification effects (Tezcan et al., 2002; İBB, 2020a). Therefore, to demonstrate how the parametric workflow functions, this framework is applied to a typical mid-rise apartment building consisting of reinforced concrete moment-resisting frames, located in the south of the district, which experiences the highest peak ground accelerations (Dlubal, 2024).

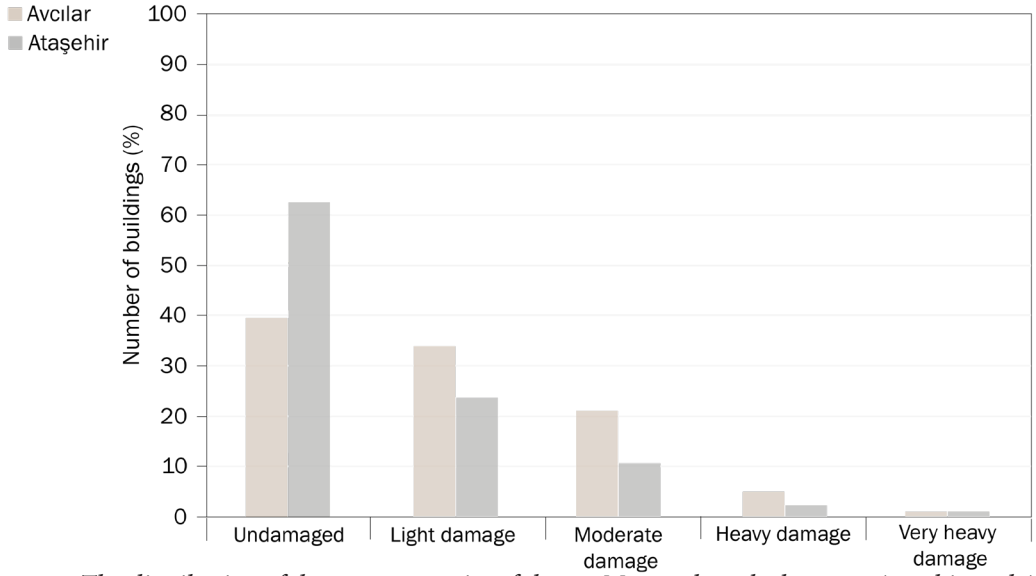

Figure 2.1: The distribution of damage categories of the 7.5 Mw earthquake between Atasehir and Avcilar

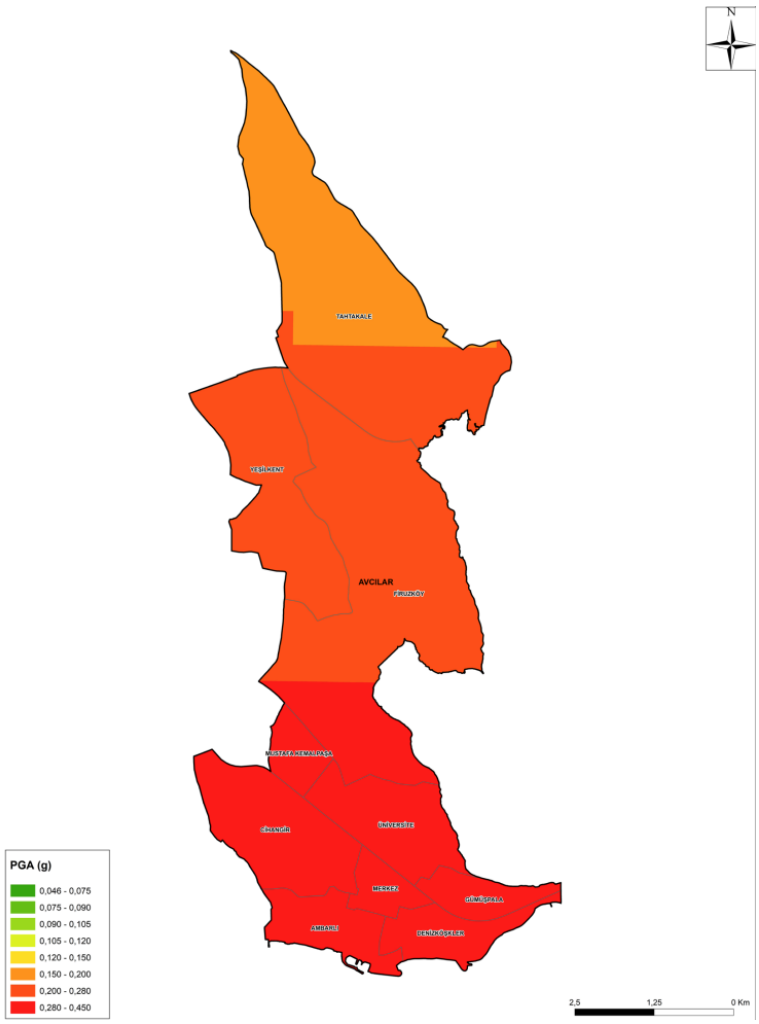

Figure 2.2: Peak ground acceleration distribution under the Mw 7.5 earthquake scenario for Avcılar, showing higher ground accelerations at the coastal zone (IBB, 2020a)

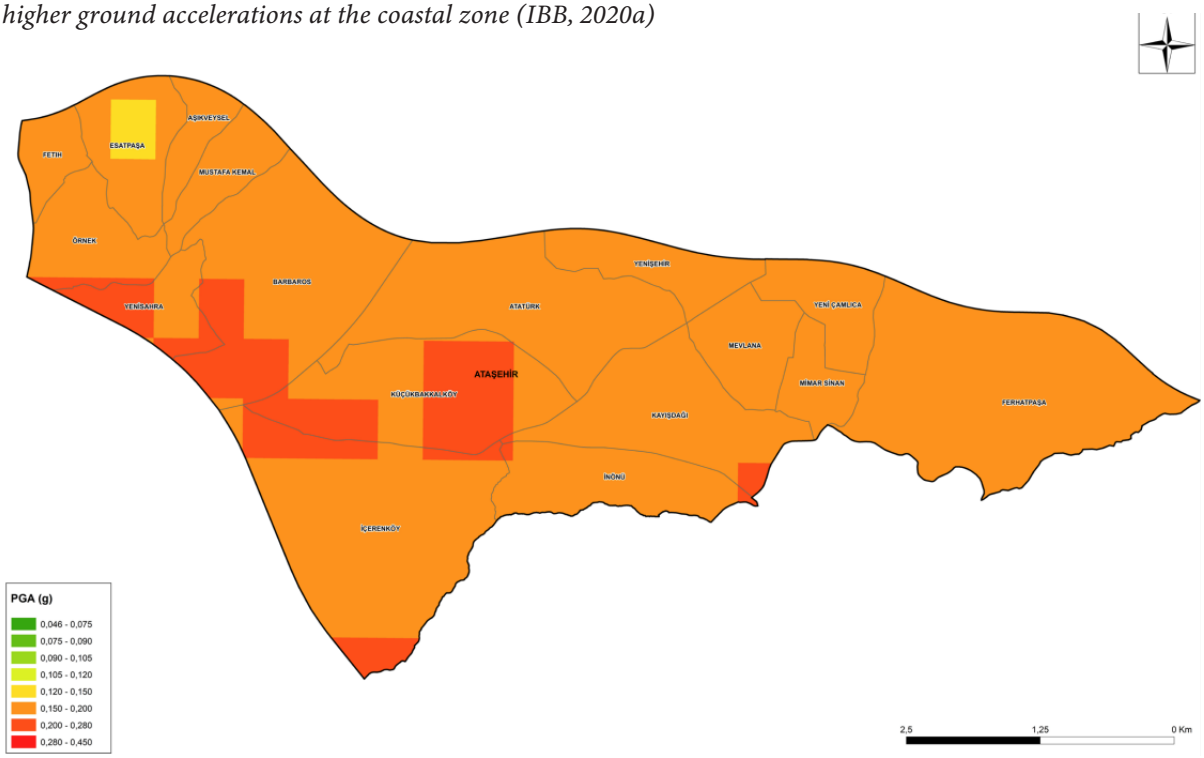

Figure 2.3: Peak ground acceleration distribution under the Mw 7.5 earthquake scenario for Atasehir (IBB, 2020b)

2.2. The building stock profile - Avcılar

Seismic hazard, as described in the previous section, characterises the physical threat posed by ground shaking at the given location. However, the extent to which that hazard translates into damage depends on the vulnerability of the built environment exposed to it. In Avcılar, the building stock profile reveals a district in which both dimensions, hazard and vulnerability, are simultaneously elevated.

Construction period
A critical indicator of structural vulnerability is the construction period of a building, as this determines which seismic design code governed its design. In Türkiye, significant revisions to seismic design requirements followed the devastating earthquake of 1999 in Izmit (Mw 7.6), which exposed severe deficiencies in the performance of the existing building stock and prompted a comprehensive update to the Turkish Seismic Code (Erberik, 2008). Buildings constructed prior to these code revisions, generally taken as the year 2000, are therefore considered particularly susceptible to seismic damage, as they were designed under codes that did not adequately account for modern seismic demands.

A substantial majority of Avcılar's building stock predates this threshold. Approximately 28% of buildings were constructed before 1980, a period during which the construction standards of that day (TEC-1975) were largely absent or poorly enforced. (Morales-Beltran, 2025). A further 37% were built between 1980 and 2000. Together, these two categories account for 65% of the district's building stock. These buildings are particularly vulnerable not only because of the limitations of TEC-1975, but also due to ineffective building inspection, poor construction control, and material-quality deficiencies that characterised much of the pre-2000 building stock (Morales-Beltran 2025). Only the remaining 35% constructed after 2000 were designed under more developed seismic regulatory contexts, following frameworks such as TEC-1998, TEC-2007, and later eventually TBEC-2018 (IBB, 2020a).

Building height
The building height distribution of Avcılar's building stock provides a further layer of vulnerability assessment. The district is dominated by low-rise buildings of one to four storeys, while mid-rise buildings of five to eight storeys constitute approximately 27% of the stock. Although low-rise buildings are not immune to earthquake damage, mid-rise reinforced concrete frame structures built before 2000 are particularly concerning. This height range coincides with the structural configuration's most susceptible failure modes like soft-storey failure or column shear failure under lateral loading (Morales-Beltran 2025). Failure modes widely observed in the 1999 Izmit earthquake and directly associated with pre-2000 construction practices prevalent in Turkish cities (Morales-Beltran, 2025; Gokdemir et al., 2013). The combination of mid-rise height and pre-2000 age therefore identifies a concentrated portion of the stock as structurally high-risk.

Structural material
The distribution of structural materials in Avcılar closely reflects the broader composition of Istanbul's urban building stock. The building stock in Avcılar is dominated by reinforced concrete, accounting for 81% of the buildings in the district. Masonry construction accounts for 15%, while tunnel formwork systems (2%), steel (1%), prefabricated (0.7%), and timber (0.3%) represent negligible shares (IBB, 2020a). This material composition is relatively consistent with national patterns, in which reinforced concrete moment-resisting frame construction (typically combined with unreinforced masonry infill walls) has been the dominant building form across Türkiye since the mid-twentieth century (Morales-Beltran, 2025; Gulkan et al., 2002). However, as Morales-Beltran (2025) notes, reinforced concrete (RC) structures generally lack lateral strength and stiffness, making them vulnerable to earthquakes.

2.3. Case study building

To demonstrate the parametric workflow tool developed in this thesis, a representative residential building in Avcılar is selected as the case study. The example building, which is shown in Figure 2.4 was selected because it displays the structural and geometric characteristics of a typical mid-rise reinforced concrete moment-resisting frame building, a typology identified by Morales-Beltran (2025) and Gulkan et al. (2002) as having elevated seismic risk.

It is important to note that no formal site investigation has been conducted for this building. As a result, no structural drawings, material certificates, or laboratory test results were prepared or available, and no on-site inspections were conducted. Therefore, the input parameters used in the on-site investigation survey are based on visual assessment and typological assumptions derived from the housing report from the Earthquake Engineering Research Institute (EERI) (Gulkan et al., 2002). The used input parameters for this case study are shown in Table 2.1 below. Within the knowledge level framework of TBDY 2018 and NEN-EN 1998-3, a Knowledge Level 2 (KL2) is assumed for this case study, on the basis that the typological database provided by Gulkan et al. (2002) documents material properties, reinforcement configurations, and geometric ranges for this building type, serving as a substitute for limited in-situ material investigation. This knowledge level has a confidence factor applied to member capacities, the implications of which are discussed in Chapter 6.

The purpose of this case study is not to produce a legal early-stage structural assessment of this specific building, but to demonstrate how the workflow functions in practice, namely from survey-based input through parametric modelling to a retrofit evaluation, using a realistic and representative building for which the tool is designed. This building therefore serves as a proof of concept.

Figure 2.4: The case study building, taken as inspiration for the input data (Google earth, 2022)

Table 2.1: The most important numerical input data used in the case study (based on Figure 2.4, Gulkan et al., 2002) and estimations

Building geometry		***Member information***		***Seismic conditions***	
Parameter	*Value*	*Parameter*	*Value*	*Parameter*	*Value*
Number of columns in X-direction	4	Column dimensions (mm)	300x300	Soil class	ZE
Number of columns in Y-direction	7	Concrete grades	C16/20	Ss – DD2 [g]	1.41
Span length X / Y (mm)	3500 / 4500	Long. Rebar	8 x ø16, S420	S1 – DD2 [g]	0.378
Ground floor height (mm)	3600	Stirrups, stirrup spacing (mm)	Ø10, 200	Fs – DD2 [g]	0.85
Upper floor height (mm)	2700	Beam dimensions (mm)	250x500	F1 – DD2 [g]	2.4
Number of storeys	5	Concrete grades	C16/20		
Overhang configuration	8	Long. Rebar	4 x ø16, S420		
Overhang lengths (mm)	1200 / 1500	Stirrups, stirrup spacing (mm)	Ø8, 250		
		Stirrup angle	90°		
		Slab thickness (mm)	120		

3. Theoretical framework

Summary
This chapter establishes the theoretical foundation for both research tracks of this thesis: the material supply chain for recycled construction and demolition waste aggregates, and the assessment of seismic analysis and retrofitting of reinforced concrete frame buildings in Istanbul. Together, these two tracks form the knowledge base from which the integrated parametric workflow in the following chapters is derived.

The material track opens by mapping Istanbul's C&D waste streams, reviews the current recycling framework in Türkiye, identifies key infrastructural and regulatory gaps, and explores the opportunities the building stock's materials offer. This is followed by an analysis of the material- and mechanical properties of recycled concrete and brick aggregates, the role of adhered mortar as their primary limitation, and the treatment strategies used to address it. The track concludes with a conceptual design for a recycling system in Istanbul, covering the incentive structure, process flow, and aggregate upgrading strategies.

The structural track characterises Türkiye's existing building stock by construction period, structural typology, and seismic vulnerability. It consequently examines the common failure mechanisms observed in reinforced concrete buildings during earthquakes. Furthermore, it classifies existing retrofitting strategies and analyses the bottlenecks of the current seismic assessment processes, which directly motivate the need for the parametric approach developed later in this thesis.

3.1: Composition and breakdown of C&D waste in Istanbul

One of the first steps in this research is systematically mapping current C&D waste streams in Istanbul. Establishing this baseline is essential. Developing retrofit products from waste requires a clear understanding of both the quantities of waste generated and the composition of material fractions in Turkish urban C&D waste. Identifying the volume, characteristics, and availability of these materials helps assess their potential for reuse in retrofitting. These insights underpin the evaluation of feasible recovery strategies and support informed decisions on integrating reclaimed resources into new materials.

3.1.1: Regional statistics and projections of C&D waste

Construction and demolition waste, accounting for 30 to 35% of total solid waste, represents a major and rapidly growing waste stream in Türkiye, especially in large metropolitan regions undergoing intensive urban transformation (Demir et al., 2017; Arslan et al., 2012). In 2013, the total amount of construction-related waste generated nationwide (including excavation soil) was approximately 130 million tonnes. More than 50% of this volume (around 67 million tonnes) originated from Istanbul alone (Demir et al., 2017).

A critical distinction within this waste stream is the dominance of excavation soil, which in Istanbul accounts for roughly 95% of the total construction-related waste by volume. When excavation soil is excluded, the remaining quantity of pure C&D waste, consisting primarily of building materials, is estimated to be approximately 2.0 to 2.5 million tonnes annually at the national level around 2010 as can be seen in Figure 3.1 (Demir et al., 2017). Despite being a smaller mass fraction, this fraction contains the materials most relevant for recycling and reuse, a perfect opportunity for creating a more circular built environment.

Projections indicate that construction-related waste generation in Türkiye will continue to increase in the coming decades, driven by population growth, urban expansion, and large-scale redevelopment initiatives. By 2033, the total volume of construction and excavation waste is expected to reach approximately 150 million tonnes per year (Demir et al., 2017). This growth is particularly pronounced in Istanbul, where urban transformation processes have intensified following the enactment of Law No. 6306 on the Regeneration of Buildings under Disaster Risk (2012), which enabled and encouraged the demolition and reconstruction of seismically vulnerable buildings (Gundes et al., 2017). This programme, involving the demolition and reconstruction of approximately 8 million buildings nationwide, has led to a sharp increase in C&D waste generation (Demir et al., 2017). In Istanbul, estimates indicate that pure C&D waste generation (excluding excavation soil) increased from approximately 2.0 to 2.5 million tonnes in 2010 to 7.0 million tonnes by 2016, as shown by the graph in Figure 3.1 (Demir et al., 2017). The scale of Istanbul's construction and demolition waste problem may become far more severe under future urban transformation scenarios. Akarsu Akdemir et al. (2025) state that Istanbul currently generates approximately 3-5 million tonnes of concrete waste annually, while large-scale urban transformation, combined with the city's earthquake vulnerability could increase this number dramatically, potentially reaching 320 million tonnes. They further argue that existing waste management practices remain inefficient, costly, environmentally damaging, and logistically impractical.

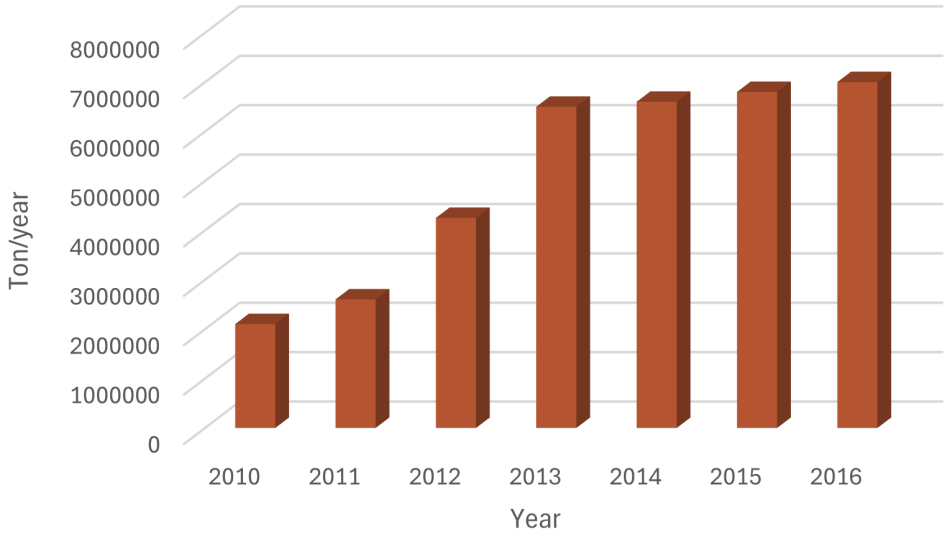

Figure 3.1: The increase of C&D waste in Istanbul, Türkiye through the years 2010-2016 (adapted from Demir et al., 2017)

3.1.2: Typical material fractions in Turkish urban construction and demolition

The Turkish building stock is predominantly composed of reinforced concrete (RC) frame buildings, which are typically combined with unreinforced masonry infill walls, resulting in a material-intensive built environment dominated by concrete and brick-based components (Morales-Beltran, 2025; Erberik, 2008). Consequently, construction and demolition waste in Türkiye reflects this structural composition. Nevertheless, C&D waste constitutes a heterogeneous waste stream, encompassing materials with diverse physical, chemical, and mechanical properties, which necessitates systematic classification to enable effective management and reuse.

C&D waste is generated in three ways, namely through a more controlled way in which C&D waste quantities are generated in a slow manner, which is through regular construction, renovation and demolition activities and the other two means, which are less controlled, lead to large, sudden amounts of C&D waste which can happen through natural disasters such as earthquakes, or which can happen through war imposed disasters (Bonifazi, et al., 2025). All of these possibilities cause a generation of C&D waste which consists of a variety of materials as is shown in Figure 3.4 to 3.6.

According to Turkish regulations, C&D waste is broadly classified into four main categories, each with corresponding material types, as shown in Figure 3.2 (Demir et al., 2017). In addition to regulatory classifications, C&D waste can be further categorised based on material behaviour and transformation potential. A primary distinction is made between inert, non-inert, hazardous, and non-hazardous waste fractions.

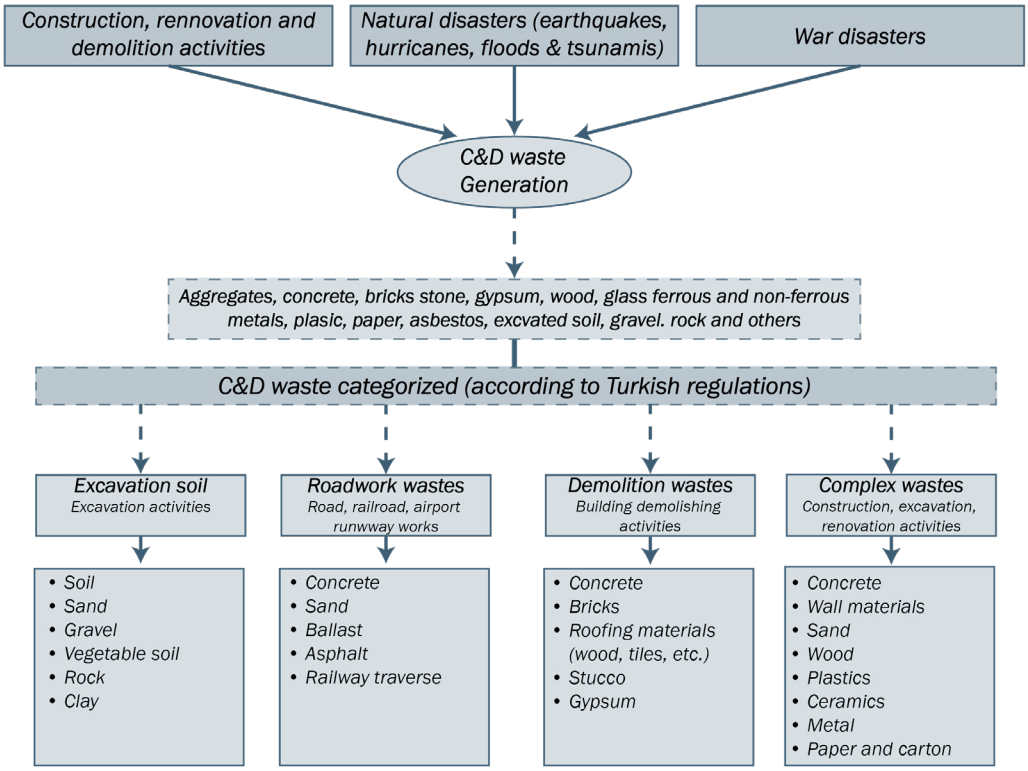

Figure 3.2: Classification and materialisation of C&D waste (adapted from Demir et al., 2017)

Inert materials are defined as waste that does not undergo significant physical, chemical, or biological changes over time, including concrete, brick, tiles, and stone. This category is further subdivided into soft-inert materials, such as soil, earth, and slurry, and hard-inert materials, such as concrete, brick, and rock. Non-inert materials comprise components that may degrade or transform over time, including wood, plastics, and organic materials Ulubeyli, S. et al. (2018). Arslan et al. (2012) additionally have a separate classification for hazardous waste, such as asbestos and heavy metals, and non-hazardous wastes are classified based on their environmental and health impacts.

Despite the dominance of concrete and masonry in the Turkish building stock, comprehensive nationwide data on detailed C&D waste material fractions remain limited. To address this gap, post-earthquake demolition waste is used as a proxy to approximate material composition. This approach is justified by the fact that earthquake-induced demolition produces material outputs comparable to planned demolition, with differences primarily related to demolition technique rather than building composition.

As illustrated in Figures 3.4 to 3.6, debris generated from the 2023 Kahramanmaraş earthquakes shows that masonry waste constitutes the largest fraction, accounting for approximately 59% of the total debris (Mavroulis et al., 2023). With an additional impact of affecting both reinforced concrete and masonry structures exhibit similar dominant material fractions, although masonry buildings contain lower proportions of concrete and steel reinforcement, and relatively higher shares of tiles and timber. These findings show that C&D waste in Türkiye is largely dominated by inert, mineral-based waste, also referred to as mineral fraction waste (Xiao et al., 2023).

The 6th of February 2023 Türkiye-Syria earthquakes reveal the magnitude of debris that can be produced by seismic disasters in Türkiye. According to Mavroulis et al. (2023), debris estimates for the event vary widely, ranging from 116-210 million tonnes according to UNDP to (450-920 million tonnes according to Xiao et al. (2023) (see Figure 3.3). This variation reflects the uncertainty involved in large-scale disaster waste estimation, yet both ranges indicate an exceptional burden from construction related debris. Using the maximum estimate, the 2023 earthquake becomes the largest debris-creating earthquake in the global dataset between 1994 and 2023. Even under the lower UNDP estimate, it remains the second-largest earthquake event in terms of debris, after the 2008 Sichuan earthquake. These figures also underline that 2.5 million people were affected by the event in Türkiye (Mavroulis et al., 2023).

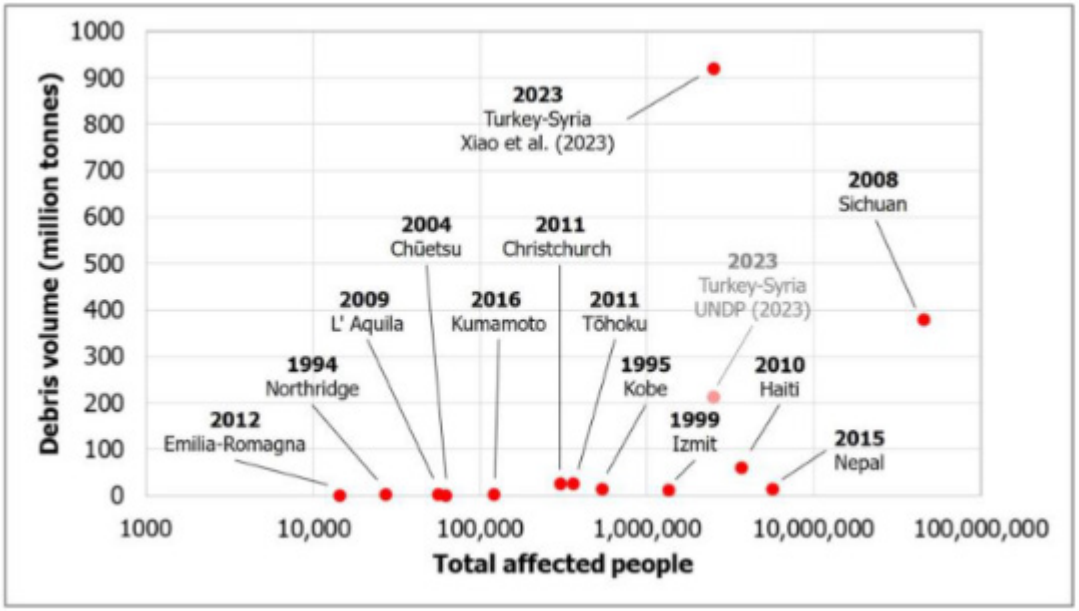

Figure 3.3: Debris volumes generated by earthquake worldwide form 1994 to 2023 against total affected people (Mavroulis et al., 2023)

Mineral fraction waste, including concrete, brick, tile, and similar inert materials, is technically recyclable and can be reused as a secondary raw material in applications such as cement production or recycled aggregate manufacturing. However, its recovery is often less economically attractive than that of higher-value materials because it is heavy, costly to transport, and usually has a relatively low market value. Temelli et al. (2023) show that when post-earthquake mineral fraction waste is evaluated as a raw material, the estimated economic gain remains moderate at approximately 37.5% after accounting for transportation and recovery costs. This indicates that mineral fraction waste has recovery potential, but that economic incentives alone may be insufficient to guarantee widespread recycling. In contrast, metallic fractions, particularly steel reinforcement, generally have a much clearer economic value and are therefore more likely to be separated and recycled during demolition processes. This difference helps explain why mineral waste is more frequently downcycled or landfilled, while scrap metals are routinely recovered. Therefore, improving the recovery of concrete and brick waste requires not only technical recycling capacity, but also stronger policy incentives, logistical planning, and dedicated processing machines.

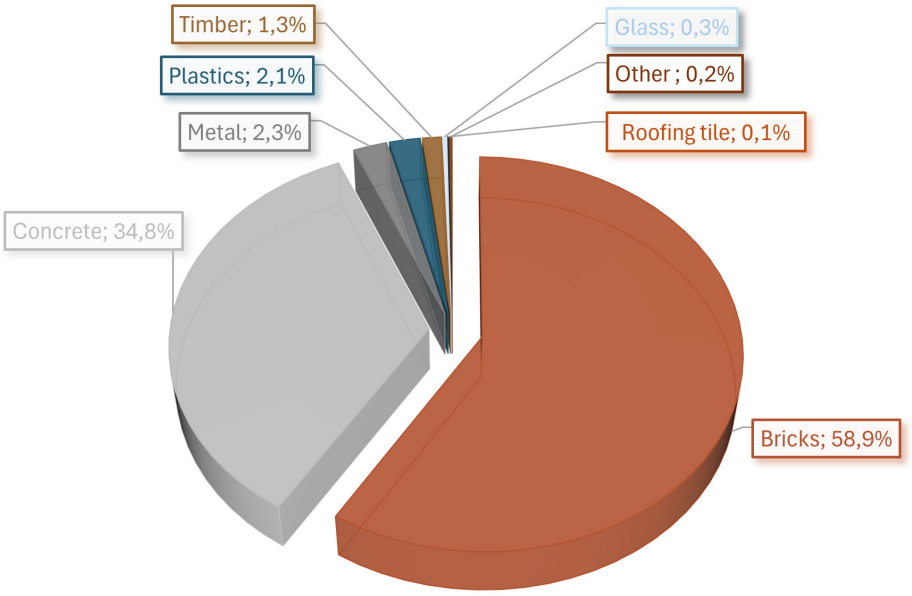

Figure 3.4: Composition of waste from demolition of reinforced concrete structures (adapted from Xiao et al., 2023)

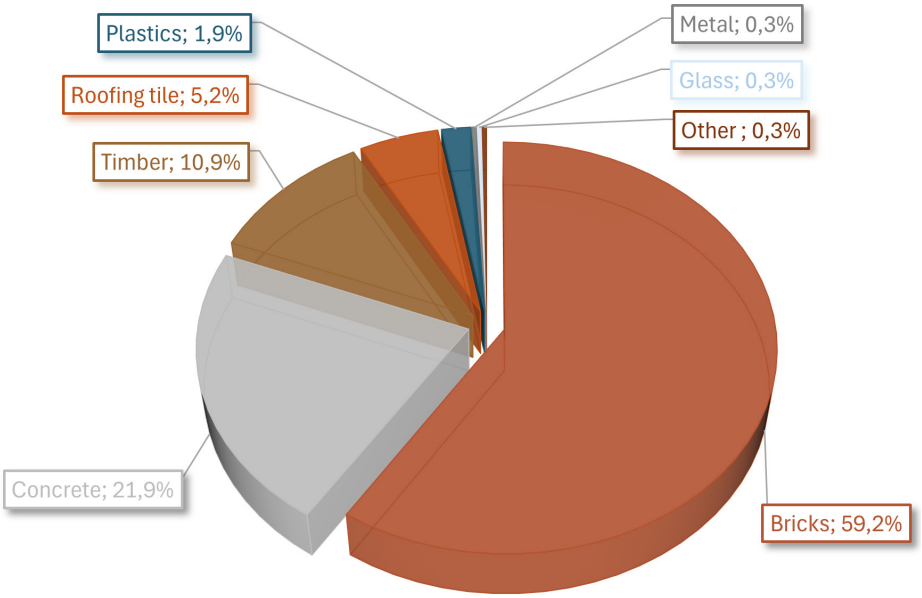

Figure 3.5: Composition of waste from demolition of masonry structures (adapted from Xiao et al., 2023)

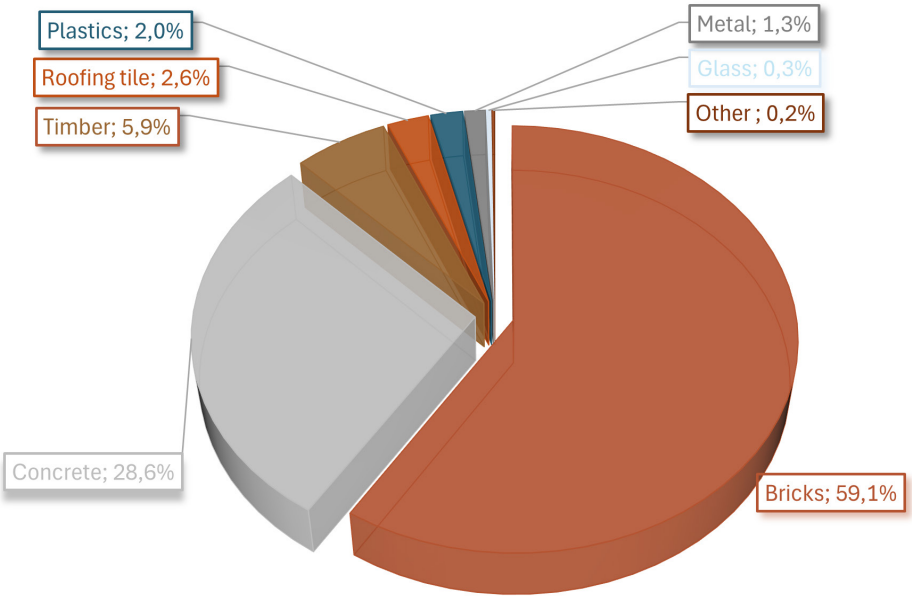

Figure 3.6: Overall composition of materials found in C&D waste in Türkiye after the Kahramanmaras earthquake (adapted from Xiao et al., 2023)

3.2: Review of current material recycling framework

It is essential to understand how C&D waste is currently processed in Türkiye. The performance, purity, and availability of recycled materials are directly determined by the quality of the recycling practices. Since this research aims to develop engineered retrofit products from C&D waste, the feasibility of such products depends not only on material properties but also on the technological, spatial, and institutional capacity of the upcycling system. Therefore, this section reviews current recycling processes, infrastructural limitations, and regulatory conditions.

3.2.1: Breakdown of current recycling process steps

The primary objective of C&D waste recycling is the production of recycled aggregates, contributing to the conservation of natural resources, the reduction of CO2 emissions, and decreased reliance on landfilling (Bonifazi et al., 2025). C&D waste comprises diverse material streams, including excavation soil, roadwork debris, demolition waste, and mixed or complex fractions, which may contain inert, non-inert, and hazardous components. In practice, source separation of C&D waste remains limited. For instance, a survey conducted in Türkiye reported that 38.5% of professionals do not sort their waste, while 75% primarily dispose of it through landfilling (Arslan & Ulubeyli, 2019), creating challenges for effective recycling. Due to the absence of standardised recycling procedures and variations in material composition, recycling processes may differ between facilities. Although additional treatments such as decontamination can improve aggregate quality, these methods are typically considered supplementary rather than integral to the core recycling process, which is therefore discussed later in this research paper.

Generally, C&D waste recycling consists of three main stages: cleaning, crushing, and sieving. Different methods and steps in the general aggregate recycling process are discussed below.

Collection and transportation

The first stage of the C&D waste recycling chain is the collection and transport of waste material to a recycling facility. The incoming waste stream as previously stated by Ulubeyli et al. (2018), this incoming waste is only accepted in Türkiye when properly separated. Waste that is properly sorted is taken in the stationary recycling facility, where subsequent sorting, crushing, and processing stages can take place (Pacheco & de Brito, 2021).

Separation of C&D waste

Since many different types of materials enter the C&D waste stream, sorting and cleaning them is essential for the efficiency of the recycling process and for ensuring sufficient quality to reuse different fractions of the waste. Therefore, this part of the recycling process is critical, complicated, and hard. Sorting is a key focus of waste management and helps enhance resource recovery and reduce reliance on landfills. In general, separation techniques undergo preliminary removal by an excavator to separate elements like wood, plasterboards, and plastics from the rest of the waste stream. Secondly, it is processed through a feeder for the removal of finer fractions like clay, soils, plastics, and paper (Pacheco & de Brito, 2021).

Manual separation

C&D waste can be separated using different techniques; first and foremost, waste can be manually separated at the construction site (Volkan and Ulubeyli, 2019) or at the recycling facility using manual labour at sorting conveyors. Pacheco & de Brito (2021) state in their research that unintended wastes are typically removed by 3 to 6 workers. These workers separate leftover contaminants and the removed materials are sent directly to storage bins below the sorting station. In the case of reinforced concrete, for example, manual separation of the rebars can be done by crushing the concrete (Ulubeyli, Personal communication, 2026).

Crushing procedure of C&D waste

After all, C&D waste is separated into metals, non-ferrous materials, plastics, timbers, etc. Through separation based on weight, size or specific material characteristics, the leftover materials, which are rubble-like brick, tiles, and concrete elements, can be reduced in size to new aggregates. Size reduction helps transfer larger particles of valuable waste into smaller particles of a desired size or shape that can be reused as a secondary raw material. The primary method of size reduction for C&D waste is crushing. This can take place in a single-stage (jaw crusher) or a two-stage jaw crusher followed by an impact crusher (Pacheco & de Brito, 2021). An illustration of a jaw and impact crusher is shown in Figure 3.8.

A jaw crusher works by squeezing materials between a movable jaw plate and a fixed jaw plate. Overall, the particle size after jaw crushing is relatively large and elongated, ranging from 10 to 350 mm. The jaw crusher is mostly used as a primary crushing method. Impact crushers are usually applied as a secondary crushing machine (Pacheco & de Brito, 2021). Impact crushers use high speed through a rotating plate hammer to crushes the particles. It applies a large crushing force and produces mostly cube-shaped particles and finer, higher-quality output particles (JXSC, 2020). The differences in particle sizes are shown in Figure 2.7.

Magnetic separation; ferrous vs. non-ferrous materials

Secondly, magnetic separation separates non-ferrous materials from ferrous materials, such as tin, iron, steel, and more. This separation technique is used both to recover metals and to purify secondary materials by removing the metals. The magnetic separation machines are found along the assembly lines, either placed above or below conveyor belts (Pacheco & de Brito, 2021).

Sieving; size-based separation

Sieving systems separate C&D waste into different particle-size fractions and can be applied before or after crushing. In recycled aggregate production, initial screening may remove oversized or elongated materials,

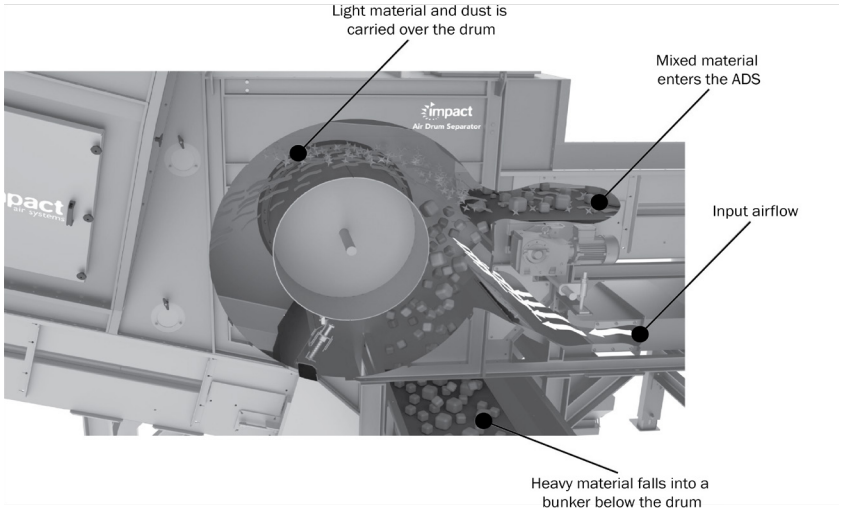

Figure 3.7: The working principle of an air drum separator (Adapted from: Impact Air Systems, n.d.)

while after the crushing stage, separation of the aggregate-sizes is carried out by using vibrating stationary screeners with slanted plates. Separating the aggregates based on the preferred sizes (Pacheco & de Brito, 2021)

Air drum separators (ADS); Weight based separation

The air drum separator is similar to a wind sifter, but it includes a rotating drum that uses air to separate mixed material streams by weight. ADS separation is very versatile. It is therefore applicable to a wide range of recycling and recovery applications. The process uses a high-velocity airstream that projects a focused airstream upward. This airflow lifts lighter materials and carries them to a designated collection zone. Heavier items roll over the infeed conveyor, remain unaffected, and drop into the drum. Figure 3.7 shows this process. For construction and demolition waste, an air drum separator can remove lighter materials, such as insulation, films, and packaging, from heavier ones, such as necessary rubble (Connelly, 2025; Pacheco & de Brito, 2021).

Final processing of C&D waste

After the particles are reduced in size by crushing, it is important to separate the clean recycled aggregates again by size. This is necessary because crushing produces both coarse and fine aggregates, depending on the type of machine. Separation methods include sieving or waste-screening applications, which sort aggregates by size (Pacheco & de Brito, 2021). In sieving, particles pass through a mesh to provide various gradations of coarse and fine aggregates (Youssef, 2025). In screening, a vibrating screen separates recycled (cement stone) powder from fine and coarse aggregates. The recycled fine and coarse aggregates are then used in new concrete elements, particularly in pavement or road-based works (Abdelfatah et al., 2011). Dehydrated cement stone can partially replace Portland cement clinker in cement production (Mulder et al., 2007). An air separator can also be used to separate fine aggregates from cement stone (Mulder et al., 2007).

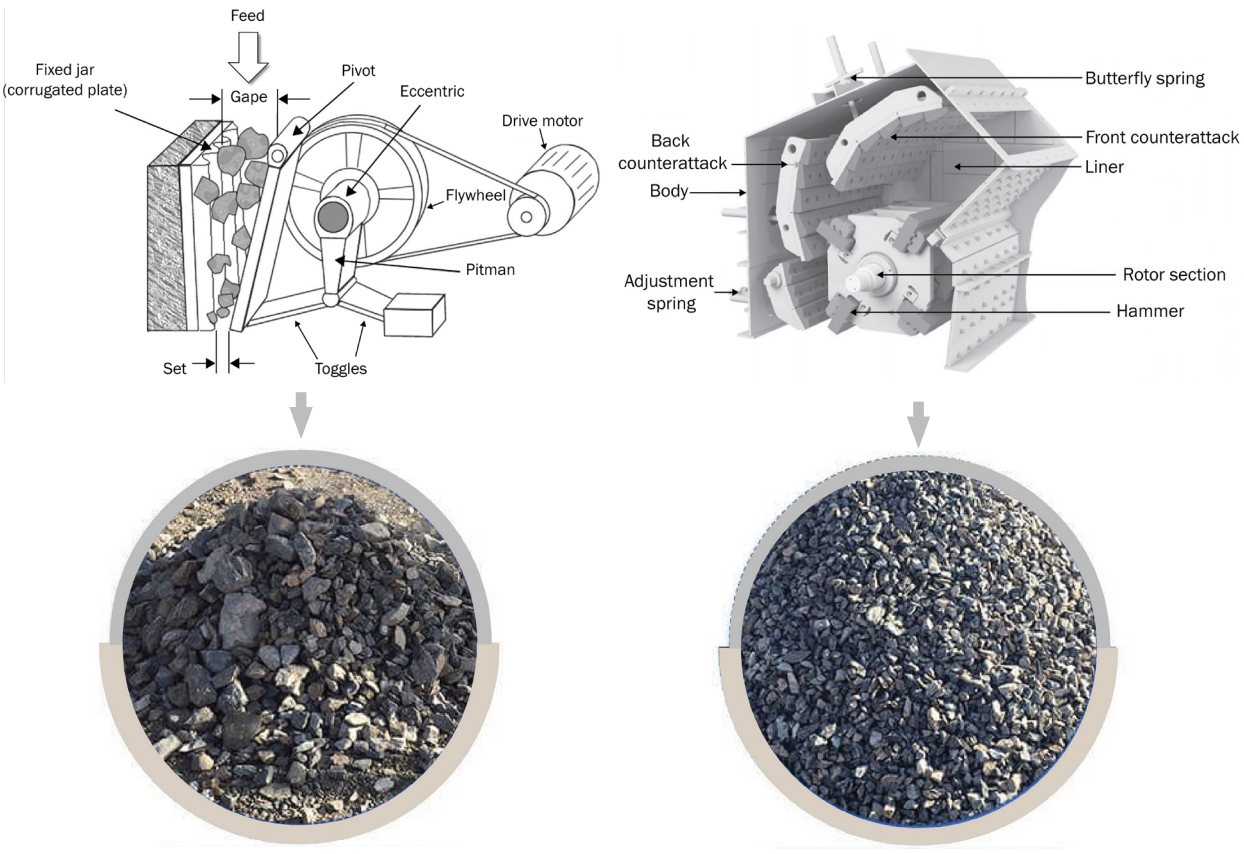

Figure 3.8: Schematic representation of a jaw crusher (left) and an impact crusher (right), illustrating the respective crushing mechanisms and resulting aggregate outputs (adapted from JXSC, 2020, Daswell, n.d. and Gupta and Yan, 2016)

3.2.2: Spatial-logistical considerations in C&D waste recycling

Since the establishment of Istanbul's first C&D waste recycling plant in 2006, the development of recycling infrastructure in Türkiye has largely stagnated. Currently, only three mobile recycling plants operate nationwide (Eskişehir, Muğla, and formerly Tuzla), with no active central facility serving the Istanbul metropolitan area, despite the Istanbul metropolitan area being the country's largest generator of C&D waste (Ulubeyli et al., 2018).

In practice, C&D waste management in Istanbul is therefore handled predominantly by certified private contractors who transport demolition waste to designated dumping sites. Although some operators use mobile crushers to produce recycled aggregates, these activities remain fragmented, small-scale, and market-driven, lacking integration within a coordinated recycling framework capable of addressing the scale of urban transformation (Ulubeyli, personal communication, 2026).

International comparison further highlights this infrastructural gap, as illustrated in Figure 3.9. This Figure shows that countries such as Germany (~1,000 plants), the Netherlands (~120), the United Kingdom (~100), and Sweden (~50) operate significantly more developed recycling networks and therefore show that Türkiye lags behind in terms of institutional capacity and infrastructure for C&D waste recycling (Ulubeyli et al., 2017).

Despite this infrastructural gap, survey results nevertheless indicate that Turkish construction professionals are willing to engage in recycling practices (Arslan & Ulubeyli, 2019). The dominance of landfilling can therefore be attributed primarily to insufficient infrastructure and limited policy enforcement rather than to a lack of technical awareness. Strengthening recycling capacity is consequently a critical precondition for enabling large-scale seismic retrofitting.

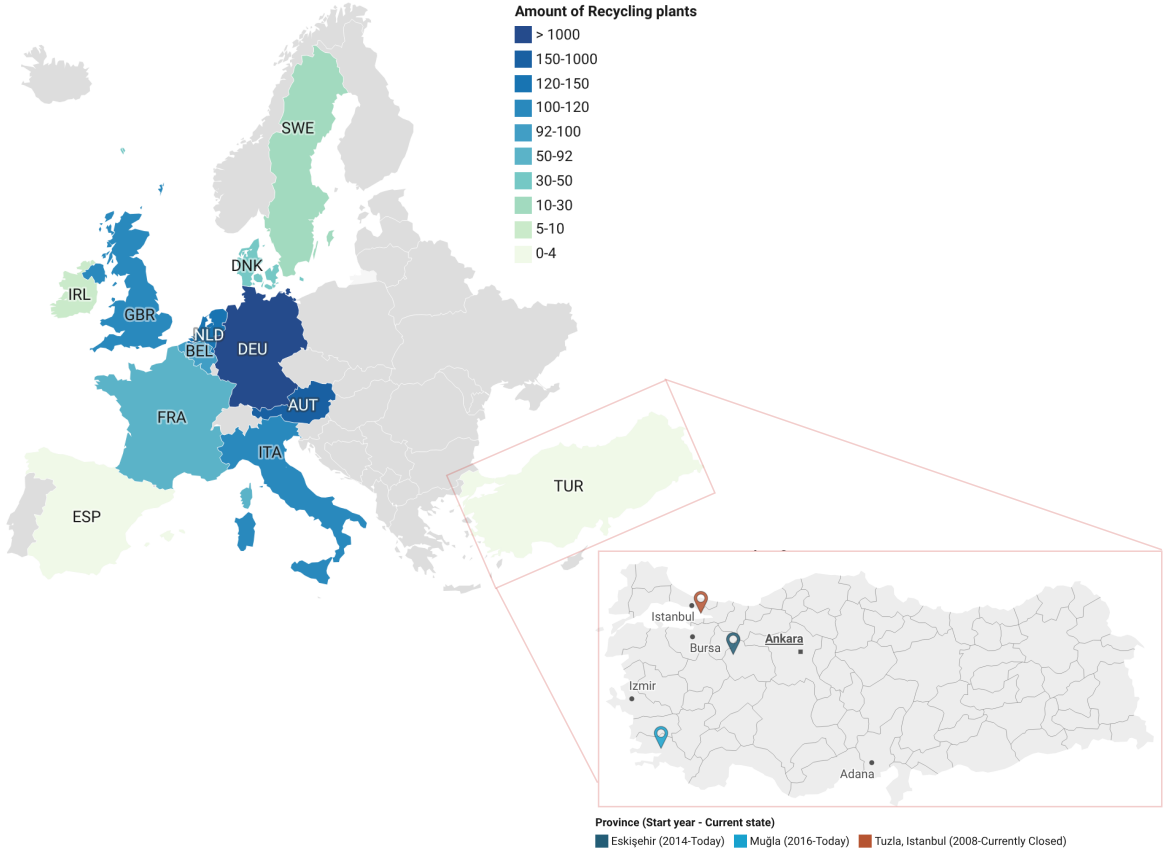

Figure 3.9: The amount of recycling plants for a selection of countries in Europe, highlighting the difference in recycling infrastructure development

The negative effects of landfilling

Despite growing awareness of the environmental and economic benefits of recycling, current C&D waste management practices in Türkiye remain largely landfill-oriented. Survey results by Arslan and Ulubeyli (2019) reveal a clear mismatch between positive attitudes toward construction and demolition waste recycling and actual site practices in Türkiye. Although awareness of reuse is relatively high, landfilling remains dominant: approximately 75% of firms report disposing of C&D waste in landfills, while 38.5% do not sort C&D waste at all. Furthermore, 57.7% of firms lack a formal waste management plan, despite such plans being legally required since 2004 under the Regulation on the Control of Excavation Soil, Construction and Demolition Waste. This regulation assigns municipalities the responsibility to prepare and implement plans for excavation and C&D waste management (Ustaoğlu and Limoncu, 2021). ranging from environmental to health hazards. Examples of hazards associated with landfilling C&D waste (as shown in Figure 3.10) include soil erosion, groundwater contamination, pest proliferation, fire risks, and the uncontrolled release of hazardous materials, including asbestos fibres, which are associated with long-term respiratory diseases and cancers (Arslan et al., 2012). Additional impacts include air and noise pollution, as well as the rapid depletion of landfill space (Bonifazi et al., 2025). Beyond environmental and health impacts, inadequate C&D waste management also results in significant economic losses. Feasibility studies from Kanat (2010) on municipal solid waste (MSW) management indicate that while landfilling is often perceived as the least effortful and therefore the least costly option, it performs poorly when compared to waste recovery and recycling strategies, as shown in Table 3.1. Economic assessments show that recycling and material recovery can yield substantially higher net benefits than landfilling, underscoring the economic potential missed by current disposal practices in Türkiye (Kanat, 2010).

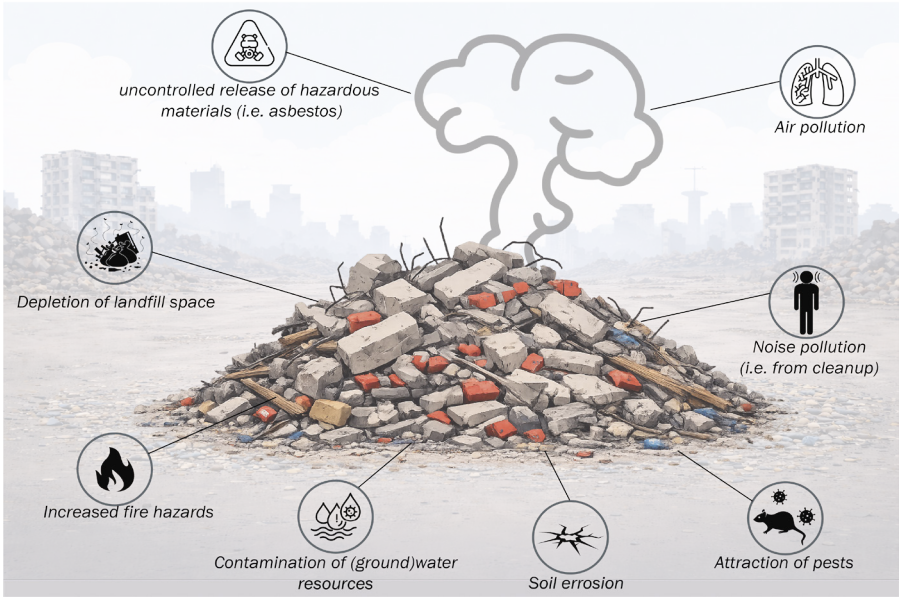

Figure 3.10: The negative impact of landfilling construction and demolition waste (image generated with assistance of AI).

Limited enforcement and insufficient municipal infrastructure have effectively made landfilling the most accessible disposal option. While landfilling has become the easiest and most accessible disposal option, its consequences are significant and often overlooked. Landfilling contributes to multiple hazards, beyond environmental and health impacts, inadequate C&D waste management also results in significant economic losses.

Feasibility studies on municipal solid waste (MSW) management indicate that while landfilling is often perceived as the least effortful and therefore the least costly option, it performs poorly when compared to waste recovery and recycling strategies, as shown in Table 3.1. Economic assessments show that recycling and material recovery can yield substantially higher net benefits than landfilling, underscoring the economic potential missed by current disposal practices in Türkiye (Kanat, 2010).

Next to immediate environmental and economic impacts, continued reliance on landfilling also poses structural limitations for future waste management. Recycling C&D waste generally requires significantly less energy than producing construction materials from virgin resources and reduces the need for raw material extraction. Furthermore, their additional advantages are that environmental damages are decreased, resulting in a reduction of pollution and protecting existing waste dumpsites (Ustaoğlu and Limoncu, 2021).

Moreover, the option of landfilling is becoming increasingly constrained, particularly in metropolitan regions such as Istanbul. Rapid urbanisation and strict siting regulations limit the availability of suitable landfill locations, which are typically situated far from the urban core. This increases transportation distances and associated costs, placing further pressure on already limited disposal infrastructure (Kanat, 2010). Maximising reuse and recycling therefore not only reduces energy, water, and raw material consumption, but also mitigates pollution and extends the operational lifespan of existing landfill sites (Ustaoğlu & Limoncu, 2021). In this context, strengthening recycling systems becomes a necessary precondition for managing the material flows associated with large-scale urban transformation and seismic retrofitting.

Currently two different approaches of handling C&D waste are illustrated in Figure 3.11 the current and most preferred way of handling C&D waste in Türkiye is predominantly linear, with large volumes of material directed toward landfilling despite their potential for reuse. This approach not only contributes to environmental degradation but also overlooks the embedded material value of demolished structures. In contrast, emerging strategies advocate for the transformation of C&D waste into secondary construction materials through mechanical processing techniques such as crushing and grading, creating a more material flow which is in this case not only beneficial for the environment, but also serves the additional structural purpose of implementing the recycled materials as seismic strengthening elements.

Table 3.1: Estimated costs of MSW disposal alternatives, adapted from Kanat, 2010.

Technology	***Net profit or [cost] (in US$/ton)***
Recovery and recycling	*2,19*
Landfilling	*[8,50]*
Composting	*[10,49]*
Incineration	*[80,97]*

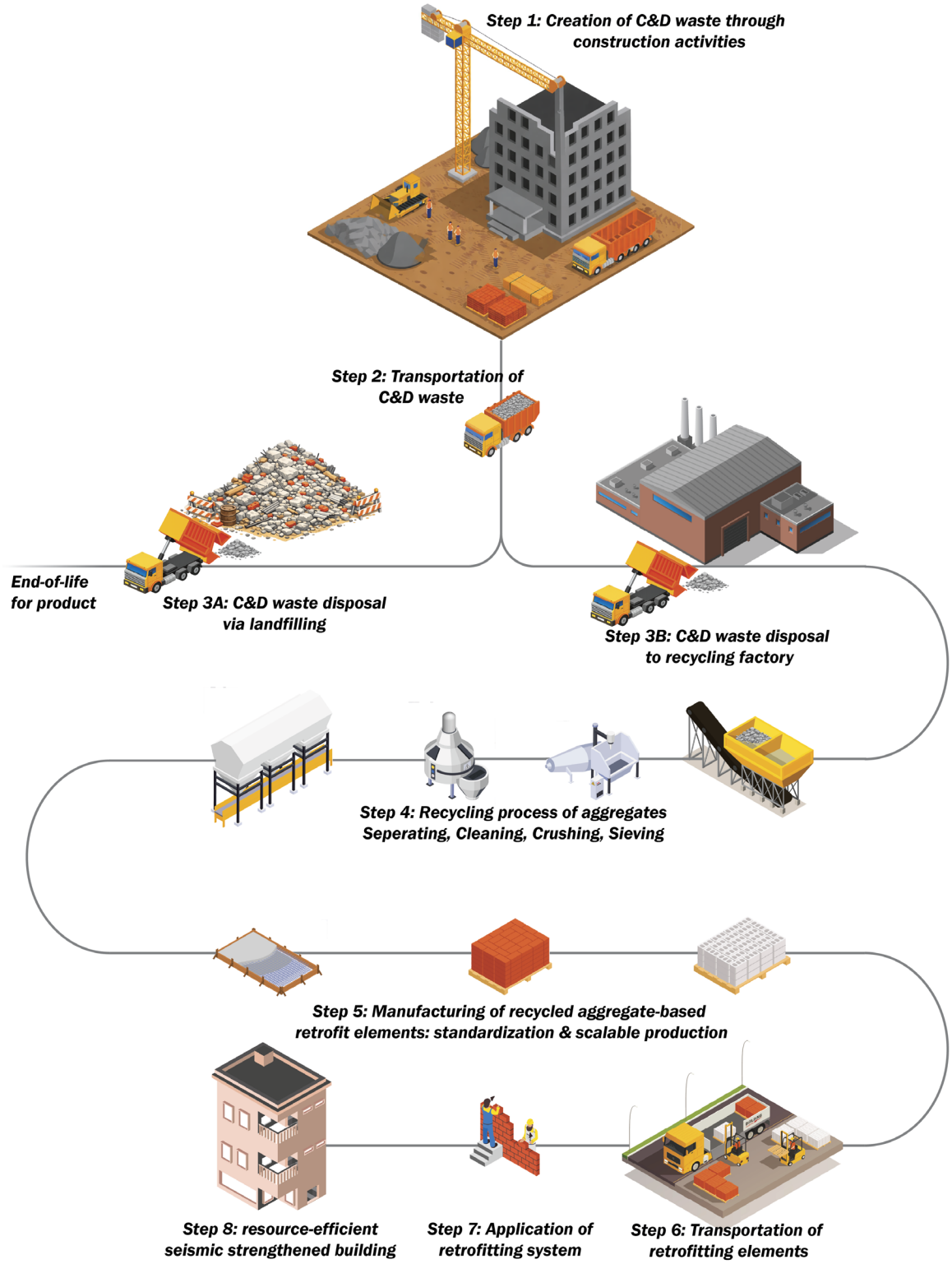

Figure 3.11: The two possible pathways for construction and demolition waste showing a linear (left) and a circular-oriented (right) material process (images generated with assistance of AI).

C&D waste recycling plant considerations

As landfilling becomes increasingly constrained both environmentally, economically and spatially, the development of dedicated recycling infrastructure emerges as a necessary alternative. In the context of large-scale urban transformation and seismic retrofitting, recycling facilities function as strategic nodes within a circular material system. Their configuration, capacity, and location directly influence the feasibility of material recovery and reuse.

Stationary vs. Mobile recycling plants

Construction and demolition waste can be processed in two main facility types, namely stationary and mobile plants. Stationary plants employ advanced sorting technologies and achieve processing capacities of 100-350 tonnes per hour. They produce more consistent and higher-quality recycled aggregates, making them particularly suitable for high-density urban regions where large waste volumes require controlled processing (Ulubeyli et al, 2017). Mobile plants, in contrast, process smaller quantities, generally up to 100 tonnes per hour, directly on or near demolition sites. While they reduce transport distances, they rely on simpler technologies, often produce lower-grade materials, and may generate dust and noise in residential areas (Ulubeyli et al, 2017). When waste volumes are insufficient for on-site processing, transfer stations can be used to sort and redirect materials to larger facilities. In addition to the type of recycling plant, recycling facilities require an evaluation of economic, environmental, locational, and administrative conditions to ensure successful operation.

Environmental considerations

From an environmental perspective, recycling plants primarily generate impacts related to noise and dust, while producing relatively few other direct emissions. Life-cycle assessments indicate that C&D waste recycling avoids three to sixteen times more environmental impact than it generates (Ulubeyli et al, 2017). Transportation is the dominant contributor, accounting for approximately 44% of total primary energy consumption (Coelho and de Brito, 2013). Overall, environmental benefits outweigh operational impacts, provided that transport distances remain limited.

Economical considerations

Recycling facilities require substantial initial investments, ranging from approximately €250,000 for a 20 t/h mobile plant to €800,000 for a 100 t/h installation (Ulubeyli et al, 2017). Although stationary plants incur higher capital costs, they benefit from economies of scale and lower unit recycling costs, driven by improved productivity and material quality. The economic feasibility of C&D waste recycling is highly context-dependent. Following the European Union's target of achieving 70% (by weight) reuse, recycling, and recovery of non-hazardous C&D waste by 2020 (European Parliament & Council of the European Union, 2008), several Member States were already approaching or exceeding this benchmark. In some countries, recycling rates of 80–90% have been achieved through a combination of policy instruments, including mandatory source separation, landfill taxation, elevated costs for primary construction materials, and financial incentives promoting recycled-content products (Ulubeyli et al, 2017). These examples demonstrate that recycling systems become economically competitive primarily when regulatory and market frameworks internalise environmental externalities and discourage reliance on virgin material extraction. Table 3.2 on the following page presents the C&D waste recycling rates across selected European Union countries.

Locational considerations

A nominal C&D waste recycling facility with an input of 350 t/h requires approximately 40.000 m² of land, preferably of low environmental value such as brownfields, former landfills, or exhausted quarries Ulubeyli et al. (2017). These locations minimise disturbance and reduce disposal and transport costs for non-recyclable residues. Facilities are therefore commonly situated outside urban centres but near major transport routes. Ulubeyli et al. (2017) state that at a regional scale, optimal performance is achieved when plants operate within a 15–50 km radius, limiting transport impacts and supporting balanced market distribution. Due to multiple sorting and transfer steps, C&D waste systems are most effective when organised regionally rather than through a single centralised facility (Ulubeyli et al., 2017).

Administrational considerations

In most countries, recycling facilities are operated by private companies, often originating from construction or excavation sectors. Public involvement is generally limited, though alternative models such as public–private partnerships and outsourced tendering exist. In Türkiye, only a small number of facilities are municipally operated, underscoring the dominant role of private initiative in the current C&D waste recycling system (Ulubeyli et al., 2017).

Table 3.2: Total- and material related recycling percentages per country in percentage (adapted from Ulubeyli, et al., 2017)

Country (recycling of C&D waste in 2005-2006)	***Percentage recycled per C&D waste category***					***Total recycling of C&D waste (in %)***
	Concrete, bricks and tiles	***Asphalt***	***Wood, glass, metals, plastics, gypsum***	***Dredging soil, soil and track ballast***	***Other mineral and C&D waste***	
Netherlands	22,1	0,0	0,0	0,0	74,0	98,1
Denmark	29,0	17,0	1,6	39,0	0,0	94,9
Estonia	10,1	3,7	21,0	54,0	0,0	91,9
Germany	19,6	12,0	0,1	71,0	20,0	86,3
Ireland	0,0	0,0	0,0	60,0	14,0	79,5
Belgium	[n/a]	[n/a]	[n/a]	[n/a]	[n/a]	67,5
United Kingdom	[n/a]	[n/a]	[n/a]	[n/a]	[n/a]	64,8
France	0,0	0,0	0,0	0,0	99,0	62,3
Norway	79,3	0,0	14,0	0,0	4,3	61,0
Lithuania	[n/a]	[n/a]	[n/a]	[n/a]	[n/a]	59,7
Austria	26,0	25,0	0,0	6,2	44,0	59,5
Latvia	[n/a]	[n/a]	[n/a]	[n/a]	[n/a]	45,8
Poland	0,6	0,0	93,0	5,2	0,1	28,3
Finland	[n/a]	[n/a]	[n/a]	[n/a]	[n/a]	26,3
Czech Republic	14,3	0,0	0,1	0,0	0,0	23,0

3.3: Material properties of recycled concrete and brick aggregates

The inherent material properties and post-processing procedures of recycled aggregates derived from construction and demolition debris significantly impact their performance. Recycled concrete and brick aggregates exhibit adherent mortar, greater porosity, higher water absorption, and more variable mechanical behaviour than natural aggregates. Workability, strength development, durability, and the dependability of structural applications are all directly impacted by these characteristics. Therefore, evaluating the applicability of recycled aggregates in the manufacturing of retrofit products requires an understanding of both their inherent constraints and potential enhancement options. To improve aggregate performance and consistency, this section examines key material and mechanical features, as well as treatment methods.

3.3.1: Material properties of recycled aggregates

Recycled concrete aggregates (RCA) and recycled brick aggregates (RBA) can be classified into coarse and fine aggregates. Compared to natural aggregates, recycled aggregates exhibit distinct material characteristics that must be considered during recycling and the structural design of new retrofitting elements. The following section therefore outlines the key material properties of RCA and later RBA. It is important to note that the properties of recycled aggregates depend heavily on their source and age. The original composition, strength, and degradation state of the parent concrete or masonry significantly influence aggregate quality (Youssef, 2025; Sivamani et al., 2021). For instance, Youssef (2025) demonstrates that the performance of recycled brick aggregates varies according to aggregate type, particle size (fine or coarse), and the percentage of natural aggregate replacement.

Shape and surface texture of RCA

When concrete elements are crushed to produce RCA, the resulting particles are generally more angular and irregular compared to natural aggregates (Ulubeyli et al., 2018). This is primarily due to the presence of adhered old mortar on the aggregate surface. Studies indicate that approximately 30 to 60% of the RCA particle surface may consist of residual cement paste (Makul et al, 2021). The presence of this attached mortar results in a rougher and more porous surface texture. Consequently, RCA exhibits higher water absorption than natural coarse aggregates. Furthermore, smaller particle sizes typically contain a higher percentage of adhered mortar, which further increases porosity and absorption capacity.

Density and porosity

RCA generally exhibits lower density than natural aggregates due to the adhered mortar and increased internal air void content. While conventional concrete has a typical density of approximately 2330-2400 kg/m^3, mixtures incorporating RCA exhibit lower unit weights, having a reduction of 3.6% to around 2250 kg/m^3 depending on the replacement level (Alkhteeb & Dawood, 2025; Rahal, 2007). Concrete produced with 100% RCA replacement demonstrated density reductions of up to 6.3% (Alkhteeb and Dawood, 2025). Porosity typically increases with higher RCA replacement ratios. However, a study from Alkhteeb and Dawood (2025) report a slight reduction in overall porosity at low replacement levels (around 20%), potentially due to improved particle packing or internal curing effects. Overall, depending on the strength grade and mix design, porosity in RCA concrete can be 10–30% higher than in concrete made with natural aggregates (Alkhteeb and Dawood, 2025). These high variations in porosity results can be attributed to:

- Differences in RCA source quality (amount of adherent mortar and microcracks and original parent concrete;
- Influence of strength class and water-to-cement ratio;
- Internal curing effects at low replacement levels;
- Curing conditions and moisture management practices.

Another interesting study conducted by Qasim et al. (2024) shows the almost linear decrease in bulk density of the concrete in relation to an increasing amount of recycled coarse concrete aggregates. For this study, a 100% replacement rate even led to a 9,5% reduction in bulk density. Results of this study are shown in Figure 3.12 below.

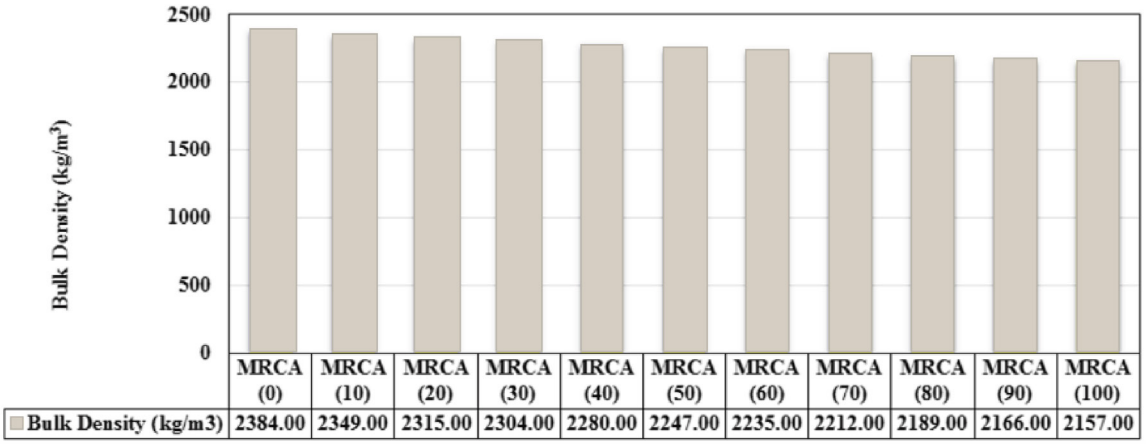

Figure 3.12: The researched bulk density of RCA consisting of different replacement rates (adapted from Qasim, et al., 2024).

Water absorption

Natural aggregates typically exhibit low water absorption values, approximately 0.9% (Alkhteeb and Dawood, 2025) . In contrast, recycled concrete aggregates exhibit significantly higher absorption rates, typically ranging from 4.7-6.4% (Ding et al., 2023).

This substantial increase is primarily attributed to the presence of adhered mortar on the RCA surface. The old cement paste is inherently more porous than natural aggregates and contains microcracks and tiny pores generated during the crushing process. These characteristics increase the particles' internal void structure and surface area, thereby increasing absorption rates.

High water absorption directly affects concrete mix design. If RCA is not pre-saturated or moisture-corrected, it may absorb part of the mixing water, effectively reducing the available water for cement hydration (García-González et al, 2014). This can lower workability and alter the effective water-to-cement ratio. In controlled conditions, however, the absorptive nature of RCA may contribute to internal curing effects, potentially improving long-term hydration (Marchi et al, 2023).

Workability and air content

Due to differences in particle shape, surface roughness, density, and absorption characteristics, the incorporation of RCA significantly affects the properties of fresh concrete. Concretes containing recycled aggregates generally exhibit reduced workability compared to conventional concrete. For mixtures targeting the same slump value, recycled aggregate concrete typically requires approximately 7% more water (Qasim et al., 2024). This increased demand is mainly caused by:

- Rougher and more angular particle surfaces;
- Higher specific surface area;
- Increased water absorption rates.

The rough surface texture increases particle-to-particle friction, reducing flowability. A study by Qasim et al. (2024) shows a relationship between an increasing percentage of recycled aggregate and a decrease in concrete workability, as shown in Figure 3.13. Simultaneously, water absorption by the adhered mortar decreases the amount of free water available for lubrication within the mix. Increasing water content can improve workability; however, it negatively affects mechanical performance. Abdelfatah et al. (2011) reported that excessive water addition may reduce compressive strength by 10 to 30%. Alternatively, workability can be maintained by using superplasticisers, allowing the water-to-cement ratio to remain constant while improving flow characteristics.

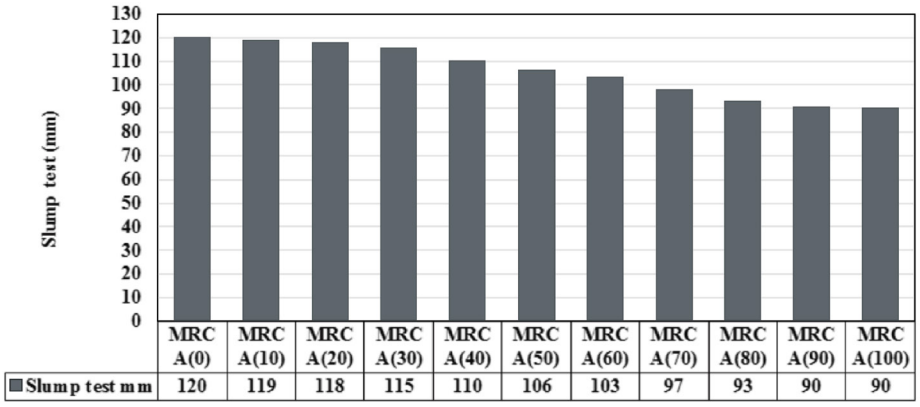

Figure 3.13: The research flowability of RCA with different replacement rates (Adapted from Qasim et al., 2024)

Recycled brick aggregates

Also derived from construction and demolition waste, brick aggregates can also be used as coarse or fine aggregates in concrete. Although fewer studies have been conducted on RBA than on RCA, similar trends in material behaviour are observed. Concrete incorporating crushed brick aggregates generally exhibits:

- Lower density;
- Higher water absorption;
- Increased porosity.

Janković et al. (2010) reported that concrete density decreased with increasing recycled brick aggregate content, ranging approximately from 2008 to 2254 kg/m^3. This reduction is directly related to the highly porous nature of clay-fired bricks

Water absorption increases proportionally with higher brick aggregate replacement levels, reflecting the intrinsic porosity of ceramic materials. Compared to natural aggregate concrete, mixtures containing RBA show significantly higher absorption values. Similar to RCA, crushed brick aggregates also display angular particle shapes and rough surface textures. However, due to the inherently higher porosity of brick compared to concrete, the magnitude of absorption and density reduction is generally greater for RBA than for RCA.

Overall, while both RCA and RBA exhibit comparable qualitative trends (lower density, higher porosity, increased absorption), brick aggregates typically demonstrate more pronounced effects due to their ceramic microstructure. Although recycled aggregates introduce higher porosity and absorption, controlled mix design and precast production methods can mitigate these drawbacks, enabling their application in structurally reliable retrofit components.

3.4: Mechanical properties of recycled aggregates

The structural feasibility of recycled aggregate-based retrofit components depends fundamentally on their mechanical performance. While recycled concrete and brick aggregates offer significant environmental advantages, their incorporation into new concrete affects key strength and stiffness parameters critical to structural applications. Across the literature, the mechanical behaviour of recycled aggregate concrete is shown to be highly dependent on aggregate source, processing quality, particle size distribution, and replacement ratio. As a result, reported performance outcomes vary considerably.

While various studies have been conducted, it is difficult to reach a precise conclusion about the mechanical properties of recycled aggregates. First and foremost, this depends on factors such as the recycled aggregate source, the recycled aggregate mix design in the new concrete, and aggregate size, all of which have specific influences on the mechanical properties. Therefore, this section dives into the general trend of the research conducted.

3.4.1: Recycled concrete aggregates

Across the literature , concrete with recycled concrete aggregates generally shows reduced mechanical performance compared to natural aggregate concrete. However, the magnitude of the reduction heavily depends on the replacement ratio and aggregate quality. Various studies have tested mechanical properties, including compressive strength, splitting tensile strength, flexural strength, and modulus of elasticity.

Compressive strength: The compressive strength of recycled aggregate concrete shows that with an increasing RCA content, the compressive strength decreases;

Splitting tensile strength: The splitting tensile strength decreases more noticeable than the compressive strength with an increase in RCA content;
Flexural strength: Only showed a more negligible effect of recycled aggregates on the flexural strength of the concrete;

Modulus of elasticity: shows the most pronounced reduction since the rate of reduction increases with higher aggregate replacement ratios;

Effect of replacement ratios of RCA
Experimental studies from Alkhteeb & Dawood (2025) have shown that using a systematic replacement ratio shows that the general trend:
Up to 20-30% replacement shows minor reductions in the strength characteristics of the new concrete;
Between 30-50% the strength characteristics become more moderate;
At a 100% replacement ratio the mechanical strength of the concrete shows more significant strength reductions, with a reduction of 15-20% in compressive strength and even a 16% reduction of the modulus of elasticity;

Despite these reductions, studies still conclude that the concrete's strength remains within acceptable limits for numerous construction applications, with some noting lower-class applications such as concrete piping or pavement use, while others conclude it is usable for structural applications (Alkhteeb & Dawood, 2025).

Coarse RCA vs fine RCA

A key finding is that, compared to coarse RCA, fine RCA has a greater effect on weakening concrete's mechanical properties (Alkhteeb & Dawood, 2025). This can be explained by the fact that fine RCA contains a higher proportion of adhered old mortar; it shows higher porosity and therefore greater water absorption. This adherence of cementitious substances influences interlocking strength, surface roughness, and the adhesion of recycled concrete to aggregate in new concrete mixtures (Qasim et al., 2024).

3.4.2: Recycled brick aggregates

As for recycled concrete aggregates, the performance of concrete made with recycled brick aggregates depends heavily on the source and size of the aggregates, as well as the processing steps used to recycle them.

A study from Youssef (2025) reported that partial substitution of coarse natural aggregate with recycled brick aggregate at levels of 10–25% yields acceptable mechanical performance. However, due to the inherently high porosity of brick, higher proportions of coarse RBA generally result in reductions in strength. In contrast, when recycled brick is used as a fine aggregate, mechanical performance can improve. This enhancement is attributed to the pozzolanic activity of fine ceramic particles, which promotes densification of the cement matrix and the ITZ. The resulting microstructural refinement contributes to improved long-term strength development (Youssef, 2025). Optimal performance was observed at approximately 50% replacement of natural sand with crushed brick fines, resulting in increases of 23%, 28%, and 19% in compressive, tensile, and flexural strength, respectively (Aboalella & Elmalky, 2023). At full (100%) replacement, however, strength gains became marginal, indicating that the beneficial pozzolanic effects diminish at excessive replacement levels.

However, an interesting conclusion by Aboalella and Elmalky (2023) is that the best overall performance was achieved when both substitutions were combined in a 50% crushed brick-50% crushed recycled concrete mix as fine and coarse aggregates, respectively. These results show a synergistic effect: the mix demonstrated 32% increases in compressive and tensile strengths, and 26% in flexural strength. This synergistic effect therefore utilised both positive properties of both recycled materials. Since rough RCA surfaces improve mechanical interlocking of particles and adhesion within the material matrix, they contribute to higher compressive strength and better stress transfer. The fine brick particles enhance the ITZ through the pozzolanic reactivity of the bricks, which results in enhanced adhesion (Diosa-Arenas et al., 2026; Aboalella and Elmalky, 2023). Therefore, relatively large amounts of recycled input material can be used without negatively affecting concrete properties, unlike when the replacement ratio of coarse or fine aggregates becomes too high. Another study conducted by Youssef (2025) showed that a combined coarse brick and fine ceramic (such as tiles) aggregate mix (75% coarse and 50% fine) shows a superior performance compared to the control mixes.

Summary

Rather than being inherently inferior to conventional concrete, recycled aggregates should be strategically used to maintain mechanical properties as effectively as possible. Clear trends emerge when distinguishing between recycled concrete aggregates (RCA) and recycled brick aggregates (RBA), as well as between coarse and fine fractions. These trends are shown in Table 3.3, which presents the mechanical properties of concrete made with recycled aggregates for the different aggregate materials, replacement rates and water to cement ratios.

Coarse RCA generally results in moderate reductions in compressive, tensile, and elastic modulus, particularly at higher replacement ratios, whereas partial replacement levels (typically 20–30%) tend to produce only limited reductions. In contrast, fine RCA has a more detrimental influence due to its higher porosity, greater water absorption, and weaker interfacial transition zones. Nevertheless, when sourced from high-quality parent concrete and combined with controlled mix design strategies, coarse RCA can achieve mechanical properties suitable for a range of structural and semi-structural applications.

Recycled brick aggregates exhibit greater variability in performance. As a coarse aggregate, RBA generally reduces strength due to its porous, brittle ceramic structure. However, when used as a fine aggregate at controlled replacement ratios, recycled brick fines can enhance mechanical performance through pozzolanic activity and microstructural densification of the cement matrix. Recent studies further highlight the potential of hybrid systems combining coarse RCA with fine RBA, where synergistic effects allow higher recycled content without compromising mechanical performance. The mechanical performance of structural elements incorporating recycled aggregates is significantly affected by the type of material and its replacement rate. These differences result in varying effects on strength, stiffness, and workability, which must be carefully balanced in structural applications to leverage the advantages of different materials, as shown in Figure 3.14.

Despite these promising findings, the widespread adoption of recycled aggregates remains constrained by two major barriers. First, much of the existing research lacks rigorous statistical validation, relying primarily on descriptive or comparative analyses. This limits the reliability and generalisability of results, making it difficult to establish design parameters, optimal replacement ratios, or confidence intervals for engineering applications. Second, current building codes remain highly conservative, restricting allowable replacement levels and largely excluding fine recycled aggregates and recycled brick or ceramic materials from structural use. This regulatory gap underscores the need for comprehensive, statistically validated performance data to inform future design guidelines and enable broader utilisation of construction and demolition waste in engineered applications (Youssef, 2025). This variability and limited statistical validation further justify the development of typology-based parametric frameworks that incorporate material uncertainty ranges in structural performance assessment.

Table 3.3: Summary table showing how different recycled aggregates (concrete and brick, fine and coarse) influence strength properties of concrete at varying replacement levels

Source	Researched aggregate	Replacement rates	Compressive strength [f_c] change (at 28 days)	Splitting tensile strength [f_s] change	Flexural strength change	Mix ratio (c:f_a:c_a) Of control mix	Water to cement ratio (w/c) of control mix
Qasim et al. (2024)	Coarse concrete aggregate	10% 20% 30% 40% 50% 60% 70% 80% 90% 100%	↓ 1,0% ↓ 1,9% ↓ 3,8% ↓ 6,3% ↓ 10,8% ↓ 13,0% ↓ 14,9% ↓ 16,8% ↓ 18,1% ↓ 19,4%	↓ 2,3% ↓ 3,9% ↓ 5,8% ↓ 8,3% ↓ 11,1% ↓ 13,2% ↓ 15,0% ↓ 17,5% ↓ 18,8% ↓ 19,6%	↓ 2,3% ↓ 4,0% ↓ 5,9% ↓ 8,4% ↓ 11,2% ↓ 12,8% ↓ 14,7% ↓ 16,2% ↓ 17,3% ↓ 18,3%	1 : 1,17 : 1,77	0,4
Aboalella & Elmalky (2023)	Coarse concrete aggregate	10% 50% 100%	↑ 13,0% ↑ 30,0% ↑ 3,0%	↑ 14,3% ↑ 28,7% ↑ 23,0%	↑ 5,0% ↑ 25,0% ↑ 16,7%	1 : 1,56 : 3,12	0,45
Ju et al. (2019)	Fine concrete aggregate	15% 30% 50% 100%	↓ 8,1% ↓ 21,7% ↓ 25,2% ↓ 28,6%	↓ 17,9% ↓ 5,1% ↓ 10,3% ↓ 12,8%	[-]	1 : 3,0 : 3,33	0,60
Hakim, et al. (2022)	Coarse brick aggregate	25% 50% 75% 100%	↓ 16,8% ↓ 48,7% ↓ 56,7% ↓ 63,1%	[-]	↓ 17,0% ↓ 22,0% ↓ 27,5% ↓ 37,5%	1 : 2,1 : 4,1	0,55
Youssef (2025)	Coarse brick aggregate	10% 20% 30% 40% 50%	↓ 7,4% ↓ 14,8% ↓ 20,4% ↓ 25,9% ↓ 31,1%	↓ 21,9% ↓ 40,5% ↓ 38,1% ↓ 60,5% ↓ 67,1%	[-]	1 : 2 : 3	0,50
Youssef (2025)	Fine brick aggregate	10% 20% 30% 40% 50%	↑ 17,4% ↑ 33,3% ↑ 28,1% ↑ 3,7% ↓ 20,7%	↓ 5,7% ↓ 8,6% ↓ 6,7% ↓ 11,4% ↓ 16,2%	[-]	1 : 2 : 3	0,50
Aboalella & Elmalky (2023)	Fine brick aggregate	10% 50% 100%	↑ 15,0% ↑ 24,0% ↑ 3,0%	↑ 14,5% ↑ 28,5% ↑ 20,0%	↑ 3,4% ↑ 16,7% ↑ 13,4%	1 : 1,56 : 3,12	0,45
Aboalella & Elmalky (2023)	Hybrid combination	50% of f_a / 50% of c_a	↑ 33,3%	↑ 34,5%	↑ 30,0%	1 : 1,56 : 3,12	0,45

c = cement, f_a = fine aggregates, c_a = coarse aggregates, w = water

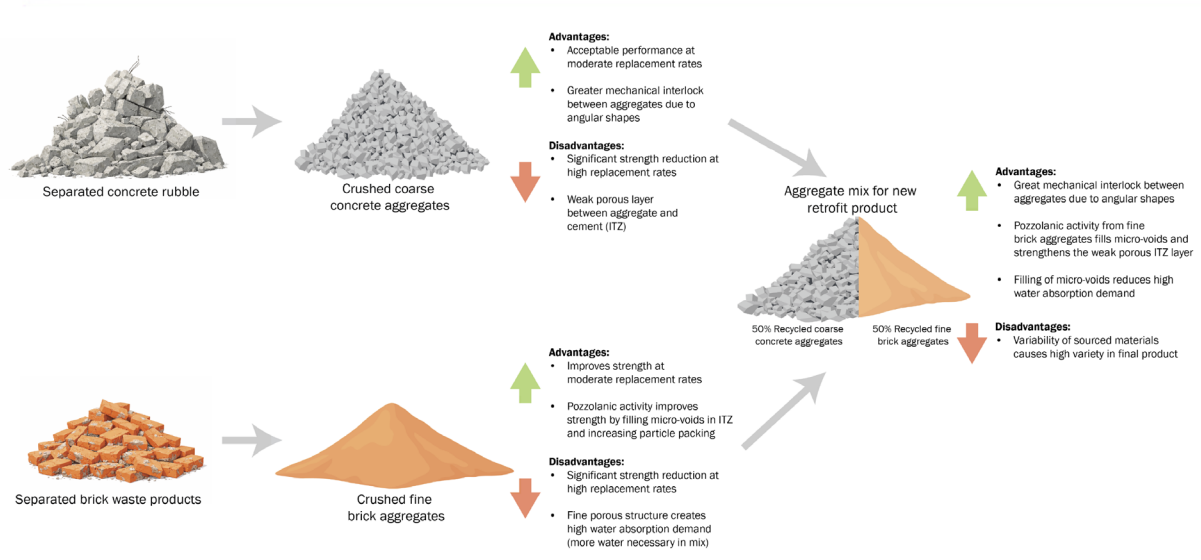

Figure 3.14: Advantages and disadvantages of RCA and RBA and the benefits of a 50–50% combination (images generated with assistance of AI).

3.5: Disadvantages and factors influencing aggregate properties

Although recycled aggregates (RA) provide clear environmental benefits, their structural applicability is limited by intrinsic material deficiencies. The principal drawback is the presence of adhered mortar, which remains attached after crushing and introduces a porous, heterogeneous phase around the aggregate particles. This results in higher water absorption, lower density, and a weaker and more permeable interfacial transition zone (Youssef, 2025) compared to natural aggregates. Additionally, the properties of RA vary significantly depending on the parent material's origin, original strength class, age, and processing method, resulting in considerable variability in mechanical performance.

To address these limitations, this research is focused on improving aggregate quality through mortar removal or surface modification techniques. Mechanical, thermal, and chemical treatments aim to partially remove the adhered mortar, while carbonation, slurry impregnation, polymer treatment, and optimised mixing methods seek to densify and strengthen the existing mortar layer. These approaches aim to reduce porosity, enhance quality, and improve the overall mechanical reliability of recycled aggregates.

3.5.1: The negative side of recycled aggregates

When particles such as concrete, brick, and tile rubble are crushed, it is still apparent that mortar or cement adheres to the aggregates. This adherent mortar significantly influences many of the recycled aggregates' material properties, which are deemed negative for their mechanical properties. This is mainly due to the mortar's porous structure (Alkhteeb & Dawood, 2025). This adherent mortar results in 2 to 3 times higher water absorption than natural aggregates (Sivamani et al., 2021), leading to lower workability and affecting the durability properties of the RCA. Secondly, the mortar's porosity means that it has a lot of air pockets which reduces the density and weakens the Interfacial Transition zone quality, since the ITZ becomes less dense and has a weaker bond with the new mortar paste due to the less hydration since the porous structure of the mortar reduces the available water for this hydration process which gives strength to the concrete (Youssef, 2025). The comparison of the interfacial transition zones of a natural coarse aggregate and a recycled coarse aggregate is shown in Figure 3.15 below.

Lastly, recycled aggregates can come from various sources, such as bricks and/or concrete. These demolished materials all have different ages, strength grades, aggregate types and sizes (Sivamani et al., 2021). This leads to significant variation in the strength of recycled aggregates, making it difficult to provide robust statistical validation and establish reliable design parameters (Youssef, 2025).

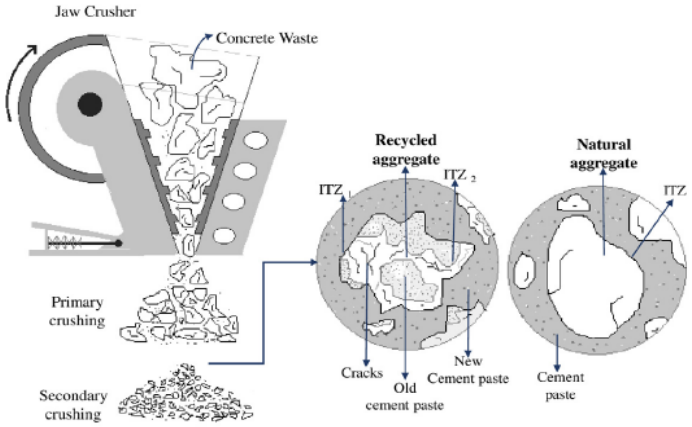

FIGURE 1. Diagram of the transformation process and RCA characteristics.

Figure 3.15: The production of RCA and the characteristics of natural and recycled aggregates (Gómez-Cano et al., 2023)

Since the adherent mortar has several negative influences on the material and mechanical properties of the RCA's, it can be stated that this mortar is a sort of contaminant to the aggregates. That is why, to reduce the negative influence of the adherent mortar, additional decontamination methods are used to clean or separate the aggregates from the adherent mortar, thereby further enhancing the quality of the recycled aggregates. The methods used to treat RCA, for example, can be divided into two main categories: removal of adhered mortar or surface coating of adhered mortar. The methods in the different categories are mapped in Figure 3.16 below.

3.5.2: Mortar removal strategies

One of the primary strategies to improve RCA is the removal of adhered mortar, which can be achieved through mechanical, chemical, thermal, or combined treatment methods. In addition to mortar removal, surface coating or densification of the existing mortar layer is also applied as an alternative improvement approach. For this research, selected methods are examined in greater depth to assess their working principles and feasibility within a C&D waste recycling process in Türkiye. The relevant aggregate upgrading methods investigated during this research are shown in the grey boxes in Figure 3.16 below, however the ones deemed interesting for application are discussed on the following pages.

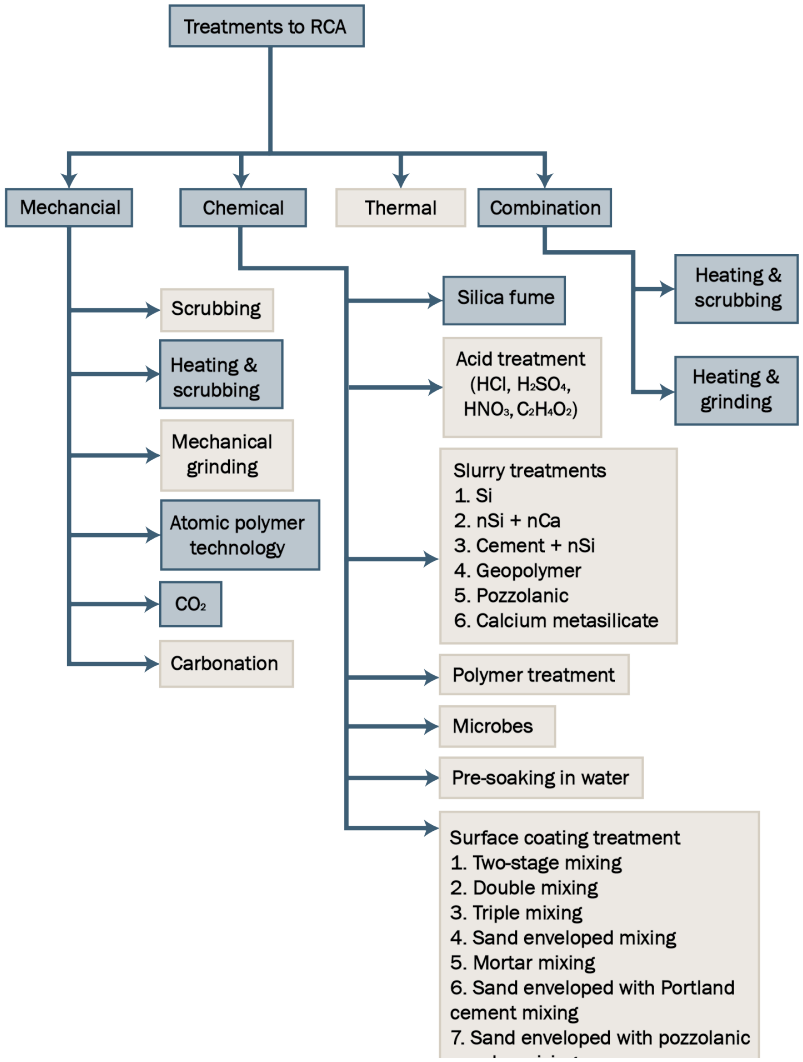

Figure 3.16: The different RCA upcycling methods (image adapted from Sivamani et al., 2021)

3.5.3: Mechanical treatment of RCA

Mechanical grinding & scrubbing

Grinding and scrubbing can help improve RCA quality by removing loose cement particles (as illustrated in Figure 3.17). Scrubbing or abrasion techniques help to reduce the abrasion value by 33%, making the aggregates more durable. Furthermore, the strength improved by 32% compared to untreated RCA (URCA) and was only 5% lower than that of natural concrete aggregates (Sivamani et al., 2021). More aggressive grinding techniques, such as shaft-rotor or ball-milling systems, remove the adhered mortar more effectively. These methods are simple to apply and improve RCA's strength compared to untreated RCA, but they also induce surface microcracks, thereby reducing efficiency due to the resulting damage (Sivamani et al., 2021).

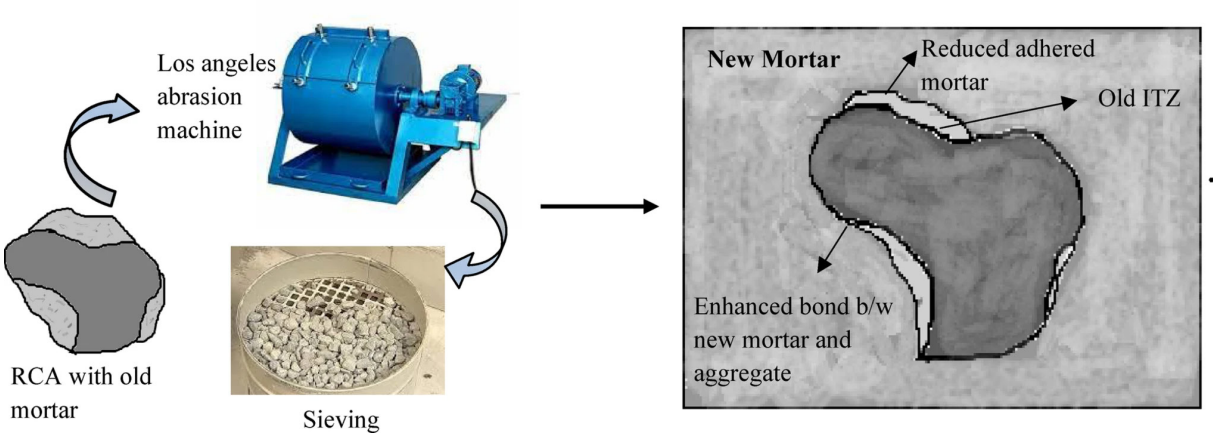

Figure 3.17: the illustrated concept of reducing adhered mortar through abrasion (Sivamani et al., 2021)

3.5.4: Chemical treatment of RCA

Pre-soaking in water

Pre-soaking is a pretreatment method in which recycled concrete aggregates are saturated with water before being mixed into concrete. This approach is relevant because recycled aggregates often contain adhered mortar and micro-cracks, which increase their water absorption compared to natural aggregates (Sivamani et al., 2021). By filling part of the aggregate pore structure before mixing, pre-soaking can reduce the uncontrolled absorption of mixing water from fresh concrete and help maintain a more stable effective water-cement ratio. As shown in Figure 3.18, the effectiveness of pre-wetting depends not only on the initial moisture content of the RCA, but also on its pre-wetting history. Khoury et al. (2017) show that long-term and short-term pre-wetting distribute water differently within the pore structure. Long-term wetting can fill less accessible pores, while short-term wetting mainly fills the easily accessible voids at the surface of the aggregate. This affects the subsequent water absorption of RCA during mixing and can influence the effective water content of recycled concrete.

Kępniak et al. (2025) showed that water immersion can improve the interfacial transition zone (ITZ) between recycled aggregate and new cement paste by supporting moisture release during hydration. In their study, concrete made with saturated recycled aggregate reached a 28-day compressive strength of approximately 49.1 MPa, which was very close to the natural aggregate reference concrete at 49.2 MPa. Its flexural strength was also similar, reaching approximately 5.8 MPa compared with 5.9 MPa for the reference concrete. Therefore, pre-soaking seems to be a practical treatment method to enhance mechanical performance of the recycled aggregates.

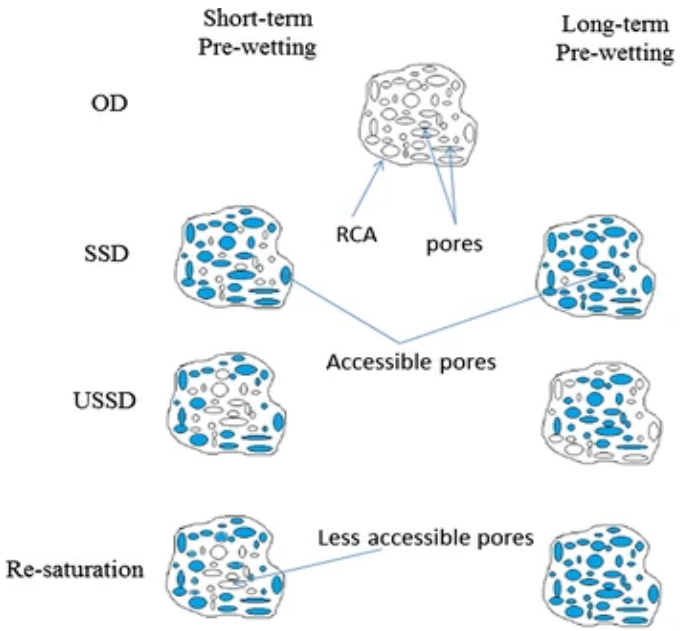

Figure 3.18: The effect between of short-term and long-term pre-wetting on accessibility to aggregate pores (Khoury, et al. 2017)

Surface coating of adhered mortar

A second method to improve recycled aggregate is to coat the adhered mortar. This is mainly done through the application of mixing techniques. This means that, in this case, the surface is coated during the concrete mixing process, whereas, for the mortar removal method, it was a separate treatment applied before concrete mixing (Sivamani et al., 2021). Surface coating of the mortar helps fill pores, gaps, and microcracks, creating a denser layer around the aggregates that strengthens the between the RCA and the new cement paste. Figure 3.19 shows various mixing techniques and pozzolanic materials (as a pre-treatment), such as fly ash, slag, silica fumes, or cement, that can be applied to improve aggregate quality. Due to their very fine particle size, these pozzolanic admixtures can penetrate the pores of the adhered mortar and react with CH to form additional C-S-H gel, which densifies the ITZ . When comparing this method to removing the old mortar, surface coating is generally simpler, more environmentally friendly, and more economical (Zheng et al., 2021). However, the properties of the improvement materials significantly affect RCA improvement. The different mixing methods that exists all have the same goal, by applying a pre-coating or pre-soaking in the mix and therefore creating additional stages in the mixing process rather than mixing all materials in one time, the RCA's pores open up, or are filled or enveloped with the corresponding filler material before being put in a final mix with the cement binder (Tam, et al., 2005).

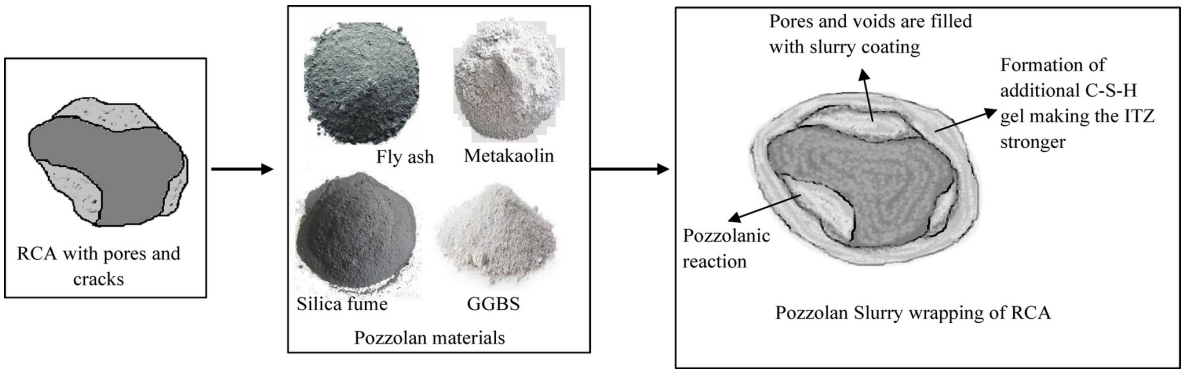

Figure 3.19: The effect of surface coating on the recycled aggregate (Sivamani et al., 2021)

3.6: System overview and design logic

Istanbul's construction and demolition waste stream presents both a logistical challenge as a material opportunity. According to Demir et al. (2017), the city generated approximately 7.0 million tonnes of pure C&D waste in 2016 alone. The largest fraction of this waste stream being masonry and concrete debris. Inert materials which are suitable for aggregate recovery. This section proposes a conceptual recycling framework that positions these waste streams as a quality-controlled supply base for seismic retrofit applications. Rather than treating C&D waste as a disposal problem, this framework demonstrates how local material recovery can unlock the path to a more resource-aware but still structurally safe retrofitting logic.

The recycling framework for the context of Istanbul is structured around three components:

- Incentivising mechanisms for improving incoming waste quality;
- The process flow logic that transforms mixed C&D waste into structurally reliable aggregate outputs;
- A following aggregate upgrading strategy that enhances the recycling outputs for use in retrofit concrete mixes.

Together, these components form the material supply-side logic of the broader retrofit framework developed in this thesis. Lastly, the goal of this supply line development is to design a recycling plant process that has a recycling capacity of 100 tonnes per hour. This aim is necessary in order to make it economically viable and to ensure a sufficient amount of supply.

3.6.1: Incentivising companies for C&D waste separation

The C&D waste recycling process is essential, as this type of waste contains a wide range of materials and contaminants. This makes recycling hard and complex. Therefore, it is proposed that the incoming C&D waste should already be pre-sorted before coming into the recycling plant; this is proposed for multiple reasons:

First of all, pre-sorting C&D waste before the recycling process can help improve aggregate quality and reduce the amount of contaminants down the line. Secondly, based on a survey by Arslan and Ulubeyli (2019), roughly 38,5% of the surveyed construction companies do not sort their generated C&D waste at all. This means that the largest fraction (61,5%) already applies some form of waste separation. Countries such as the Netherlands and Germany, with recycling rates of 80-90% for C&D waste, achieve these high numbers because the government provides incentives to increase the willingness to actively recycle C&D waste. According to Ulubeyli et al. (2017) these incentives, which are mostly formed by imposing certain taxes, which would be particularly effective for the process design in Istanbul, are:

1. Taxing landfilled recyclable materials as is done in Austria, Belgium, Czech Republic, Denmark, Spain, France, Ireland, Italy, the Netherlands, Slovenia, and the UK;
2. Taxing unsorted waste delivered to recycling plants by applying a higher gate fee;
3. Promoting introduction in the market perhaps by lowering taxes on construction products with a recycled content;
4. Subsidising the companies for disposing waste in the recycling centres.

The multitude of incentives, which have shown great success in other European countries, are therefore expected to improve, incentivise, and increase the amount and quality of C&D waste entering the recycling plant.

3.7: Recycling process design

Now that the incoming material strategy has been proposed, the recycling proces for C&D waste can be contextualized. In simple terms, the process consists of cleaning, crushing, and separating the incoming rubble to produce recycled aggregates with the best possible output quality. An image of the proposed recycling process is shown in Figure 3.20 and described below.

Step 0: Separation before entering the recycling plant

The quality of recycled aggregates depends directly on the quality of the incoming C&D waste. Therefore, contractors should be encouraged to deliver pre-sorted waste that falls below a defined contamination threshold. Although some waste separation is already practised in Türkiye, on-site sorting is still not standard, with 38.5% of the firms not sorting their construction waste at all (Arslan & Ulubeyli, 2019). Even when results from Poon et al (2001) indicate that at-source separation leads to better segregation of inert and non-inert waste, contractors are often reluctant to sort waste without financial incentives, as it is perceived as time-consuming and labour intensive, even when the environmental benefits are understood.

Since the quality of the recycled aggregates at the end of the process depend directly on the quality of the incoming C&D waste, a financial incentive mechanism is proposed. The construction and Demolition Diversion Deposit (CDDD) system offers a relevant model: a refundable deposit is charged when a demolition permit is issued and returned only when waste is delivered to an approved recycling facility and contamination levels remain below a defined threshold. This discourages landfilling and illegal dumping while improving the quality of the material entering the plant. A comparable system in San José, California, achieved a 75% diversion rate from landfilling (City of San José Environmental Services Department, n.d.) showing that financial incentives can support sorting behaviour even at a city-wide scale.

Step 1: Transportation of C&D waste to recycling plant

The recycling process begins with the delivery of pre-sorted C&D waste to the plant. To reduce contamination, machinery wear, and additional separation costs, the input stream is

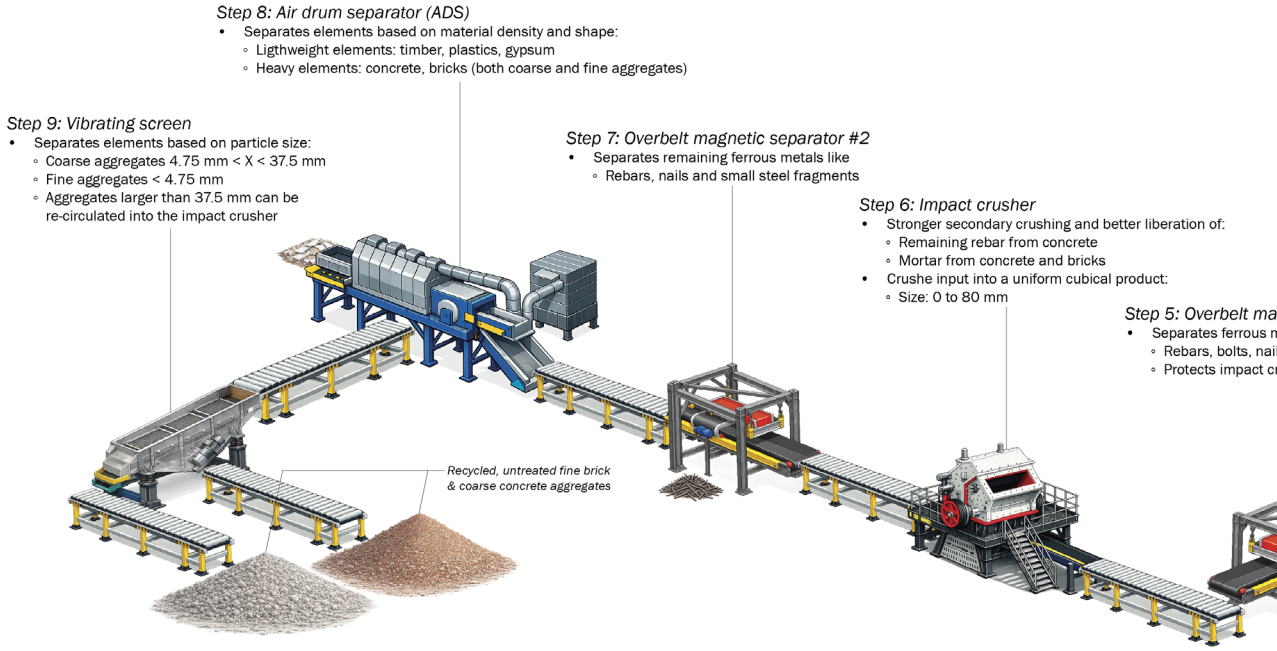

Figure 3.20: The set-up of the recycling process for construction and demolition waste into coarse concrete aggregates, and fine brick aggregates (images are created with the assistance of AI)

divided into two main batches: brick-dominated waste and concrete-dominated waste. This source separation is important because fine brick and concrete fractions are difficult to separate after crushing. Final visual separation can still be carried out before the C&D waste enters the recycling process. This can be done using equipment such as excavators, since concrete and brick elements can often be distinguished by colour.

Step 2: Grizzly feeder

The incoming C&D waste is fed into a grizzly feeder using an excavator. At this stage, the excavator operator also acts as a first line of defense by removing oversized elements, soil, visible contaminants and other unwanted materials that could damage downstream machinery. Additionally, the excavator can break pieces larger than 800 mm so that it fits in the feeder opening. The grizzly feeder stabilises the material input to approximately 100 tonnes per hour and removes smaller unwanted fractions, such as soil and loose residues. The selected feeder for the process is the FABO TBX-25, a heavy-duty grizzly feeder with a capacity of 100-250 t/h and a maximum feeding width of 800 mm (FABO, 2024a).

Step 3: Manual sorting station

After the grizzly feeder, the material passes through a manual sorting station. Although the waste has already been pre-sorted, it may still contain timber, aluminium, plastics, insulation, glass, packaging, or hazardous residues. This step functions as a final quality-control layer, protecting the aggregate quality and preventing damage or downtime in the machinery further in the process.

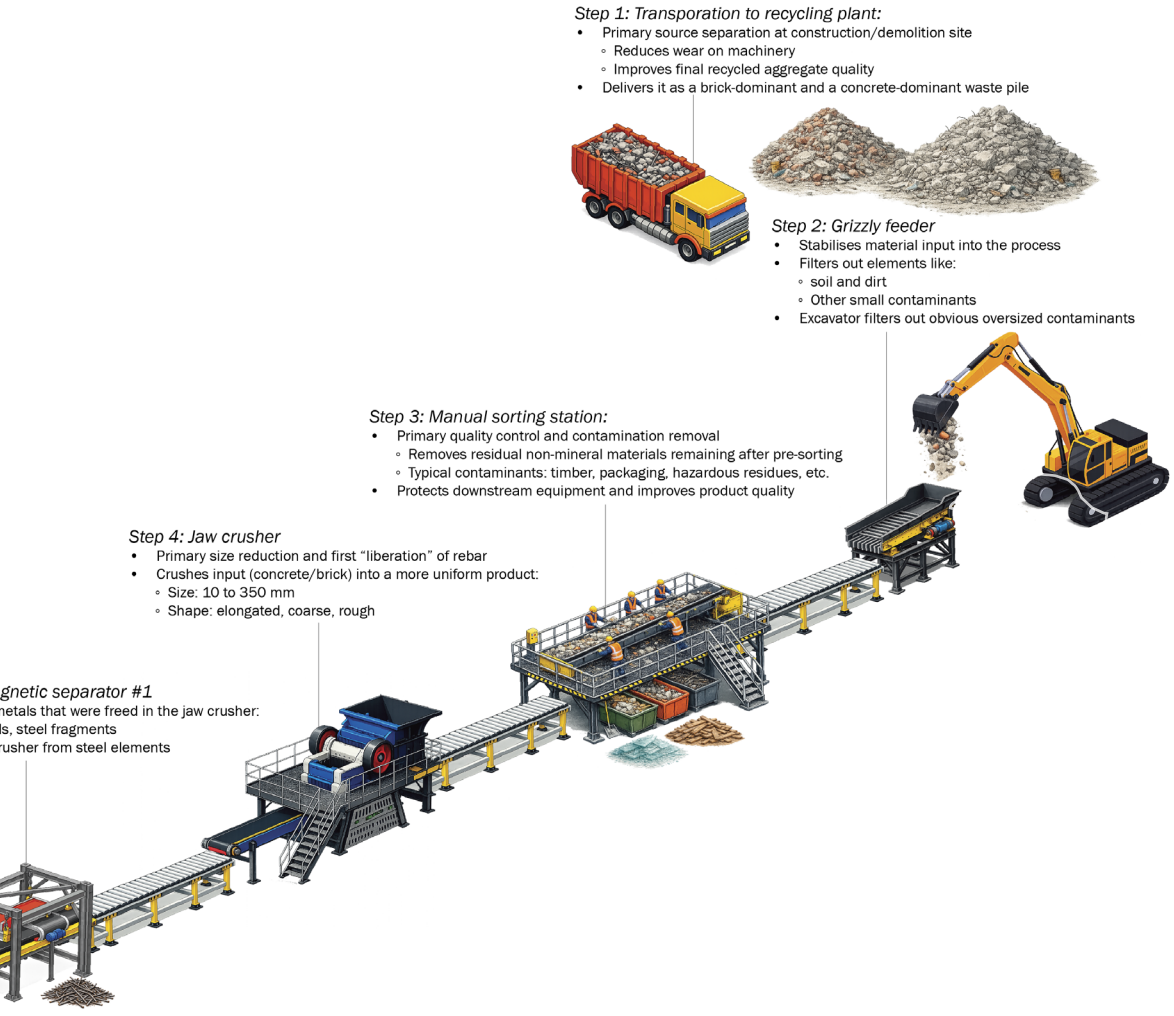

A join American-Canadian study on material recovery facilities provides benchmark manual sorting rates of approximately 0.4 tonnes per hour per sorter (Illinois Recycling Association, 2005). Since this stage is intended as quality control rather than full sorting, and because preliminary sorting has already taken place, an estimated 8 to 12 sorting employees are considered sufficient.

Step 4: Jaw crusher
The jaw crusher serves as the primary size-reduction station. It reduces large C&D fragments into coarse particles of approximately 10-350 mm and helps to liberate rebar and other metal fragments embedded in the concrete matrix. This is important since reinforced concrete waste is often contaminated with steel reinforcement, which therefore must be removed before further processing. The selected jaw crusher is the FABO CLK-60, chosen for its 600 by 400 mm feed opening and its capacity range of 60 to 120 t/h (FABO, n.d.-a).

Step 5: Overbelt magnetic separator #1
Since one of the main functions of the jaw crusher is to free the rebar and other metal fragments that are stuck in the matrix, the first magnetic separator functions to separate these metals from the main recycling elements. This overbelt magnetic separator separates the ferrous metals such as rebars, nails, bolts and other steel fragments. The overbelt magnetic separator is ideal because it is simple to install. In addition to its role in material recovery, the separator protects downstream equipment from mechanical damage caused by metals.

Step 6: Secondary impact crusher
The secondary crusher, namely the impact crusher, further reduces the 10-350 mm particles into more cubical and well-graded aggregates of approximately 0-80 mm. Oversized fractions can later be recirculated into the crusher after the screening proces. The impact action from the crusher additionally helps to remove remaining rebars and weak adherent mortar from brick and concrete particles, improving the quality of the recycled aggregates. The selected impact crusher is the FABO PDK-70, with a maximum feed size of 350 mm and a capacity of 70-100 t/h, matching the jaw crusher aggregate output size and the desired plant capacity (FABO, n.d.-b).

Step 7: Overbelt magnetic separator #2
The second magnetic separator separates the last remaining ferrous metals in the concrete elements. Therefore, it ensures that no ferrous metals are left in the waste matrix.

Table 3.4: The manual sorting speed (in kilogram per hours) for different MSW waste types (adapted from Illinois Recycling Association, 2005)

Waste material	***Manual sorting benchmark (kg/h/sorter)***
HDPE (natural)	*450*
HDPE (coloured)	*420*
HDPE (mixed)	*450*
PETE	*450*
Tubs (mixed plastics)	*200*
Glass (flint)	*600*
Glass (coloured)	*600*
Cardboard (OCC)	*400*
Boxboard (OBB)	*300*
Mixed waste paper (MWP)	*450*
Hardpack (OBB/OCC)	*350*

Step 8: Air drum separator (ADS)
The air drum separator is used to remove remaining lightweight contaminants from the aggregate stream. Using airflow and density-based separation, heavier brick and concrete particles remain in the main output stream, while lighter materials such as timber, plastics, insulation, and gypsum are separated. This stage is especially important because small non-ferrous contaminants may pass through manual sorting but still could reduce the quality of the final aggregate.

The selected system is the SFX 1200 air density separator, with a feeding width of 1200 mm and a processing capacity of approximately 120 m^3/h (Arcler Projects LLP, n.d.). Although the overall plant is designed for 100 t/h, the material flow decreases after crushing, magnetic separation, and manual sorting. Based on typical bulk densities of mixed C&D waste, the expected input to the air separator is approximately 65-85 m^3/h making the SFX 1200 sufficient for the required capacity and operational flexibility (Lu et al., 2021).

Step 9: Vibrating screen
The final step before aggregate upgrading is size classification. At this stage, the remaining stream consists mainly of inert brick or concrete aggregates, which must be separated into fine, coarse, and oversized fractions. Fine and coarse aggregates can be used for their intended applications, while the oversized particles are recirculated into the impact crusher to reach the desired size rang.

The selected screen is the FABO TE-1650 inclined vibrating screen, with three screen surfaces, a 1.6 by 5.0 metre screen area, and a capacity of 100-130 t/h. This allows the material to be classified into multiple size fractions through vibration and gravity-driven flow (FABO, n.d.-c).

3.7.1: Aggregate upgrading design

Since C&D waste is processed into coarse and fine recycled aggregates, the issue of reduced mechanical quality caused by adhered mortar remains important to address. Recycled aggregates often show higher porosity, higher water absorption, weaker interfacial transition zones, and greater variability depending on the parent material (Qasim, 2024; Youssef, 2025; Sivamani et al., 2021). Therefore, aggregate upgrading is included in the recycling process to reduce these weaknesses and create a more consistent material quality. Figure 3.21 below shows the additional equipment required for this aggregate upgrading stage.

Pre-saturation

For upgrading the recycled aggregates, this process focuses on two relatively simple strategies: pre-saturation and coating. These methods are selected since these methods are less complex and likely cheaper to implement than chemical or highly specialised treatments, while also being more widely studied than many advanced alternatives (Gómez-Cano et al., 2023)

Pre-saturation addresses the high water absorption of recycled aggregates. Because recycled aggregates are more porous, they tend to absorb part of the mixing water and reduce concrete workability (Ding et al., 2023). By pre-soaking the aggregates, the internal pores are partly filled with water, helping to stabilise the effective water-cement ratio of the mix. This may also support internal curing, as the absorbed water can be gradually released into the surrounding cement paste, promoting further hydration and densifying the ITZ. Marchi et al. (2023) show that the pre-saturated recycled aggregate concrete can achieve compressive strengths comparable to, and in some cases slightly higher than conventional mixes.

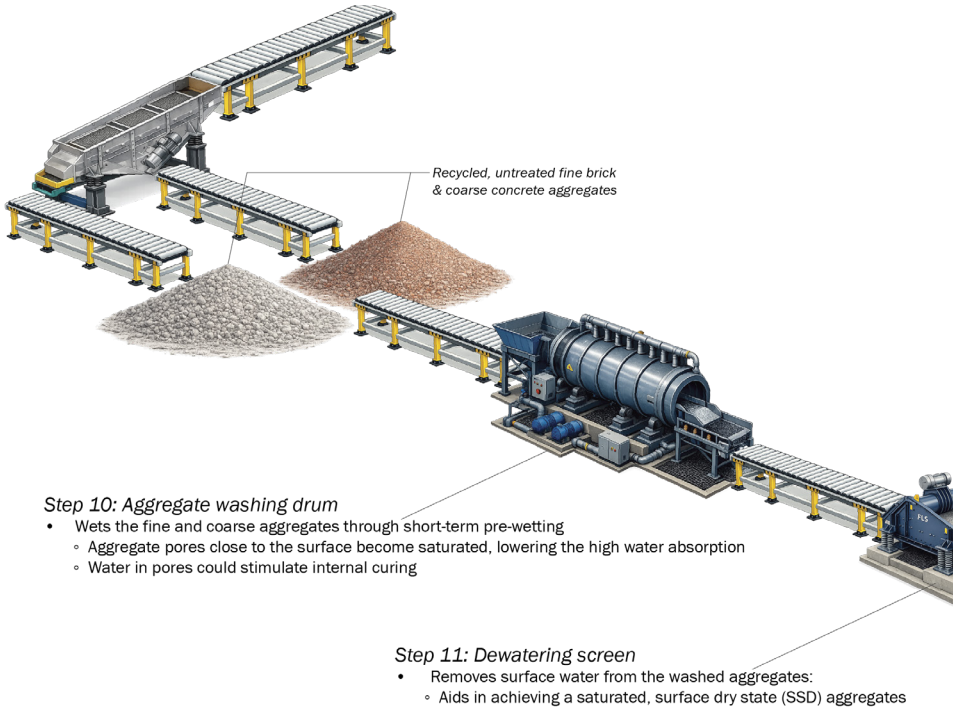

Figure 3.21: The subsequent steps of the aggregate recycling line focussing on the aggregate upcycling of the concrete and brick aggregates (images are created with the assistance of AI)

For the upgrading process, a GTX1530 rotary trommel scrubber is selected. With a processing capacity of 70-140 t/h and a maximum feed size of 50 mm, it is suitable for both recycled coarse and fine aggregates (Longzhong Machinery, n.d.). Besides washing dust and small contaminants from the aggregates, the scrubber also contributes to partial saturation. A DSHC-1224 dewatering screen is then used to remove excess water and bring the aggregates closer to a saturated surface-dry condition. With a capacity of 70 t/h, this machine is suitable for the proposed process scale (FABO Global, n.d.)

Aggregate coating

A second strategy that is applied in the upgrading process is aggregate coating. A cement-fly ash slurry coating can fill surface pores, improve surface uniformity, reduce water absorption, and strengthen the bond between old and new mortar. Fly ash is included since it functions as a supplementary cementitious material, improving durability while reducing the need for Portland cement (Li et al., 2022). The coating strategy should not be applied tot fine recycled brick aggregates, as their higher surface area would require significantly more binder and could lead to lumping or agglomeration (Nedeljković et al., 2021; Siletani et al., 2024). Therefore, fine brick aggregates are upgraded only through pre-saturation and dewatering. For the coating process, A FEECO surface coating drum is proposed (FEECO international, n.d.). This rotating drum provides continuous, high-capacity treatment of granular materials through tumbling action. It can be equipped with an integrated spray system to apply the cement-fly ash slurry evenly, while adjustable speed and slope allow the process to be adapted to different capacities and aggregate conditions.

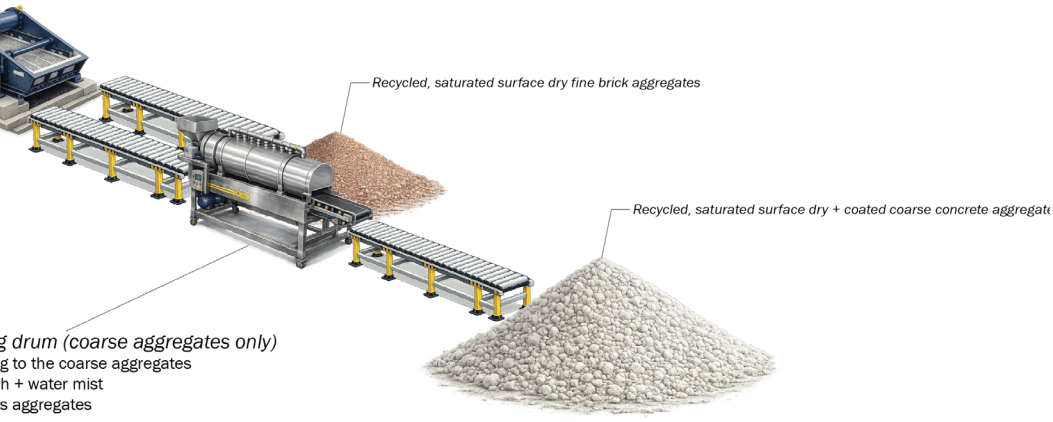

3.8: Seismic performance of current Turkish building stock

Given the country's location within an active seismic region, the performance of the built environment remains a critical factor for public safety and urban resilience. A large proportion of the Turkish building stock was constructed before the enforcement of modern, coherent seismic regulations, and buildings, some still under construction, continue to exhibit deficiencies related to age, structural typology, material quality, and construction practices. These conditions increase the likelihood of damage and collapse under earthquake loading, as demonstrated by repeated collapse patterns observed in past seismic events.

This chapter first reviews Türkiye's building stock, focusing on age, height, and structural systems. It then examines seismic performance in past earthquakes to identify damage patterns. Next, it discusses common global and local failure mechanisms in reinforced concrete frame structures, including the effects construction- and material quality. Finally, it summarises current retrofitting methods and the challenges of strengthening vulnerable buildings at scale.

3.8.1: A profile of Türkiye's Existing Building Stock

Türkiye is located within one of the most seismically active regions in the world, where large urban populations are exposed to significant earthquake hazards. Understanding how the built environment responds to these hazards is therefore a critical component of seismic risk assessment. In particular, the characteristics of the existing building stock play a decisive role in determining cities' earthquake vulnerability.

Mapping the composition of Türkiye's current building stock provides valuable insight into these vulnerabilities, as building materials, structural systems, age, and height categories strongly influence seismic performance. As noted by Güneş, vulnerability measures whether empirical or derived from rigorous analytical approaches are often closely related to these building characteristics (Güneş, 2015).

According to the World Population Review (2026), Türkiye currently has a population of approximately 87.9 million, which continues to grow. Demographic growth has driven rapid urbanisation, particularly in major metropolitan areas such as Istanbul, Ankara, and Izmir, placing increasing pressure on the built environment. At the same time, 52.9% of Türkiye's population resides within first- or second-degree earthquake zones, indicating that approximately 45 million people live in areas exposed to significant seismic hazard (Gülgün et al., 2016). This combination of population concentration and seismic exposure highlights the importance of understanding the characteristics and vulnerabilities of the existing building stock, as shown in Figure 3.22.

Beyond demographic growth, Türkiye also faces the challenge of a large and ageing building stock, much of which was constructed prior to the widespread enforcement of modern seismic design regulations. Gaining insight into the age distribution and structural characteristics of this building stock is therefore essential for assessing seismic vulnerability at both national and urban scales.

According to a 2021 national building inventory, Türkiye has approximately 25.3 million buildings. Of these, 3.18 million buildings (12.6%) were constructed before 1981, 7.83 million buildings (30.9%) between 1981 and 2000, and 12.01 million buildings (47.4%) after 2000. An additional 9.1% of buildings are classified as having an unknown construction year (Türkiye İstatistik Kurumu (TÜİK), n.d.). These numbers indicate that nearly half of the building stock was constructed before 2000, a year commonly used in seismic risk studies as a reference point due to the regulatory and enforcement changes following the 1999 Marmara earthquakes, which significantly increased awareness of seismic safety and led to improved design practices (Gurbuz & Cengiz, 2025).

A similar pattern is observed in Istanbul, Türkiye's largest metropolitan area, which contains approximately 4.78 million buildings. Of these, 10.4% were built before 1981, 36.8% between 1981 and 2000, and 45.7% after 2000, with 7.1% of unknown age (Türkiye İstatistik Kurumu (TÜİK), n.d.). These numbers again suggest that roughly half of the known building stock predates 2000, reinforcing concerns regarding seismic vulnerability in one of the country's most densely populated and seismically exposed cities (Türkiye İstatistik Kurumu (TÜİK), n.d.). When Istanbul is taken as the scope, recent studies indicate that approximately 70% of the existing buildings in Istanbul were constructed before the 1999 earthquake. (Demir & Doğan, n.d.).

In addition to building age, building height is another critical parameter influencing seismic performance. National data indicate that approximately 8.7 million buildings in Türkiye have six or more storeys, a category particularly relevant due to its sensitivity to long-period ground motions. In Istanbul, where the average building height is approximately 6.8 storeys, more than 54.9% of buildings are six or more storeys (Türkiye İstatistik Kurumu (TÜİK), n.d.).

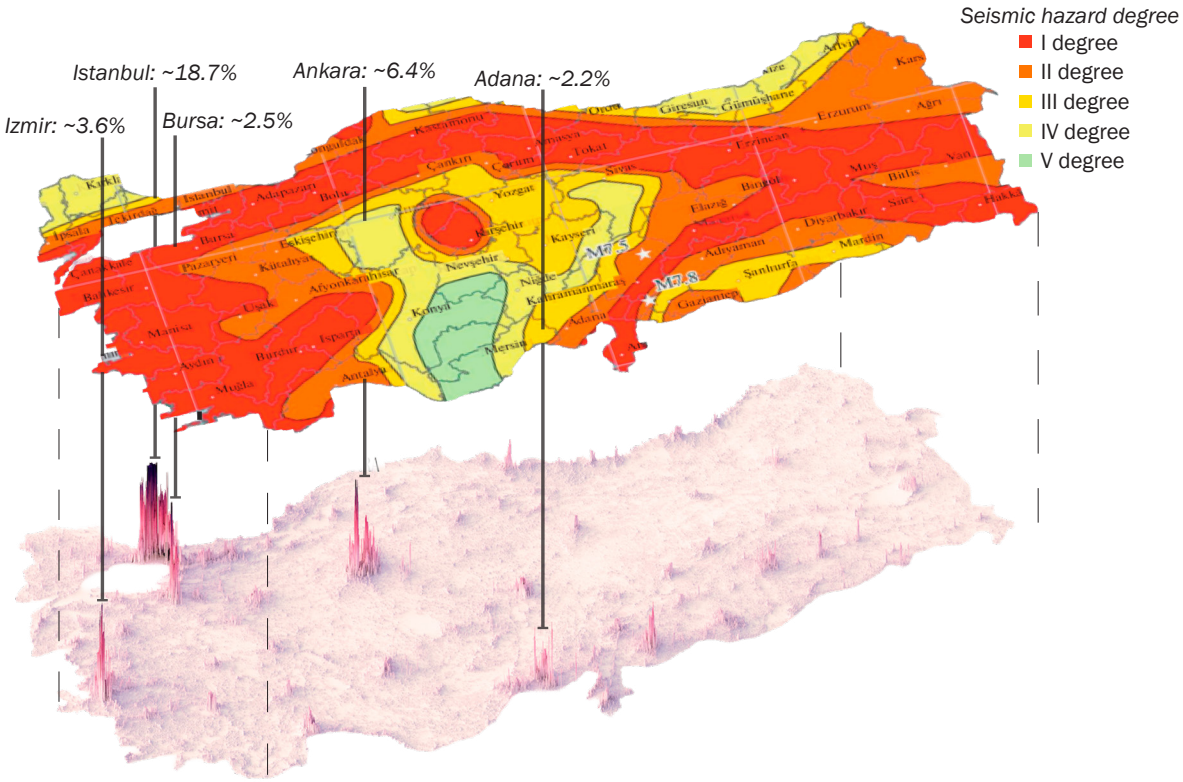

Figure 3.22: The population distribution map of Türkiye overlayed with the corresponding seismic hazard risk degree (adapted from Terence (2022); Günes (2015)

3.8.2: Mapping of most common structural systems in Türkiye

The structural building stock in Türkiye is predominantly composed of RC moment resisting frame structures, particularly in urban areas. Buildings constructed using this system typically employ unreinforced masonry infill walls, which serve as enclosure elements rather than load-bearing components. Additionally, in regions affected by the 2023 Türkiye–Syria earthquakes, this typology likewise dominated the building stock, with approximately 86.7% of buildings identified as reinforced concrete structures, alongside low-rise masonry and brick buildings in rural areas (Gurbuz & Cengiz, 2025). As illustrated in Figure 3.23, Türkiye's building stock has undergone a remarkable transition over the past few decades. In 1984, load-bearing masonry structures accounted for approximately 70% of buildings, whereas reinforced concrete frame structures represented only around 30%. By 2010, the proportion of masonry buildings had decreased to 47.7%, while RC frame structures had become the dominant system nationwide (Güneş, 2015). This trend reflects the increasing adoption of reinforced concrete as the dominant construction material for residential and mixed-use buildings.

The dominance of RC frame structures is even more pronounced in Istanbul, where they account for approximately 76.4% of the total building stock (see Figure 3.23) and up to 90% for buildings constructed after 2000 (Güneş, 2015; Morales-Beltrán, 2025). Much of this housing stock consists of relatively simple mixed-use residential buildings, typically organised with commercial spaces at the ground floor and regular apartment units above containing limited spatial variation. Within this development context, architectural and structural designs are frequently copied and reused across multiple projects, with only minor adjustments made to accommodate different parcels. As a result, large numbers of buildings share highly similar architectural configurations and structural systems, reflecting a building stock characterised by repeated and basic building types and streamlined design processes aimed at minimising cost and design complexity (Demir & Doğan, n.d.).

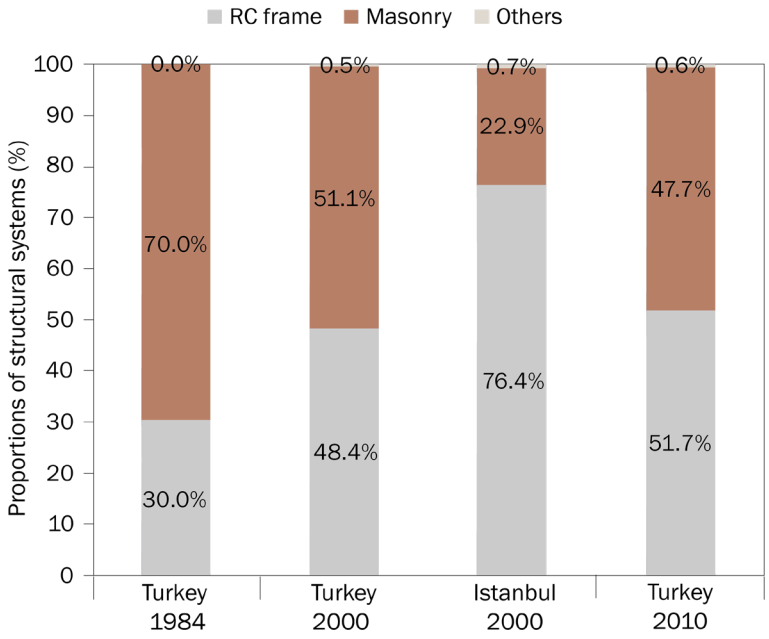

Figure 3.23: Proportion of structural material usage for Türkiye and Istanbul (adapted from: Günes, 2015)

3.9: Common failure mechanisms in RC buildings in earthquakes

After many earthquakes in Türkiye, engineers have studied the causes and mechanisms of building collapse extensively. This research led to post-earthquake reconnaissance studies. In these, teams of engineers visit affected areas soon after an event. They document damage and identify recurring failure patterns. As reinforced concrete structures are common, these studies focus mainly on this type of system.

Failure mechanisms can be divided into three categories: global mechanisms, related to overall structural or architectural configurations; local mechanisms, associated with individual elements such as columns or shear walls; and the influence of non-structural elements on structural behaviour. The purpose of analysing these mechanisms is to determine how they can be effectively mitigated through retrofitting strategies and to identify solutions that can be applied efficiently at scale. The following sections therefore discuss the most common failure mechanisms observed in reconnaissance studies, with particular reference to the 2023 Türkiye earthquakes.

3.9.1: Global damage mechanisms

Global damage mechanisms refer to failure modes that occur at the scale of the entire structural system, rather than at the level of individual elements. These mechanisms are typically associated with deficiencies in the overall structural configuration, such as irregular stiffness distribution, soft-storey behaviour, or insufficient lateral load resistance. When such weaknesses are present, seismic forces can cause a loss of global stability, leading to partial or total collapse of a building.

Weak-column strong-beam mechanism

When the fundamental design principle of strong-column–weak-beam behaviour is not satisfied, brittle failure mechanisms may occur, leading to sudden collapse. Seismic design aims to ensure ductility by allowing plastic hinges to form in beams rather than columns. Plastic hinges are regions in beams or columns where controlled yielding occurs, enabling the structure to deform plastically and absorb seismic energy, thereby maintaining global stability during large deformations. However, if columns are weaker than beams, plastic hinges may form in the columns first, leading to a weak-column–strong-beam mechanism. Since column failure compromises the vertical load-carrying system, it can trigger rapid, often catastrophic, global collapse (Sezgin et al., 2024). Figure 3.24 illustrates the differences between these two design principles and the global structural behaviour that results from the formation of plastic hinges.

Figure 3.24: The difference between weak-column strong-beam mechanism (right) and strong column weak beam mechanism (left) with the corresponding plastic hinge formation shown in red (author's own work

Short column mechanism

Short columns are formed when infill walls or openings partially restrict the open height of a column within a column–beam framework. This reduction in effective height limits the column's capacity to deform laterally and significantly increases shear demand. As a result, the structural response becomes governed by concentrated shear forces rather than flexural behaviour. If the column is not designed for these increased shear forces, brittle failure may occur instead of the desired ductile flexural response. This type of damage is typically characterised by the formation of (double) diagonal cracks in the column, as illustrated in Figure 3.25. To prevent this mechanism, it is essential to account for the interaction between non-structural elements and the structural system, as infill walls can strongly influence the deformation behaviour of load-bearing elements (Sezgin et al., 2024).

Figure 3.25: The short-column effect illustrated (left; author's own work) and seen in the reconnaissance study (right) (Sezgin et al., 2024)

Soft-storey mechanism

A soft-storey mechanism is observed when a building displays significant vertical irregularities in stiffness, causing one storey to possess substantially lower lateral stiffness than the others. This condition typically results in concentrated deformation demands and reduced shear capacity within the weaker storey. Such vulnerabilities often stem from architectural and functional design choices, especially when ground floors are allocated for commercial use (Gulkan et al., 2002). This practice is common in dense urban environments and leads to open floor plans with higher storey heights, increasing deformation demands (Sezgin et al., 2024). Furthermore, increased storey heights and the replacement of infill walls with windows or curtain walls further diminish stiffness and amplify lateral displacements. Consequently, seismic forces become concentrated in the soft storey, promoting the formation of plastic hinges and elevating the risk of local failure that can precipitate a catastrophic global collapse, as illustrated in Figure 3.26 (Gurbuz and Cengiz, 2025).

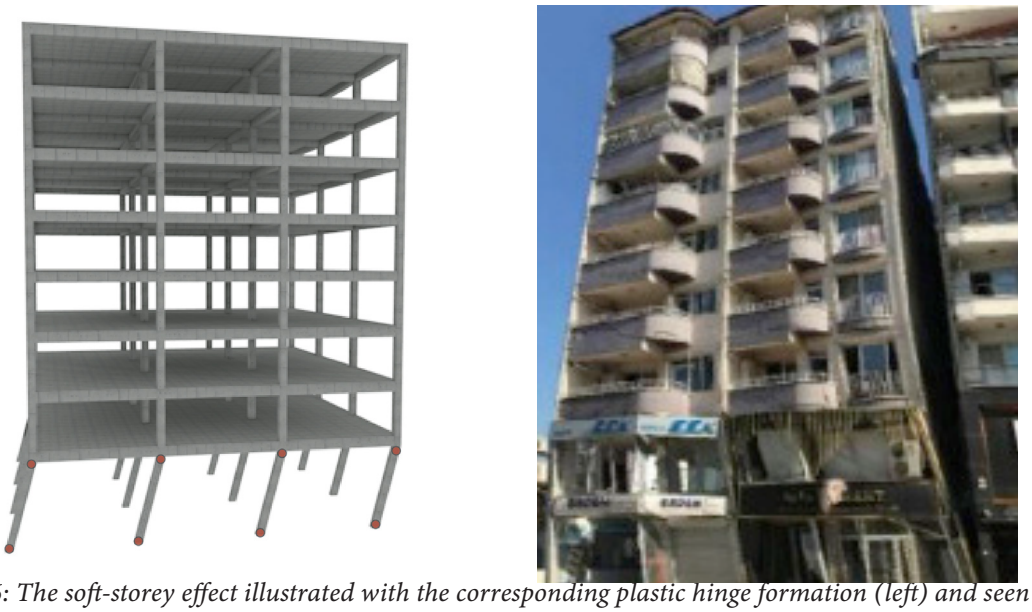

Figure 3.26: The soft-storey effect illustrated with the corresponding plastic hinge formation (left) and seen in the reconnaissance study (right) (Sezgin et al., 2024)

Torsional instability mechanism

Torsional irregularity represents another form of instability that can result in the failure of concrete walls and columns. This phenomenon arises when the centre of mass of a building does not coincide with the centre of rigidity. The centre of mass is determined by the distribution of weight within the building plan, whereas the centre of rigidity is governed by the concentration of lateral stiffness in structural elements such as columns, walls, and cores. When these distributions differ, the resulting misalignment creates an eccentricity that induces a torsional response under lateral loading (see Figure 3.27) (Gokdemir et al., 2013). This rotational response can amplify lateral displacements and subsequently increase shear demands on structural elements, particularly at the edges of columns and walls. Consequently, these elements may undergo brittle failure, potentially resulting in partial or complete structural collapse. Furthermore, differential displacements can elevate the risk of pounding between adjacent buildings (see Figure 3.28). Torsional instability has been documented in previous earthquakes, including the 1999 İzmit and Düzce events (Gokdemir et al., 2013).

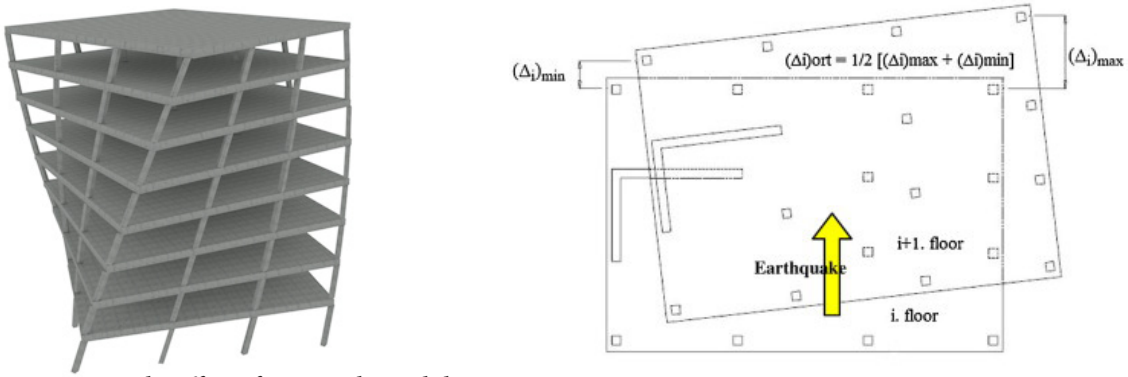

Figure 3.27: The effect of torsional instability on structure (left; author's own work) and as seen through a plan view (right) (Gokdemir et al., 2013)

Pounding effect

The pounding effect occurs when adjacent buildings with different dynamic characteristics respond out of phase during seismic excitation, resulting in collisions. Differences in structural properties like mass, stiffness, and height result in unequal lateral displacements, which can cause impact when insufficient separation or seismic joints are provided. Depending on the alignment of storey levels, pounding may occur between floor slabs of adjacent buildings or, more critically, between a floor slab and a column when storey heights differ (see Figure 3.28 on the right). The latter case is particularly dangerous, as it can induce high localised shear forces in columns, potentially leading to brittle failure (Sezgin et al., 2024). Furthermore, torsional or rotational responses may amplify relative displacements, increasing the likelihood of pounding occurring. The different pounding mechanisms are schematized in Figure 3.28.

Figure 3.28: The effect of pounding between buildings having similar storey heights (left) and different storey heights (right) (author's own work)

Diaphragm action

Floor systems generally contain a large volume of concrete due to their extensive surface area, resulting in a significant mass concentration at each storey. As seismic forces are proportional to mass, variations in floor weight have a substantial influence on the structural response during earthquake loading. In Türkiye, ribbed floor systems, such as hollow block floor slabs shown in Figure 3.29, are commonly used due to their cost efficiency, as they require less formwork and fewer finishing surfaces (Sezgin et al., 2024). However, these systems often lead to increased structural mass, which amplifies seismic forces, particularly shear demands. Moreover, due to their directional configuration, ribbed floors exhibit anisotropic behaviour, providing greater stiffness along the direction of the concrete beams while offering limited resistance in the perpendicular direction. As seismic loading occurs in multiple directions, this can result in increased shear demands perpendicular to the ribs, where load transfer relies primarily on the thin slab layer, potentially compromising diaphragm action (Sezgin et al., 2024).

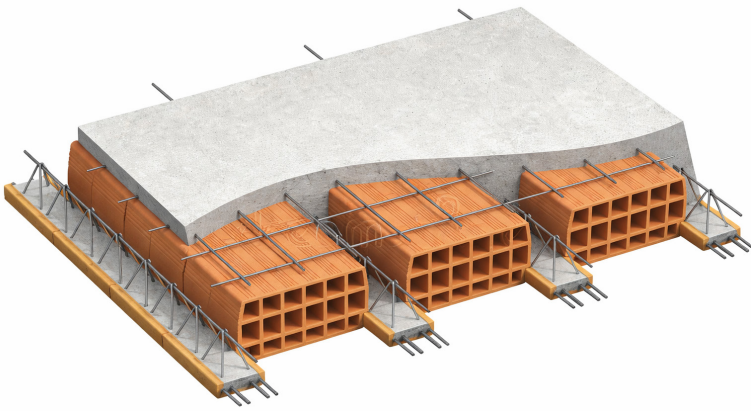

Figure 3.29: the typical ribbed floor system utilized in Türkiye (also known as: asmolen döseme) (Shutterstock, n.d.)

Summary
This section showed multiple global damage and collapse mechanisms observed in buildings in Türkiye during reconnaissance studies. However, it is important to note that short columns and soft storeys with heavy overhangs show the most negative impact on the seismic resistance of buildings. The collapse mechanisms of soft storeys are influenced by the presence of overhangs in the buildings. A study conducted in Izmir found that of the 140 buildings studied, 90% featured soft storeys, and 72% had overhangs. Furthermore, 35% of the buildings showed plan irregularity, a driving factor for soft storeys and torsional instability. Of the buildings that experienced an earthquake, 60% of the collapsed buildings experienced soft-storey failure, indicating that addressing soft storeys, induced by various irregularities and short columns, requires urgent priority to prevent seismic collapse (Morales-Beltran, 2025).

3.9.2: Local damage mechanisms

Local damage mechanisms refer to failure modes that occur at the level of individual structural elements, such as beams, columns, or connections. Unlike global mechanisms, these forms of damage do not necessarily lead to immediate collapse, but may compromise the performance of specific components. However, if local failures are not properly controlled, they can trigger progressive collapse or contribute to global instability. Therefore, understanding the causes and locations of local damage mechanisms is essential for assessing structural vulnerability and designing effective retrofit strategies.

Damage mechanisms to foundations
Seismic damage can also occur at the foundation level, often due to inadequate design and poor construction practices. The primary causes of local foundation damage are closely related to insufficient or improper reinforcement detailing. Common deficiencies include inadequate anchorage between tie beams and spread footings, insufficient confinement due to poorly detailed stirrups, and weak column–foundation connections. These shortcomings can lead to excessive crack widths, loss of confinement, and reduced load transfer capacity. In addition, failure modes such as buckling of longitudinal reinforcement (see the left image in Figure 3.30), rebars fracturing, and stirrup dislodgement are frequently observed. Consequently, inadequate reinforcement detailing can result in concrete crushing, cracking, and separation of structural elements. Figure 3.30 illustrates some typical local damage mechanisms observed in post-earthquake reconnaissance studies (Sezgin et al., 2024).

Figure 3.30: Images from the reconnaissance study depicting damage mechanisms to foundations (Sezgin et al., 2024)

Damage mechanisms to beams

Local damage in beams during seismic events is primarily associated with excessive shear and inadequate reinforcement detailing. A common failure mechanism is the formation of diagonal (X-shaped) cracks, which may extend into the floor slab and indicate high shear stresses. In addition, seismic loading can lead to buckling of longitudinal reinforcement, concrete crushing, and, in some cases, pull-out of reinforcing bars, as shown in Figure 3.31. These damage patterns are typically linked to poor detailing practices, such as insufficient confinement, inadequate stirrup spacing, and insufficient development or lap lengths. A less common but critical configuration is the beam–beam connection, where intersecting beams create localised stress concentrations, leading to cracking and potential shear failure (Sezgin et al., 2024).

Figure 3.31: Images from the reconnaissance study depicting damage mechanisms to beams (Sezgin et al., 2024)

Damage mechanisms to columns

Vertical load-bearing elements, such as columns, are critical to a building's structural stability, as their failure can trigger progressive collapse and lead to global structural failure. During seismic events, columns often fail in shear due to lateral sway demands, particularly in short columns where deformation is constrained by adjacent walls. These failures are primarily associated with inadequate reinforcement detailing, including insufficient stirrup spacing, improper anchorage, the use of smooth (non-ribbed) reinforcement, incorrect stirrup hook configurations, and the absence of crossties. In addition, low concrete strength significantly reduces the shear capacity of columns. As a result, shear failure, typically occurring near the column base, leads to the loss of confinement, dislodgement of stirrups, buckling of longitudinal reinforcement, and eventual crushing of the concrete (Sezgin et al., 2024). The damage mechanisms observed in post-earthquake reconnaissance studies are depicted in Figure 3.32.

Figure 3.32: Images from the reconnaissance study depicting damage mechanisms to beams (Sezgin et al., 2024)

Damage mechanisms to column-beam joints

Beam–column joints are identified as highly vulnerable regions in reinforced concrete structures, as observed in post-earthquake reconnaissance studies (Sezgin et al., 2024). In moment-resisting frames, these joints are critical zones where significant stress transfer occurs between beams and columns, requiring adequate confinement and ductile detailing. However, failures are frequently associated with low concrete strength and inadequate reinforcement detailing. A common deficiency is the improper placement of lap splices, where column reinforcement is extended into beams or floor slabs, leading to premature pull-out and loss of load transfer, as shown in Figure 3.33. In addition, the use of smooth (non-ribbed) reinforcement and insufficient development or overlap lengths further reduces bond strength, increasing the likelihood of joint failure (Sezgin et al., 2024).

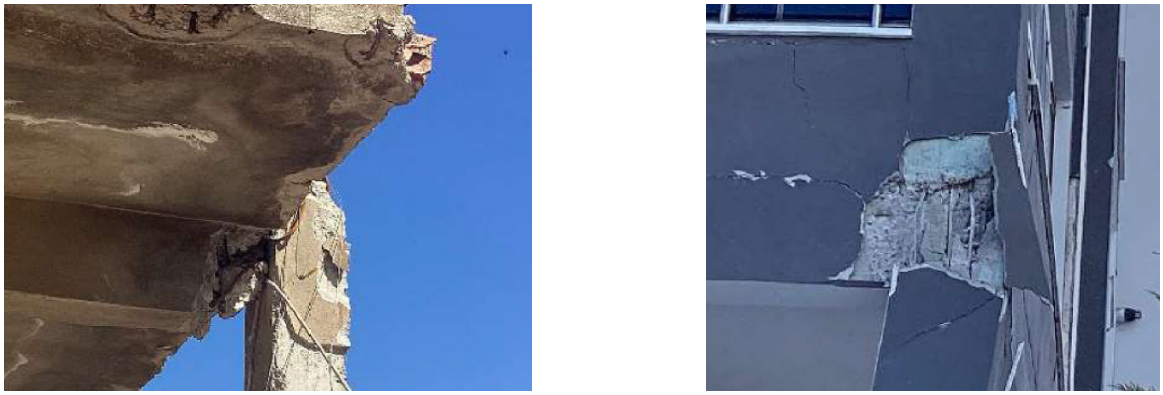

Figure 3.33: Pictures from the reconnaissance study depicting damage mechanisms to member joints (Sezgin et al., 2024)

Damage mechanisms to shear walls

When properly designed and detailed, shear walls perform effectively under seismic loading by resisting a significant portion of lateral forces and reducing overall structural deformation. However, inadequate reinforcement detailing, irregular or asymmetrical placement, and non-compliance with design regulations can lead to failure even in these primary load-bearing elements. Such failures may occur both in-plane and out-of-plane, and are typically characterised by the formation of shear and flexural cracks, particularly at the wall boundaries. Examples of these local damage mechanisms are illustrated in Figure 3.34 (Sezgin et al., 2024). The occurrence of local damage in structural elements is closely related to reinforcement detailing and material quality. As observed across the different failure mechanisms, many deficiencies stem from improper reinforcement application and the use of low-strength concrete. Therefore, further investigation into the underlying causes of these deficiencies is essential to better understand and mitigate such failures.

Figure 3.34: Images from the reconnaissance study depicting damage mechanisms to shear walls (Sezgin et al., 2024)

3.9.3: Damage from material quality

Based on the reconnaissance study, numerous deficiencies related to material quality and workmanship have been identified, which are key contributors to local structural failures and, in some cases, may lead to global collapse. These issues primarily affect the load-bearing capacity, ductility, and overall seismic performance of structural elements. Hence, understanding the role of material properties and construction practices is essential for evaluating structural vulnerability.

Aggregate related problems

Many older buildings constructed before 2000 commonly used all-in mixtures of sand, gravel, and coarse particles often sourced from riverbeds. These aggregates are typically composed of rounded, smooth particles and frequently contain impurities such as clay and silt. Due to their smooth surface and rounded shape, all-in aggregates exhibit poor mechanical interlocking and weak adhesion with cement paste, especially when combined with the low cement contents commonly used in older concrete. As a result, cracking tends to initiate at the interfacial transition zone, reducing concrete strength and integrity.

In addition, excessively large aggregate sizes (70–80 mm, as shown in Figure 3.35) observed in many older concretes significantly reduce workability. Such large particles can block the flow of fresh concrete between reinforcement bars, leading to segregation and poor compaction. This often results in insufficient concrete cover and a poor bond between the reinforcement and the surrounding concrete. Previous studies have shown that large aggregates induce microcrack formation in the structural element, as there is insufficient cement paste to fully coat and restrain the aggregate skeleton. Together, weak aggregate–paste bonding, impurities, and oversized aggregates contribute to brittle concrete behaviour and poor seismic performance, increasing vulnerability to earthquake-induced damage.

Concrete quality related problems

In many older buildings, poor concrete quality occurred, which performed even below requirements stated in the seismic codes. The poor quality can largely be attributed to the lack of ready-mixed concrete and to uncontrolled concrete preparation on construction sites. Concrete was often mixed manually or with small mixers, without systematic quality control of proportions, materials, or workmanship. As a result, the amount of cement in the concrete was frequently insufficient relative to the aggregate content, indicating a lack of cement and directly limiting achievable strength. To compensate for poor workability, especially in the absence of modern water-reducing admixtures, excessive amounts of water were commonly added. While this temporarily improved flow, it significantly reduced compressive strength and durability by increasing porosity.

Figure 3.35: Images from the reconnaissance study depicting aggregate related issues in a structure (Sezgin et al., 2024)

In addition, the frequent use of oversized coarse aggregates further impaired workability and contributed to segregation. These issues were often exacerbated by insufficient or improper vibration, leading to inadequate compaction, trapped air voids, and non-uniform concrete. Core samples taken from such structures have shown compressive strengths below the minimum C18 requirement specified in the 1975 seismic code, confirming systemic deficiencies in material quality. Collectively, poor mix control, excessive water addition, improper aggregate grading, and inadequate compaction resulted in weak, brittle concrete, significantly increasing vulnerability to earthquake-induced damage.

Reinforcement-related problems

As shown earlier, improper reinforcement design and detailing significantly contribute to local damage mechanisms in reinforced concrete structures during earthquakes. One of the most critical issues is reinforcement corrosion, which is initiated by environmental agents such as chlorides and carbon dioxide. When the protective alkaline environment of concrete is compromised, often due to insufficient concrete cover or high concrete permeability, steel reinforcement corrodes, producing rust that expands and induces cracking and spalling of the concrete cover. This process reduces both the bond strength and the effective cross-sectional area of the reinforcement, leading to a loss of load-bearing capacity.

Inadequate reinforcement arrangement, particularly the insufficient use or improper spacing of stirrups, further increases seismic vulnerability. Transverse reinforcement is essential for carrying shear forces and confining the concrete core, thereby ensuring ductile behaviour. Poor detailing, such as incorrect hook angles (using a 90° angle instead of a 135° angle), hook lengths, stirrup spacing, insufficient lap splice lengths, or the continued use of plain (smooth) reinforcement bars, results in weak anchorage and bar slippage. These deficiencies cause buckling of longitudinal bars, which eventually leads to crushing of the concrete core and brittle failure modes. Post-earthquake investigations have shown significant cross-sectional losses due to corroded stirrups and brittle reinforcement failure that failed to meet TS708 standards, highlighting the critical role of proper reinforcement detailing and durability in seismic performance (Sezgin et al., 2024). Some failure mechanisms of the reconnaissance study are shown in Figure 3.36.

Figure 3.36: Photos from the reconnaissance study depicting rebar related issues in a structure (Sezgin et al., 2024)

3.10: Classification of existing retrofitting strategies

Structures deteriorate over time due to environmental exposure, material ageing, and, in many cases, prior seismic events. As a result, their structural performance may no longer meet current safety or design requirements. Retrofitting therefore plays a crucial role in extending the service life of buildings, enhancing their seismic resilience, and adapting them to improved performance demands. Over the past decades, significant research and technological development have led to a wide range of retrofitting techniques, each targeting specific structural deficiencies and performance objectives. This section provides an overview and classification of these retrofitting strategies, which serve as a structured basis for their evaluation and application.

3.10.1: Current retrofitting techniques

Retrofitting is crucial for extending a structure's lifespan, improving its adaptability, and enhancing its response to future earthquake loadings. Over time, research and development have produced a wide range of retrofitting techniques, each with different advantages, limitations, and levels of intervention. Therefore, the selection of a suitable method must be project-specific, balancing factors such as structural performance, cost, execution speed and invasiveness (Tsionis et al., 2014).

Furthermore, Tsionis et al. (2014) state that no single retrofitting method is universally suitable for all buildings. Instead, the chosen strategy should respond to the specific failure mechanisms and structural weaknesses identified in the seismic assessment (such as insufficient strength, stiffness, ductility, or displacement capacity). Since many different types and subtypes of retrofitting strategies exists, it is useful to categorise them according to their main purpose. In general, seismic retrofitting can be divided into two groups: techniques that reduce seismic demand by lowering earthquake loads acting on the building, and techniques that enhance the seismic capacity by strengthening the global lateral load resisting system or specific members of the structure itself.

1. Seismic demand-reduction techniques
   - Seismic isolation
   - Energy dissipation/damping techniques

2. Capacity enhancement techniques
   - Jacketing techniques
   - Concrete jacketing
   - Steel jacketing
   - FRP jacketing

3. Global lateral load–resisting strengthening techniques
   - Shear wall addition
   - Addition of infill walls
   - Addition of steel bracings
   - Buckling restraint bracings

Next to the textual explanations on the following pages, additional information about the retrofitting strategies are described in Appendix B.

Seismic demand-reduction techniques

One way to protect a structure against damage from seismic events is to reduce the seismic-induced forces acting on it. By cleverly reducing induced shear forces, such as base shear, a building does not even need to be strengthened, allowing the structural members to be designed as if they were not subjected to additional seismic forces.

Seismic isolation techniques

When seismic isolation is applied, the building is in principle decoupled from the ground by installing flexible bearing elements, also called isolators, between the foundation and the building. This decoupling allows the building to move independently of the ground during a seismic event. This independent movement significantly reduces swing, deformation and drift, therefore preventing damage (Asadi-manesh & Jalilifard, 2025).

Energy dissipations/damping techniques
Energy dissipation systems are used to increase structural damping and reduce earthquake-induced response. These devices absorb part of the seismic input energy and convert it into other forms, such as heat or plastic deformation, thereby reducing vibrations, displacements, internal forces, and accelerations within the structure (Asadimanesh & Jalilifard, 2025).

Friction pendulum systems (FPS)
FPS systems utilise a bearing based on the friction between sliding surfaces in a pendulum motion. Friction pendulum systems provide high damping capacity by dissipating the seismic energy through friction. The base is designed to exhibit low shear stiffness while accommodating large displacements, so that the input energy from an earthquake is concentrated and dissipated in these isolators. Therefore, this leaves the main structure free of seismic forces (Barrera-Vargas et al. 2020).

Capacity enhancement techniques
The second group of retrofitting techniques focuses on enhancing the structural capacity of buildings. Rather than reducing seismic demand, these methods improve the building's ability to resist earthquakes by increasing strength and stiffness. This can be achieved through several local or building-level strengthening strategies, discussed in Appendix B.

Jacketing techniques
Jacketing is the strengthening of structural members, such as columns, after damage or to withstand increased (seismic) load demands. Jacketing involves improving the structural capacity of a member (column or beam) by adding extra materials, such as additional dimensions or other materials that enhance its capacity. Jacketing is an important retrofitting technique, since columns are a critical element in earthquake design. If a column fails in an earthquake, the failure mode is often sudden and brittle (Lew et al., 2002). The multiple jacketing techniques are described in Appendix B.

Concrete jacketing
Concrete jacketing is a traditional yet highly effective strengthening technique in which a new concrete layer is cast around the existing concrete member to increase its cross-sectional dimensions and, consequently, its load-bearing capacity and stiffness (Asadimanesh & Jalilifard, 2025). This method is commonly applied to strengthen low- to medium-rise residential, commercial, and industrial buildings, as well as bridges and other ordinary concrete structures. With a larger cross section, the compressive, flexural and shear strength of a column can increase. Additionally, concrete jacketing can improve durability by protecting the existing concrete from environmental effects. Members are jacketed by installing steel reinforcement bars, also called connection bars, to create a new confinement cage consisting of longitudinal and stirrup rebars. In the formwork, the new concrete is cast (Asadimanesh & Jalilifard, 2025).

Global lateral load resisting strengthening techniques
Another important load-bearing system crucial to earthquake design is the application of global lateral load-resisting systems. This entails elements such as shear walls, infill walls, structural bracing, and floors. These elements, which could be made of concrete, bricks, or steel, provide strong resistance to lateral forces. Lateral load-bearing systems increase lateral strength and stiffness and are effective at preventing global collapse mechanisms, such as soft-storey mechanisms or torsional instability, thereby preventing a critical progressive collapse mechanism. Appendix B describes the different retrofitting techniques that apply to this system.

3.11: Retrofitting at scale

Accordingly, this section presents the underlying logic of the assessment procedure, including data collection strategies, modelling requirements, and analysis methods. Together, these elements form a structured workflow that supports performance evaluation and decision-making regarding structural intervention.

3.11.1: Current practices and workflow for seismic assessment of buildings

Current seismic assessment practices in Türkiye are primarily based on a building-by-building methodology. This approach is reflected in existing design and assessment frameworks, such as Eurocode 1998 Part 3, which explicitly states that retrofitting procedures are intended for the evaluation of individual buildings rather than building clusters or building blocks (European Committee for Standardization, 2005).

While the Turkish Seismic Code does not explicitly prohibit alternative approaches, its provisions are similarly formulated at the scale of individual buildings. As a result, current engineering practice is inherently oriented towards case-by-case assessment, without providing a framework for scalable or typology-based evaluation.

The seismic assessment of an existing building follows a structured workflow, in which each stage requires specialised input data and engineering judgement. This process, described by Güneş (2015) can be broadly divided into the following steps:

1. Data acquisition → field surveys, documentation review, material (sample) testing;
2. Development of a structural model → based on the collected geometric data from the survey;
3. Seismic analysis → using the corresponding (non) linear method based on building type;
4. Performance evaluation and decision-making → implementation of retrofitting strategy.

The seismic assessment of existing buildings typically follows a workflow consisting of data acquisition, structural modelling, seismic analysis, and performance evaluation. However, as noted by Güneş (2015), applying these procedures at the scale of entire urban building stocks remains impractical due to the time-intensive nature of conventional methods.

This workflow is inherently linear, meaning that each stage depends on the reliability and the completeness of the previous one. As a result, uncertainties in early stages directly affect the accuracy of the final evaluation. Therefore, knowledge levels are introduced.

Knowledge level concept

A central concept within the seismic assessment framework is the definition of knowledge levels, which describe the reliability and completeness of the available information regarding a building's geometry, material properties, and structural detailing. In the European Seismic retrofitting code (European Committee for Standardization, 2005), three knowledge levels are defined: Limited (KL1), Intermediate (KL2), and Comprehensive (KL3). Each knowledge level is associated with a confidence factor (CF), which is used to modify the calculated structural capacity in order to account for uncertainty in the available data. Typical values defined in TBDY (2018) are:

- KL1 (Limited knowledge level) → CF = 0.75;
- KL2 (Normal knowledge level) → CF = 0.90*;
- KL3 (Comprehensive knowledge level) → CF = 1.00.

*Only specified in Eurocode 1998-3 table 3.1 (European Committee for Standardization, 2005).

These factors are applied to reduce the estimated material strengths or member capacities when knowledge is limited, thereby ensuring a conservative assessment.

The required level of knowledge directly influences the extent of data acquisition and verification procedures. Achieving higher knowledge levels requires more detailed and time-intensive field investigations, including additional measurements, material testing, and verification of structural detailing. As a result, there is a clear trade-off between accuracy and effort, where increased reliability of the assessment comes at the cost of increased time, labour, and invasiveness of testing methods.

3.11.2: Current bottlenecks of seismic assessment

Before a building can be retrofitted, a thorough assessment must be conducted. The provisions in the TSC. Ch. 7 (Turkish seismic code from 2007) represents the current state of the art and outlines the elements necessary for a good evaluation of buildings. However, this methodology has potential time-related problems, as it relies heavily on full structural accuracy. Therefore, implementing this methodology from beginning to end requires a small team of engineers and technicians and takes in the order of a month, and can only be shortened to a certain extent (Güneş, 2015). Considering that, according to 2021, 6.7 million buildings still need to be evaluated, especially given the regulation of the urban transformation initiative (World Bank, 2021). This would make full coverage of all buildings unrealistic within the meaningful timeframe when earthquakes strike in Türkiye. Therefore, there is an urgent need for rapid condition assessment and evaluation methodologies.

Therefore, the problem can be framed as a national-scale feasibility challenge. The difficulty is not that assessment methods are insufficient; rather, they cannot be applied quickly enough to match the scale of the risk. The current methodology used for assessment remains manual, slow and most of all, difficult to scale.

Another challenge for the assessment (at scale) of the seismic performance of buildings is the limited information available in structural (and detail) drawings. The gathering of these drawings and the information can become difficult and time-consuming. This is especially the case when structural drawings do not exist or do not match the existing structure. This is too often the case in Türkiye and therefore leads to a more time-consuming, lower-quality evaluation, which directly affects evaluations that show an insufficient seismic resistance of a building. One way to obtain structural models more quickly is to adopt Photogrammetry, for example. This can be useful for obtaining a quick structural representation of the building, including geometric dimensions such as the structural grid and individual members (Güneş, 2015).

3.11.3: Duration of the current seismic assessment process

Based on Güneş's (2015) findings, conventional seismic assessment processes represent a major bottleneck within Türkiye's wider retrofitting and urban transformation challenge. Full implementation of the existing assessment methodology for a single building, from initial investigation to structural evaluation, requires a small professional team of engineers and technicians in the order of a month. The time frame is significant because it includes stages such as visual inspection, collecting structural and material information, conducting on-site investigations and material tests, generating a structural model, performing seismic analysis, and evaluating the building's performance in relation to retrofit or renewal decisions. It is also argued that substantial time savings can be achieved only when the techniques and tools used at each stage of the workflow are improved (Güneş, 2015).

4: Spatial, economic and material feasibility of the C&D waste recycling plant

Summary
This chapter translates the conceptual recycling framework developed in the previous chapter into a spatially and economically situated proposal for Istanbul, demonstrating that circular retrofit is not only technically feasible but also practically implementable within the city's existing infrastructure.

The first section examines where a C&D waste recycling plant could realistically be located in Istanbul, considering land requirements, proximity to waste-generating sources, and the suitability of existing landfills and industrial areas for such a facility. Secondly, the economic dimension of the framework is addressed, evaluating the plant's financial viability and exploring funding mechanisms to support large-scale retrofit activity in Türkiye.

4.1: Locational considerations

Since the recycling process setup is known, it is important to consider the next important step. The plant's location and size. According to Coelho and de Brito (2013) and Ulubeyli et al. (2017), a nominal automated C&D recycling facility requires a surface area of about 27.500-40.000 m^2. However, it is worth noting that, in the research by Coelho and de Brito (2013), this would be a 350 t/h recycling plant. Therefore, as these estimates are taken as a conservative measure of the space needed for the 100 t/h C&D waste recycling plant, it is deemed that sufficient space will be provided to accommodate the factory, machinery, and incoming and outgoing materials.

Now, the necessary area might seem a lot, given Istanbul's dense urban centre and the fact that the city can use all the space they need. However, considering that Istanbul already has 3 landfill areas for municipal solid waste, which are used for energy production through waste incineration or landfill-gas-to-energy technologies (Istaç, n.d.), namely Şile-Kömürcüoda on the Asian side and Götürk-Odayeri and Silivri Seymen on the European side. A solution could be to locate the recycling plant on or near these landfill sites. This is because the current MSW plants are already well connected by road and located outside urban centres.

If it were not possible to locate the new C&D waste recycling plant on or around the current landfilling areas, a multitude of studies have been conducted to identify suitable alternative landfill sites. A study conducted by Güler and Yomralıoğlu (2017) shows that, based on a series of environmental and economic factors, landfill suitability is classified and presented in Figure 4.1. Lastly, Ulubeyli et al. (2017) state that optimal performance is achieved when plants operate within a 15-50 km radius. If this ratio is put right on top of the old centre of Istanbul, it can be seen that a 50 km radius provides a scale of possibilities, both using C&D recycling plants on current landfill-energy facilities but also a lot of possibilities for constructing a new facility area on a scale of suitable to very suitable land, mostly located on the outskirts of the European side in the province.

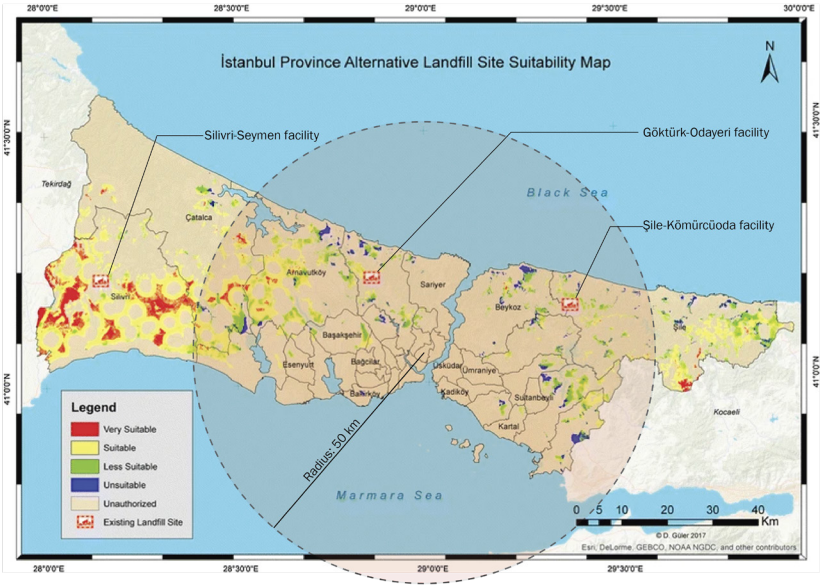

Figure 4.1: A map depicting the three landfilling-energy production facilities and the suitability for alternative landfilling areas (adapted from Güler and Yomralıoğlu, 2017)

Lastly, to demonstrate the efficiency of the space required for a 100 t/h waste recycling plant, Figure 4.2 compares the reserved area for the Götürk-Odayeri landfill-incineration facility. Rough estimates, made with the polygon measurement tool from Google Earth indicate that the Götürk-Odayeri facility, with a capacity of 9500 t/day (Demir et al., 2016), has an area of 2.34 km^2 (Google, n.d.). Compared to a very conservative 40.000 m^2 required for the C&D waste plant with a 1200 t/day (based on 12 hours per day operation), this means that a C&D waste recycling plant roughly uses 1,7% of the designated area compared to just one landfill-waste incineration site. This shows the specific area efficiency of using recycling strategies compared to landfilling the waste.

Figure 4.2: The comparison between the current Götürk-Odayeri landfill-incineration facility area (bright-red) and the estimated necessary area for a C&D waste recycling facility plant with a 100 t/h capacity (image adapted from Google Earth, n.d.)

4.2: Economical considerations

Next to location, another important question is the cost of setting up a C&D waste recycling plant in Istanbul. While economic considerations are based on many different costs, for instance, initial investments (costs of land, construction, machinery) and operational costs (costs of employees, fuel, and electricity), almost no reliable cost data are available. Therefore, instead of focusing on the costs, the focus shifts to facilitating this through investment. In Türkiye, a specific homeowners insurance policy called DASK (Doğal Afet Sigortaları Kurumu) is available. This insurance is a catastrophe insurance pool established in 1999 (Turkish Catastrophe Insurance Pool, 2024, p. 115). This insurance pool has been established by the government for a multitude of reasons, namely: to create a government-mandated, self-sustaining insurance system designed to provide affordable earthquake protection to all registered homeowners, to limit the government's financial exposure to natural disasters, to build long-term catastrophe reserves to finance future earthquake losses, and to encourage risk reduction and mitigation practices in residential construction.

The cost of this mandatory insurance depends on factors such as the building's location and the type of materials used, and therefore varies per homeowner. This is because premiums are divided into different risk groups based on the Turkish earthquake hazard map, ground and soil conditions, and building characteristics. This creates differences in the premiums per homeowner. The annual premium rates are shown in Table 4.1 below. Based on the premiums as stated by the Natural Disaster Insurance institution (n.d.).

Table 4.1: Annual payment per homeowner for the earthquake insurance in Lira's and Euro's - per risk group and building style (Natural Insurance institution, n.d.)

	Yearly premium payment per risk group per homeowner (in Turkish Lira & Euro's calculated at conversion rate €1 = ₺53,01 in may 2026)						
Building style (structural material)	*Risk group I*	*Risk group II*	*Risk group III*	*Risk group IV*	*Risk group V*	*Risk group VI*	*Risk group VII*
Reinforced concrete structures	*₺ 3.021 € 56,99*	*₺ 2.689 € 50,73*	*₺ 2.282 € 43,05*	*₺ 2.143 € 40,43*	*₺ 1.607 € 30,32*	*₺ 1.146 € 21,62*	*₺ 782 14,75*
Dwellings made from other structural materials	*₺ 3.543 € 66,84*	*₺ 3.036 € 57,27*	*₺ 2.664 € 50,25*	*₺ 2.493 € 47,03*	*₺ 1.993 € 37,60*	*₺ 1.328 € 25,05*	*₺ 779 € 14,70*

These premiums are deliberately kept low to make it more affordable for all income groups. These premiums all go into a large insurance pool that serves as a financial buffer and pays out after an earthquake. However, when an earthquake hits, the financial damage to buildings can quickly run into the billions of euros. For instance, the World Bank estimated that the 2023 earthquake in Türkiye caused 34.2 billion dollars in direct physical damage (World Bank, 2023).

According to the DASK 2024 annual report, the average annual premium nationwide is 1166 Turkish lira, or 22,05 Euro. This report also states that, in Istanbul, with a total of 4.153.000 residences, 2.591.491 are insured. This gives a policy penetration rate of 62% and generates 3.492.307.733 Turkish lira, or 66.057.000 Euro, per year (Turkish Catastrophe Insurance Pool, 2024, pp. 28, 34). Now, this annual amount would never cover billions of dollars in damages, even after years of saving. Instead, a proposal could be to shift from a reactive compensation-based disaster finance model to a proactive prevention-oriented risk-reduction model. The money generated from premiums could be used to invest in C&D waste recycling factories that produce retrofitting products for homeowners, thereby helping prevent structural and financial damage during earthquakes.

Therefore, even when investment costs for a recycling plant remain vague, the money generated for the insurance pool could, for example, be used to invest in a C&D waste recycling plant that provides partial risk reduction in dwellings.

5: Parametric workflow for seismic vulnerability and retrofit assessment

Summary
This chapter presents the development of the parametric workflow that forms the operational core of this research, namely a typology-based tool for rapid screening of the seismic vulnerability of existing reinforced concrete frame buildings and for designing targeted retrofit interventions within the same environment.

The chapter opens by arguing that, given the scale of the vulnerable building stock, conventional building-by-building assessment would be too slow to have an impact on the problem. A parametric, typology-based workflow is proposed as a response to this constraint, a tool that enables the rapid evaluation of structurally similar buildings. The workflow is built around a representative structural typology which is among the most common and most seismically vulnerable building types in Istanbul (Gulkan et al., 2002; Günes, 2015), making it a meaningful starting point for a proof-of-concept demonstration.

Data acquisition combines a standardised on-site survey with existing structural documentation to capture the parameters that drive automatic generation of a 3D structural model in Grasshopper. Following this, seismic performance is evaluated using the equivalent static method, producing utilisation factors that identify which members are overstressed and the most likely failure mode, thereby directly guiding the definition of the best retrofit strategy. Once the vulnerabilities are identified, the workflow transitions into a retrofit design tool, where column jacketing and shear wall interventions are configured within the same environment and verified through final capacity checks.

5.1: The necessity behind scaling up

Türkiye and its major cities face a critical challenge from the seismic vulnerability of their built environment. Much of the existing residential building stock was constructed before modern seismic design regulations. According to the World Bank, most residential buildings in Turkish cities were built before 2000, when improved building codes and stricter standards were implemented. As a result, a significant share of the housing stock remains vulnerable to earthquake hazards and requires structural strengthening. This vulnerability is worsened by decades of rapid urbanisation and inadequate design and construction practices. These factors have led to many buildings not meeting current seismic safety standards. Demolishing and reconstructing these structures is often economically and socially unfeasible, making large-scale retrofitting programs necessary for reducing seismic risk.

The magnitude of this challenge is immense. Building on the vulnerabilities described above, it is estimated that approximately 6.7 million residential buildings in Türkiye require structural retrofitting, representing an investment of roughly 465 billion USD (World Bank, 2021). Despite the urgency of the situation, progress remains limited; currently only around 4% of the necessary residential buildings have undergone strengthening interventions. At the current pace, addressing the full scope of the problem would require several decades.

A closer examination of Istanbul highlights how the urgency is further intensified by the anticipated occurrence of a major earthquake along the North Anatolian Fault. As prominent geologist Celal Şengör warns:

"The most severe earthquake we are currently expecting is the Istanbul earthquake" (Habertürk, 2017).

"While a precise date cannot be given, we are under threat of an earthquake averaging 7.2 magnitude by 2030." (Habertürk, 2017).

Together, these conditions create immense time pressure on a problem of extraordinary scale. Istanbul's dense urban fabric, ageing building stock, and complex socio-economic conditions make large-scale retrofitting particularly challenging. Consequently, Türkiye faces a dual challenge: the slow pace of seismic retrofitting and the increasing probability of a major earthquake striking its most populous city in the coming years.

5.1.1. Limitations of the current approach

As discussed earlier, the current approach to seismic demand assessment typically operates on a building-by-building basis. Each structure must be individually surveyed, modelled, analysed, and evaluated by teams of engineers and technicians before retrofit solutions can be designed and implemented. This process often requires weeks or even months per building (Güneş, 2015). While this approach ensures high analytical accuracy, it creates a significant bottleneck when applied at the scale of entire cities. Given the millions of buildings that require evaluation, the conventional workflow is too slow to effectively address the urgency of seismic risk.

For this reason, the seismic assessment process itself must be scaled up. Rather than analysing buildings solely as individual cases, new approaches must be developed that allow large groups of structurally similar buildings to be assessed more efficiently without compromising reliability. Without such innovations, the current pace of retrofitting will remain time-intensive. In the face of the anticipated Istanbul earthquake, this delay risks leaving large segments of the population exposed to catastrophic structural failure.

5.2: Proposed procedure

To address the limitations of conventional building-by-building seismic assessment, this research proposes a parametric, typology-based workflow that enables the rapid evaluation of large groups of structurally similar buildings. As outlined in the previous chapter, the current assessment practice is too slow to respond to the scale and urgency of seismic risk, particularly in cities such as Istanbul where millions of residential buildings require evaluation and potential retrofitting.

This parametric approach builds on the observation that a significant portion of the existing residential building stock shares recurring structural characteristics. Instead of analysing each building individually, these similarities are used to define building typologies, within which variations can be captured through a limited set of geometric and structural parameters. Consequently, the assessment process can shift from a case-by-case methodology to a parametric modelling strategy, where building configurations can be generated swiftly and analysed efficiently.

As a further step, by structuring the assessment process into a parametric workflow, the methodology significantly accelerates the evaluation of existing buildings. It enables rapid generation of structural models, automated seismic analysis, and efficient implementation and verification of retrofit strategies. This reduces the need for repetitive manual modelling and allows engineers to quickly assess both the current and retrofitted structural performance. As a result, the approach improves the feasibility of seismic assessment at scale, enabling faster retrofit decisions.

The workflow integrates multiple software environments and code-based calculations into a coherent process, combining parametric geometric modelling, structural analysis, and simplified capacity verification. As illustrated in Figure 5.1, the procedure consists of sequential steps: data input and model generation, seismic performance evaluation, and implementation and verification of retrofit strategies.

The following subchapters describe each step of this workflow in more detail, including the definition of input parameters, the development of the parametric structural model, the applied loading strategy, and the evaluation of structural performance before and after retrofit intervention.

From Assessment to Retrofit: A Parametric Workflow for Seismic Evaluation

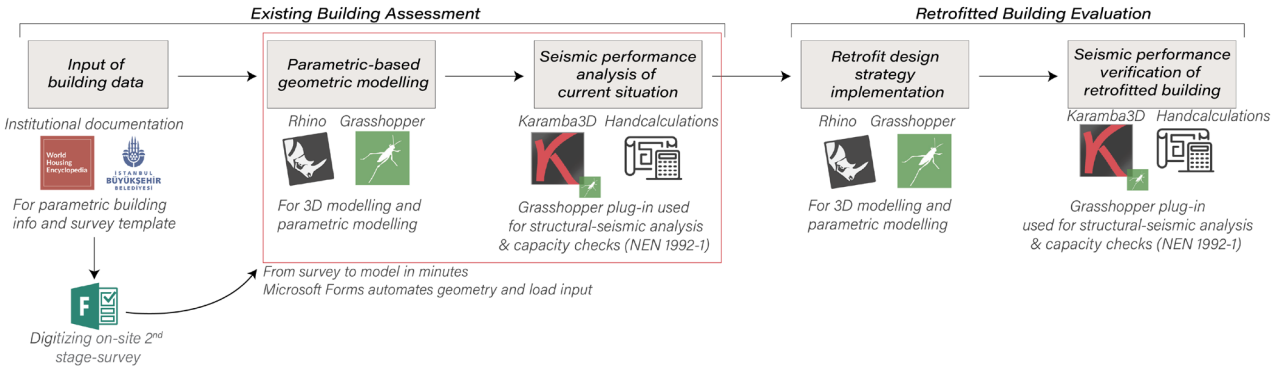

Figure 5.1: The general steps of the parametric workflow for seismic evaluation (author's own work)

5.3 Building typology selection

Since the tool cannot serve as a one-size-fits-all model for all building types, the research focuses on one representative structural typology: mid-rise reinforced concrete moment-resisting frame apartment buildings. This typology is selected because it is one of the most widespread forms of urban housing in Türkiye and can be found across many Turkish cities, including Istanbul, Izmir, and Ankara. As stated by the World Housing Encyclopedia (Gulkan et al., 2002), approximately 80 per cent of Türkiye's urban households live in mid-rise apartment blocks made of cast-in-situ reinforced concrete, making this typology highly relevant to the focus on large-scale seismic assessment.

From the perspective of the tool, this typology is also suitable for a parametric early-stage assessment tool because it contains recurring structural features that help define parameter ranges for this typology. The structure has typical storey heights of around 3 meters and is usually 3 to 7 storeys tall, with typical cantilevers at its upper floors. At the same time, this typology is known to be vulnerable due to insufficient lateral resistance, poor detailing, variable concrete quality and soft-storey conditions caused by open commercial ground floors.

Therefore, focusing on this typology allows us to address a building stock that is both technically relatively easy to assess and socially significant. By developing the workflow for this recurring residential typology first, the tool can support faster vulnerability screening and targeted selection of retrofitting strategies for a large portion of Türkiye's urban housing stock. Figure 5.2 shows what this building type looks like and that it can be found in multiple districts across Istanbul, on both the European and Asian sides.

Figure 5.2: Typical mid-rise RC moment-resisting frame apartment buildings in Istanbul: (left top) [Avcılar], (right top) [Üsküdar], (left bottom) [Besiktas], (right bottom) [Kadıköy]. (Google Earth Street View (2014, 2018, 2020, 2025).

5.4 Data acquisition

To parameterise a building typology, it is necessary to define both which parameters are required and how these parameters are obtained. The proposed workflow relies on two complementary sources of information to establish the framework's base: typological databases and on-site building surveys.

The first source concerns which parameters should be surveyed in individual projects. The building assessment forms developed by the Geology and Earthquake Investigation Department as part of the 2003 Istanbul Earthquake Master Plan provide a structured overview of the building characteristics to be documented during field surveys. In particular, the second-stage assessment form (see Appendix C) identifies essential geometric and structural properties, including building height, number of storeys, structural system, member dimensions, and infill characteristics. The form is designed to be completed by a team of three technical personnel in approximately 1 to 2 hours per building, making it a practical basis for defining the input parameters required for the parametric modelling process.

In practice, the required survey data is obtained through a combination of visual inspection, measurements, and targeted testing, depending on the available documentation and the desired level of knowledge. When structural or detail drawings are incomplete or unavailable, non-destructive testing methods are preferred in order to minimise intervention in the existing structure. For example, a covermeter can be used to detect the location, spacing, and concrete cover of reinforcement bars, enabling an estimate of member detailing without exposing the reinforcement. Similarly, basic geometric information can be acquired through manual measurements or laser-based distance tools. If necessary, these measurement methods may be complemented by limited intrusive investigations, such as localised opening of concrete elements or core sampling, to verify critical structural properties. In general, the data acquisition strategy aims to maximise the reliability of the collected information while minimising damage to the building. The survey data is structured into four main categories:

- General building information → building age, documentation availability;
- Geometric building properties → storeys, storey heights, spans, layouts, irregularities;
- Structural system characteristics → lateral load resisting system, materials;
- Material and detailing condition → condition of materials, workmanship.

While the survey forms identify which parameters must be recorded during field inspections, the ranges within which these parameters vary for specific building typologies must also be defined. This information can be obtained in documents from the World Housing Encyclopedia, developed by the Earthquake Engineering Research Institute (EERI) and the International Association for Earthquake Engineering (IAEE). The encyclopedia provides extensive documentation of common structural typologies across different regions, including their architectural configuration, lateral load-resisting systems, construction materials, and typical structural layouts. In addition, it describes characteristic geometric properties such as typical building heights, span lengths, member dimensions, and structural detailing. By compiling this information, the encyclopedia establishes representative parameter ranges for each typology, which can be used to define the boundaries of the parametric model and capture the variability present within the building stock.

Based on the two different sources, a list of important geometrical and structural parameters related to the typology is illustrated. These parameters attempt to capture both aspects of the building as clearly, quickly, and as detailed as possible. Some parameters, for example, the availability of structural, detail, or architectural drawings, can be answered with a simple yes-or-no, but this information affects the level of knowledge about the building. The knowledge level describes how detailed the building's knowledge is, based on available and accessible information and materials. This influences the admissible analysis type and the confidence factor values, which, in turn, influence the structural capacity checks.

5.4.1 Implementation of on-site survey

To connect the physical site assessment directly to the parametric model, a Microsoft Forms survey was developed, structured similarly to the second-stage on-site survey. The form is intended to be filled in by the responsible engineer or technical survey team during the site visit. The survey organises the required input data into a standardised digital format that can later be exported as a comma-delimited CSV file and imported directly into the Grasshopper workflow.

The survey collects the main parameters needed to generate and assess the building model. These include, for instance, the general building geometry, such as the number of storeys, storey height, bay dimensions, overhang configurations, and overall grid characteristics. It also records detailed information about the members, such as dimensions, reinforcement sizes and configurations and material properties. Another important part of the survey is the input of seismic- and soil-related parameters, which, based on the site location, allows the model to calculate preliminary structural loads on the building without requiring the engineer to manually enter all values in Grasshopper.

The main advantage of this survey-based input system is that it establishes a direct link between on-site observation and parametric structural assessment, enabling quick vulnerability screening of the building. Once the form is completed, the collected data can be transferred to the model almost instantly, replacing a large part of the manual geometry modelling and load input process. This reduces the risk of transcription errors, ensures consistency across different building assessments, and makes the workflow easier to replicate across multiple buildings of the same typology. As a result, the Microsoft Forms survey serves as the first step in the tool's automation logic, translating site data into structured model input and enabling faster early-stage vulnerability screening. An example of the survey setup and the corresponding link is in Appendix D.

5.5 Parametric-based geometry modelling

Following the definition of the input parameters and their respective ranges, the next step in the workflow is to generate a parametric building model. This part of the model explains how parametric logic translates survey data into a structural geometry model of the building, thereby providing the geometric basis for subsequent structural analysis. As shown, this part of the model is developed using a combination of Rhino and Grasshopper. Rhino provides the modelling environment for visualisation and spatial control, Grasshopper enables the implementation of a rule-based parametric system in which the building geometry is generated from the defined input parameters.

The parametric model is structured around a set of key geometric descriptors derived from the survey data as shown in Appendix D. These parameters are translated into a hierarchical modelling logic, where the building is constructed from fundamental structural elements in which:

- nodes represent joints between column and beam elements;
- Lines represent linear elements like columns and beams
- Surfaces represent planar elements such as (shear) walls and floor slabs;

5.5.1 Modelling of the ground floor

The modelling process starts with generating the ground floor, which establishes the building's primary structural framework. A structural grid is defined by user-defined parameters, such as the number of bays and span lengths in both principal directions. This grid serves as the basis for node generation, which subsequently defines the locations of structural elements.
From these nodes, vertical elements representing columns are generated based on the specified ground-floor storey height (see Figure 5.3). The ground floor is particularly important, as it often exhibits higher storey heights due to commercial functions. Typical values range from 3.5 to 4.5 metres, which significantly influence susceptibility to soft-storey mechanisms under seismic loading (Gulkan et al., 2002).

In addition, the model includes the option to incorporate a basement level, including its corresponding storey height. This allows for a more accurate representation of building mass distribution and foundation-level boundary conditions.

5.5.2 Modelling of the upper floors

Following the definition of the ground floor, the upper floors are generated based on the number of storeys and their associated storey heights. For the selected building typology of urban mid-rise apartments, this typically ranges from three to seven storeys with storey heights between 2.7 and 3.0 metres (Gulkan et al., 2002).

Another essential characteristic of this building typology is the presence of cantilevered upper floors, which introduce geometric irregularities that could significantly influence seismic behaviour. These overhangs can lead to an eccentric mass distribution and unfavourable load paths, increasing the risk of torsional instability or weak-storey effects at lower levels.

To capture these effects, the parametric model includes multiple predefined overhang configurations (as shown in Figure 5.4), allowing the user to select the appropriate geometric condition. Additional parameters such as overhang length and the presence of corner columns are incorporated to further refine the geometric model. Lastly, based on the defined input parameters, structural elements such as beams, slabs, and the total floor area are automatically generated which results in a model as is shown in Figure 5.5.

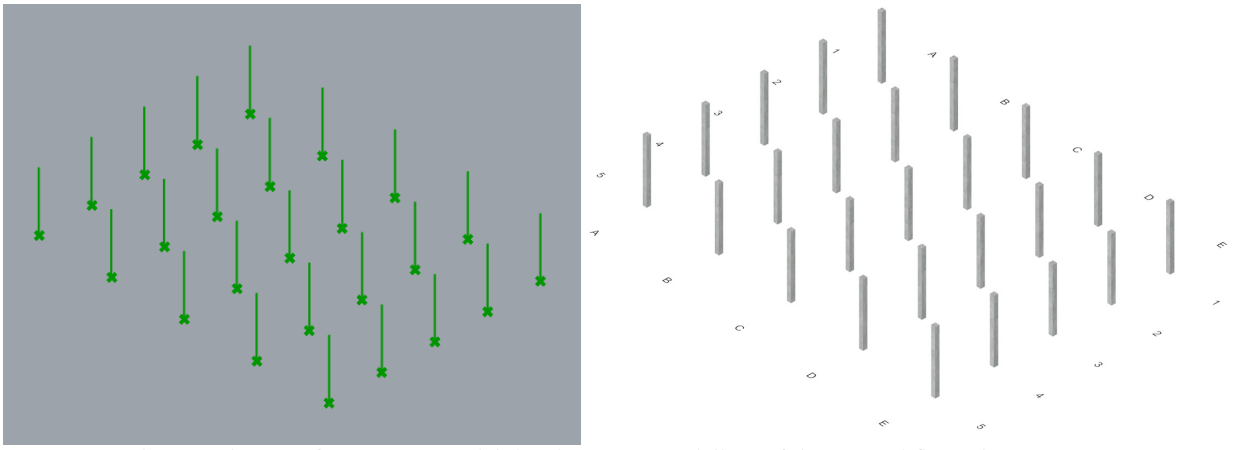

Figure 5.3: The initial stage of geometric model development, modelling of the ground floor, shown as a parametric wireframe in Rhino (left image) and as a refined model for contextual visualisation (right image) (author's own work)

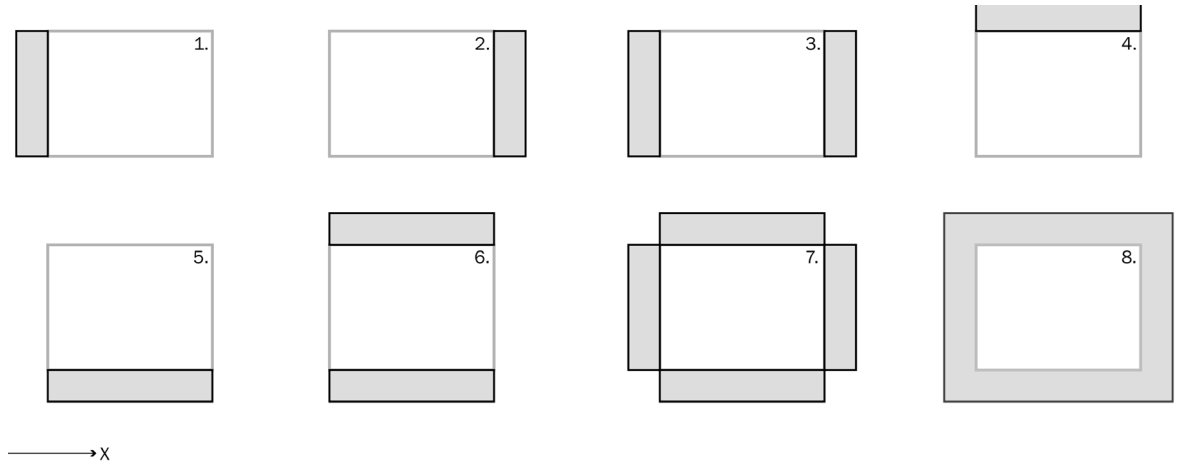

Figure 5.4: The different possible overhang configuration possibilities in the parametric model (author's own work)

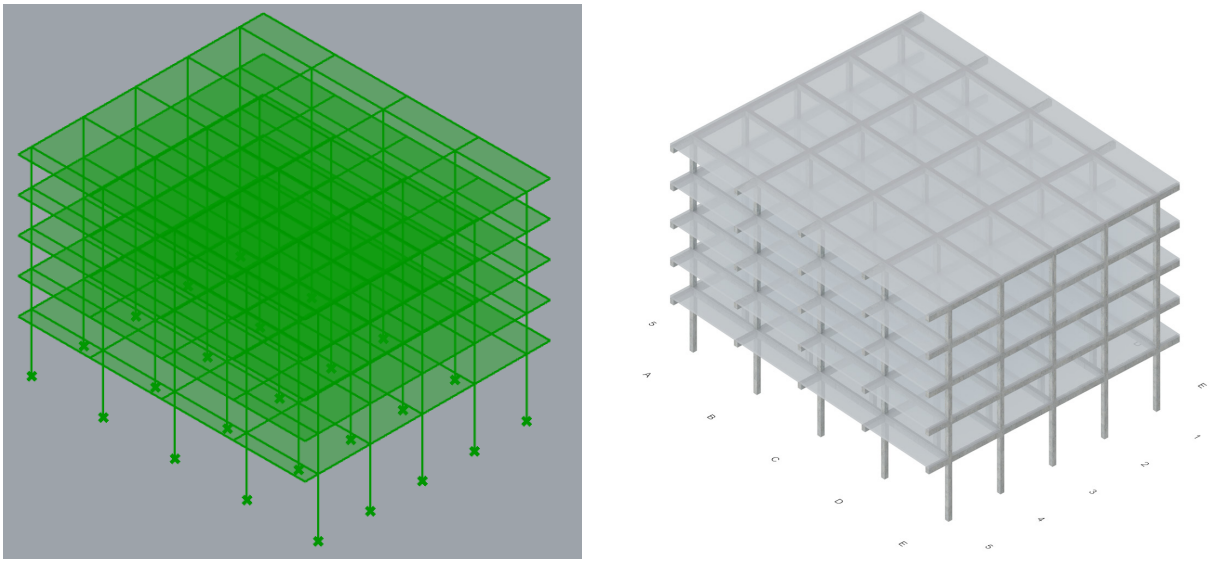

Figure 5.5: The second stage of geometric model development, modelling of the upper floors, shown as a parametric wireframe in Rhino (left image) and as a refined model for contextual visualisation (right image) (author's own work)

5.6 Seismic analysis modelling

After the geometric structural model of the building has been established, it is time to assess the building's structural performance in its current condition under seismic loading. The seismic analysis is done via a Grasshopper plug-in named Karamba3D. In this plug-in, the most structural-member-related information is put in:

- Type and location of supports;
- Load input through load cases and load combinations;
- Cross sections of the structural members;
- Material & material grade of structural members.

For the seismic analysis, the equivalent static method (ESM) has been chosen. The ESM approach attempts to model dynamic earthquake effects using simplified static lateral forces distributed over the height of a building. The reason for applying this method is due to the ease of implementation in the tool and its computational efficiency, which would work well with the fast parametric workflow. However, while it is a simplified representation and therefore less accurate than dynamic analysis methods, it is an acceptable trade-off for speed and scalability, especially considering that this method is still considered a very valid method for low- to mid-rise buildings which are relatively regular, with a low torsional irregularity (TBDY 2018 section 4.7).

5.6.1 Load inputs & load combinations

To capture the full effect of the earthquake and the internal forces and stresses it produces on the structural members, it is crucial to include all loads and their corresponding combinations. The different loads which are modelled on the structure are defined in load cases, as shown below:

- Load case 0 (Lc0) → dead load from self-weight of structural elements = defined through geometric and member modelling of material and cross section;
- Load case 1 (Lc1) → dead load from self-weight of other building elements, such as partition walls, facades, installations) = 3.0 kN/m^2;
- Load case 2 (Lc2) → Live loads = 2.0 kN/m^2;

Seismic load cases

- Load case 3 (Lc3) → Horizontal seismic loading in + X-direction = mass-height dependent;
- Load case 4 (Lc4) → Horizontal seismic loading in - X-direction = mass-height dependent;
- Load case 5 (Lc5) → Horizontal seismic loading in + Y-direction = mass-height dependent;
- Load case 6 (Lc6) → Horizontal seismic loading in - Y-direction = mass-height dependent.

Since the seismic loadings are mass and height dependent, they have to be calculated for every floor. This is done based on the formulas 4.21 to 4.23 from TBDY 2018 (Afet ve Acil Durum Yönetimi Başkanlığı [AFAD], 2018)

The value of the additional equivalent earthquake load affecting the N floor (top) of the building $\Delta F^{(X)}_{NE}$ (eq. 4.22 section 4.7.2.2 in TBDY2018):

$$\Delta F^{(X)}_{NE} = 0.0075\ N\ V^{(X)}_{tE}$$

The remainder of the total equivalent earthquake load (X), including the N-th layer $\Delta F^{(X)}_{NE}$, equivalently to the floors of the building (formula 4.23, section 4.7.2.3):

$$\Delta F^{(X)}_{iE} = (V^{(X)}_{tE} - \Delta F^{(X)}_{NE}) \frac{m_i \cdot H_i}{\Sigma^N_{j=1} m_j \cdot H_j}$$

Where:

- $\Delta F^{(X)}_{iE}$ = the equivalent seismic force at storey i in X-direction (in kN);
- $V^{(X)}_{tE}$ = the base shear force acting on the building in X-direction (in kN);
- m_i = mass of storey i;
- H_i = height of storey i from base;
- $\Sigma^N_{j=1} m_j \cdot H_j$ = weighted sum of all storey masses and heights.

It is important to note that, for proper force distribution throughout the floor elements, a mesh of the floor elements has been created; the nodal points extracted from the mesh serve as locations to apply the divided seismic floor load; these loads are subsequently distributed to all column nodes. Figure 5.6 on the following page shows how these forces are subsequently distributed in a 4-storey building.

Now the individual load cases are known, it is time to combine them into different load combinations. This is done in order to capture the effect of the seismic loadings in all directions and is based on equation 4.9 and 4.11 as described in TBDY 2018:

The composition of the horizontal earthquake load based on the combined effect of earthquake loading in the X- and Y-direction

$$E_d^{(H)} = \pm E_d^{(X)} \pm 0.3 E_d^{(Y)}$$

$$E_d^{(H)} = \pm 0.3 E_d^{(X)} \pm E_d^{(Y)}$$

Where:

- $E_d^{(X)}$ = seismic loading in the ±X-direction;
- $E_d^{(Y)}$ = seismic loading in the ±Y-direction;
- $E_d^{(H)}$ = total horizontal earthquake loading;

Based on the total horizontal seismic loadings, the total load combination can be made based on the equation:

$$G + Q + (0.2S)^* + E_d^{(X)} + 0.3\, E_d^{(Z)}$$

Where G: dead load and Q: live load

*Note: the influence of snow loading (0.2 S) and the vertical earthquake forces ($E_d^{(Z)}$) are left out of the code due to its mostly negligible influence on the total outcome.

Based on the significance of the components in the load combinations, the following eight load combinations are created taking into account the different earthquake loading directions:

- Load combination 1 → 1.0 · (Lc0+Lc1) + 1.0 · (Lc2) + 1.0 · (Lc3) + 0.3 · (Lc5); (+X & +Y direction)
- Load combination 2 → 1.0 · (Lc0+Lc1) + 1.0 · (Lc2) + 1.0 · (Lc3) + 0.3 · (Lc6); (+X & -Y direction)
- Load combination 3 → 1.0 · (Lc0+Lc1) + 1.0 · (Lc2) + 1.0 · (Lc4) + 0.3 · (Lc5); (-X & +Y direction)
- Load combination 4 → 1.0 · (Lc0+Lc1) + 1.0 · (Lc2) + 1.0 · (Lc4) + 0.3 · (Lc6); (-X & -Y direction)
- Load combination 5 → 1.0 · (Lc0+Lc1) + 1.0 · (Lc2) + 1.0 · (Lc5) + 0.3 · (Lc3); (+X & +Y direction)
- Load combination 6 → 1.0 · (Lc0+Lc1) + 1.0 · (Lc2) + 1.0 · (Lc5) + 0.3 · (Lc4); (+X & -Y direction)
- Load combination 7 → 1.0 · (Lc0+Lc1) + 1.0 · (Lc2) + 1.0 · (Lc6) + 0.3 · (Lc3); (-X & +Y direction)
- Load combination 8 → 1.0 · (Lc0+Lc1) + 1.0 · (Lc2) + 1.0 · (Lc6) + 0.3 · (Lc4); (-X & -Y direction)

Appendix E shows an illustration from the software dissecting the different load cases.

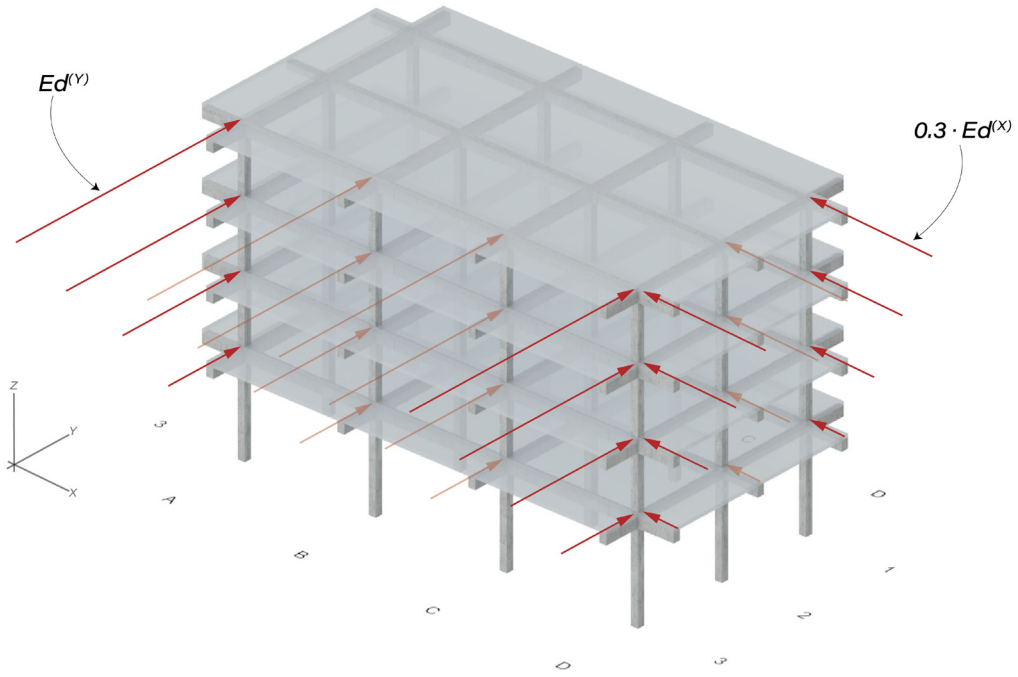

Figure 5.6: Contextual visualisation of a seismic loading case, illustrating load application in both X- and Y-directions and the corresponding force distribution over the building height (author's own work)

5.6.2. Structural member inputs

The structural members require information on their materiality and cross-sectional sizes. This is subsequently divided into input information for the columns, beams, floor slabs and walls. The parameter ranges for cross-section dimensioning are again based on the document provided in the housing encyclopedia for low- to mid-rise apartment buildings.

The materiality, on the other hand, is more difficult to capture, as Karamba3D does not provide material inputs for composite materials such as reinforced concrete. It does for pure concrete; however, this would skew the results by creating very large utilisation factors due to the very low tensile resistance of pure concrete, whereas for reinforced concrete the steel would take the tensile forces, thereby protecting the concrete itself against tensile loadings. Therefore, in order to capture the effect of reinforced concrete, some additional steps have to be taken in the model to fill in important information, for instance:

- Material property information → concrete strength class, reinforcing steel grade;
- Geometric data → cross-sectional dimensions, effective depth, effective span, concrete cover;
- Reinforcement detailing:
  - Longitudinal reinforcement → area, size, spacing of bars
  - Transverse reinforcement → diameter, spacing and inclination of stirrups

This extra information will create a small model, providing the user with clear information about the subsequent structural element and showing the steel rebar layout within the element.

However, it should be noted that, for subsequent floor weight calculations, the density of pure concrete is used, as the rebars have a negligible influence on the weight.

5.6.3 load outputs

Since all geometric and structural information is provided, the Karamba3D software can perform structural analysis of the current situation. Engineers are interested in a select set of so-called engineering demand parameters (EPDs) that describe how the building responds to imposed forces. This therefore helps us examine them to form a judgement about the structure's safety. These EPDs that are important load outputs related to seismic demand analysis are:

- Internal shear forces (V_y & V_z);
- Internal bending moments (M_y, M_z & M_t);
- Interstorey displacements (drift) (u_x, u_y, u_z).

Furthermore, the utilisation factor is used to identify weak members. Due to the inability of the Karamba3D software to properly capture the composite effect of reinforced concrete, the utilisation factor values cannot be used, as pure concrete is used as the material input. However, the location of the weakest members can still be visually extracted and helps the user identify the type of failure most likely to occur in the building under seismic loading, thereby providing guidance for applying targeted retrofitting techniques in the right locations. The visualisation of the utilisation factor for two different geometrical configurations (a shift in 3.5 to 4.5 meter tall columns on the bottom floor) and the corresponding influence on the utilisation factor can be seen in Figure 5.7. It is important to note that, in this case, steel is chosen as the element material to demonstrate the effect of column length on the utilisation factors of the elements.

Other elements that can be visualised quickly in the Karamba3D output include the building's deformation under loading. Figure 5.8, for instance, shows a render of the deformation between a building without a shear wall core and with a shear wall core. Therefore, it shows what influence shear walls can have on reducing lateral displacement. A numerical difference in the displacement of a different geometrical configuration is presented in Appendix E.

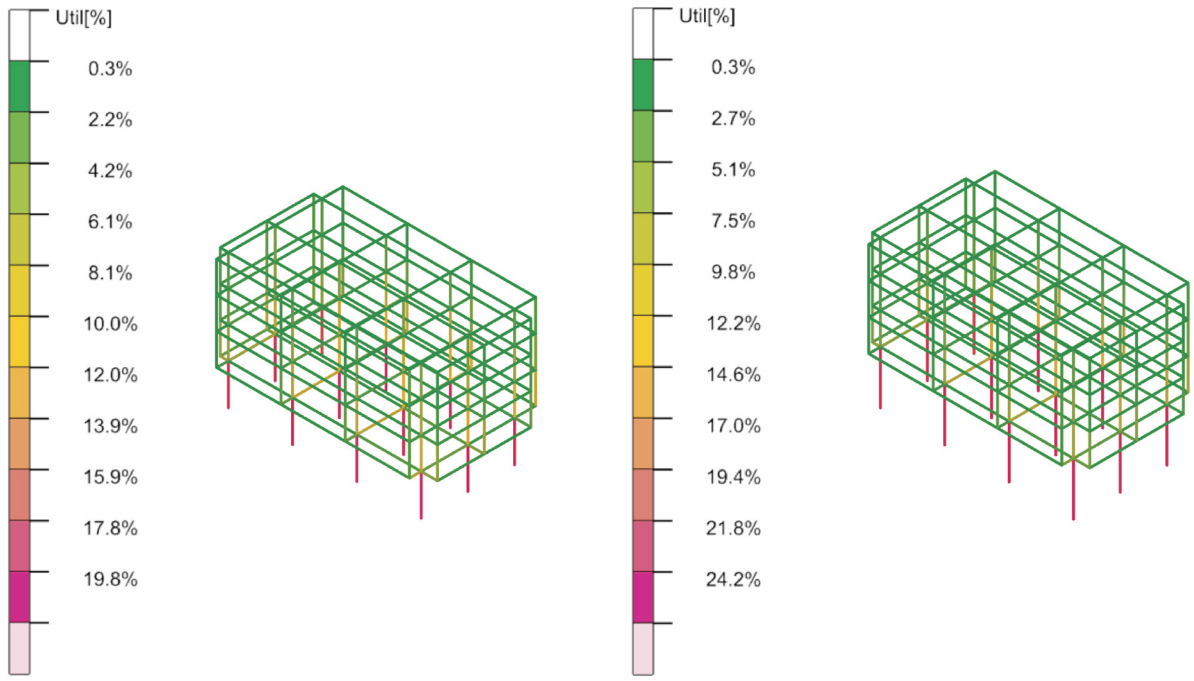

Figure 5.7: Comparison of utilization factor distributions for ground floor heights of 3.5 m (left) and 4.5 m (right), illustrating the variation in member demand and the location of the most critical members (author's own work)

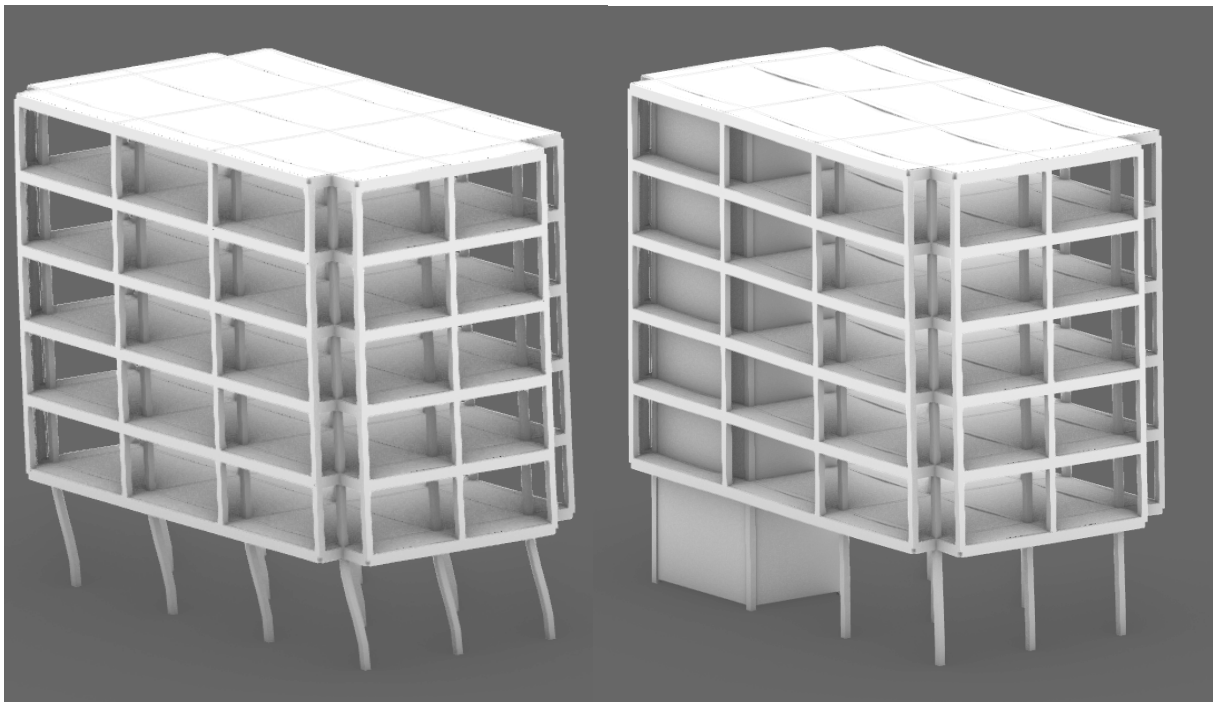

Figure 5.8: Deformation comparison between structural model renders without (left) and with (right) a shear wall core, demonstrating the effect of shear walls on reducing lateral displacements (author's own work)

Additionally, the internal forces acting on the structural elements are numerically extracted. This is done in a manner where the minimum and maximum forces in order to capture forces in both positive and negative directions. These internal forces are important because they are used in subsequent capacity checks of the elements, as elaborated on in 5.6.4.

The output information for the interstorey drift is performed by extracting the nodal lateral displacement results from a representative vertical line of nodes in the Grasshopper model (as depicted in red in Figure 5.9). These nodal displacements are consequently separated into X- and Y-axis components and are furthermore sorted by storey number. Furthermore, the relative displacements between two consecutive floor levels were calculated and divided by the corresponding storey height, giving an interstorey drift value for every storey. The maximum drift ratio is then extracted separately for the X- and Y-directions. This can be done both numerically and visually (as is shown in Appendix F), which are subsequently compared to the TBDY 2018 calculated interstorey drift limit, for which its corresponding formulas are shown in Appendix G.

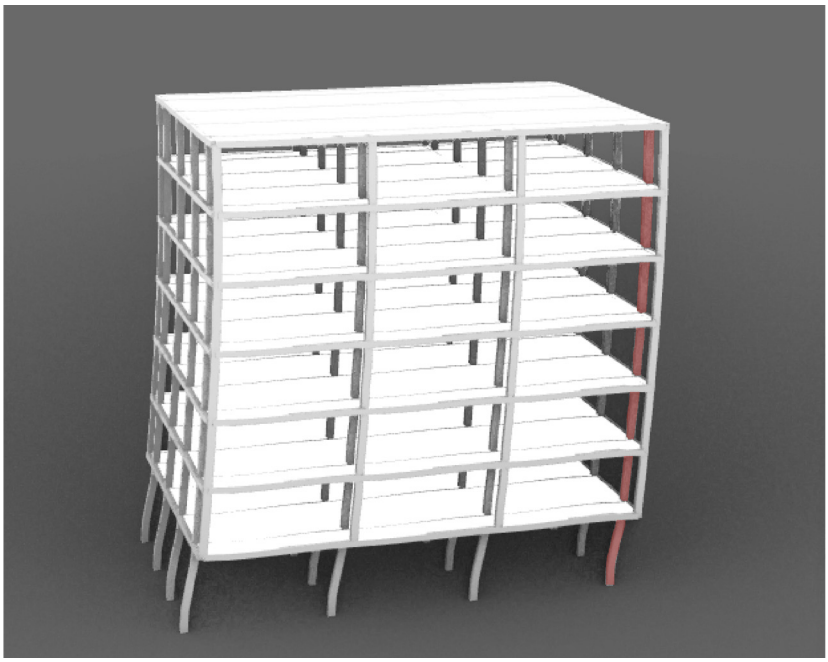

Figure 5.9: Deformation of a multi-storey frame building, schematically depicting the extraction of the nodal lateral displacement results form the representative vertical line (author's own work)

5.6.4. Verification of current situation

After the load outputs are provided, certain outputs must be filtered to perform the capacity checks. These filterings are the engineering design parameters (EDP's). EDP's are the key parameters that must be checked to assess the seismic capacity of the building and its members.

First of all, it is important to note that there may be a lack of information about the building, for example, due to improper or missing drawings. The model accounts for this by factoring in different levels of knowledge. These knowledge levels determine the reliability of the data collected about the structure. These levels directly determine the Knowledge Factor, a safety factor that reduces the calculated capacity of structural elements based on the extent of their investigation. The three given knowledge levels and their corresponding confidence factors are (From NEN 1998-3 and TBDY 2018):

- Knowledge level 1 - Limited, reduction factor: 0.75;
- Knowledge level 2 - Normal, reduction factor: 0.90;
- Knowledge level 3 - Full, reduction factor: 1.00 (no reduction);

Next to the definition of the knowledge level for the reduction factors, different formulas are used to perform the capacity checks. The reason for performing semi-manual capacity checks is that Karamba3D does not allow reinforced steel to be selected as a modelling material. Therefore, only pure concrete or steel can be selected, which do not properly represent how reinforced steel is dealt with tensile and compressive stresses.

This limitation affects the utilisation factor in the model, making it untrustworthy; for that reason, semi-manual capacity checks are performed, which allow greater flexibility in inputting member-specific information, such as different relevant concrete, longitudinal rebars, and stirrup properties. Through information gained by the engineer during the survey on site, with, for instance, a rebar scanner and sampling of the concrete, specific data can be gathered that allows a quick structural model of the column and beam elements in the structure and also directly feeds as input for the capacity calculations.

In this study, local member capacity checks were separated from global seismic deformation checks. Bending, axial-force, and shear capacities were evaluated according to NEN-EN 1992-1-1 (European Committee for Standardization, 2004), as these are local reinforced-concrete resistance checks, and the Dutch/European formulation provides a clear and familiar basis for interpretation. However, interstorey drift was evaluated using TBDY 2018, since this check represents a seismic performance limitation related to damage control, storey deformation compatibility and non-structural interaction under earthquake loading. Therefore, TBDY 2018 was adopted as the reference seismic-performance criterion, while NEN-EN 1992-1-1 was retained for concrete member resistance. The different member capacity check formulas are in Appendix G.

After these relevant member parameters are known, the capacity checks are performed. The members are checked to determine whether they have sufficient capacity to resist the maximum occurring shear forces, bending moments, axial forces, and the critical combination of bending moments and axial forces. For this, simple unit checks are performed in which the maximum forces are compared to the capacity of the column and beam members, and the results directly indicate whether the capacity is sufficient.

One last critical engineering demand parameter is the interstorey drift, which is the relative horizontal displacement (sway) between two consecutive floors of a building. It is calculated as the difference in horizontal deflection between the top and bottom of a specific story, often expressed as a ratio of that difference to the story's total height. It is another important parameter for structural engineers that indicates how much a building bends or deforms under lateral loads. Figure 5.10 below illustrates the key elements required to calculate a building's interstorey drift.

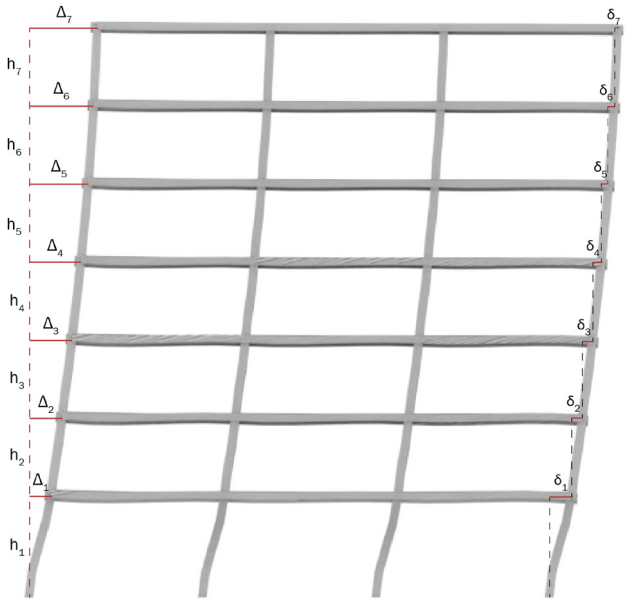

Figure 5.10: Definition of interstorey drift of a multi-storey frame structure showing the relative horizontal displacement (Δ), the lateral displacement and the interstorey drift between the consecutive floors (δ) (author's own work)

5.7 Retrofit design implementation

Once the building's seismic performance is evaluated through capacity checks and interstorey drift assessment, the workflow transitions directly to retrofit design implementation. The unity check results reveal both the location and nature of the structural deficiencies. Whether individual members fail in bending, shear, or axial capacity, or whether the building as a whole exceeds the allowable interstorey drift limit. This distinction is important, as member-level capacity failures are most effectively addressed through column jacketing, which directly increases the cross-sectional capacity and confinement of the critical elements, whereas global lateral stiffness deficiencies are best resolved through the addition of shear walls, which fundamentally alter the building's lateral load-resisting system. However, the user can also choose to apply both shear walls and column jacketing to the building.

Both currently available retrofit strategies are chosen because they are directly compatible with the precast C&D waste-recycled blocks developed in the material design track, creating a coherent link between the parametric structural workflow and the material supply chain. The engineer can select the appropriate intervention based on the identified failure modes and then configure the retrofit geometry to be applied within the building, within the same parametric environment.

For the shear wall intervention option, four predefined configurations are available (as is shown in Figure 5.11 and 5.12): a shear core of which the location can be freely positioned anywhere within the structural grid, perimeter walls applied along the full building perimeter or selectively in the X- or Y-direction only, and corner walls placed at the building's corner nodes, while also allowing the engineer to choose the vertical continuity of these retrofit walls. These configurations cover the most common retrofit scenarios, but when none of the predefined configurations adequately address the identified vulnerabilities, for instance when the building geometry or failure pattern requires a non-standard wall arrangement, the engineer can bypass the presets entirely and define shear wall locations manually by inputting the corresponding structural node ID numbers directly, as is shown in Appendix H. This node-based selection gives the user complete freedom over placement without requiring any modifications to the underlying parametric model. The images below illustrate examples of the different shear wall retrofit strategy configurations.

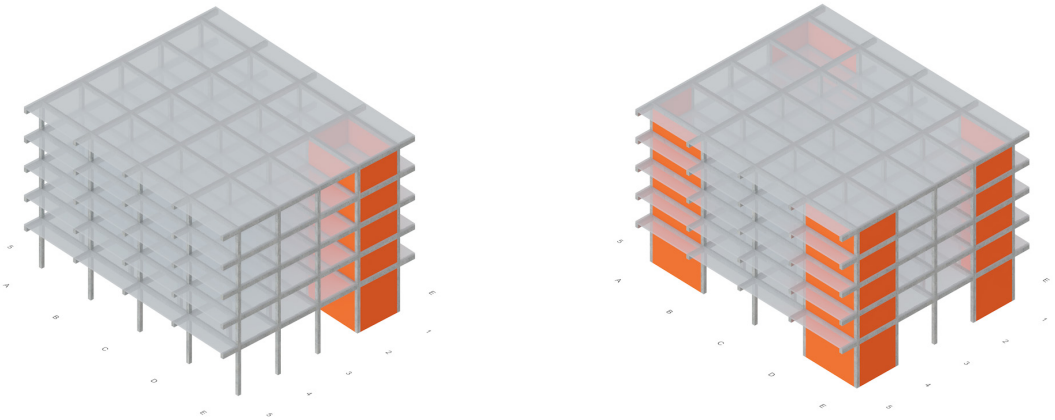

Figure 5.11: : Shear walls applied as a building core (left image) and at the corners frames of the structure (right image) (author's own work)

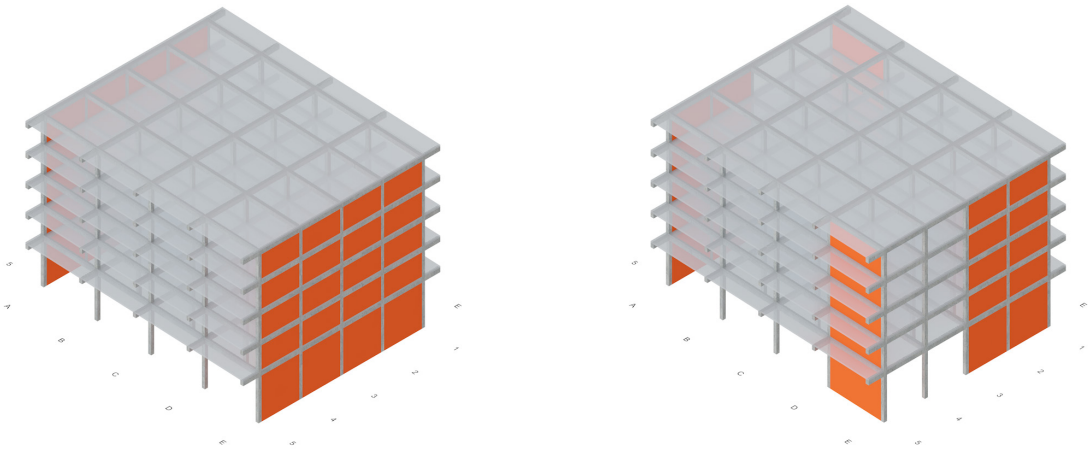

Figure 5.12: Shear walls applied to all perimeter frames following the direction of the x-axis (left image) and to all frames based on the engineer's choice (author's own work)

The column jacketing intervention follows the same logic, offering predefined options to jacket all columns on the bottom floor, all columns on a specific upper floor, or any individual floor level, alongside a fully flexible node-based selection for targeted jacketing of specific columns anywhere in the building (see Figure 5.13 and 5.14). Together, these two interventions ensure that the parametric workflow remains useful across the wide variety of building configurations and failure patterns that can occur in the building stock. Additionally, the column jacket block thicknesses can be selected. These thicknesses are defined as adding blocks of 100, 150 or 200 mm thick to the existing column.

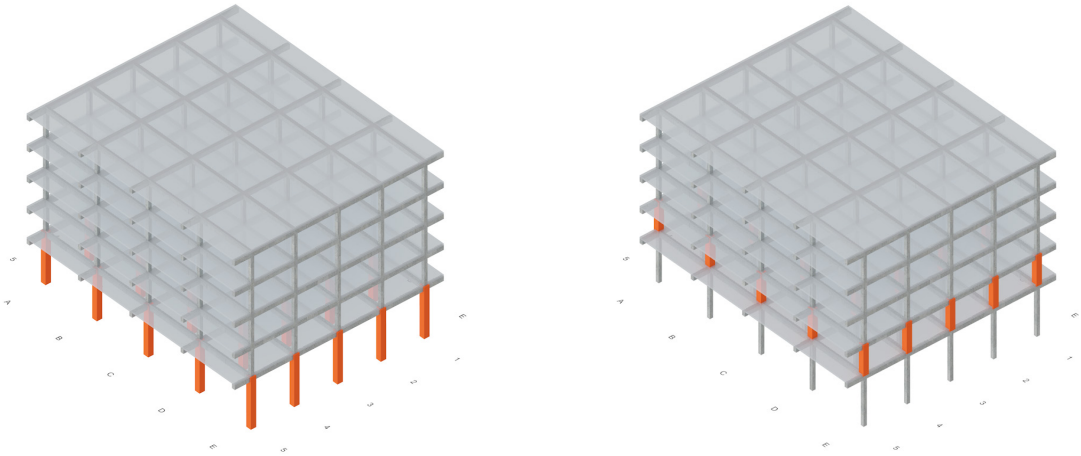

Figure 5.13: Column jacketing applied to all ground floor columns only (left image) and to all first-floor columns only (right) (author's own work)

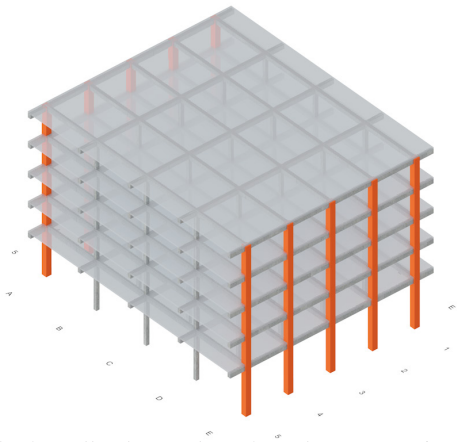

Figure 5.14: Column jacketing applied to all columns based on the engineer's choice (author's own work)

5.8 Final capacity checks

After selecting a retrofit strategy, the parametric workflow allows the modified building geometry to be re-analysed under similar seismic demand (adjusted for additional weight of retrofitting elements) and the same type of capacity-check procedure. This enables the engineer to verify whether the proposed intervention sufficiently improves seismic performance. A representative case study building from the district of Avcılar is implemented to demonstrate this, comparing the current and retrofitted situation and showing how the added retrofit geometries influence behaviour and demand-capacity checks.

The workflow incorporates two interventions, column jacketing and shear wall addition, both based on the proposed precast recycled C&D waste block system. However, using recycled aggregate-based blocks introduces material uncertainties not present in conventional retrofit materials. Unlike standard materials covered by codes such as the European NEN-EN 1992-1-1 or TBDY 2018, the modular retrofit blocks in this study are part of an early-stage material design, and their mechanical properties have not yet been validated through standardised testing.

5.8.1 Implementation of the material reduction factor

To avoid overestimating the structural contribution of these blocks, a conservative material confidence factor is applied. To account for this uncertainty in a conservative but academically grounded manner, a material confidence factor of 0.60 is applied to the structural contribution of the retrofit blocks in all column capacity calculations. This factor is derived by extending the knowledge level framework already embedded in this study. NEN 1998-3 and TBDY 2018 define a minimum confidence factor of 0.75 for Knowledge level 1, representing limited investigation with incomplete documentation. Given that the material has no standardised characterisation data whatsoever, a further 20% reduction is applied by engineering judgement, yielding a confidence factor of $0.75 \cdot 0.80 = 0.60$. This factor is applied exclusively to the additional capacity contributed by the block layer and is intentionally conservative, reflecting the proof-of-concept nature of the material. Once the mechanical strength is established through laboratory testing, a less conservative value can be adopted.

This conservative approach also reflects a deliberate design philosophy: rather than excluding recycled materials on the grounds of uncertainty, this system is designed to accommodate that uncertainty in a quantifiable structural way. Therefore, the goal is not perfect materials, but a structural logic intelligent enough to use imperfect ones responsibly.

In the model, the factor is applied exclusively to the additional capacity provided by the retrofit blocks in column jacketing, specifically to the increase in cross-sectional area and confinement contributed by the new material layer. The existing column core retains its original assessed capacity without reduction, as its material properties are established through on-site investigation under the applicable knowledge level. For shear wall interventions, no material reduction factor is applied at the member capacity level. This is because shear walls in this workflow are evaluated primarily for their contribution to the global lateral stiffness and interstorey drift reduction, rather than isolated member resistance. Their addition fundamentally alters the lateral load path of the structure, redistributing seismic demand away from frame members and reducing drift to within code-compliant limits.

5.8.2 Case study building

To demonstrate the operational output of the parametric workflow, a hypothetical case study building is introduced. The building is assumed to be located in Avcılar, Istanbul.

6: Case study application & integration of material workflow

Summary
This chapter applies the parametric workflow developed in the previous section to the Avcılar case study building, integrating the structural assessment with the material workflow to demonstrate the full supply-to-retrofit loop in practice.

The section opens with the seismic performance evaluation of the case study building in its current, unretrofitted state. Using the parametric model, unity checks and interstorey drift values are extracted, revealing the building's critical vulnerabilities, such as overstressed ground-floor columns or exceeding interstorey drift capacity.

With the failure mode established, the section introduces the retrofit application. The C&D waste currently burdening Istanbul's landfills is repurposed as a material input for the retrofit elements. The recycled aggregate concrete mix, incorporating enhanced recycled aggregates and virgin aggregates, is used to produce precast modular retrofit components. Two retrofit systems are designed around this material input: precast column jacketing blocks that enclose and confine existing columns, and precast shear wall blocks stacked to form infill panels within the building's frame.

The retrofitted model is then re-analysed under the seismic loads. The results demonstrate a significant improvement in structural performance, with unity checks falling well below 1.0 and interstorey drift reduced within the limits stated in TBDY 2018, confirming the viability of the proposed system.

6.1: Seismic assessment of the current structure

Using the survey input parameters summarised in Table 6.1, the parametric workflow generates the structural geometry of the case study building and evaluates its seismic performance in the current, unretrofitted state. The purpose of this step is to demonstrate how the workflow can rapidly translate basic geometric, material, and seismic input data into a structural model with an initial set of performance indicators, providing a quick screening-level understanding of where the building's main vulnerabilities are likely to occur.

Figure 6.1 shows the deformed shape of the current structure under the applied seismic load case. This deformation pattern indicates a concentration of lateral displacement in the ground floor. This behaviour is consistent with the expected weaknesses of mid-rise reinforced concrete frame buildings with relatively open or taller ground floors, where lateral stiffness is reduced. Therefore, Figure 6.1 indicates the probable development of a soft-storey mechanism. Figure 6.2 further illustrates the distribution of the internal forces throughout the structure. The visual output shows that the ground-floor columns are more heavily stressed than the upper-storey members, confirming that the lower part of the building governs the seismic response.

The maximum internal forces and corresponding unity check values for load case 1 (ULS_1) are presented in Table 6.1. The results show that the building fails in several critical parameters. Column shear reaches a unity check value of 1.48, indicating insufficient shear capacity in the columns. Although column moment, axial, and biaxial moment checks remain within the allowable range, the shear failure is structurally significant because columns are critical load-bearing members under seismic loading. Beam performance seems problematic: the beam shear capacity check reaches 2.22, while the beam moment check reaches 1.64, both exceeding the allowable limit of 1.0. These results indicate that the existing frame does not have sufficient member-level capacity to safely resist the applied seismic demand.

Lastly, the drift results further confirm the current structure's vulnerability. The interstorey drift check in the X-direction reaches a unity check value of 1.87 and therefore fails, while the Y-direction drift remains within the allowable limit. Overall, the current state assessment shows that the building is vulnerable at both global and local levels: globally through excessive interstorey drift in one direction, and locally through insufficient shear and moment capacity in selected columns and beams. These findings justify the need for a retrofit intervention that increases lateral stiffness, improves member capacity and reduces the concentration of demand in the lower storeys. The assessment therefore defines the retrofit demand that the following section addresses, using recycled aggregate-based column jackets and shear wall elements as targeted interventions to improve the building's seismic performance.

Internal forces (ULS_1) – Current situation		***Unity check values (ULS_1)***		
Parameter	Value ranges (kN/kNm)	Parameter	Unity check value	PASS/FAIL
Columns – Shear (Vz)	-114,6 to 18,2	Columns – Shear (Vz/Vy)	1,48	FAIL
Columns – Shear (Vy)	-9,0 to 33,0	Columns – Moment (Mz/My)	0,39	PASS
Columns – Moment (My)	-186,1 to 226,4	Columns – Axial (compr./tens.)	0,63 / 0,46	PASS / PASS
Columns – Moment (Mz)	-49,8 to 68,9	Columns – Biaxial moment	0,49	PASS
Columns – Axial (N)	-969,6 to 304,4	Beams – Shear (Vz/Vy)	2,22	FAIL
		Beams – Moment (Mz/My)	1,64	FAIL
Beams – Shear (Vz)	-146,7 to 115,3	Beams – Axial (compr./tens.)	0,03 / 0,15	PASS / PASS
Beams – Shear (Vy)	-7,1 to 4,9			
Beams – Moment (My)	-197,7 to 202,7			
Beams – Moment (Mz)	-4,5 to 4,1	Interstorey drift in X-direction	1,87	FAIL
Beams – Axial (N)	-53,4 to 62,2	Interstorey drift in Y-direction	0,53	PASS

Table 6.1: Numerical seismic analysis results of current building - maximum internal forces and unity checks of column and beam elements

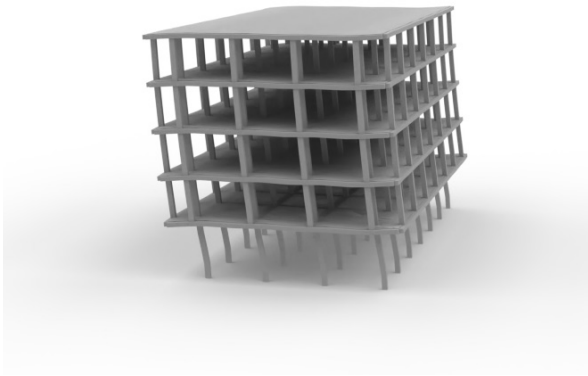

Figure 6.1: Deformation of the case study building in the current situation - load case: ULS-1 (deformation is exaggerated 20x) (author's own work)

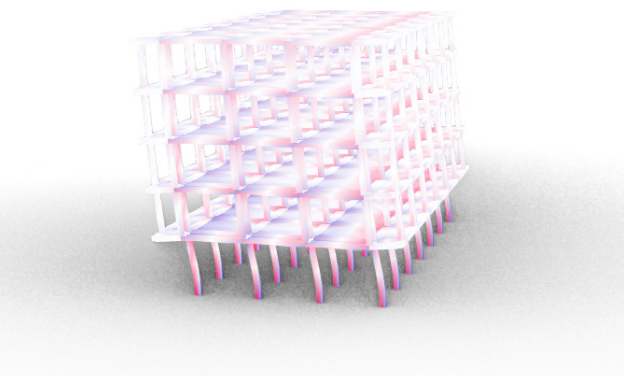

Figure 6.2: Stress strain relation of the members of the case study building in the current situation (red = compression stresses, blue = tension stresses) - load case: ULS-1 (author's own work)

6.2: Retrofit application

The C&D waste that currently burdens Istanbul's landfills and contributes to the waste crisis is, within this proposed system, no longer treated as a disposal problem but rather as a material resource. Now that the recycling process, aggregate upgrading and supply chain are established, the recovered aggregates can serve as input material for the retrofit products. In this way, the C&D waste stream originating from the city's existing and deteriorating building stock is directly redirected to strengthen that same building stock against seismic risk. This section describes the process by which these recycled aggregates are translated into a conceptual precast block design for two retrofit interventions: column jacketing and shear wall application.

6.2.1: Material input: C&D waste properties and mix design

As previously explained, the properties of recycled aggregates are different from those of virgin aggregates. With recycled aggregates, issues such as lower density due to adhered mortar, higher water absorption, and variable strength, since the waste contains a mix of different concrete grades and parent materials, are important factors to keep in mind when designing these resource-aware retrofitting products.

Drawing on the promising results shown in Table 3.3, a hybrid aggregate combination is selected to balance structural performance with recycled content. Aboalella and Elmalky (2023) have shown promising results using a combination of 50% recycled coarse concrete aggregates and 50% recycled fine brick aggregates. The recycled coarse concrete aggregates contribute to mechanical interlocking through their rough surface texture and angular particle shapes, increasing friction and bond with surrounding cement paste, which allows stresses to be transferred more effectively (Diosa-Arenas et al., 2026). However, the fine recycled brick aggregates contain reactive silica and alumina, which, when crushed, can form additional cementitious products through the hydration reaction. This pozzolanic effect helps create additional C-S-H products, which fill pores and improve bond strength at the interfacial transition zone (Aboalella and Elmalky, 2023). While both RCA and RBA offer distinct structural benefits, both are also more porous and water-absorptive than virgin aggregates, meaning pre-soaking, grading and quality control remain essential to ensure reliable aggregate performance.

To make use of both recycled aggregates while keeping the risks associated with high replacement rates manageable, the hybrid mix design proposed by Aboalella and Elmalky (2023) with a 50% aggregate replacement ratio is adopted. This strategy balances circular material use with the need for reliable mechanical performance. For early-stage material design, the mix is specified as a 1:1:2 ratio of cement, fine aggregates, and coarse aggregates. This means that the coarse aggregate fraction accounts for the larger share of the total aggregate content, while the fine aggregate fraction accounts for the smaller share. Within these fractions, 50% of the aggregates are replaced with recycled C&D waste aggregates. However, final proportions, water demand, workability, and mechanical strength properties must be verified through future laboratory mix design and testing to ensure reliable performance. The indicative hybrid aggregate mix design is shown in Figure 6.3 below.

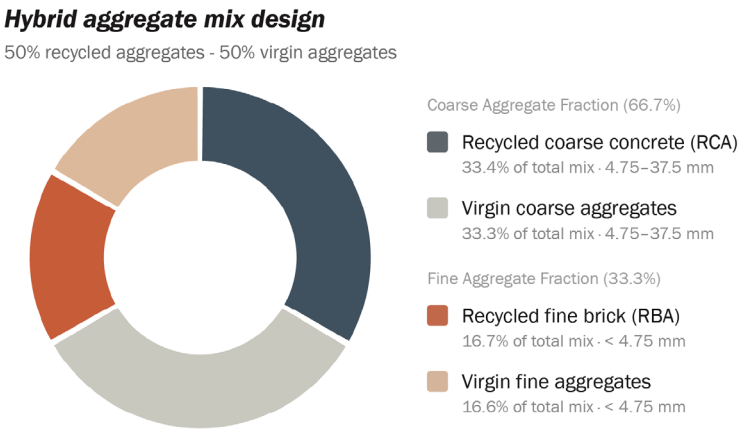

Figure 6.3: The distribution of aggregate type (virgin vs recycled) and aggregate material (coarse concrete vs fine brick) in the hybrid design mix

Scalability and implementation

The retrofit elements are produced as precast concrete elements rather than cast-in-place (CIP) for several reasons related to quality control, material reliability, and site efficiency. A fundamental challenge of using recycled aggregates in structural concrete is their inherent variability in mechanical properties and water absorption, which makes consistent quality difficult to achieve, especially under typical site conditions (Youssef, 2025).

Precast concrete production in a controlled factory environment directly addresses this, as mix proportions, curing conditions, water-cement ratios, and compaction can be strictly monitored and adjusted, ensuring better product consistency. Beyond material quality, precast production offers significant advantages for on-site implementation in Istanbul's dense urban context. Column jacketing and shear wall placement are interventions that typically need to be carried out in occupied or partially occupied residential buildings, meaning construction disruption must be minimised. Precast elements arrive on site ready to install, eliminating the need for large formwork assembly, wet concrete pouring, and extended curing times. This reduces the active construction period per dwelling considerably (Jaillon and Poon, 2007). Additionally, the modular nature of the precast retrofit elements allows them to be produced in standardised sizes to accommodate varying column dimensions and wall configurations, making the system scalable across Istanbul's diverse building stock without requiring tailor-made solutions for every building.

6.2.2: Retrofit product design principles

The fundamental design challenge of using recycled aggregates in structural retrofit elements is that material uncertainty cannot be fully eliminated; it can only be managed. The design strategy therefore deliberately shifts structural responsibility away from reliance on material strength and instead distributes load transfer through multiple mechanical mechanisms: interlocking geometry, reinforcement continuity, and cast-in-place concrete at the critical stress zones of the elements. Each design feature is therefore a direct response to a specific material or structural limitation.

1. Increasing shear bearing capacity

Since seismic forces act laterally on a building, the retrofit system must have strong shear capacity. A critical feature of the precast block design is the incorporation of interlocking shear teeth on all horizontal and vertical mating faces between blocks, inspired by the System3E interlocking masonry principle (see Figure 6.4). These shear teeth serve as the primary mechanism for transferring shear forces between individual blocks under seismic loading. In conventional masonry, for example, the horizontal shear resistance between bricks relies almost entirely on the adhesive bond of the grout joint. However, adhesive bond strength is limited and susceptible to degradation under cyclic loading imposed by earthquakes.

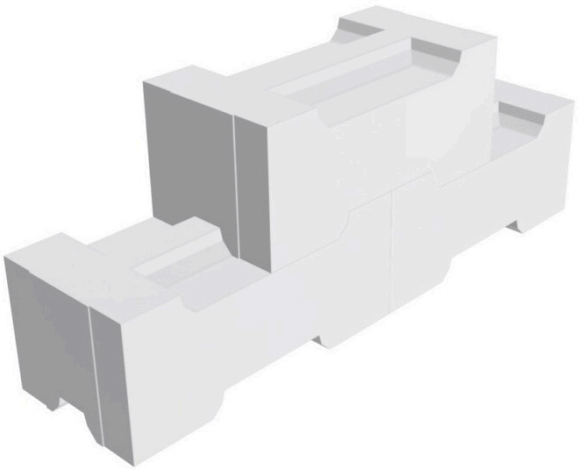

Figure 6.4: Geometry and interlocking masonry stacking-principle of the System3E blocks (SYSTEM 3E Australia, n.d.)

The interlocking teeth overcome this limitation by transferring shear forces through direct mechanical bearing and an adhesive bond. During horizontal shear force application, the protruding teeth of one block bear directly against the recessed teeth of the adjacent block, creating a physical interlock that resists sliding of the blocks. This means that even when the grout bond in between the bricks is partially lost due to seismic cycling, the mechanical interlock ensures continued shear transfer capacity. The suitability of this interlocking principle for seismic zones is computationally tested and supported by System 3E; however, it is explicitly recommended to apply confined or reinforced System 3E constructions to ensure the necessary structural stability and resistance to seismic forces, since unreinforced masonry has a lower ductility and energy dissipation capacity. This is applied in the design philosophy of the precast blocks through adhesion bonds between the blocks and the use of continuous reinforcement.

2. Enabling reinforcement continuity

While the interlocking shear teeth provide mechanical resistance between the blocks, steel reinforcements are essential for the retrofit element. Since concrete is inherently weak in tension, and seismic loading generates significant tensile demands through bending and shear, reinforcements should be incorporated to take on the tensile demands of the structure and provide the necessary tensile resistance and ductility. In these precast blocks, holes and grooves are applied in the mould to ensure sufficient open space is left to accommodate various types of steel rebars. These different types of rebars and the corresponding accommodation within the element are elaborated below.

- Longitudinal rebars - vertical holes

The longitudinal rebars provide the vertical reinforcement continuity and transfer axial and bending forces through the retrofit element. Since longitudinal rebars are steel elements with a larger diameter (typically 8 mm to 32 mm+), large 35 mm holes are used in the blocks to accommodate them. Since full-length bars are impractical, mechanical rebar couplers are applied in the system, allowing shorter bars to be used and connected during the modular installation. Since vertical rebars are used in residential buildings, a smaller diameter is usually required. Together with these mechanical rebar couplers, sufficient space is provided to accommodate them.

- Stirrups - horizontal grooves

In order to provide confinement to the system and prevent the longitudinal reinforcement from buckling under load, stirrups are provided in the blocks. These stirrup elements are accommodated through smaller 16 mm horizontal grooves. After each stack of bricks, these stirrup elements can be placed in the grooves and tied to the longitudinal rebars.

- Shear dowels

To connect the new retrofitting element to the existing frame or column, shear dowels are applied (as shown in Figure 6.5). These shear dowels penetrate pre-drilled holes in the building's current framework and transfer horizontal shear forces between the new strengthening system and the original frame. These shear dowels are essential to ensure composite action; without adequate anchorage, the retrofit block could slide or separate from the existing structural member under lateral loading. In the column jacketing block, shear dowels are accommodated by a small hole, while for the shear wall blocks, it is not accommodated since it is applied at the location where cast-in-place concrete is used.

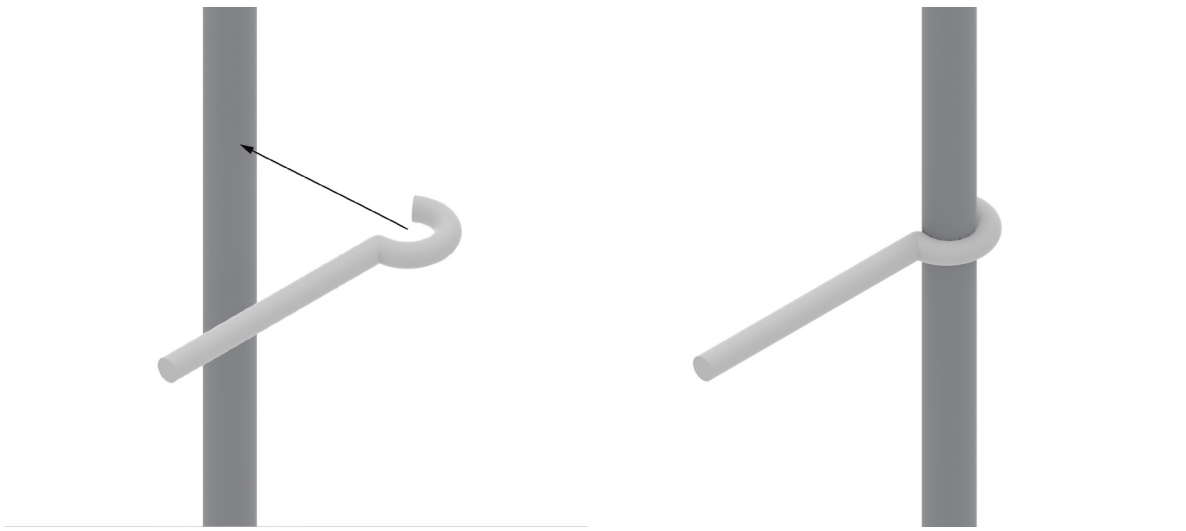

Figure 6.5: Shear dowel connection detail for column jacketing (left) before connection with the longitudinal rebar (right) after connection with the longitudinal rebar (author's own work)

- Cross-ties (only applied at shear walls)

These elements generally have a diameter of 8 mm (as shown in Figure 6.6) and run transversely through the block, connecting the longitudinal reinforcement bars on opposite faces of the shear wall. They improve the overall confinement by preventing the longitudinal bars from buckling. By applying these elements in an S-shape, confinement is improved and the reinforcement cage is prevented from spreading.

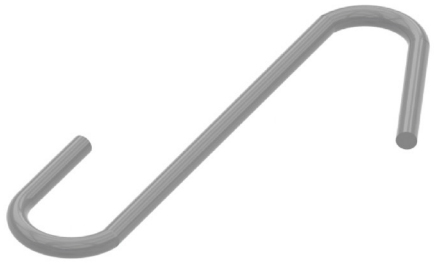

Figure 6.6: Geometry of the S-shaped cross-tie rebar for the connection between two longitudinal rebars in the shear walls (author's own work)

3. Ensuring monolithic connection

To ensure that the applied retrofit element functions as a single system with the existing structural elements, it is important that the connection between the structural frame and the reinforcement of the precast blocks is properly established. For the rebar-to-block connection, a non-shrink cementitious injection grout is applied, which, through its high flowability, fills all gaps between the precast blocks and the steel reinforcement elements, solidifying the assembly into a single composite system. As shown in the previous section, the holes and grooves in the block element are deliberately made thicker than the rebar elements, allowing for different rebar thicknesses, rebar couplers, and, most importantly, space for the cementitious grout to flow through these gaps. The reason to use non-shrink grout is that it maintains its volume during curing, helping ensure permanent contact at all interfaces and reducing the formation of air pockets in the system. This product is injected into the vertical holes of the longitudinal bars and is applied when all precast block elements are stacked. Through the gaps, this grout flows throughout the hole system, solidifying it into a single monolithic structural element.

4. Cast in place boundary zones

The final design principle of the retrofit system is the strategic use of cast-in-place concrete at the boundary zones. Specifically, these zones include the edge areas of the shear walls and the joint regions of the columns, where the highest structural stresses concentrate. Using precast recycled aggregate blocks in such critical zones would be less reliable, since the inherent variability of RCA concrete makes it difficult to guarantee the required strength and ductility precisely where the structural system is most stressed.

For this reason, the boundary zones are cast in place using virgin aggregates and a higher, more reliable concrete strength grade. This ensures more predictable performance at the locations that govern the retrofit capacity. Furthermore, these critical zones typically require additional reinforcement, such as at the shear wall edges, which is difficult to achieve within the precast blocks' fixed holes and grooves. At the top of the retrofitting elements, modular bricks cannot be used due to limited space and the need for rebar continuity. Therefore, cast-in-place concrete in these areas supports a deliberate material zoning strategy: high-reliability CIP concrete where demands are highest, and precast recycled aggregate blocks where demands are lower. In this way, the system maximises circular material use across most of the retrofit element while concentrating structural reliability where it is needed most.

6.2.3: Modular precast column jacketing blocks

The column jacketing retrofit system consists of L-shaped precast modular blocks (see Figure 6.7). Four blocks are assembled per course around the existing column, forming a continuous closed jacket at each layer. Successive rows of blocks are applied in an alternating bond pattern to ensure that vertical joints are never continuous, as such continuity could otherwise present a plane of structural weakness. Between each course, a layer of cementitious adhesive is applied to provide a solid connection alongside the shear bearing connection provided by the shear teeth.

Each block weighs approximately 10 kg, allowing a single site worker to handle and place each block without lifting equipment, which is a deliberate design consideration for constrained residential building conditions. Reinforcement continuity from top to bottom is ensured by using smaller rebar segments connected through compact mechanical rebar couplers, allowing vertical rebar to be connected quickly and avoiding impractical lap splices. Figure 6.8 on the following page shows the additional reinforcement and how the block geometries accommodate it. At the top of the column, where insufficient clearance remains for a full block course, the final rebar segments are inserted by temporarily sliding the couplers down, placing the rebar, and locking the couplers back into position (as shown in Figure I.12 and I.13 in Appendix I). A cast-in-place formwork element then closes the gap between the last blocks and the beam with virgin concrete, ensuring the jacket is fully continuous up to the beam-column joint.

Once all blocks and reinforcements are placed, the assembly is solidified by applying non-shrink cementitious injection grout. This grout is injected into all remaining voids, including the longitudinal reinforcement hole gaps that connect to the stirrup grooves and, more critically, the interface between the inner face of the precast blocks and the existing column surface. This interface connection, visible as the highlighted joint layer in Figure 6.9, is the primary load transfer plane between the new jacketing and the old column. The non-shrink property ensures that no gaps form upon curing, guaranteeing continuous stress transfer. This enables the existing column and the precast jacket to act as a single composite element under seismic loading. Appendix A provides a step-by-step installation plan detailing each phase of the process.

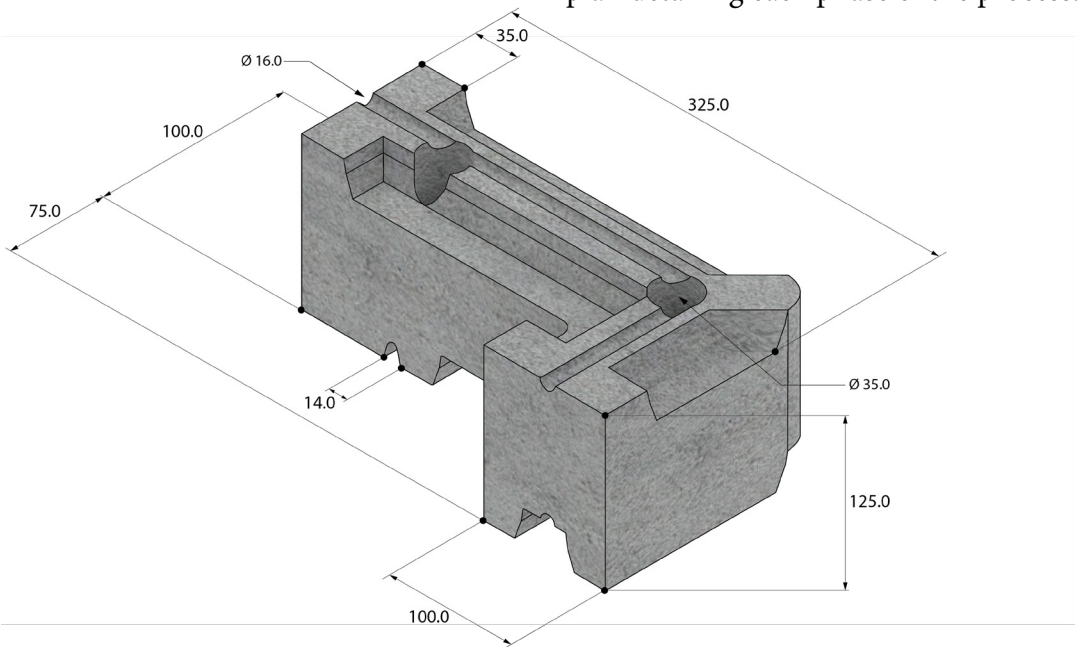

Figure 6.7: Annotated dimensions of the modular precast column jacketing block (all dimensions are in mm) (author's own work)

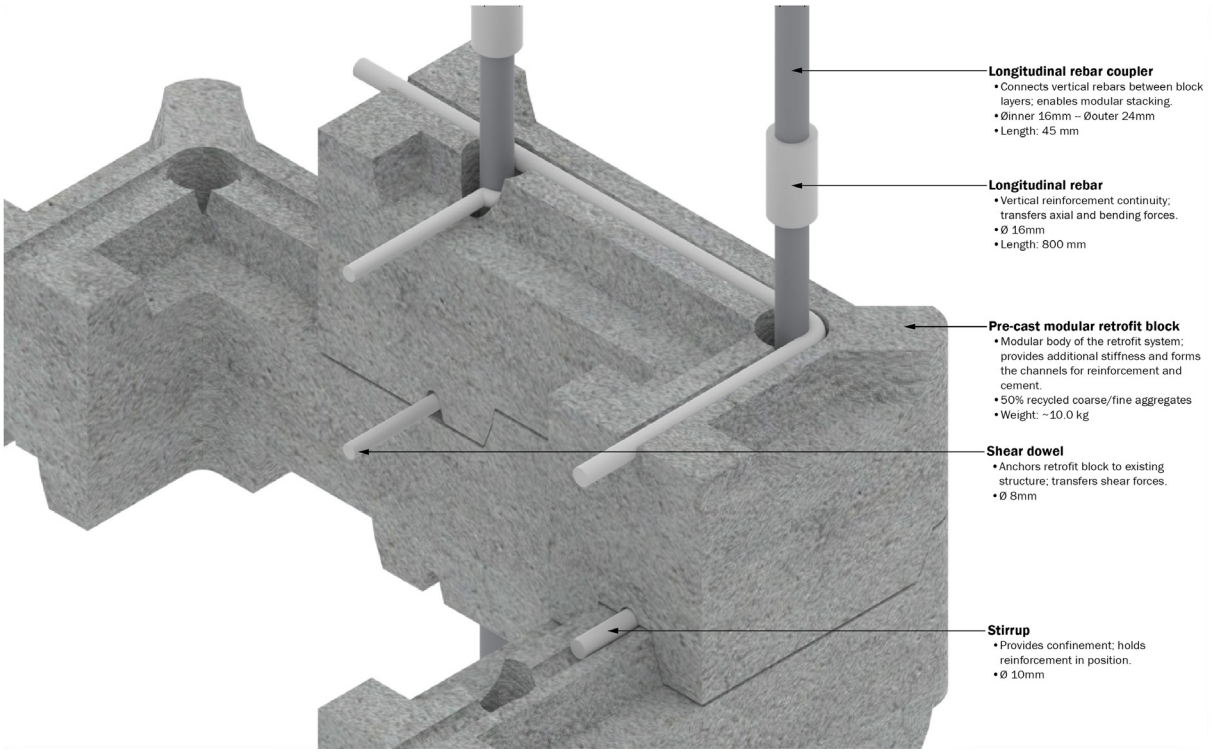

Figure 6.8: The configuration of the modular precast column jacketing block system, showing the different steel components and their functions (author's own work)

Figure 6.9: Application of the non-shrink grout (highlighted in yellow) ensuring proper shear/load transfer between the old column and the new retrofit elements (author's own work)

6.2.4: Modular precast shear wall blocks

The shear wall retrofit system consists of rectangular precast modular blocks stacked in horizontal courses to form the main wall panel, with the same alternating bond pattern as in the column jacketing system (see Figure 6.10), using a cementitious adhesive between courses. At approximately 20 kilograms per block, units remain handleable by two site workers without lifting equipment. To provide transverse confinement around the longitudinal reinforcement, stirrups are looped around the edge rebars and finished with 135° hooks. These stirrups are placed in an alternating pattern along the wall edge, filling one stirrup groove per brick, as shown in Figures 6.11 and 6.12.

While the precast blocks form the main wall body, the bottom foundation strip, the top connection zone, and the vertical boundary elements at both wall edges are cast-in-place using virgin concrete. This is structurally deliberate since the base and top of a shear wall are the primary zones for force transfer under seismic loading, demanding the most reliable concrete. The vertical boundary elements also use cast-in-place to accommodate the dense reinforcement configuration of the stirrup confinements, longitudinal rebars, and shear dowels (which connect to the existing concrete frame), as shown in Figure 6.13. This many reinforcement elements cannot be easily incorporated into the precast block geometry. The resulting hybrid system, shown in Figure J.19 in Appendix J, where the darker precast bricks are framed by the lighter-coloured cast-in-place concrete, concentrates material reliability where structural demand is highest while maximising recycled aggregate use across the middle of the wall.

To keep elements manageable on site, the stirrups are split into shorter segments and connected with mechanical couplers, preventing unwieldy, long stirrup elements while maintaining full reinforcement continuity. Once all block elements are in place and the reinforcements are connected, a non-shrinkage injection grout is used to fill all remaining voids within the block holes and grooves, solidifying the panel into a continuous structural assembly. A step-by-step installation plan is provided in Appendix J.

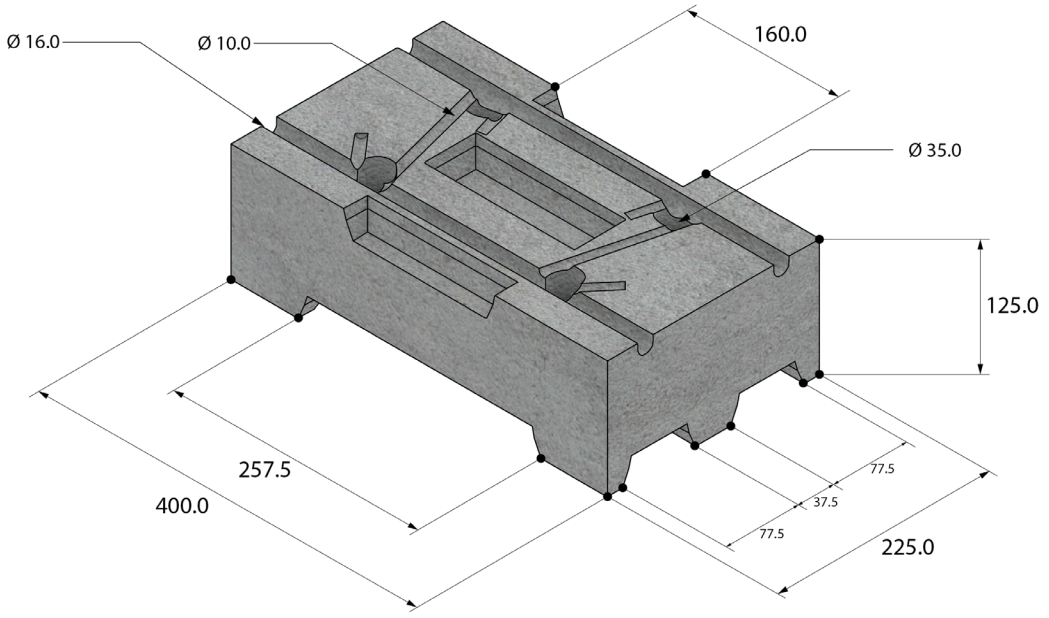

Figure 6.10: Annotated dimensions of the modular precast shear wall block (all dimensions are in mm) (author's own work)

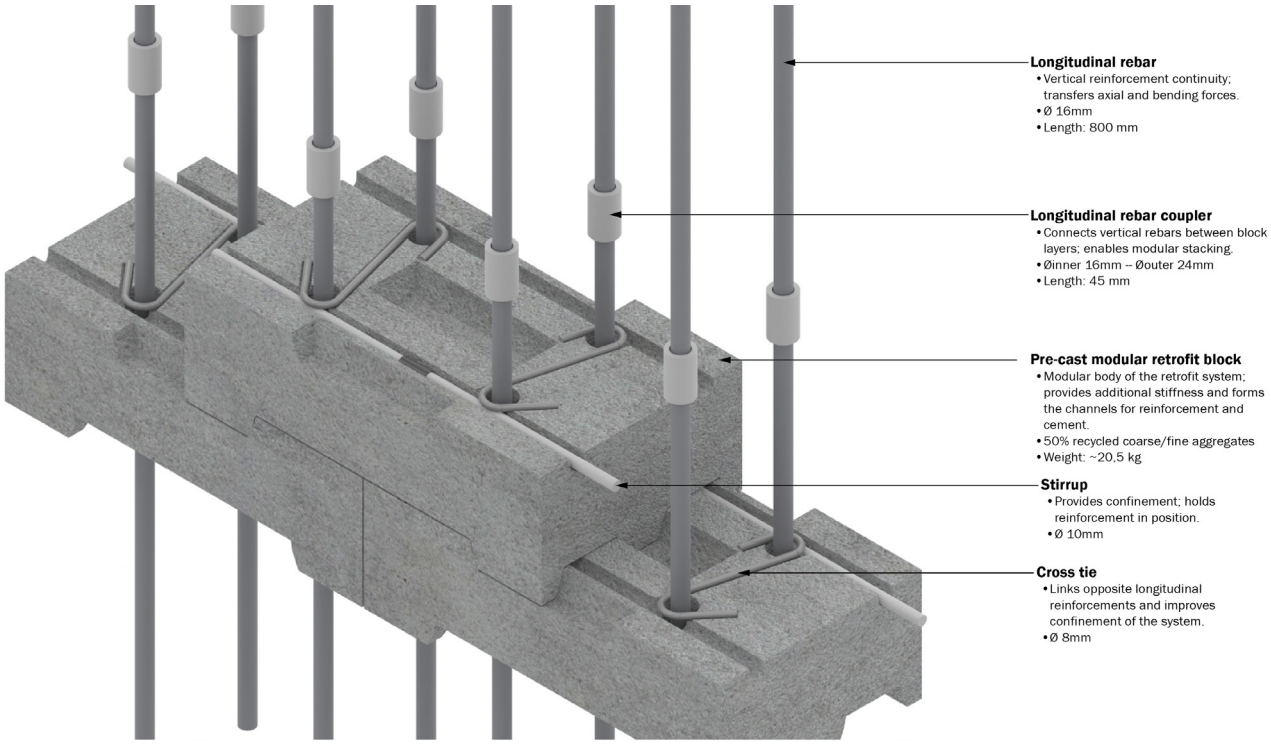

Figure 6.11: The configuration of the modular precast shear wall block system, showing the different steel components and their functions (author's own work)

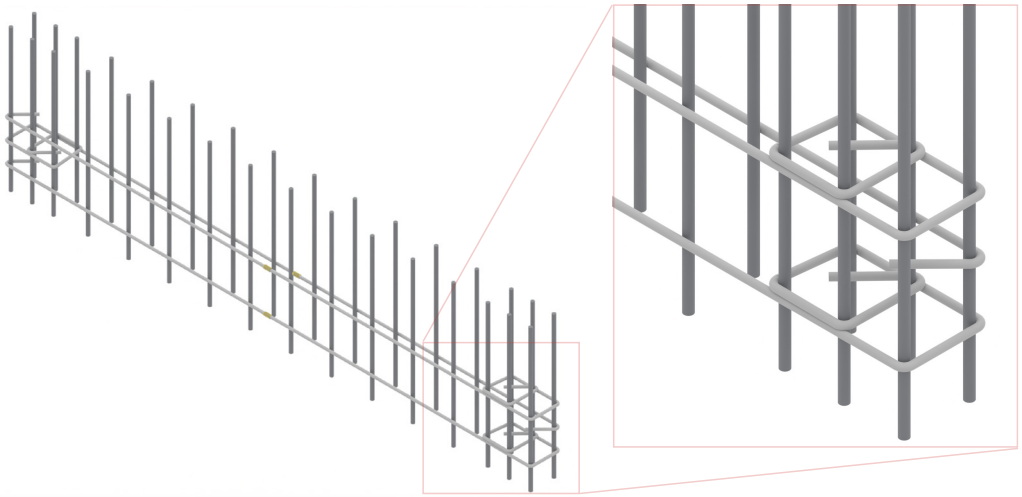

Figure 6.12: Reinforcement cage of the shear wall showing the longitudinal rebars and alternating stirrup placement, with stirrups looping around the edge longitudinal rebars and finished with 135° hooks on alternating faces of the wall (author's own work)

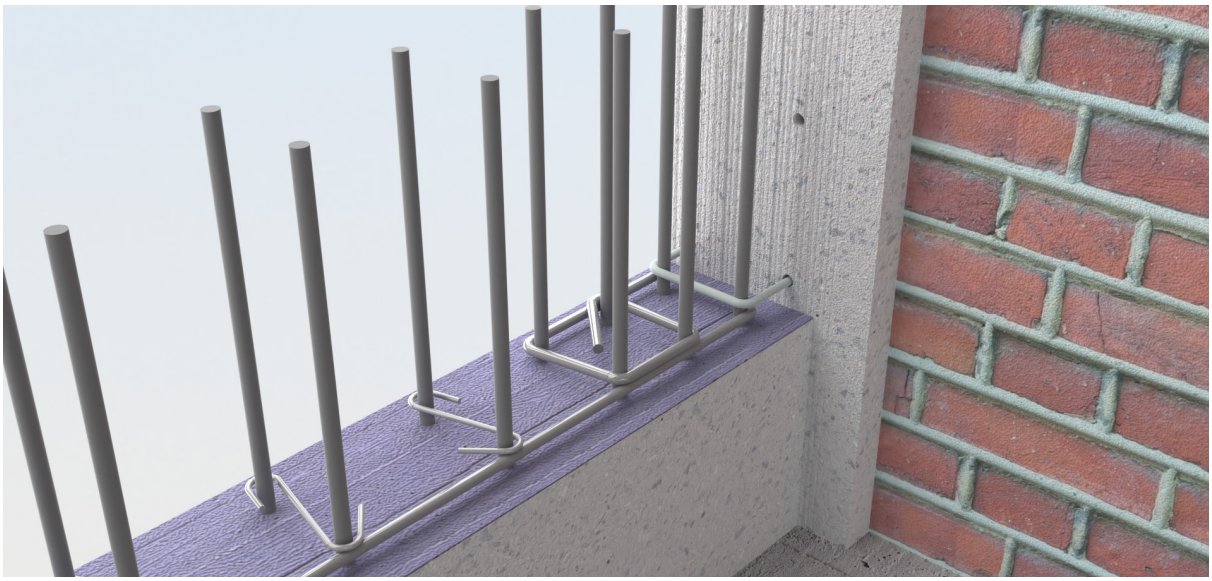

Figure 6.13: Reinforcement configuration at the base of the precast shear wall blocks, showing the dense arrangement of longitudinal rebars, stirrups, cross-ties, and shear dowels at the boundary zone, illustrating the need for cast-in-place concrete (author's own work)

6.2.5: Advantages and disadvantages of modular retrofitting blocks

The retrofit interventions proposed in this research, column jacketing and shear wall addition, are not new techniques in seismic retrofitting. What is novel is the execution method. While conventional column jacketing and shear wall construction rely heavily on cast-in-place concrete, this approach is often reliable but challenging in Istanbul's densely populated residential areas. The modular precast block system proposed here addresses these practical issues. However, the system also introduces its own trade-offs, which are important to acknowledge.

The most immediate benefit of the modular approach is reduced construction invasiveness at the building level. By shifting most wet concrete work to an off-site factory, noise, dust, vibration, and long curing times are minimised for residents. Factory production also improves material control, especially when recycled aggregates are used, since mix proportions, curing conditions, compaction, and water demand can be more consistently monitored than on-site. On-site installation then mainly involves assembly of precast block structure, placing reinforcement, connecting couplers, and injecting grout, thereby reducing the need for extensive formwork and large concrete pours. Each element in the retrofit system is also sized for manual placement by just one on-site worker, making the process more feasible within the spatial constraints of Istanbul's dense neighbourhoods.

However, reducing invasiveness does not necessarily reduce complexity. The modular installation process requires several sequential steps, including wet-pouring concrete in critical zones, precast block placement, reinforcement positioning, dowel anchorage, alignment, and grout injection. Each of these steps is critical to the structural integrity. Therefore, quality control is not eliminated but rather shifted from concrete casting on site to the accuracy of installation, connection detailing, and grout filling. Claims of speed compared to cast-in-place methods should therefore be made carefully. It is more accurate to state that the disruption is more predictable and contained, placing a high priority on using resource-aware materials, modular elements, and easier installation, rather than definitively stating that the process will be shorter.

Furthermore, the system does not completely eliminate cast-in-place concrete. At the boundary zones of shear walls and columns, where stress concentrations are highest and dense reinforcement cannot always easily fit within fixed precast geometries, cast-in-place concrete with virgin aggregates is deliberately used. This is both a structural and a process necessity (how else are blocks at the top placed?), ensuring more reliable performance where structural demands are greatest.

Finally, because this system is not yet a standardised retrofit product, it would require experimental validation, cyclic testing, and regulatory approval before real-world implementation. Its behaviour under repeated seismic loading must be verified. Underlying all these considerations, however, the system remains intentionally resource-aware. The C&D waste currently filling Istanbul's landfills is redirected into retrofit elements that reinforce the very buildings that need it the most. In this way, the demolition waste burden becomes a response to seismic vulnerability.

6.3: Seismic analysis of the retrofitted structure

Based on the vulnerabilities identified in the current-state assessment in 6.1, a combined retrofit strategy is applied to the case study building. The intervention consists of ground-floor column jacketing and the addition of shear wall elements along both outer edges of the building, extending over four storeys (see Figure 6.14). The column jackets are introduced to improve the local capacity of the most critical ground-floor columns, while the shear walls are added to increase the structure's global lateral stiffness and reduce excessive interstorey drift.

Figure 6.15 shows the retrofitted building configuration. The added shear walls create a more continuous lateral load-resisting system. The ground-floor jackets strengthen the columns that previously showed the highest stresses. Figure 6.16 visualises the internal force distribution after the retrofit intervention. Compared with the current state, the demand is less concentrated in the ground-floor columns, indicating that the retrofit strategy effectively redistributes seismic forces through the strengthened frame and the newly added shear walls.

The numerical results in Table 6.2 confirm this improvement. All column capacity checks are reduced to well below the allowable limit. Furthermore, the interstorey drift performance also improves significantly, with the X-direction drift reduced to 0.78 and the Y-direction drift still within the allowable range. This indicates that the shear wall addition successfully reduces the excessive lateral deformation observed in the original structure.

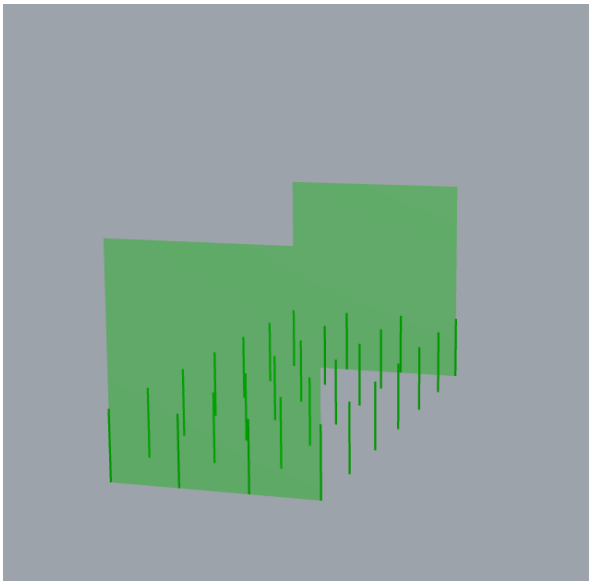

Figure 6.14: The retrofit geometries applied for retrofitting of the current building, showing the location of shear wall application and column jacketing (author's own work)

Internal forces (ULS_1) – Retrofitted situation		***Unity check values (ULS_1)***		
Parameter	Value ranges (kN/kNm)	Parameter	Unity check value	PASS/FAIL
Columns – Shear (Vz)	-11,9 to -0,5	Columns – Shear (Vz/Vy)	0.07	PASS
Columns – Shear (Vy)	19,8 to 48,6	Columns – Moment (Mz/My)	0.13	PASS
Columns – Moment (My)	-18,2 to 24,8	Columns – Axial (compr./tens.)	0,18 / 0,467	PASS / PASS
Columns – Moment (Mz)	-12,6 to 162,4	Columns – Biaxial moment	0.15	PASS
Columns – Axial (N)	-1209,4 to 943,3	Beams – Shear (Vz/Vy)	1,38	FAIL
		Beams – Moment (Mz/My)	0,66	PASS
Beams – Shear (Vz)	-91,3 to 61,6	Beams – Axial (compr./tens.)	0,10 / 0,37	PASS / PASS
Beams – Shear (Vy)	-10,2 to 9,9			
Beams – Moment (My)	-66,6 to 82,2			
Beams – Moment (Mz)	-7,1 to 6,8	Interstorey drift in X-direction	0,78	Pass
Beams – Axial (N)	-164,0 to 148,6	Interstorey drift in Y-direction	0,73	PASS

Table 6.2: Numerical seismic analysis results of retrofitted situation - maximum internal forces and unity checks of column and beam elements

However, the retrofit does not fully eliminate all local deficiencies. The beam shear capacity check remains above the allowable limit, with a value of 1.38. This does not indicate that the retrofit has worsened the beam response; in fact, the beam shear capacity check is lower than in the unretrofitted situation. Rather, it shows that the global intervention successfully reduces demand, but the existing beams still do not have sufficient shear capacity to pass the check. Since the selected retrofit strategy mainly targets ground-floor column capacity and global lateral stiffness through shear wall addition, the beams are not directly strengthened. Therefore, the remaining beam shear failure indicates a local member-level weakness that would require an additional intervention, such as FRP wrapping.

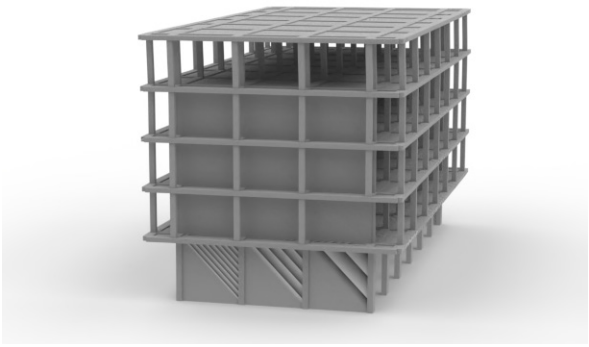

Figure 6.15: Deformation of the case study building in the retrofitted situation - load case: ULS-1 (deformation is exaggerated 20x) (author's own work)

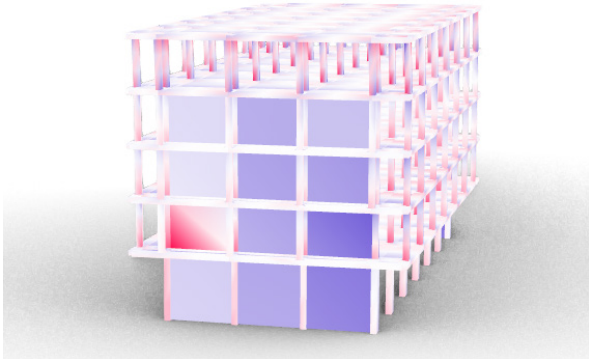

Figure 6.16: Stress strain relation of the members of the case study building in the retrofitted situation (red = compression stresses, blue = tension stresses) - load case: ULS-1 (author's own work)

For a complete retrofit design, this remaining beam shear deficiency would need to be addressed through a supplementary local strengthening measure, such as fibre-reinforced polymer wrapping. In this sense, the workflow demonstrates its value as an iterative assessment tool: it shows how recycled aggregate-based column jackets and shear wall blocks can substantially improve the global seismic response, while also identifying the remaining weaknesses that must be resolved in the next design step.

Beyond the numerical improvement itself, this step demonstrates the value of the parametric workflow as an early-stage retrofit design tool. Once the vulnerability of the current structure is identified, different retrofit strategies can be selected, inserted into the model, adapted and rechecked within the same workflow. This allows engineers and other decision-makers to receive direct feedback on how each intervention affects drift behaviour, internal forces, and member capacity. Instead of treating assessment and retrofit design as separate, time-consuming processes, the workflow enables rapid progression from vulnerability screening to design testing. In this way, the tool supports more rapid and informed decision-making by showing where the building is vulnerable, which retrofit strategy is most appropriate, and whether the chosen intervention sufficiently improves the structural response.

7: Discussion and Conclusions

7.1 Discussion

The developed system design demonstrates that a typology-based parametric approach can meaningfully compress the preliminary stages of seismic assessment and retrofit design into a single structured environment. Where conventional building-by-building assessment can take weeks to months per structure, the proposed workflow significantly reduces this for modelling, analysis, and initial retrofit verification. This acceleration should not be understood as a substitute for detailed engineering analysis. Rather, it functions as a rapid, preliminary assessment tool that streamlines selected stages of the process to identify potential structural vulnerabilities and compare potential retrofit strategies at an early design stage, thereby speeding the process. Given the scale of the problem in Türkiye, where approximately 6.7 million residential buildings require structural intervention, the current assessment pace leaves the majority of the vulnerable population unaddressed.

The case study performed in 5.6.2. demonstrated that the workflow functions as intended end-to-end. Survey input was translated directly into a parametric model, seismic loads were calculated and distributed, and capacity deficiencies were identified in an instance. After the building's vulnerability screening, a retrofit intervention strategy was implemented, and improved performance was verified. The remaining beam moment deficiency also shows the honesty of the tool, in a way that the tool does not oversimplify structural behaviour and correctly signals that the chosen intervention does not resolve all failure modes, a quality which is essential for a reliable decision support tool.

A key implication of the work is the shift from isolated assessment to the ability, for instance, of municipalities to apply typological reasoning. Buildings that share similar construction periods, structural systems and other geometric characteristics could be grouped into comparable archetypes. This allows recurring vulnerabilities, such as soft-storey behaviour, interstorey drift or insufficient member capacity to be identified more rapidly. The workflow therefore has potential value not only for individual engineers, but also for municipalities and public authorities seeking to prioritise seismic risk reduction at district scale.

Perhaps one of the most fundamental lessons this research reveals is not just technical but philosophical. The system designed here does not work because the aggregates are of perfect quality, but because the structural and material logic is designed to function responsibly with the quality they offer. This is achieved by distributing structural responsibility across geometry, connection detailing, and composite action rather than concentrating it solely on material strength. The integration of recycled C&D waste is central to this logic: by positioning demolition rubble as a material input rather than a disposal problem, the framework proposes a system in which the same urban transformation processes that generate waste also supply the material for strengthening the vulnerable buildings that remain. This reflects a broader shift in design thinking that the construction industry will increasingly be forced to confront. Virgin materials are becoming scarcer and more costly, while demolition waste is accumulating in volumes that landfill infrastructure cannot sustainably handle. The instinct to wait for something cleaner, stronger, or better characterised is understandable, but it is a missed opportunity at exactly where opportunity is needed.

The case study demonstrates that, even with a confidence factor of 0.60, column jacketing delivers sufficient capacity gain, providing this material concept with some engineering ground. However, systematic physical testing remains essential before field application. What this thesis argues, implicitly through its design and confidence factor, is that the question is not whether recycled materials should be made perfect, but whether our structural systems are robust and intelligent enough to use them responsibly. Designing around material imperfection is not a compromise. It is the direction that engineers and designers will ultimately have to take, considering that in this world, where the mines are emptying and the rubble pile is growing, most responsible materials are those already around us.

7.2 Limitations

The designed framework is subject to several limitations that must be acknowledged. One of the most significant limitations relates to the material uncertainty of the recycled C&D waste blocks. Their compressive strength, elastic modulus, durability, and long-term behaviour under cyclic seismic loading have not yet been characterised through standardised testing. The material confidence factor of 0.60 was therefore introduced as a conservative engineering assumption, rather than as a code-prescribed value. Until laboratory testing provides reliable mechanical properties and validated confidence factors, the tool should be understood as a vulnerability screener and early-stage design tool rather than a final design verification tool.

A second limitation concerns economic feasibility. The cost of producing, transporting, and installing precast recycled C&D waste blocks at scale is currently unknown. Material costs, labour requirements, recycling plant economics, and the market price of recycled aggregates compared with virgin aggregates could strongly influence whether the proposed system is competitive with conventional retrofit techniques. A detailed cost analysis is therefore critical.

There are also limitations related to structural modelling. The Karamba3D analysis is based on elastic modelling and therefore does not capture nonlinear or post-yield behaviour, such as plastic hinge formation, stiffness degradation, or progression toward collapse. In addition, Karamba3D does not have the ability to model reinforced concrete as a composite interaction between concrete and reinforcement. This required the workflow to use workarounds through analytical calculations. As a result, the model is useful for early-stage comparison and vulnerability screening, but not for detailed nonlinear reinforced-concrete verification.

A further limitation concerns the verification of the retrofit interventions themselves. In the current workflow, retrofit performance is assessed by inserting the proposed column jackets and shear wall elements into the model and comparing drift, internal forces, and unit checks before and after intervention. This gives useful early-stage feedback on whether a retrofit strategy improves the seismic response. However, critical aspects of connections, such as dowel anchorage, interface shear transfer, reinforcement coupler performance, diaphragm action, and the cyclic behaviour of precast blocks, are not explicitly checked. Therefore, the workflow should be understood as a screening tool, while real-world implementation would require detailed code-compliant design, nonlinear assessment and laboratory testing.

Finally, full N-M interaction for columns, combining axial force with biaxial bending simultaneously, is not implemented in the current version of the tool. Constructing a full interaction diagram for every column would require section-level analysis and cross-section sweeping, both of which are complex and time-intensive within the current Grasshopper environment. A simplified linear interaction check was considered but proved too conservative because it combines peak internal force values that may not occur simultaneously at the same location within the cross-section. Therefore, axial force and bending moments are currently checked independently, while full N-M interaction verification is considered an important direction for future development.

7.3 Future research

The current system design represents an early-stage foundation with clearly defined boundaries. The following steps are critical for future development of both the tool and the broader system.

The most urgent next step is full-scale mechanical testing of the recycled C&D waste blocks. This would allow the confidence factor of 0.60 to be replaced with a code-compliant partial factor for a code-compliant material, transitioning the tool from a proof-of-concept to an engineering-grade application. Alongside this, a cost framework should be developed that maps the full economics of the process from waste collection and aggregate processing through block production to on-site application. Given that cost feasibility can fundamentally influence the viability of the proposed system, this is not an optional addition but a necessary validation step.

A further refinement of the workflow concerns the formulations used for capacity checks during local member verifications. Due to time constraints and the interpretational challenges associated with working in a different language, the member capacity checks in this study are based on NEN-EN-1992-1-1 rather than the Turkish seismic code. For full compliance and practical deployment within a Turkish engineering context, these formulations should be replaced by the corresponding provisions of TBDY 2018 in future development of the tool.

A further development of the workflow that could be added in future research is the direct quantification of the material demand directly from the retrofit output. Once a retrofit intervention is selected and configured in the parametric environment, the model contains all the geometric information needed to calculate the required material quantities. The number of precast blocks, volume of cast-in-place concrete, total rebar length and diameter, stirrup quantity and diameter. As a direct function of the building geometry and the chosen intervention, this would allow the workflow to directly link the identified retrofit demand to a quantified supply requirement.

Extension to the tool itself represents another logical direction. The flexible parametric environment can be expanded by incorporating additional retrofit intervention types, such as steel bracings or fibre-reinforced polymer wrapping (the latter already identified as necessary by the beam moment deficiency in the case study). Furthermore, if a way can be found to more accurately model the composite behaviour of reinforced concrete within Karamba3D, the tool could reduce reliance on separate numerical capacity checks and shift toward more visual, immediate output through utilisation diagrams and stress visualisations directly in the model, significantly enhancing the workflow.

Once the tool is sufficiently developed for the current typology, extending it to other common Turkish building typologies is a natural next step, though this may require more advanced seismic calculation methods beyond the equivalent static approach, potentially requiring an alteration of the current workflow.

A key longer-term achievement would be the possibility of grouping buildings that share similar construction periods, structural systems, and geometric characteristics into comparable archetypes, for which this tool provides a foundation for an archetype database. Once populated, this database would allow recurring vulnerabilities to be identified rapidly across entire building groups without having to repeat the full assessment for each individual structure. The workflow therefore has the potential value to provide insight for municipalities and public authorities seeking to prioritise seismic risk reduction at a larger scale in a more systematic way.

7.4 Answering of research questions

"How can a system design strategy be developed to accelerate the seismic assessment and by extension retrofit design of mid-rise reinforced concrete frame buildings in Türkiye, while enabling the integration of recycled construction and demolition materials?"

The answer this research proposes is not a single tool, but a system where two independently developed tracks, a structural assessment workflow and a material recovery process, are deliberately designed to converge. By making the assessment and retrofit process faster, more resource-efficient, and grounded in locally available waste streams, the system aims to lower the threshold for seismic intervention, making retrofitting not only quicker and more resource-aware, but ultimately more accessible to the communities that need it most.

The structural design track demonstrates that acceleration is achievable by shifting assessment from a building-by-building approach to one grounded in typological backing. By recognising that a significant portion of Türkiye's vulnerable residential stock shares recurring geometric and structural characteristics, the workflow replaces repetitive building-specific modelling with a parametric logic in which a structured survey translates directly into an automated geometric model, seismic load calculation, structural analysis, and capacity verification. All within a single tool. What conventionally takes a lot of time is now compressed significantly. Critically, this time-saving does not eliminate engineering judgement; it redirects it. The engineer is no longer occupied with manual modelling and load input but with interpreting results and selecting interventions, the decisions that actually require engineering expertise.

The material track demonstrates that C&D waste, currently treated as a disposal problem in Türkiye, can be repositioned as a structural resource. Concrete and brick rubble, the dominant material fractions of Turkish urban demolition, can be processed into recycled aggregates and cast into precast modular blocks suitable for column jacketing and shear wall applications. Currently, the material confidence factor of 0.60 ensures that the integration of this unverified material into a structural context is handled conservatively. The case study confirmed that even under these conservative assumptions, the retrofit delivers sufficient capacity gains to the members.

The system design emerges precisely where these two tracks meet. The structural workflow generates a quantified retrofit demand, what members fail, by how much and through what mechanism. The material track generates a supply of retrofit elements derived from local demolition waste. By aligning demand with supply within the same parametric framework, the system closes a loop that conventional practice leaves open: the same urban transformation processes that demolish vulnerable buildings and generate rubble can now also create the material needed to strengthen what remains. Vulnerable buildings serve as both a source of recycled material and a target for seismic resilience.

Answering of sub-questions

The sub-questions, which have been introduced in the beginning of this report, guided the development of the material, structural, and system design track. This section briefly reflects on how each question has been addressed in this research.

Material design sub-questions

The material design questions were addressed by identifying concrete and brick rubble as the most relevant C&D waste fractions for structural retrofit applications in Türkiye. These fractions are closely connected to the dominant reinforced concrete frame and masonry infill building stock, making them both available and materially relevant. The proposed recycling process shows how these waste streams can be separated, crushed, cleaned, graded, and upgraded into recycled concrete and brick aggregates suitable for conceptual retrofit products. Finally, the thesis demonstrates how these aggregates can be translated into modular precast elements for column jacketing and shear wall applications.

Structural design sub-questions

The structural design questions were addressed through the development of a parametric seismic assessment workflow for a representative mid-rise reinforced concrete frame building typology. The workflow uses survey-based input data to generate a simplified structural model, apply seismic loading, assess interstorey drift and member capacity, and identify critical vulnerabilities. These assessment outputs then inform the selection of retrofit strategies, such as column jacketing where member capacity is insufficient and shear wall addition where lateral stiffness and drift performance require improvement. The case study demonstrates that these interventions can be incorporated into the same parametric model and rapidly rechecked, enabling rapid, iterative design evaluation.

System design sub-questions

The system design questions were answered by integrating the structural demand side with the material supply side. The structural workflow identifies the type and location of needed retrofit, while the material workflow proposes how recycled C&D waste can be processed into retrofit components that meet that demand. The system therefore functions as an early-stage decision-support framework, since it does not replace detailed engineering verification, but helps identify vulnerabilities, test retrofit strategies, and compare performance improvements more quickly. Its potential for standardisation lies in its typology-based logic, in which buildings with similar structural characteristics can be assessed using comparable input parameters and retrofit decision pathways.

7.5 Conclusion

This thesis demonstrated that integrating survey-based input, parametric modelling, and structural analysis into a single coherent environment enables rapid early-stage seismic assessment and retrofit design for typologically similar buildings. The results have shown that the implementation of retrofitting strategies influences the seismic behaviour of mid-rise reinforced concrete frame buildings in measurable, predictable ways. These insights informed the development of a parametric workflow designed to make typology-based vulnerability screening applicable. However, if the current limitations in verifying the mechanical strength of recycled C&D waste blocks and in the cost framework are validated, the results could serve as a foundation for implementation across the broader vulnerable building stock in Türkiye.

The thesis set out to explore whether a parametric system design could accelerate seismic assessment and retrofit design while integrating recycled construction and demolition materials. The proposed workflow proved to be structured, repeatable, and functional even in its early development stage. The combination of a digital survey, rule-based parametric geometry, automated load calculation, and integrated capacity verification enabled a complete assessment in a quick environment. These findings not only validate the design methodology but also open the door to early-stage seismic vulnerability screening tools that go beyond a single building typology and the implementation of just a few retrofitting intervention strategies.

Beyond structural feasibility, the material integration confirmed that concrete and brick rubble from construction and demolition waste processes in Istanbul represents a large, locally available, and technically recyclable resource that is currently largely lost to landfilling. By embedding recycled aggregates into precast retrofit blocks, the proposed system reduces reliance on virgin construction materials and redirects the waste towards a standardised structural solution. This positions vulnerable buildings not only as targets for seismic intervention, but also as part of a wider material system in which demolition waste can be recovered, processed and reintroduced into the strengthening of the existing building stock. In this way, the workflow connects seismic vulnerability with material circularity, demonstrating how retrofit demand and recycled-material supply can be addressed within a single integrated framework.

The workflow reframes seismic retrofitting as a system design challenge rather than a purely technical one. The results suggest that structural performance and material circularity can coexist within a single integrated framework. If proven economically feasible and materially validated, the proposed system could be extended across additional building typologies and types of retrofit interventions, developing it into a comprehensive decision-support tool for engineers, municipalities, and public authorities involved in seismic risk reduction. This contributes not only to the design of a single retrofit product or digital model, but also to the demonstration of a scalable framework for approaching Türkiye's seismic resilience challenge more systematically.

7.6 Reflection

Looking back on this thesis, the research process worked out better than originally anticipated. The decision to immerse broadly in the problem context, spanning seismic engineering, material science, recycling infrastructure, and urban policy, proved to be foundational to this research, even though it also brought a necessary degree of chaos. Understanding the full chain of the issue before narrowing it down to the workflow development allowed it to be planned with a coherence that would have been more difficult to achieve had the research been differently scoped. Within the graduation studio, the project is positioned between building technology, structural design, and circular material thinking. It therefore does not treat seismic retrofitting only as an engineering calculation, but as a system design problem in which seismic assessment, material supply, and implementation must be connected.

The relationship between research and design became clearer throughout the process. The research defined the scale of the problem, the vulnerable building typology, the limitations of current assessment methods, and the potential of recycled aggregate-based retrofit elements. The design work then translated these findings into a parametric workflow and a conceptual retrofit system. In that sense, the method directly shaped the outcome: because the research question focused on speed, scalability, and resource-awareness, the final output became an early-stage decision-support tool that automates repetitive steps.

At the same time, knowing that this tool is still in its early stages generates more motivation than satisfaction. Being deeply involved in the parametric workflow and system design made it clear that there are still many directions for refinement, validation, and testing. The intended result was not to produce a legally complete retrofit assessment, as this would be impossible within the given time, but to demonstrate how vulnerability screening and retrofit strategy testing could be accelerated. In retrospect, the project achieved its main aim, while also making its limitations visible.

The parametric workflow also represented a personal learning curve. Entering the project without extensive Grasshopper experience meant that large ambitions had to be broken down into small, testable steps. In retrospect, this constraint became an asset to me. It enforced a discipline of taking incremental steps in the tool's design, keeping it organised and grounded in what was verifiable or doable at each stage, rather than allowing the project to become too speculative and thereby losing its essence.

At last, the main ethical dilemma was the risk of overclaiming. Since seismic safety is directly connected to human lives, the workflow cannot be presented as a replacement for professional engineering judgement or a final code-compliant assessment. I dealt with this by framing the tool as an early-stage design and decision-support workflow: useful for swiftly identifying vulnerabilities, comparing retrofit options, and guiding faster prioritisation and decision-making, but always requiring further detailed verification. The ambition is not to simplify seismic safety irresponsibly, but to make the first step towards safer buildings in a faster, clearer and more accessible way.

8: Bibliography

Abdelfatah, A., Tabsh, S., & Yehia, S. (2011). Utilization of Recycled Coarse Aggregate in Concrete Mixes. Journal of Civil Engineering and Architecture, 562-566.

Aboalella, A. A., & Elmalky, A. (2023). Use of crushed bricks and recycled concrete as replacement for fine and coarse aggregates for sustainable concrete production. Challenge Journal Of Concrete Research Letters, 39-46.

Arcler Projects LLP. (n.d.). Air density separator. Retrieved June 10, 2026, from https://arclerprojects.com/cms-product/air-density-separator/

Afet ve Acil Durum Yönetimi Başkanlığı. (2018). Türkiye bina deprem yönetmeliği: Deprem etkisi altında binaların tasarımı için esaslar. T.C. İçişleri Bakanlığı, Afet ve Acil Durum Yönetimi Başkanlığı.

Akarsu Akdemir, B., Bozkurt, F. S., & Aluçlu Armutcu, G. (2025, May 12–14). UrbanReCrete: A sustainable approach to concrete waste recycling in Istanbul [Conference paper]. 4th International Graduate Research Symposium, İstanbul, Türkiye. https://www.researchgate.net/publication/399755313_UrbanReCrete_A_Sustainable_Approach_to_Concrete_Waste_Recycling_in_Istanbul

Alkhteeb, L., & Dawood, M. B. (2025). The effect of recycled aggregate on properties of concrete: A review. Hybrid Advances, 1-16.

Akın, M., Tuncer, H. B., & Yastı, A. Ç. (2024). One disaster two traumas: Being under rubble and burn injuries in the 2023 Maraş, Turkey earthquakes. Burns, 50(6), 1456–1462. https://doi.org/10.1016/j.burns.2024.03.001

Arslan, H., Coşgun, N., & Salgın, B. (2012). Construction and Demolition Waste Management in Turkey. In L. F. Rebellon, Waste Management - An Integrated Vision (pp. 313-332). IntechOpen.

Arslan, V., & Ulubeyli, S. (2019). SORTING AT SOURCE AND REUSING: THE CASE OF CONSTRUCTION AND DEMOLITION WASTE IN TURKEY. International Civil Engineering And Architecture Conference, (pp. 230-236). Trabzon.

Asadimanesh, M., & Jalilifard, F. (2025). Review of Modern Methods for Seismic Retrofitting of Reinforced Concrete Structures. Concept and Function in The Building Engineering, 27-43.

Barrera-Vargas, C. A., Díaz, I. M., Soria, J. M., & Garacía-Palacios, J. H. (2020). Enhancing Friction Pendulum Isolation Systems Using Passive and Semi-Active Dampers. Applied Sciences, 1-23.

Bonifazi, G., Grosso, C., Palmieri, R., & Serranti, S. (2025). Current trends and challenges in construction and demolition waste recycling. Green and Sustainable Chemistry, 1-9.

City of San José Environmental Services Department. (n.d.). San José construction and demolition diversion program (CR&D Case Study 8). Government of British Columbia. https://www2.gov.bc.ca/assets/gov/environment/waste-management/zero-waste/case-studies/cs_sanjose.pdf

Coelho, A., & de Brito, J. (2013). Economic viability analysis of a construction and demolition waste recycling plant in Portugal—Part I: Location, materials, technology and economic analysis. Journal of Cleaner Production, 39, 338–352. https://doi.org/10.1016/j.jclepro.2012.08.024

Connelly, T. (2025, June 4). Impact Air Systems launches a next-gen material drum separator. Retrieved from wastetoday magazine.com: https://www.wastetodaymagazine.com/news/impact-air-systems-drum-separator/#:~:text=The%20versatility%20of%20the%20ADS,for%20downstream%20recovery%20or%20processing.

Damptech Earthquake Protection. (n.d.). Description of Friction Dampers. Retrieved from Damptech.com: https://www.damptech.com/description

Demir, G., Kolay, U. E., Ökten, H. E., & Alyüz, Ü. (2016). Selection of alternative landfill location by using a geographical information system: European side of Istanbul case study. Environment Protection Engineering, 42(1). https://doi.org/10.37190/epe160110

Demir, I., Arıkan, O. A., & Maçin, K. E. (2017). Construction and Demolition Waste Management in Turkey. International Conference on Engineering Technology and Innovation. Sarajevo.

Demir, U., & Doğan, F. (n.d.). Structural Lessons from Türkiye's Earthquakes: Design-Inspection-Destruction Nexus. Structures, 30(5), 1360–1374.

Designing buildings - The construction wiki. (2022, March 9). Trial pit. Retrieved from designingbuildings.co.uk: https://www.designingbuildings.co.uk/wiki/Trial_pit

Ding, Y., She, A., & Yao, W. (2023). Investigation of water absorption behavior of recycled aggregates and its effect on con crete strength. Materials, 16(13), Article 4505. https://doi.org/10.3390/ma16134505

Diosa-Arenas, J. S., Rojas-Manzano, M. A., Madera-Sierra, I. E., & Maury-Ramírez, A. (2026). Influence of High-Perfor mance Recycled Aggregates on Mechanical Properties of High-Strength Concrete. Infrastructures, 11(2), 66. https://doi.org/10.3390/infrastructures11020066

Dlubal. (2024, April 24). Seismic zones of Turkey according to TBEC:2018. Dlubal. Retrieved May 29, 2026, from https://www.dlubal.com/en/load-zones-for-snow-wind-earthquake/seismic-tbec.html

Erberik, M. A. (2008). Fragility-based assessment of typical mid-rise and low-rise RC buildings in Turkey. Engineering Structures, 30(5), 1360–1374. https://doi.org/10.1016/j.engstruct.2007.07.016

European Committee for Standardization (2004, December). Eurocode 2: Design of concrete structures—Part 1-1: General rules and rules for buildings (BS EN 1992-1-1:2004). BSI. https://www.phd.eng.br/wp-content/uploads/2015/12/en.1992.1.1.2004.pdf

European Committee for Standardization (2005, June). Eurocode 8: Design of structures for earthquake resistance—Part 3: Assessment and retrofitting of buildings (BS EN 1998-3:2005). BSI.

European Parliament and Council of the European Union. (2008). Directive 2008/98/EC of the European Parliament and of the Council of 19 November 2008 on waste and repealing certain Directives. Official Journal of the European Union, L 312, 3–30. https://eur-lex.europa.eu/legal-content/EN/TXT/?uri=CELEX:32008L0098

FABO. (2024a). FABO 2024 catalog. Récupéré sur https://www.scribd.com/document/757468382/FABO-2024-Catalog

FABO. (n.d.-a). CLK-60 Jaw Crusher. Récupéré sur fabo.com: https://fabo.com.tr/en/product/stationary-crushing-plants/jaw-crushers/clk-60-jaw-crusher/

FABO (n.d.-b). PDK-70 primary impact crusher [Product brochure]. FABO.

FABO Company. (n.d.-c). TE16-50 vibrating screen. Retrieved May 31, 2026, from https://fabocompany.com/tek-1650-vibrating-screen

FABO Global. (n.d.). DSHC-1224 dewatering screen. Retrieved May 31, 2026, from https://faboglobal.com/products/stationary-crushing-screening-plant/dshc-series-dewatering-screens/dshc-1224-dewatering-screen/

FEECO International. (n.d.). Agglomeration equipment [Product brochure]. FEECO International.

García-González, J., Rodríguez-Robles, D., Juan-Valdés, A., Morán-del Pozo, J. M., & Guerra-Romero, M. I. (2014). Pre-Saturation Technique of the Recycled Aggregates: Solution to the Water Absorption Drawback in the Recycled Concrete Manufacture. Materials, 7(9), 6224-6236. https://doi.org/10.3390/ma7096224

Gokdemir, H., Ozbasaran, H., Doğan, M., Unluoğlu, E., & Albayrak, U. (2013). Effects of torsional irregularity to structures during earthquakes. Engineering Failure Analysis, 713-717.

Gómez-Cano, D., Arias-Jaramillo, Y. P., Bernal-Correa, R., & Tobón, J. I. (2023). Effect of enhancement treatments applied to recycled concrete aggregates on concrete durability: A review. Materiales de Construcción, 73(349), e308. https://doi.org/10.3989/mc.2023.296522

Google. (n.d.). Google Earth [Web mapping service]. Retrieved March 17, 2026, from https://earth.google.com/

Gülgün, B., Yazici, K., Dursun, S., & Tahta, B. T. (2016). Earthquake Park Design and Some Examples from the World and Turkey. Journal of International Environmental Application and Science, 159-165.

Gulkan P., Aschheim, M., & Spence, R. (2002, June 05). World Housing Encyclopedia - an Encyclopedia of Housing Construction in Seismically Active Areas of the World. Turkey.

Gundes, S., Atakul, N. & Büyükyoran, F. (2017). Earthquake Preparedness: Evaluation of Urban Transformation Law in Turkey. 16th World Conference on Earthquake Engineering, Santiago, Chile.

Güneş, O. (2015). Turkey's grand challenge: Disaster-proof building inventory within 20 years. Case Studies in Construction Materials, 2, 18–34. https://doi.org/10.1016/j.cscm.2014.12.003

Gupta, A., & Yan, D. S. (2016). Jaw crusher. In Mineral processing design and operations: An introduction (2nd ed.). Else vier. https://www.sciencedirect.com/science/chapter/edited-volume/pii/B9780444635891000046

Gurbuz, T., & Cengiz, A. (2025). Structural damages during the February 06, 2023 Kahramanmaraş Earthquakes in Turkey. Soil Dynamics and Earthquake Engineering.

Habertürk. (2017, August 16). Prof. Celal Şengör uyardı: İstanbul depreminin eli kulağında. Habertürk. https://www.haber turk.com/gundem/haber/1599735-prof-celal-sengor-uyardi-istanbul-depreminin-eli-kulaginda

Ilki, A., & Celep, Z. (2012). Earthquakes, Existing Buildings and Seismic Design Codes in Turkey. Arabian Journal for Science and Engineering, 365-380.

Illinois Recycling Association. (2005, September). Best operational practices manual for materials recovery facilities and recycling drop-off facilities. Retrieved from csu.edu: https://www.csu.edu/cerc/researchreports/documents/ BestOperationalPracticesManualForIllinoisRecyclers.pdf

Impact Air Systems. (n.d.). Air Drum Separator (ADS). https://impactairsystems.com/solutions/air-drum-separator-wind shifter/

İSTAÇ. (n.d.). Enerji üretim tesisleri. Retrieved March 15, 2026, from https://www.istac.istanbul/tesislerimiz/enerji-ure tim-tesisleri

İstanbul Büyükşehir Belediyesi Deprem ve Zemin İnceleme Şube Müdürlüğü. (n.d.). Possible earthquake loss estimates district booklets. İBB Deprem Zemin. Retrieved May 28, 2026, from https://depremzemin.ibb.istanbul/en/possi ble-earthquake-loss-estimates-district-booklets

İstanbul Büyükşehir Belediyesi, Deprem ve Zemin İnceleme Müdürlüğü. (2020a). İstanbul ili Avcılar ilçesi olası deprem kayıp tahminleri kitapçığı. https://depremzemin.ibb.istanbul/uploads/prefix-avcilar-666ad4f31841f.pdf

İstanbul Büyükşehir Belediyesi, Deprem ve Zemin İnceleme Müdürlüğü. (2020b). İstanbul ili Ataşehir ilçesi olası deprem kayıp tahminleri kitapçığı. https://depremzemin.ibb.istanbul/uploads/prefix-atasehir-666ad4e9b40b3.pdf

Jaillon, L., & Poon, C.S. (2007). Advantages and limitations of precast concrete construction in high-rise buildings: Hong Kong case studies. Proceedings of the CIB World Building Congress 2007, 2504-2514. CIB.

Janković, K., Bojović, D., Nikolić, D., Lončar, L., & Romakov, Z. (2010). Frost resistance of concrete with crushed brick as aggregate. Architecture and Civil Engineering, 155-162.

Javidan, M. M., Ali, A., & Kim, J. (2022). A steel hysteretic damper for seismic design and retrofit of precast portal frames. Journal of Building Engineering, 1-12.

JXSC. (2020, February 28). Jaw Crusher VS Impact Crusher. Retrieved from jxscmachine.com: https://www.jxscmachine. com/new/jaw-crusher-vs-impact-crusher/

Kanat, G. (2010). Municipal solid-waste management in Istanbul. Waste Management, 1737-1745.
Li, J., Fomin, N. I., Xiao, S., Yang, K., Zhao, S., & Yang, H. (2025). Seismic Enhancement Techniques for Rein forced Concrete Frame Buildings: A Contemporary Review. Buildings, 1-48.

Kalkan, E., & Gülkan, P. (2023). Assessing seismic risk in the built environment of Istanbul: High-resolution hazard map ping and ground motion analysis in the sea of Marmara region. Building Engineering, 1(1), 403. https://doi. org/10.59400/be.v1i1.403

Kępniak, M., Chyliński, F. & Woyciechowski, P. Enhancing the performance of recycled aggregate concrete through opti mized pretreatment methods: a microstructural perspective. Sci Rep 15, 29998 (2025). https://doi.org/10.1038/ s41598-025-14834-y

Lew, H. S., Simiu, E., Gross, J. L., & Starnes, M. A. (2002). Manual for seismic and windstorm evaluation of existing con crete buildings for the Dominican Republic (NISTIR 6867). National Institute of Standards and Technology.

Li, G., Zhou, C., Ahmad, W., Usanova, K. I., Karelina, M., Mohamed, A. M., & Khallaf, R. (2022). Fly Ash Application as Supplementary Cementitious Material: A Review. Materials, 15(7), 2664. https://doi.org/10.3390/ma15072664

Lu, W., Yuan, L., & Xue, F. (2021). Investigating the bulk density of construction waste: A big data-driven approach. Re sources, Conservation and Recycling, https://doi.org/10.1016/j.resconrec.2021.105480.

Luoyang Longzhong Heavy Machinery Co., Ltd. (n.d.). Rotary trommel scrubbers. LZZG. Retrieved May 30, 2026, from https://www.lzzgchina.com/products/sand-processing-equipment/rotary-trommel-scrubbers.html

Marchi, T., Garcia Diaz, E., Salgues, M., Souche, J. C., & Devillers, P. (2023). Internal curing capacity of recycled coarse ag gregates incorporated in concretes with low water/cement ratios. Construction and Building Materials, 409, Arti cle 133893. https://doi.org/10.1016/j.conbuildmat.2023.133893

Makul, N. (2021). Use of recycled concrete aggregates in production of green cement-based concrete composites: A review. Crystals, 11(3), 232. https://doi.org/10.3390/cryst11030232

Mavroulis, S., Mavrouli, M., Vassilakis, E., Argyropoulos, I., Carydis, P., & Lekkas, E. (2023). Debris management in Turkey provinces affected by the 6 February 2023 earthquakes: Challenges during recovery and potential health and environmental risks. Applied Sciences, 13(15), Article 8823. https://doi.org/10.3390/app13158823

Metropolitan Municipality of Istanbul, Planning and Construction Directorate, Geotechnical and Earthquake Investigation Department. (2003). Earthquake master plan for Istanbul. Boğaziçi University, Istanbul Technical University, Middle East Technical University, & Yıldız Technical University.

Morales-Beltran, M. (2025). Understanding 60 years of soft storey in Türkiye: an interdisciplinary perspective. Natural Hazards, 11297-11336.

Mulder, E., de Jong, T. P., & Feenstra, L. (2007). Closed Cycle Construction: An integrated process for the separation and reuse of C&D waste. Waste Management, 1408-1415.

Natural Disaster Insurance Institution. (n.d.). Tariffs and premiums. DASK. https://www.dask.gov.tr/en/tariffs-and-premi ums

Nedeljković, M., Visser, J., Šavija, B., Valcke, S., & Schlangen, E. (2021). Use of fine recycled concrete aggregates in concrete: A critical review. Journal of Building Engineering, 38, Article 102196. https://doi.org/10.1016/j.jobe.2021.102196

Pacheco, J., & de Brito, J. (2021). Recycled aggregates produced from construction and demolition waste for structural con crete: Constituents, properties and production. Materials, 14(19), Article 5748. https://doi.org/10.3390/ ma14195748

Parsons, T., Barka, A., Toda, S., Stein, R. S., & Dieterich, J. H. (2000). Influence of the 17 August 1999 Izmit earthquake on seismic hazards in Istanbul. In A. Barka, O. Kozacı, S. Akyüz, & E. Altunel (Eds.), The 1999 Izmit and Duzce earthquakes: Preliminary results (pp. 295–310). Istanbul Technical University Press. https://web.itu.edu.tr/barka/ pubs/ist_haz2/Seismic_Hazards_in_istanbul.pdf

Poon, C. S., Yu, A. T. W., & Ng, L. H. (2001). On-site sorting of construction and demolition waste in Hong Kong. Resourc es, Conservation and Recycling, 32(2), 157–172. https://doi.org/10.1016/S0921-3449(01)00052-0

Qasim, O. A., Hilal, N., Al Biajawi, M. I., Sor, N. H., & Tawfik, T. A. (2024). Studying the usability of recycled aggregate to produce new concrete. Journal of Engineering and Applied Science, 1-24.

Rahal, K. (2007). Mechanical properties of concrete with recycled coarse aggregate. Building and Environment, 42(1), 407–415. https://doi.org/10.1016/j.buildenv.2005.07.033

Sezgin, S. K., Sakcalı, G. B., Özen, S., Yıldırım, E., Eyübhan, A., Bayhan, B., & Çağlar, N. (2024). Reconnaissance report on damage caused by the February 6, 2023, Kahramanmaras Earthquakes in reinforced-concrete structures. Journal of Building Engineering.

Siletani, A. H., Asayesh, S., Shirzadi Javid, A. A., Habibnejad Korayem, A., & Ghanbari, M. A. (2024). Influence of coating recycled aggregate surface with different pozzolanic slurries on mechanical performance, durability, and mi cro-structure properties of recycled aggregate concrete. Journal of Building Engineering, 83, Article 108457. https:// doi.org/10.1016/j.jobe.2024.108457

Sivamani, J., Renganathan, N. T., & Palaniraj, S. (2021). Enhancing the quality of recycled coarse aggregates by different treat ment techniques—a review. Environmental Science and Pollution Research, 60346-60365.

SYSTEM 3E Australia. (n.d.). B2B. https://system3e.com.au/b2b/

Tam, V. W. Y., Gao, X. F., & Tam, C. M. (2005). Microstructural analysis of recycled aggregate concrete produced from two-stage mixing approach. Cement and Concrete Research, 35(6), 1195–1203. https://doi.org/10.1016/j.cemcon res.2004.10.025

Temelli, U. E., Sezgin, N., & Cumalı, B. Ö. (2023). Determination of construction demolition wastes after kahramanmaraş earthquake and evaluation of wastes: the case of Hatay province. 9TH INTERNATIONAL "BAŞKENT" CON GRESS ON PHYSICAL, ENGINEERING, AND APPLIED SCIENCES, (pp. 218-224). Ankara.

Terence. (2022). Population density of Turkey [Data visualization]. In Milhaud Maps. https://mapasmilhaud.com/en/data-maps/population-density-of-turkey-2022/

Tezcan, S. S., Kaya, E., Bal, İ. E., & Özdemir, Z. (2002). Seismic amplification at Avcılar, Istanbul. Engineering Structures, 24(5), 661–667. https://doi.org/10.1016/S0141-0296(02)00002-0

Tsionis, G., Apostolska, R., & Taucer, F. (2014). Seismic strengthening of RC buildings. Luxembourg: Publications Office of the European Union.

Turkish Catastrophe Insurance Pool. (2024). TCIP 2024 annual report. Türk Reasürans A.Ş.

Türkiye İstatistik Kurumu. (n.d.). Bina istatistikleri. Nüfus İstatistikleri Portalı. Retrieved June 10, 2026, from https://nip.tuik.gov.tr/?value=BinaIstatistikleri

Ulubeyli, S. (2026, January 5). Personal communication.

Ulubeyli, S., Arslan, V., & Kazaz, A. (2018). Construction and Demolition Waste Recycling Plants in Turkey. International Conference On Engineering And Natural Science, (pp. 476-482). Kiev.

Ulubeyli, S., Kazaz, A., & Arslan, V. (2017). Construction and demolition waste recycling plants revisited: management issues. Procedia Engineering, 1190-1197.

Ustaoğlu, S. S., & Limoncu, S. (2021). C&D Waste Management Model for Deconstruction-Demolition of Buildings: A Case of Istanbul in Turke. In R. Rahbarianyazd, Contemporary Approaches in Urbanism and Heritage Studies (pp. 143-153). Istanbul: Cinius yayinlari.

World Bank. (2021, December 21). Towards Resilient Housing in Turkey – a Virtual Knowledge Exchange with Japan Housing Finance Agency on Housing Upgrading and Retrofitting for Seismic and Flood Resilience. https://www.worldbank.org/en/events/2021/12/21/drmhubtokyo-towards-resilient-housing-in-turkey

World Bank. (2023, February 27). Earthquake damage in Türkiye estimated to exceed $34 billion: World Bank disaster assess ment report [ress releases]. https://www.worldbank.org/en/news/press-release/2023/02/27/earthquake-damage-in-turkiye-estimated-to-exceed-34-billion-world-bank-disaster-assessment-report

World Population Review. (2026). Turkey population 2026. Retrieved May 31, 2026, from https://worldpopulationreview.com/countries/turkey

Xiao, J., Deng, Q., Hou, M., Shen, j., & Gencel, O. (2023). Where are demolition wastes going: reflection and analysis of the February 6, 2023 earthquake disaster in Turkey. Low-carbon Materials and Green Construction, 1-9.

Youssef, O. F. (2025). Sustainable concrete with recycled brick and ceramic aggregates: A statistical validation and perfor mance evaluation. Next Materials, 1-15.

Zheng, Y., Zhang, Y., & Zhang, P. (2021). Methods for improving the durability of recycled aggregate concrete: A review. Jour nal of Materials Research and Technology, 6367-6386.

9: Appendix

Appendix A: Integrated workflow diagram for seismic assessment and recyc

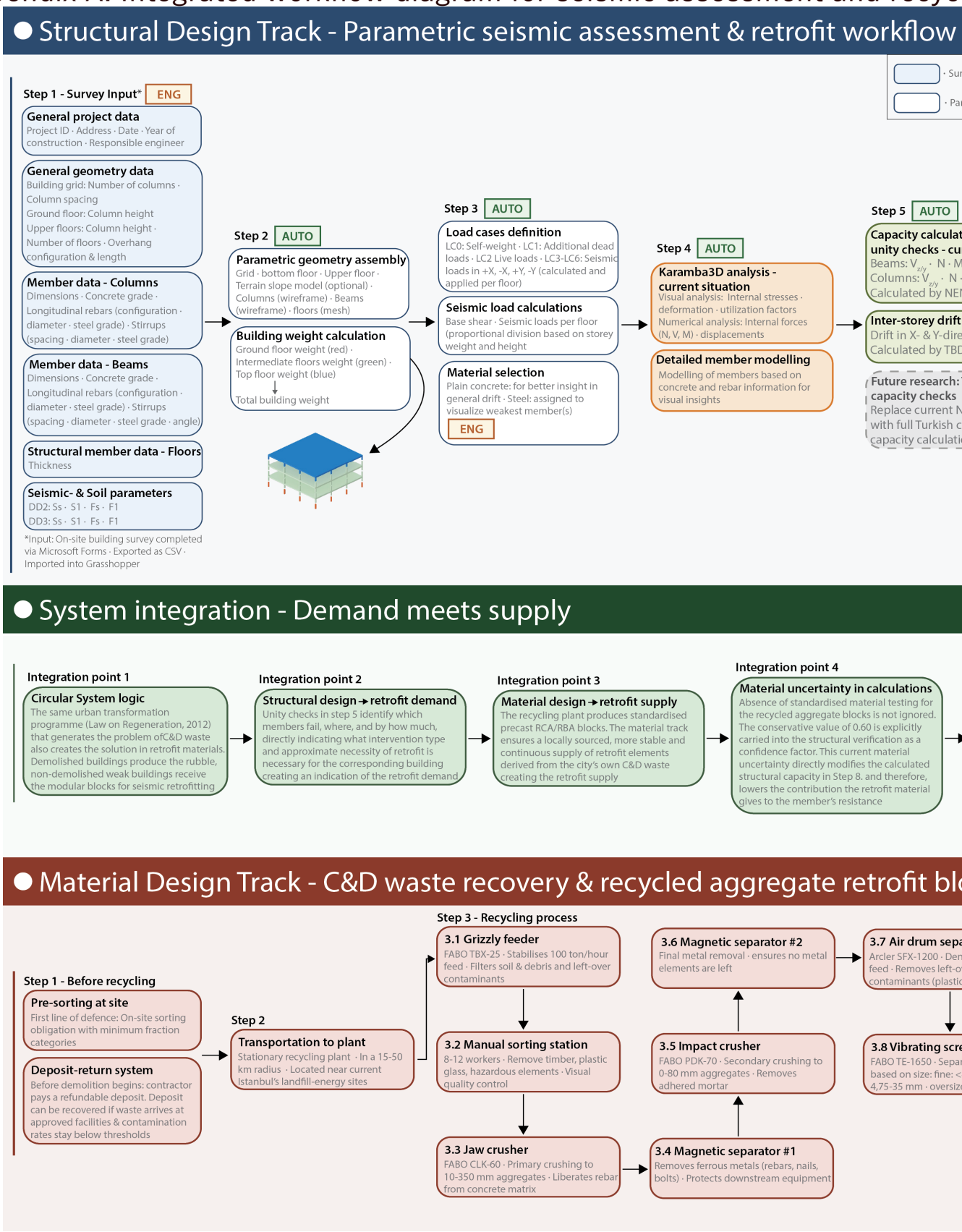

Figure A.1: Dual-track flowchart showing the integration of how parametric seismic assessment identifies retrofit demand, while C&D waste recycling and aggregate upgrading generate the material supply for recycled aggregate retrofit components (author's own work)

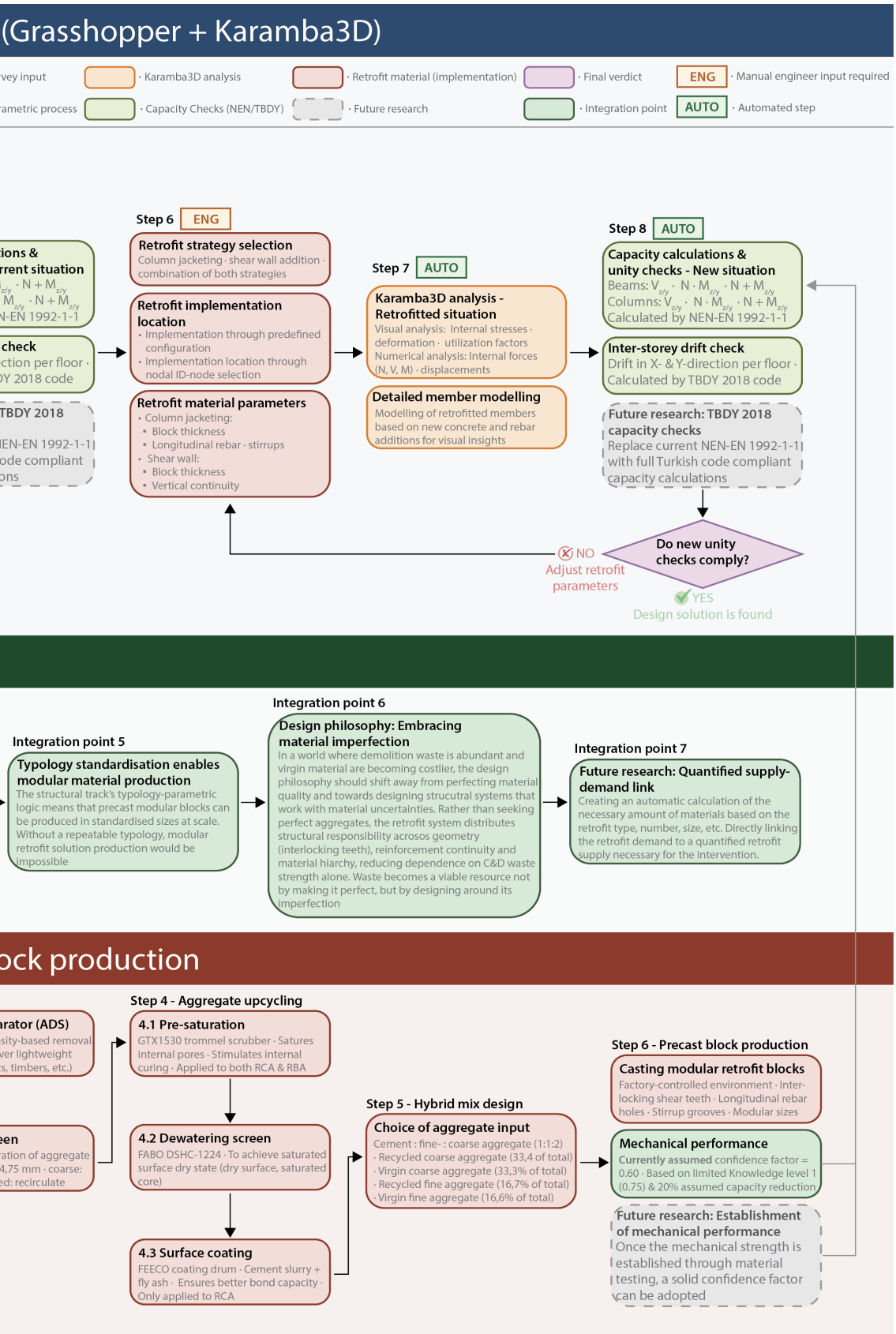
(Grasshopper + Karamba3D)
· Karamba3D analysis
· Retrofit material (implementation)
· Final verdict
ENG · Manual engineer input required
· Capacity Checks (NEN/TBDY)
· Future research
· Integration point
AUTO · Automated step
Step 6 ENG
Retrofit strategy selection
Column jacketing · shear wall addition · combination of both strategies
Retrofit implementation location
• Implementation through predefined configuration
• Implementation location through nodal ID-node selection
Retrofit material parameters
• Column jacketing:
▪ Block thickness
▪ Longitudinal rebar · stirrups
• Shear wall:
▪ Block thickness
▪ Vertical continuity
Step 7 AUTO
Karamba3D analysis - Retrofitted situation
Visual analysis: Internal stresses · deformation · utilization factors
Numerical analysis: Internal forces (N, V, M) · displacements
Detailed member modelling
Modelling of retrofitted members based on new concrete and rebar additions for visual insights
Step 8 AUTO
Capacity calculations & unity checks - New situation
Beams: $V_{z/y}$ · N · $M_{z/y}$ · N + $M_{z/y}$
Columns: $V_{z/y}$ · N · $M_{z/y}$ · N + $M_{z/y}$
Calculated by NEN-EN 1992-1-1
Inter-storey drift check
Drift in X- & Y-direction per floor · Calculated by TBDY 2018 code
Future research: TBDY 2018 capacity checks
Replace current NEN-EN 1992-1-1 with full Turkish code compliant capacity calculations
Do new unity checks comply?
NO
Adjust retrofit parameters
YES
Design solution is found
Integration point 5
Typology standardisation enables modular material production
The structural track's typology-parametric logic means that precast modular blocks can be produced in standardised sizes at scale. Without a repeatable typology, modular retrofit solution production would be impossible
Integration point 6
Design philosophy: Embracing material imperfection
In a world where demolition waste is abundant and virgin material are becoming costlier, the design philosophy should shift away from perfecting material quality and towards designing strucutral systems that work with material uncertainties. Rather than seeking perfect aggregates, the retrofit system distributes structural responsibility acrosos geometry (interlocking teeth), reinforcement continuity and material hiarchy, reducing dependence on C&D waste strength alone. Waste becomes a viable resource not by making it perfect, but by designing around its imperfection
Integration point 7
Future research: Quantified supply-demand link
Creating an automatic calculation of the necessary amount of materials based on the retrofit type, number, size, etc. Directly linking the retrofit demand to a quantified retrofit supply necessary for the intervention.
ock production
Step 4 - Aggregate upcycling
4.1 Pre-saturation
GTX1530 trommel scrubber · Satures internal pores · Stimulates internal curing · Applied to both RCA & RBA
4.2 Dewatering screen
FABO DSHC-1224 · To achieve saturated surface dry state (dry surface, saturated core)
4.3 Surface coating
FEECO coating drum · Cement slurry + fly ash · Ensures better bond capacity · Only applied to RCA
Step 5 - Hybrid mix design
Choice of aggregate input
Cement : fine- : coarse aggregate (1:1:2)
· Recycled coarse aggregate (33,4 of total)
· Virgin coarse aggregate (33,3% of total)
· Recycled fine aggregate (16,7% of total)
· Virgin fine aggregate (16,6% of total)
Step 6 - Precast block production
Casting modular retrofit blocks
Factory-controlled environment · Inter-locking shear teeth · Longitudinal rebar holes · Stirrup grooves · Modular sizes
Mechanical performance
Currently assumed confidence factor = 0.60 · Based on limited Knowledge level 1 (0.75) & 20% assumed capacity reduction
Future research: Establishment of mechanical performance
Once the mechanical strength is established through material testing, a solid confidence factor can be adopted

Appendix B: Retrofit strategy tables

	Retrofitting technique	Primary mechanism	Suited for what building type	Modifies structural parameters
Seismic isolation techniques	***Elastomeric isolation system***	*Uses laminated rubber bearings with alternating layers of rubber and steel with a lead core to offer high lateral flexibility and giving great vertical stiffness. Therefore increases damping and reduces earthquake forces*	*Especially effective for stiff (concrete) bulky buildings, culutural heritage buildings and buildings that host valuable contents or critical services (i.e. hospitals). (Source: european commission)*	• Structure's vibration period (T) ↑ • Base shear forces (V_b) ↓ • Damping (ξ) ↑
	Friction pendulum system (FPS)	*Dissipates seismic energy through friction between sliding surfaces and a pendulum motion at the foundation of a structure*	*Structures that require high damping and precise control of lateral displacements* *Due to frequency-independent behaviour FPS is suitable for wide range of earthquake frequencies*	• Structure's vibration period (T) ↑ • Damping (ξ) ↑ • Base shear forces (V_b) ↓ • Accelerations (S_a) ↓
	Hybrid isolation system	*Combines single-type systems (i.e. elastomeric and friction pendulum bearings) to leverage all advantages through fine-tuning of bearing types*	*Structures requiring maximum safety or other highly sensitive and important structures*	
Energy dissipations/damping techniques	***Fluid viscous damping (FVD)***	*Earthquake energy forces a flow of a viscous fluid (i.e. silicone oil) through a nozzle, converting kinetic energy into thermal energy which then dissipates*	*Tall buildings, high-rise and buildings with long natural periods (T)*	• Damping (ξ) ↑ • Lateral displacement (u) ↓ • Floor accelerations (S_a) ↓
	Steel hysteretic dampers	*Works based on plastic deformation of steel under loading cycles which dissipates earthquake energy in the steel*	*Mid- and high rise framed structures*	• Damping (ξ) ↑ • Lateral displacement (u) ↓ • Floor accelerations (S_a) ↓
	Friction dampers	*Placed within the structural system, these dampers dissipate kinetic energy by friction between solid surface during relative movement*	*Mid- and high rise framed structures*	• Damage prevention to non-structural elements ↑ • Damping (ξ) ↓ • Lateral displacement (u) ↓
	Tuned mass dampers (TMD)	*An additional damper mass is attached to the structure (including a spring system and viscous damper), the damper mass vibrates, absorbs and dissipates the seismic energy*	*Tall buildings in mild to moderate earthquakes*	• Damping (ξ) ↑ • Structure specific vibration period (T) ↑

Key advantages	*Key limitations*	*Retrofitting product image*
• Both improves seismic performance by reducing both earthquake forces and increasing damping • Reliable mechanism	• Degradation over time and environmental factors, requiring maintenance and potential periodic replacement • limited vertical load bearing capacity[8]	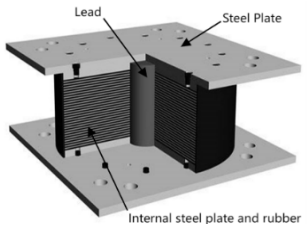 *Figure B.1: A laminated rubber bearing seismic isolation system (LI et al., 2025)*
• Relatively compact design technique compared to other base isolation systems[8]	• Complex design and installation • Higher initial cost compared to other base isolation systems • Requires maintenance and potential periodic replacement [8]	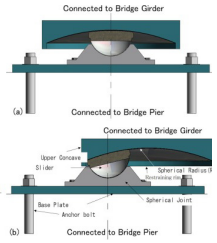 *Figure B.2: A description of a frictio pendulum system at stationary condition (top) and in moving condition (bottom) (Moestopo et al., 2022)*
• Leverages the advantages of both systems • can optimize a structure's performance for a wide range of earthquake motions	• Complex design and installation • Higher initial cost compared to other base isolation systems	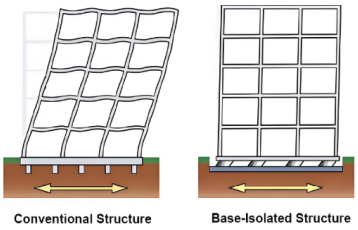 *Figure B.3: The general principle of seismic isolation of a building (Li et al., 2025)*
• Highly reliable mechanism • Most commonly used type of energy dissipator	• Requires maintenance and inspection • Higher costs compared to other types of dampers[8]	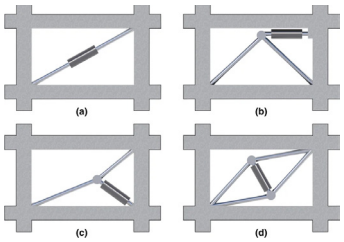 *Figure B.4: Different bracing layouts for viscous damping elements (Parajuli, et al. 2023)*
• Particularly useful in preventing damage on structural members • High stability • Ability to be designed for various energy capacities	• Plastic deformation of the steel component leads to the need to replace after an earthquake	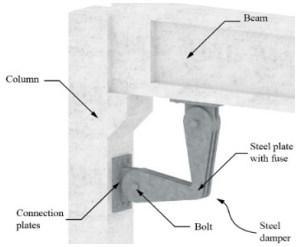 *Figure B.5: An example of a steel hysteretic dampling system (Javidan, et al., 2022)*
• Economical and efficient option • Simple construction • Adjustable friction force allows to tailor the system to specific seismic demands	• Susceptible to wear and aging of friction materials • Limited energy dissipation capacity compared to fluid viscous damping techniques[8]	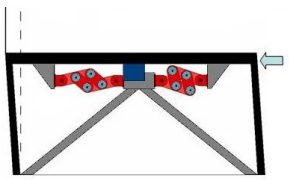 *Figure B.6: The working principle of friction damperening system in a frame (damptech., n.d.)*
• Improves occupant comfort • Most commonly used type of energy dissipator	• Mostly a limited effect for strong earthquakes • Requires tuning of the mass	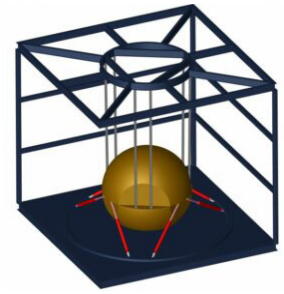 *Figure B.7: A fastened tuned mass damper system (Deicon, n.d.)*

	Retrofitting technique	Primary mechanism	Suited for what building type	Modifies structural parameters
Jacketing techniques	**Concrete jacketing** *(High-strength concrete, Self-consolidating concrete (SCC) & precast concrete jacketing)* *High applicability as C&D waste based retrofit element!*	*Increases cross-sectional area and confinement in order to increase load-bearing capacity and stiffness*	*Commonly applied in low- to mid-rise residential, commercial and industrial buildings & buildings that require a significant increase in strength and stiffness or that suffered severe damage*	• Members strength (compressive, flexural shear) ↑ • Stiffness (K) ↑
	Steel jacketing	*In steel jacketing, a member's section is enlarged by welding or bolting a steel section cage around the column. This gap between the concrete and steel can consequently be filled with grout.*	*Commonly applied in low- to mid-rise residential, commercial and industrial buildings*	• Members strength (compressive, flexural shear) ↑ • Stiffness (K) ↑
	Fibre reinforced polymer - Externally bonded reinforcement systems (EBR)	*Using epoxy adhesives, FRP strips or sheets are adhered to the external surface of a concrete member in order to provide a 'protective skin' against seismic forces*	*Suitable for existing residential, commercial and office buildings that require fast and economical strengthening*	• Members strength (shear, flexural confinement depends on way of application) ↑ • Stiffness (K) ↑ • Crack propagation ↓
	Fibre reinforced polymer - Near surface mounted system (NMS)	*Pre-cut grooves in members surfaces are filled with FRP bars or strips and filled with a special cement-based or epoxy resin mortar*	*Suitable for structures or structural members that are exposed to harsh enviromental conditions (i.e. marine structures)*	• Member strength ↑ • Stiffness (K) ↑

Key advantages	*Key limitations*	*Retrofitting product image*
• It is a well-established and widely used technique • Improves durability of the structure • Low costs and easy to execute	• High invasiveness and consumes space • Labour-intensive and time consuming • Increases structural weight of the building	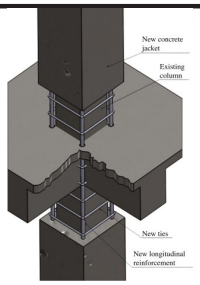 *Figure B.8: An illustration showing the different elements of concrete retrofitting (Anwar and Najam, 2017)*
• Faster installation compared to concrete jacketing • Minimal section enlargement, so less spatial impact	• Generally costly and labour intensive • Chance of rusting or corrosion • Increases structural weight of the building (if grout is applied)	 *Figure B.9: Jacketing of a column through application of steel plates (Horse construction, n.d.)*
• No need for extensive demolition of the existing structure • Great ease and speed of application • Relatively low costs • Very lightweight measure	• Lower efficiency (30-35%) due to risk of debonding • Poor properties on exposure to high temperature and wet environments	 *Figure B.10: The application of fibre reinforced polymers to a column (Structural technologies, n.d.)*
• Greater resistance to fire and mechanical damage due to mortar cover protection • Provides better bonding and higher load capacity compared to EBR technique	• Higher execution complexity (compared to EBR) • More invasive since it requires pre-cutting	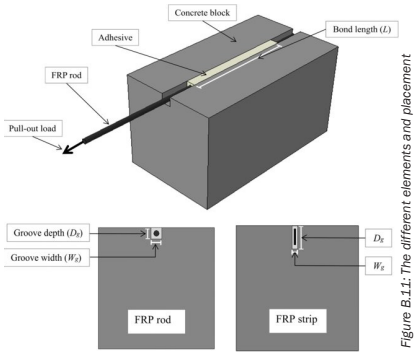 *Figure B.11: The different elements and placement methods of near surface mounted FRP (Nasrollahzadeh and Afzali, 2017)*

	Retrofitting technique	Primary mechanism	Suited for what building type	Modifies structural parameters
Seismic bracing techniques	**Steel bracing addition**	*Steel bracings help to create parallel lateral load paths alongside the frame and therefore transfers them safely to the foundation, absorbing earthquake forces*	*particularly efficient for mid- and high-rise concrete buildings and buildings with irregular floorplans or large openings*	• (Lateral) stiffness (K) • Natural vibration period (T)
	Concentrically braced frames (CBF)	*Centrically braced frames dissipate seismic energy through axial forces in brace members, creating efficient triangulated load paths*	*More suitable for low and mid-rise structures*	• (Lateral) stiffness (K) • Natural vibration period (T)
	Eccentrically braced frames (EBF)	*Eccentrically braced frames dissipate seismic energy through controlled plastic deformation of a link beam between braces, providing stable energy dissipation*	*More suitable for medium to high-rise structures and structures exposed to severe seismic events*	• (Lateral) stiffness (K) • Natural vibration period (T)
	Buckling-restrained bracings (BRB)	*Buckling-restrained bracings dissipate seismic energy through the controlled yielding of a steel core that is encased in a concrete restraining system, preventing buckling of the member*	*Mostly used in tall and critical buildings that require a high ductility and damping*	• Ductility (μ) • Damping (ξ)
Infill wall techniques	**FRP strengthening + masonry infills**	*Enhances in-plane strength and deformation behaviour of masonry infills by providing reinforcement, redistributing stresses and preventing brittle failure modes*	*(Existing) RC frame buildings with masonry infills, particularly low- to mid-rise structures*	• Crack propagation
	Precast concrete infill panels *High applicability as C&D waste based retrofit element!*	*Transforms a building frame action into wall-like behaviour through infill action and load transfer via connections*	*Low- to mid-rise frame buildings*	• Drift (u_i) • Stiffness (K) • Lateral load capacity strength (V)
	Reinforced concrete shear walls *High applicability as C&D waste based retrofit element!*	*Reinforced concrete shear walls resist seismic forces by acting as stiff vertical elements that effectively transfer lateral loads to the foundation*	*Can be applied to low-, mid- and high-rise structures and buildings in high seismic hazard regions*	• Storey drift (u_i) • Stiffness (K) • Lateral load capacity strength (V)
	Rocking shear walls	*Shear walls that allow controlled uplift and rotation at the base, with self-centring provided by post-tensioned tendons and optional energy dissipation through energy dissipaters*	*Mostly mid- to high rise strcutures rerquiring low damage and better post-earthquake functionality*	• Drift (u_i) • (Controlled) stiffness (K) • Lateral load capacity strength (V)

Key advantages	*Key limitations*	*Retrofitting product image*
• rapid installation • possibility of external application • very economical method	• A high slenderness ratio can cause buckling of the bracing elements under high seismic loading	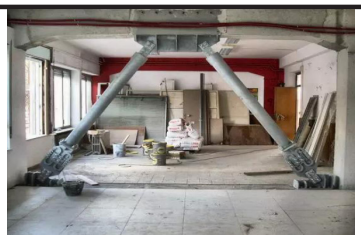 *Figure B.12: A photo depicting the use of eccentrically steel braced frames (Asadimanes, 2025)*
• Based on simple design and construction • Provides high efficiency • Relatively low costs	• Limited ductility due to brace buckling in compression, leading to reduced energy dissipation capacit	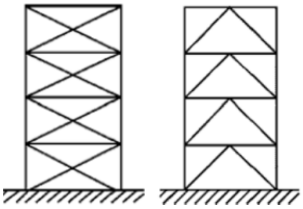 *Figure B.13: Examples of concentrically- (top) and eccentrically braced frames (bottom) (Tsionis, et al., 2014)*
• Both brace- and link beam elements can be designed independently, enabling control over both stiffness and strength allowing for seismic tailoring of the structure	• the link beam undergoes significant plastic deformation during earthquakes, often requiring inspection, repair, or replacement after a seismic event	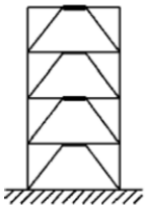
• Provides superior seismic performance and damage control	• Buckling-restrained bracings are more expensive than conventional steel bracings	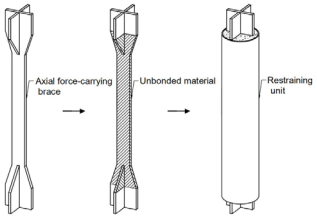 *Figure B.14: The build up of a buckling restrained bracing elementt (Li et al., 2017)*
• Prevents brittle failure and distributes cracking of infill walls • Easy to apply	• Performance is often highly variable and limited • Sometimes negligible improvement	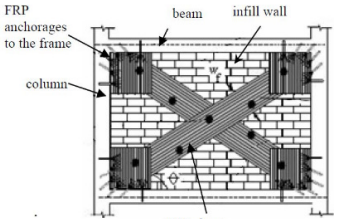 *Figure B.15: Application example of fibre reinforced polymers on a masonry infill wall (Tsionis, et al., 2014)*
• Less time consuming due to precasting of panels	• Strong dependence on connection quality	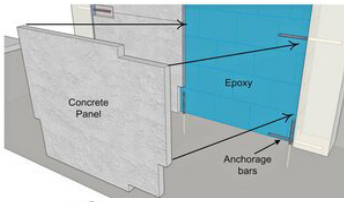 *Figure B.16: An example of pre-cast shear wall application (Kurt, et al., 2012)*
• Greatly prevents (soft) storey collapse • Possibly reduces irregularities of a building, both hiehgt-wise and in plan	• Effectiveness of shear wall depends on how it is connected to the frame • Applications of shear walls are an invasive measure • local strengthening of existing elements might be necessary	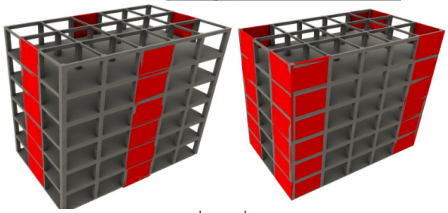 *Figure B.17: two possible design options for shear wall application (Li et al., 2017)*
• Intended to maintain their stength and stiffness even after seismic events • minimal structural damage and deformation	• Less effective when applied in irregular shaped buildings • May increase force demand in existing members	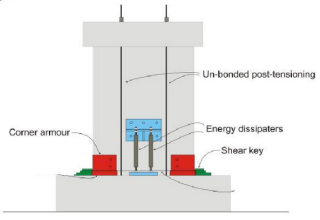 *Figure : The build up of a rocking shear wall system using post tesioning cables and energy dissipators (Tsionis et al., 2014)*

Appendix C: 2nd-stage assessment form from Istanbul municipality

This appendix presents the second-stage assessment form applied in the structural evaluation methodology. Opposed from a first-stage assessment form, which is a rapid street-survey form, used to screen many buildings quickly Istanbul Metropolitan Municipality (2003), the second-stage survey outlines the parameters and the criteria used for detailed assessment of building performance in greater detail.

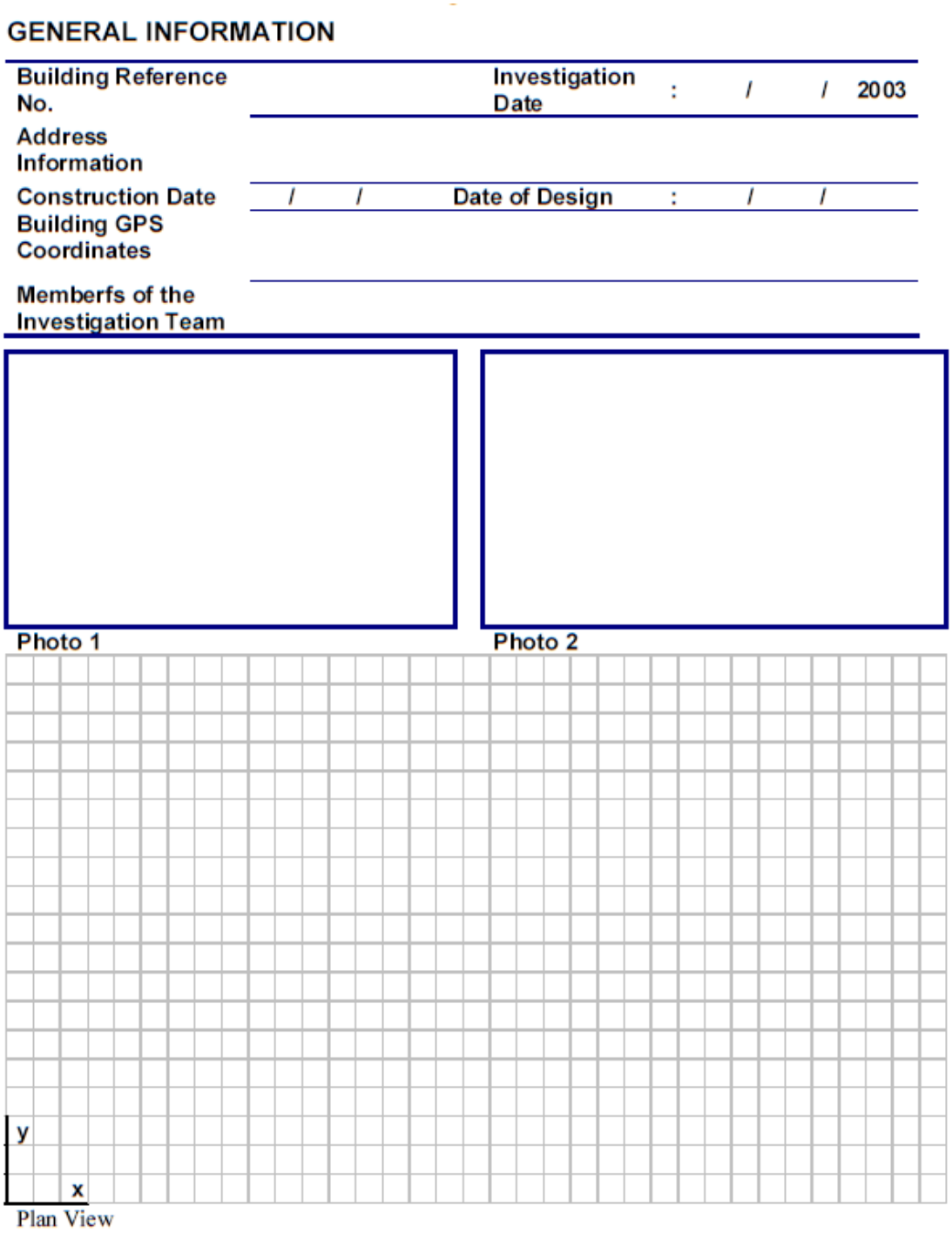
GENERAL INFORMATION

Building Reference No.		Investigation Date	: / / 2003
Address Information			
Construction Date	/ /	Date of Design	: / /
Building GPS Coordinates			
Memberfs of the Investigation Team			

Photo 1

Photo 2

y

x

Plan View

Figure C.1: The second-stage assessment form (1st part) as presented by the Metropolitan Municipality of Istanbul, 2003

Story	Number of Repetition	Floor Height (m)	Floor Area (m^2)	Remarks
Basement				
Ground				
Mezzanine				
Normal Story				
Penthouse				

Is there any increase in story numbers due to change of municipal construction regulations?	Yes		No			

Location	Detached		Appending corner building		Appending on both sides in a row of housing	
	Building on a slopping terrain?	Yes			No	
	Slope	≥ 30°			< 30°	

Does seismic dilatation with neighboring buildings exist?	Yes		Yok		NA	

Does floor height difference between adjacent neighboring buildings exist	No		Yes		NA	

Irregularities		
	Exist	Does not exist
Irregularities in plan		
Irregularites in the elevation		
Floor discontinuity		
Non-parallel frame lines		
Soft story		
Discontinuity in vertical elements		

Figure C.2: The second-stage assessment form (2nd part) as presented by the Metropolitan Municipality of Istanbul, 2003

Properties of the Structural System

Type of the Structural System:	RC Frame	
	RC Wall-Frame System	
	Mixed (RC+Masonry)	
	Masonry	

For RC Buildings		
Infil Wall Material	Hollow clay tiles	
	Solid clay tiles	
	Concrete briquettes	
	Kiln-fired bricks	
	AAC	
	Others (please specify) -	

Mixed/Masonry Buildings		
Structural Wall Material	Hollow clay tiles	
	Solid clay tiles	
	Concrete briquettes	
	Kiln-fired tiles	
	AAC	
	Stone	
	Others (please specify) -	

Bodrum Perdesi Malzemesi:	Stone masonry (pointed or rubble)	
	RC wall	
	Kiln-fired or solid clay tiles	
	Concrete briquettes	
	Others (please specify) -	

Floor System	Two-way slab with beams	
	Hollow joist slab system	
	Joist slab	
	Flat slab	
	Others (please specify) -	

Reinforcement						
Grade	S220 (St I)		S420 (St III)		S500 (St IV)	
Type	Plane:		Deformed:			
Any sign of corrosion?	Yes:		No:			
Any sign of longitudinal cracks in exterior columns or beams?	Yes:		No:			

- If it can be determined.

Figure C.3: The second-stage assessment form (3rd part) as presented by the Metropolitan Municipality of Istanbul, 2003

Structural System Information

(1) Any stores in the ground floor?	Yes:		No:	
(2) Any story height difference b/w the ground story and the first story?	Yes:		No:	
(3) Is there any difference in the number of stories as tey apper from the front and rear facades of the building?	Yes:		No:	
(4) In case the answer to Question 3 is negative, please answer:				
Apparent number of stories as seen from the front façade				
Apparent number of stories as seen from the front façade				
(5) Is there any short columns?	Yes:		No:	
(6) Binanin kirişlerinin yüksekliği kolonlarin genişliğinden fazla mi? (Belirlemek mümkün değilse boş birakiniz).	Yes:		No:	
If there are any other thing that must be mentioned, please specify.				

OVERALL WORKMANSHIP EVALUATION

		Yes/Good	No/Bad
Apparent quality of the building is:			
Material Quality	Concrete		
	Infill		
	Structural wall		
Beams and columns meet at joint without any significan offset, i.e. confined beam-column joints.			
Are there significant change b/w the architectural plans of the successive floors?			
Are there any damage in RC structural elements, i.e. cracks, excessive deformation, etc.			
Others, please specify.			

Figure C.4: The second-stage assessment form (4th part) as presented by the Metropolitan Municipality of Istanbul, 2003

Appendix D: 2nd-stage assessment form seismic analysis

This appendix shows the setup of the Microsoft Forms which can be used during the site-visit to collect the relevant geometry-, member and soil parameters. The full survey can also be found by following this link:

2nd Stage assessment form for Seismic analysis – Fill out form

https://forms.office.com/Pages/ResponsePage.aspx?id=TVJuCSlpMECM04q0LeCIe91sxYQf-pZpEvT36HVahcAZUOUwyTE9LNUgwSEM0VVFNQTdMS1JZQVJMNC4u

Appendix E: Dissection of load combintions into separate loads

This appendix shows illustrations of some of the different load cases and how they are applied to the geometrical model. This is done in order to give more clearance on how loads are applied and distributed on (mainly) the floor elements of the model.

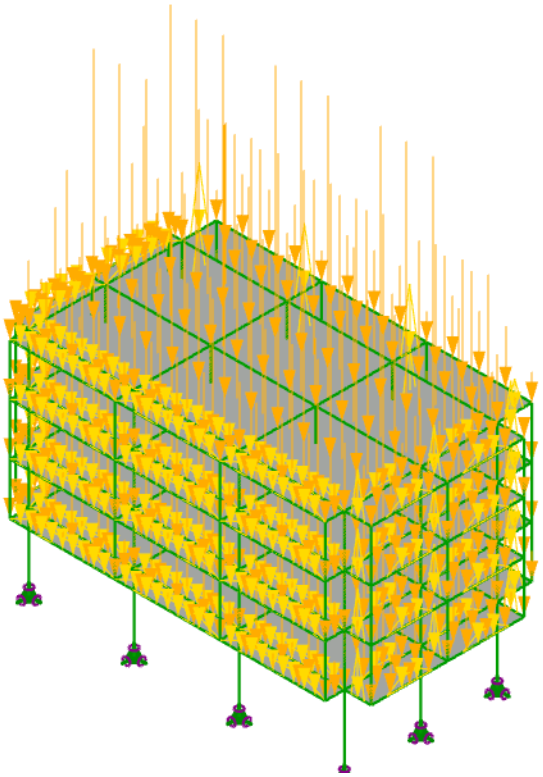

Figure E.1: The load case application of the live loads (Lc2). The dirrection and the type of load application is similar to the dead loads (Lc0 and Lc1).

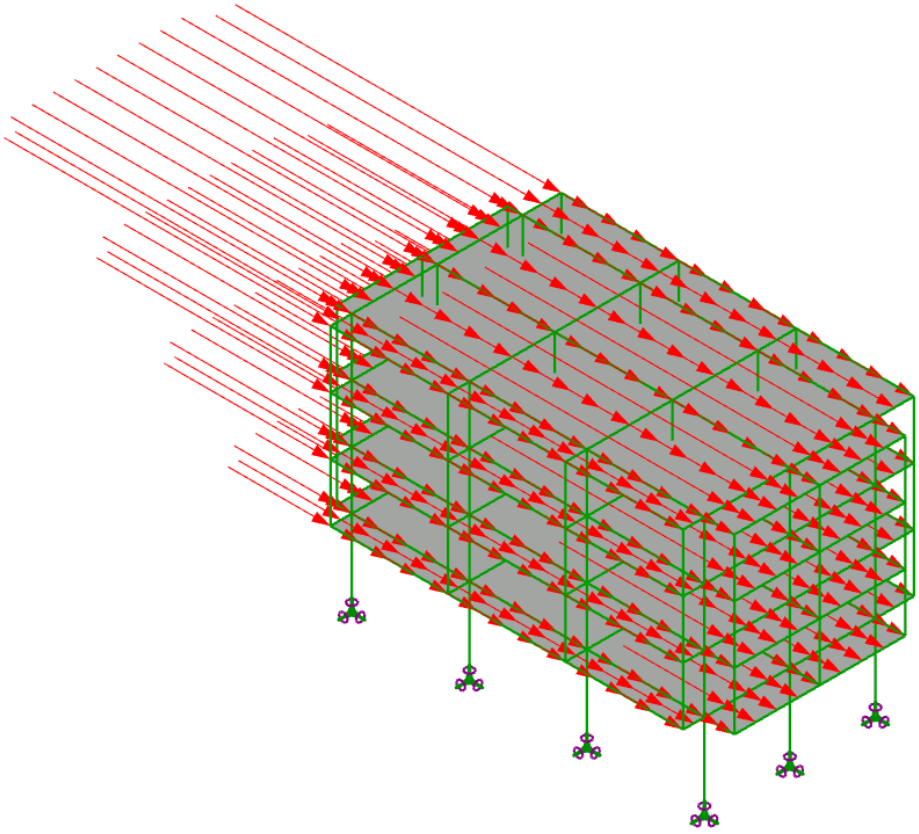

Figure E.2: The load case application of the seimic loads in +X-direction (Lc3). The seismic load case Lc4 show similar loads but in the opposite direction.

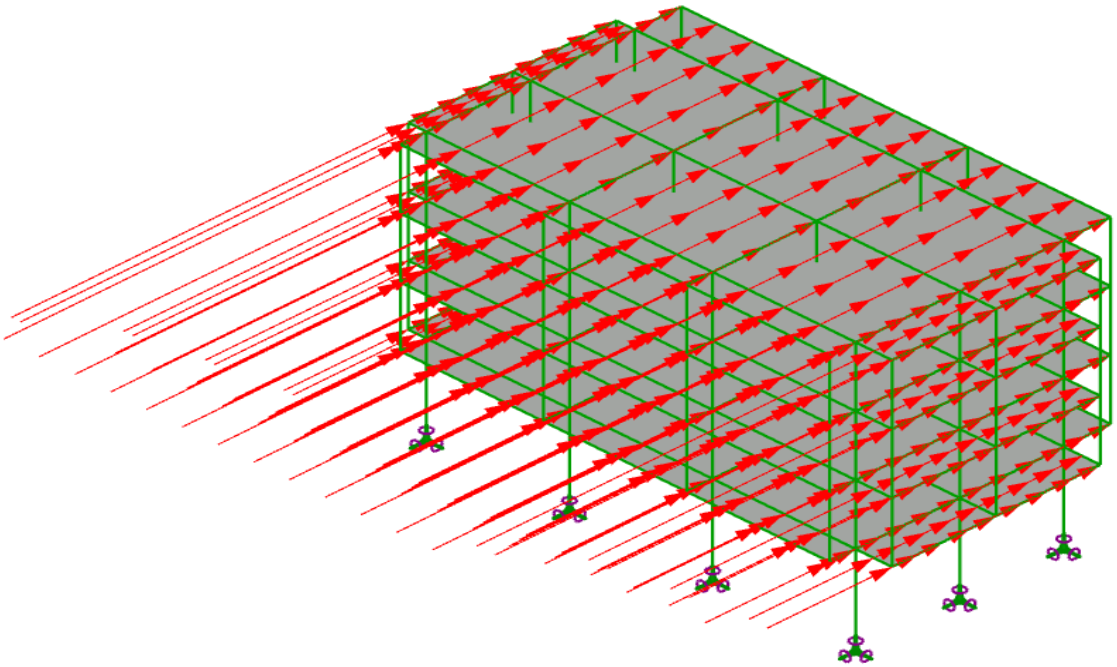

Figure E.3: The load case application of the seimic loads in +Y-direction (Lc5). The seismic load case Lc6 show similar loads but in the opposite direction.

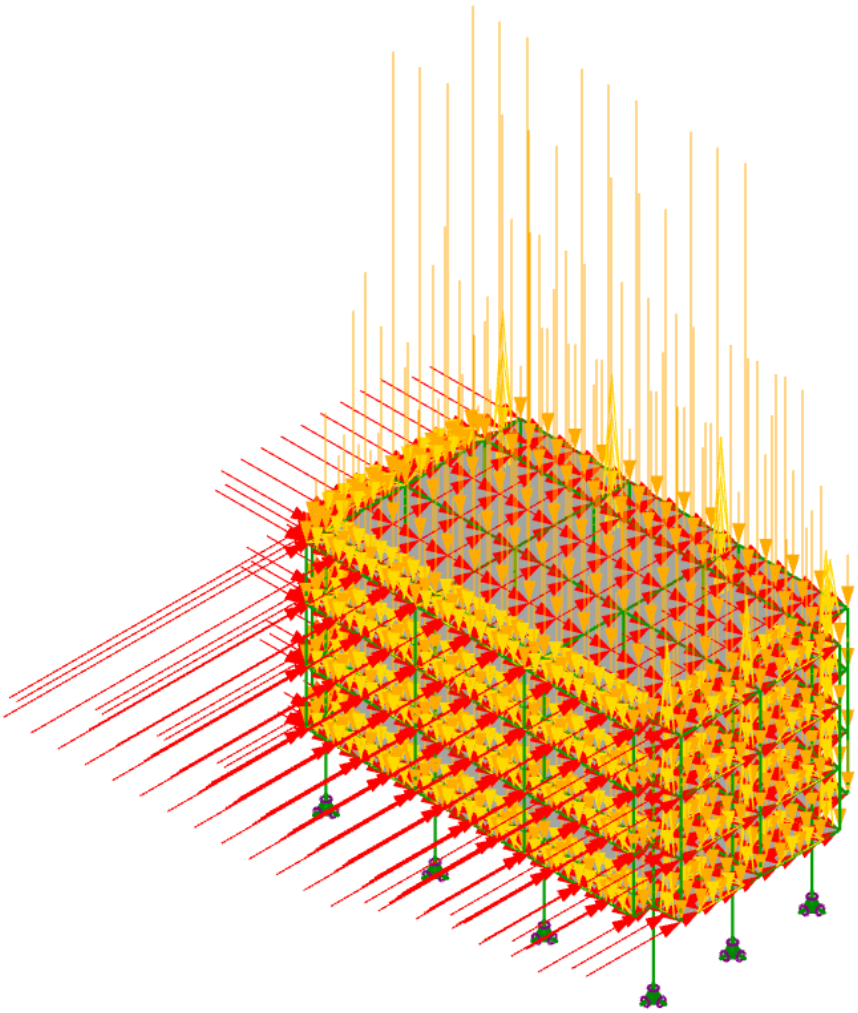

Figure E.4: This model shows the application of one of the Load combinations applying the vertical load applications from the dead- and live loads and the horizontal seismic load applications.

Appendix F: Displacement output of model

In this appendix, more clearance is given on how the numerical lateral displacements output could be presented visually in the model. Furthermore, it shows the effectiveness of shear walls application to reduce this lateral displacement of the building.

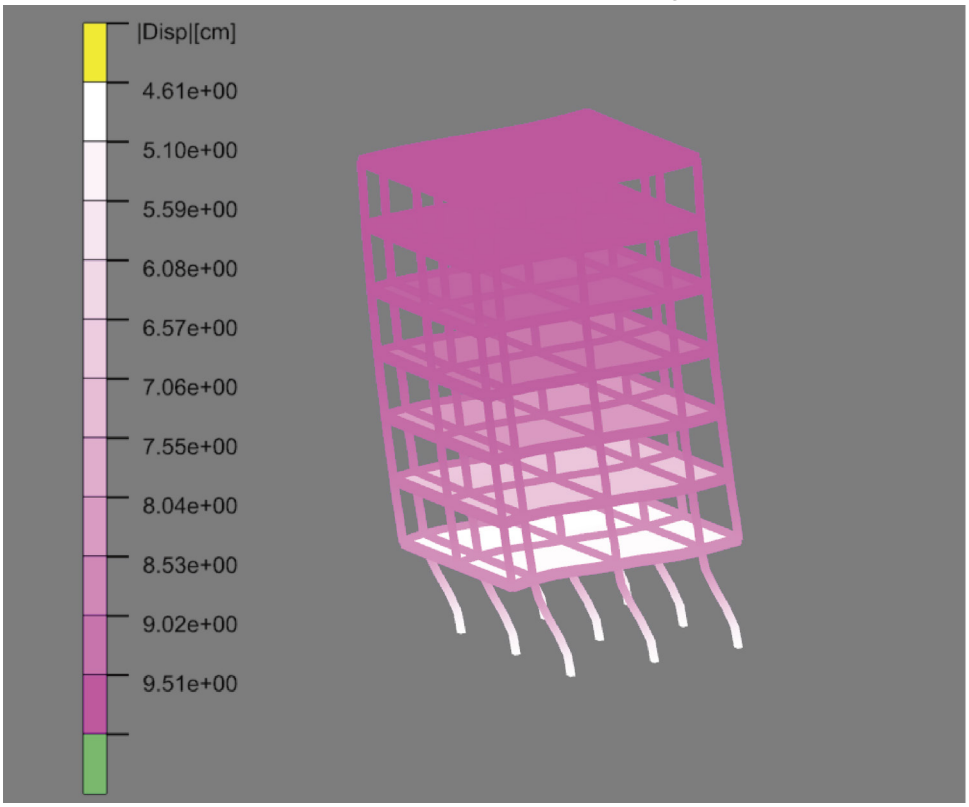

Figure F.1: Numerical displacement distribution of a 7-storey building without a shear wall core, showing significant lateral deformation.

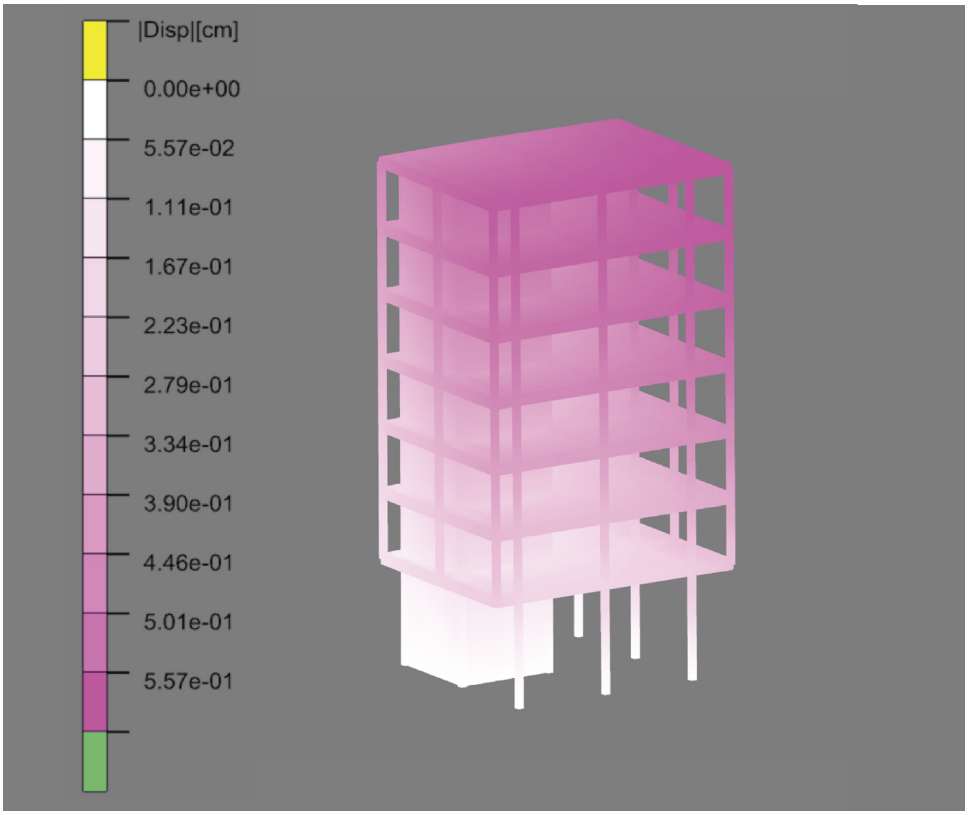

Figure F.2: Numerical displacement distribution of a 7-storey building with a shear wall core, illustrating reduced lateral deformation

Appendix G: Formulas from NEN-EN 1992-1-1 & TBDY 2018

Within the Grasshopper environment, building codes are utilised for numerous tasks. In the model both NEN-EN 1992-1-1 and TBDY 2018 are used to find the corresponding formulas necessary for the calculations. These calculations range from calculating the earthquake loads on the building (calculated by TBDY2018), the calculation of the member capacity for the shear-, moment-, and axial forces (calculated through NEN-EN 1992-1-1), to check if the internal forces do not exceed the capacity of the members. Lastly, TBDY 2018 is utilised to check whether the interstorey drift is within limits. In this appendix, the corresponding formulas used within the model are shown and discussed.

Calculation of earthquake loads

In order to calculate the earthquake loads on the structure through the equivalent static method for seismic analysis. The following formulas are utilised.

Calculation of seismic load combination

In order to find out what the total design action is on the building, the earthquake effects are combined with all other loads acting simultaneously which are decreased by a certain safety-factor based on the chance of simultaneously occurence. In the model calculation, snow loads are ignored since the 0,2 already indicates that snow plays a minor role. The vertical seismic loads are also not taken in the calculations of the model due to simplifications.

$$1.0 \cdot G + 1.0 \cdot Q + 0.2 \cdot S + E_d^{(H)} + 0.3 \cdot E_d^{(Z)} \qquad \text{(eq. 4.11 in TBDY 2018)}$$

Where:

G = dead loads (this includes structural members and an additional 3.0 kN/m^2 is added to take into account partition walls, facades, installations, etc.)

Q = Live loads (taken as 2.0 kN/m^2 in the model)

S = Snow loads (ignored in model)

$E_d^{(H)}$ = combined horizontal earthquake effect

$E_d^{(Z)}$ = combined vertical earthquake effect

Calculation of horizontal combined earthquake loads $E_d(H)$

The combined horizontal earthquake effect is calculated based on different directions and magnitudes for the X- and Y-directions as is shown in the formula below:

$$E_d^{(H)} = \pm E_d^{(X)} \pm 0.3 \cdot E_d^{(Y)} \qquad \text{(eq. 4.9 in TBDY 2018)}$$
$$E_d^{(H)} = \pm 0.3 \cdot E_d^{(X)} \pm E_d^{(Y)}$$

Where:

$E_d^{(X)}$ = Earthquake load in X-direction

$E_d^{(Y)}$ = Earthquake load in Y-direction

Calculation of base shear V_{tE}

The base shear is the total horizontal earthquake force that acts at the base of a building, representing the inertial resistance of the entire structure to the ground motion. This value forms the starting point of the equivalent static calculation method and once calculated, it gets distributed up the height of the building at every floor level. The base shear depends on the building's mass, its dynamic characteristics, the seismic hazard level at the site, and the ductility level of the structural system.

In the model the S_{DS} and S_{D1} have to be calculated for both DD2 & DD3 earthquake levels.

$$S_{DS} = S_s \cdot F_s$$
$$S_{D1} = S_1 \cdot F_1 \qquad \text{(eq. 2.1 in TBDY 2018)}$$

Where:

S_s = Short period spectral acceleration coefficient (found at the dlubal website for the respective site)
S_1 = Long period [1.0 sec.] spectral acceleration coefficient (found at the dlubal website for the respective site)
F_s = Short period soil amplification factor (found in table 2.1 in TBDY based on Soil conditions and S_s)
F_1 = Long period soil [1.0 sec.] amplification factor (found in table 2.2 in TBDY based on Soil conditions and S_1)
S_{DS} = Short period design spectral acceleration coefficient
S_{D1} = Long period soil [1.0 sec] design spectral acceleration coefficient

Empirical dominant period T_{pA}

To calculate the base shear of a building, it is necessary to gain information about its natural vibration period as well. Since this cannot be known precisely before the model calculations are done, an approximation is found through the following formula:

$$T_{pA} = C_t \cdot H_N^{3/4} \qquad \text{(eq. 4.27 in TBDY 2018)}$$

Where:

C_t = Coefficient for structural system type (reinforced concrete frame = 0.1)
H_N = total height of the building above basement (in meters)

Calculation of horizontal elastic design spectral acceleration $S_{ae}(T)$

The horizontal elastic design spectral acceleration is essentialy the earthquake's demand curve, telling how hard the ground shakes a building, depending on how flexible that building is. The horizontal elastic design spectral acceleration is calculated based on how the natural vibration period falls compared to the spectrum corner periods T_A and T_B

$$S_{ae}(T) = (0.4 + 0.6 \cdot T / Ta) \cdot S_{DS} \qquad \text{for } 0 \le T \le T_A$$
$$S_{ae}(T) = S_{DS} \qquad \text{for } T_A \le T \le T_B$$
$$S_{ae}(T) = S_{DS} / T \qquad \text{for } T_B \le T \le T_L$$
$$S_{ae}(T) = (S_{D1} \cdot T_L) / T \qquad \text{for } T_L \le T,\ T_L = 6 \text{ sec.} \qquad \text{(eq. 2.2 in TBDY 2018)}$$

Where:

T_A = Spectrum corner period, calculated as $0.2 \cdot S_{D1}/S_{DS}$
T_B = Spectrum corner period, calculated as S_{D1}/S_{DS} (eq. 2.3 in TBDY 2018)

Seismic load reduction factor $R_a(T)$

Based on the ductility of the structural system, earthquake forces can be reduced. This reduction factor is calculated based on the behaviour factor and the building importance and is as follows;

$$R_A(T) = R / I \quad \text{(eq. 4.1a in TBDY 2018)}$$

or

$$R_A(T) = D\,(R / I - D) \cdot T / T_B \quad \text{(eq. 4.1b in TBDY 2018)}$$

Where:

R = Structural system behaviour factor (found in Table 4.1 in TBDY 2018) - Taken as A31, R = 4.0 in the model

I = Building importance factor found in Table 3.1 in TBDY 2018) - For residential buildings this value is 1.0

D = Overstrength factor (found in Table 4.1 in TBDY 2018)

Reduced design spectral acceleration $S_{aR}(T)$

Based on the seismic load reduction factor $R_a(T)$ and the horizontal elastic design spectral acceleration $S_{ae}(T)$, the final reduced design spectral acceleration can be calculated which tells what the earthquake demands from the building in a non-elastic way, since the structural system is designed to yield and absorb the seismic energy. The reduced design spectral acceleration $S_{aR}(T)$ is calculated based on the following formula:

$$S_{aR}(T) = S_{ae}(T) / R_a(T) \quad \text{(eq. 4.8 in TBDY 2018)}$$

Base shear calculation

Once the building's mass and its reduced design acceleration are known, the base shear is calculated. It captures everything in one number: how heavy the building is, how the ground shakes at that site, how flexible the structure is, and how ductile the structural system is. The code also enforces a minimum value regardless of what the calculation gives, ensuring that no building is designed for a trivially small earthquake force.

$$V_{tE}^{(X)} = m_t \cdot S_{aR}(T) \cdot (T_P^{(X)}) \geq 0.04\, m_t \cdot S_{DS} \cdot g \quad \text{(eq. 4.19 in TBDY 2018)}$$

Where:

$V_{tE}^{(X)}$ = Base shear force as total equivalent earthquake load

m_t = The total building mass (in tonnes, 10^3 kg)

$T_P^{(X)}$ = The dominant natural vibration period of the building in (X) direction (in seconds), in the model this is taken as the T_{pA} for the current situation calculations and the calculated natural vibration (T) from karamba3D for the retrofitted situation

g = gravitational acceleration (9,81 m/s)

Calculation of seismic load per floor

After the building weight is calculated, the equivalent seismic load at the roof floor $\Delta F_{NE}^{(X)}$ needs to be calculated, since this force has an influence in the distribution of the seismic loads between the intermediate floors. The corresponding formula in TBDY 2018:

$$\Delta F_{NE}^{(X)} = 0.0075 \cdot N \cdot V_{tE}^{(X)} \qquad \text{(eq. 4.22 in TBDY 2018)}$$

Where:

$\Delta F_{NE}^{(X)}$ = Additional equivalent earthquake load applied at roof level (in x-direction

N = total number of stories above basement level

$V_{tE}^{(X)}$ = base shear force (in x-direction)

After the seismic load at the roof is calculated, the load at the intermediate floors must be calculated. This is proportional based on mass and height per floor as is described in the following formula:

$$F_{iE}^{(X)} = (V_{tE}^{(X)} - \Delta F_{NE}^{(X)}) \cdot \frac{m_i H_i}{\sum_{j=1}^{N} m_j H_j} \qquad \text{(eq. 4.23 in TBDY 2018)}$$

Where:

$F_{iE}^{(X)}$ = Additional equivalent earthquake load applied at roof level

m_i = Seismic mass of the i-th floor

H_i = Height of i-th floor above the building base (in meters)

m_j = Seismic mass of the summation of all floors

H_j = Summation of height of all floors (in meters)

Calculation of interstorey drift capacity

In the model, the building is assumed to behave as a rigid diaphragm at each floor level, meaning all nodes at the same storey move essentially together as one plane. Based on this assumption, a single vertical line of column nodes is tracked throughout the height of the building. By monitoring the node IDs in both the X- and Y-direction, their displacements remain unambiguously identifiable regardless of the building geometry. The interstorey drift at each level is then simply the difference in horizontal displacement between two consecutive floors, which is amplified back to a realistic deformation level and checked against the code limits defined in TBDY 2018 section 4.9.1, which is explained further.

Calculation of interstorey drift

The following formula describes the calculation of the reduced interstorey drift at i-th storey (in X-direction) in meters, and is basically calculated based on the lateral displacement at the top of storey i minus the lateral displacement of the top of the floor below.

$$\Delta_i^{(X)} = u_i^{(X)} - u_{i-1}^{(X)} \qquad \text{(eq. 4.32 in TBDY 2018)}$$

Where:

$\Delta_i^{(X)}$ = Reduced interstorey drift at i-th storey in X-direction (in meter)

$u_i^{(X)}$= Lateral displacement at top of i-th storey under reduced earthquake loads in X-direction (in meter)

$u_{i-1}^{(X)}$ = Lateral displacement at top of storey i-1th under reduced earthquake loads in X-direction (in meter)

Calculation of effective interstorey drift

The effective interstorey drift represents the realistic lateral displacement difference between two consecutive floors, scaled back up to account for the ductility reduction applied. It is the actual deformation the building is expected to undergo during the design earthquake.

$$\delta_i^{(X)} = (R / I) \cdot \Delta_i^{(X)} \qquad \text{(eq. 4.33 in TBDY 2018)}$$

Where:

$\delta_i^{(X)}$ = Effective interstorey drift at i-th storey in X-direction (in meter)

R = Structural system behaviour factor (found in Table 4.1 in TBDY 2018) - Taken as A31, R = 4.0 in the model

I = Building importance factor found in Table 3.1 in TBDY 2018) - For residential buildings this value is 1.0

Spectral ratio coefficient calculation

Since the drift check is a serviceability check aimed at the frequent everyday earthquake rather than the full design earthquake, a scaling factor (λ) is needed to bring the DD-2 level displacements down to the DD-3 level. This ratio compares the spectral acceleration of the frequent earthquake to that of the design earthquake at the building's own period, and directly reduces the strictness of the drift limit accordingly.

$$\lambda = S_{ae}^{DD\text{-}3}(T_P) / S_{ae}^{DD\text{-}2}(T_P) \qquad \text{(derived from section 4.9.1.4 in TBDY 2018)}$$

Where:

λ = Spectral ratio of DD-3 to DD-2 elastic design spectral acceleration at T_P

$S_{ae}^{DD\text{-}3}(T_P)$ = The elastic spectral acceleration your building experiences during the design-level earthquake (72-year return period), read at your building's own period

$S_{ae}^{DD\text{-}2}(T_P)$ = The elastic spectral acceleration your building experiences during the design-level earthquake (475-year return period), read at your building's own period

Calculation of interstorey drift ratio limit

The interstorey drift ratio limit checks whether the building deforms acceptably at each floor during the frequent earthquake, ensuring non-structural elements such as infill walss and facades are not damaged beyond repair. This formula comes with a difference in limit, depending on hohw the infill walls are connected to the structural frame. When brittle infill walls are rigidly and directly attached to the frame with no flexible joints between them, the stricter limit of 0.008κ is utitlised. When flexible joints are applied, or when independently supported, the looser limit of 0.016κ can be applied, since the frame can deform more freely without causing non-structural damage. In the model, the stricter limit is used since the building typology contains no infill walls or brittle infill walls without flexible joints.

$$\lambda \cdot (\delta_i^{(X)},max / h_i) \leq 0.008\kappa \qquad \text{(eq. 4.34a in TBDY 2018)}$$

Where:

$\delta_i^{(X)}$,max = Maximum effective interstorey drift among all columns/walls at i-th storey (in meters)

h_i = Clear storey height of the i-th floor (in meters)

κ = Material coefficient, κ = 1.0 for RC buildings (which is taken in the model), κ = 0.5 for steel buildings

Calculation of member capacities

In order to perform the unity checks for the reinforced concrete column and beam members of the building, a capcity check of the corresponding members have to be performed as well. The member and material information, which is filled in the Microsoft Forms survey, is fed into the following formulas in order to calculate the shear-, moment- & axial capacity of the member. The following member capacities are calculated using NEN-EN 1992-1-1 which is the primary European standard for concrete structures.

Calculation of shear capacity (non-inclined stirrups)

The calculation formula of the shear capacity of a reinforced concrete member is dependent on if the stirrups are inclined or not. For members with non-inclined stirrups, the shear capacity of a reinforced concrete member is the smaller value between the following formulas:

$$V_{Rd,s} = (A_{sw} / s) \cdot z \cdot f_{ywd} \cdot \cot(\theta) \qquad \text{(eq. 6.8 in NEN-EN 1992-1-1)}$$

and

$$V_{Rd,max} = \alpha_{cw} \cdot b_w \cdot z \cdot \nu_1 \cdot f_{cd} \cdot (\cot(\theta) + \tan(\theta)) \qquad \text{(eq. 6.9 in NEN-EN 1992-1-1)}$$

Where:

$V_{Rd,s}$ = Shear capacity with shear reinforcement
$V_{Rd,max}$ = Maximum shear resistance (due to concrete strut crushing)
A_{sw} = Cross-sectional area of shear reinforcement
s =spacing of stirrups
z = lever arm ($\approx 0.9 \cdot d$ (where d: effective depth of cross-section))
f_{ywd} = Design yield strength of shear reinforcement (in N/mm^2)
f_{cd} = Design compressive strength of concrete (f_{ck}/γ_c, in N/mm^2)
θ = Angle of concrete compression strut (taken as most conservative value of 45 ° in the model)
α_{cw} = coefficient taking account of the state of the stress in the compression cord (1.0 for non-prestressed members)
b_w = Width of cross-section
ν_1 = strength reduction factor for cracked concrete, calculated as $0.6 \cdot (1 - f_{ck} / 250)$

Calculation of shear capacity (inclined stirrups)

For stirrups placed under an angle in the member, different formulas act. For these members, the shear capacity of a reinforced concrete member is the smaller value between the following formulas:

$$V_{Rd,s} = (A_{sw} / s) \cdot z \cdot f_{ywd} \cdot (\cot(\theta) + \cot(\alpha)) \cdot \sin(\alpha) \qquad \text{(eq. 6.13 in NEN-EN 1992-1-1)}$$

and

$$V_{Rd,max} = \alpha_{cw} \cdot b_w \cdot z \cdot \nu_1 \cdot f_{cd} \cdot (\cot(\theta) + \cot(\alpha)) / (1 + \cot^2(\theta)) \qquad \text{(eq. 6.14 NEN-EN 1992-1-1)}$$

Where:

α = angle of the shear reinforcement (between 0 ° and 45 °)

Calculation of moment capacity
To start the calculation of the moment capacity, it is first important to calculate the neutral axis depth at ultimate limit state, which is done as follows:

$$x_u = N_s / (\alpha \cdot b \cdot f_{cd})$$

Where:
x_u = The depth of the neutral axis at ultimate limit state (in mm)
N_s = The tensile resistance in the steel reinforcement ($A_s \cdot f_{yd}$)
α = Concrete compression stress-block factor, which is equal to 0.75
b = The width of the cross-section (in mm)

Secondly, the internal lever arm of the member is calculated. The internal lever arm is the distance between the tensile force in the steel reinforcement and the compressive force in the concrete block and is calculated as follows

$$z_u = d - \beta \cdot x_u$$

Where:
z_u = The internal lever arm of the member at ultimate limit state (in mm)
d = Effective depth of the member (in mm)
β = The location factor of the concrete compression resultant ≈ 7/18

Based on the steel reinforcement resistance (N_s) and the internal lever arm (z_u), the bending moment capacity of the concrete member can be calculated with the formula below:

$$M_{Rd} = N_s \cdot z_u$$ (derived from section 6.1 in NEN-EN 1992-1-1)

Calculation of axial force capacity
In the model the axial force capacity in compression is calculated by using the compression capacity of the concrete together with the compression capacity of the steel reinforcement. The compression capacity of the member can be calculated according to the following formula:

$$N_{Rd,c} = A_c \cdot f_{cd} + A_s \cdot f_{yd}$$

Where:
$N_{Rd,c}$ = The axial compression resistance of the member
A_c = The cross-sectional surface area of the concrete (in mm²)
f_{cd} = Design compressive strength of concrete (f_{ck}/γ_c, in N/mm²)
A_s = The cross-sectional surface area of the steel reinforcement (in mm²)
f_{yd} = Design strength of the steel reinforcement (f_{yk}/γ_s, in N/mm²)

Note: the model also shows that net axial tension occurs (mainly in the columns) due to sway and overturning of the building under seismic loads. This means that a separate capacity check for axial tension resistance of the members is performed by using the following formula:

$$N_{Rd,t} = A_s \cdot f_{yd}$$

Where:
$N_{Rd,t}$ = The axial tension resistance of the member

Calculation of biaxial bending moment interaction ($M_z + M_y$)

In structures, columns are almost never loaded in just one direction. Seismic forces, eccentricities, and asymmetric loading cause bending about both axis simultaneously. Since the combined effect of biaxial bending reduces a column's load-carrying capacity below of what either axis could carry independently, verifying both moment components together is essential for an accurate and safe structural assessment. Therefore, the biaxial bending moment interaction is calculated using the following eurocode formulas:

$$(M_{Edz} / M_{Rdz})^a + (M_{Edy} / M_{Rdy})^a \leq 1.0 \qquad \text{(eq. 5.39 in NEN-EN 1992-1-1)}$$

Where:

M_{Edz} = The design moment around the z-axis
M_{Rdz} = The moment resistance in the z-axis direction
M_{Edy} = The design moment around the y-axis
M_{Rdy} = The moment resistance in the y-axis direction
a = The exponent based on N_{Ed}/N_{Rd} Where for:

$N_{Ed}/N_{Rd} = 0.1$	a = 1.0
$N_{Ed}/N_{Rd} = 0.7$	a = 1.5
$N_{Ed}/N_{Rd} = 1.0$	a = 2.0

Appendix H: Retrofit configuration based on nodal-ID numbers

If during the retrofit strategy implementation phase of the model, the engineer requires more flexibility in the chose where to apply the column jacketings or the shear walls within the building, the option to make a selection based on the ID numbers of the nodes is also a possibility. In this configuration, the engineer can click the component "Point List", which assigns a number to every node in the geometry (as is shown in Figure H.1). The engineer can then type the nodes from which a column jacketing is erected or the corner points of the shear wall implementation, and following this, the retrofit intervention is now located at the place of the choice of the engineer as is illustrated in Figure H.2.

Imagine if the engineer looks for a solution to apply shear walls at diagonally opposite sites, the engineer fills in the ID numbers of the corners of the shear walls, and this is directly implemented in the geometry.

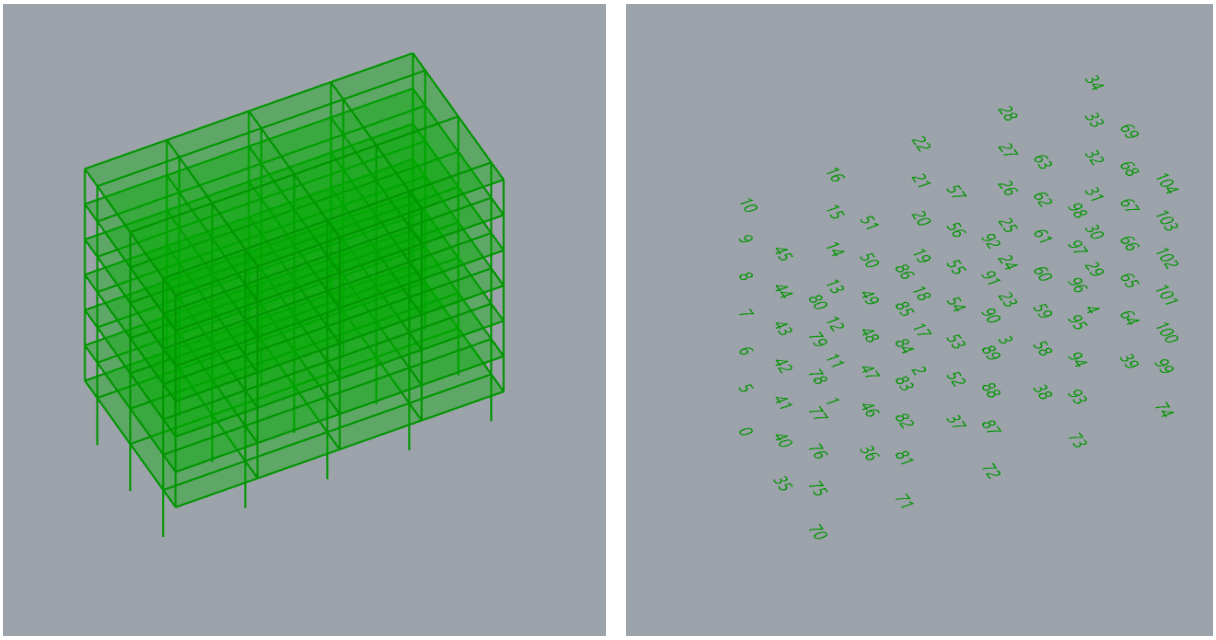

Figure H.1: Parametric building geometry in Rhino/Grasshopper environment: the wireframe geometry of a structure (left image) and the corresponding Nodal-ID point distribution (right image) (author's own work)

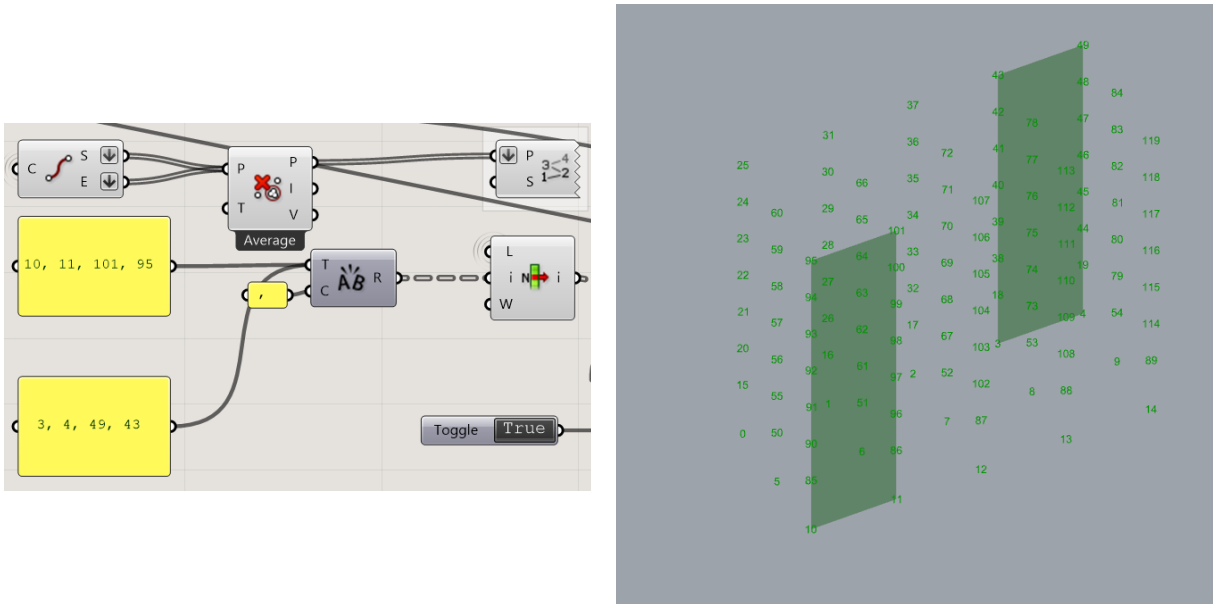

Figure H.2: Nodal-ID based retrofit configuration in Grasshopper: input component for node ID selection within the Grasshopper code (left image) and the resulsting shear wall geometry output at the engineer-defined locations (right image)

Appendix I: Retrofit application of column jacketing

In this appendix, the steps to install the column jacketing with the precast column jacketing blocks is shown. What exactly is done per step is discussed in greater detail in this section in order to get a good understanding of the installation process.

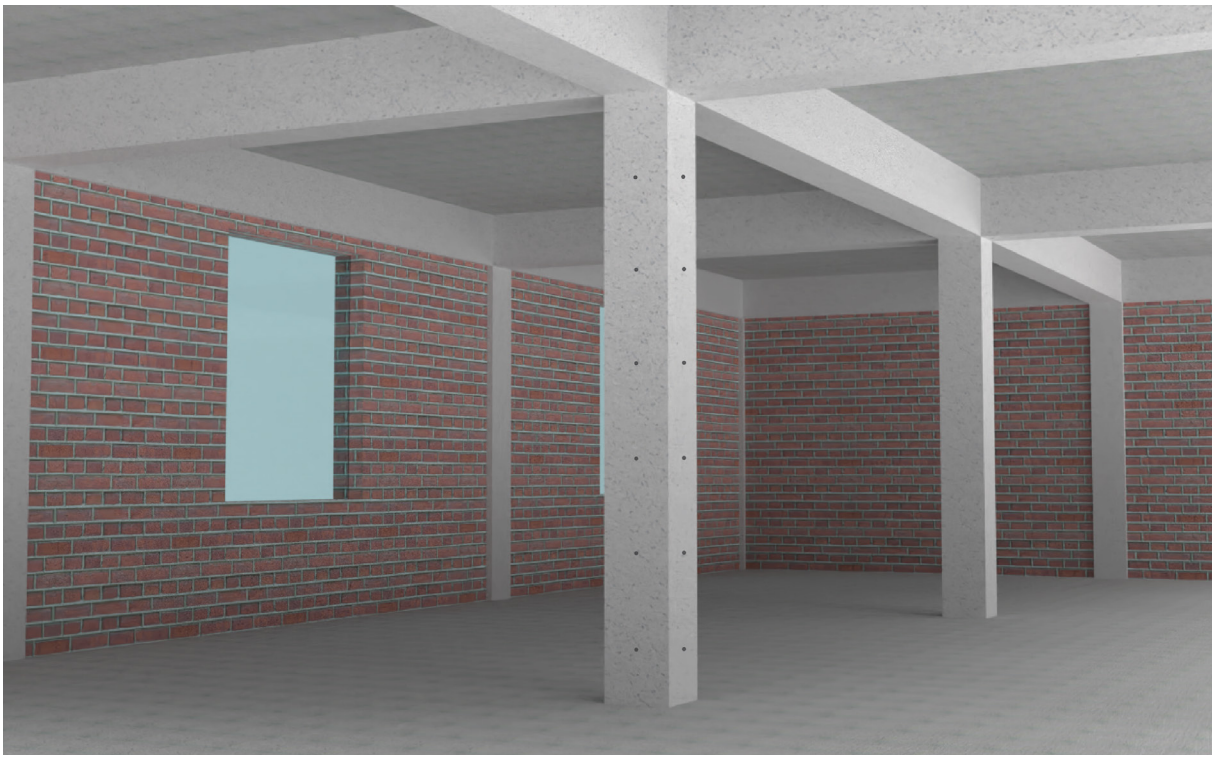

Figure I.1 - Step 1: In this step, holes are drilled in the existing column at certain distances in order to accommodate the shear dowels later in the process.

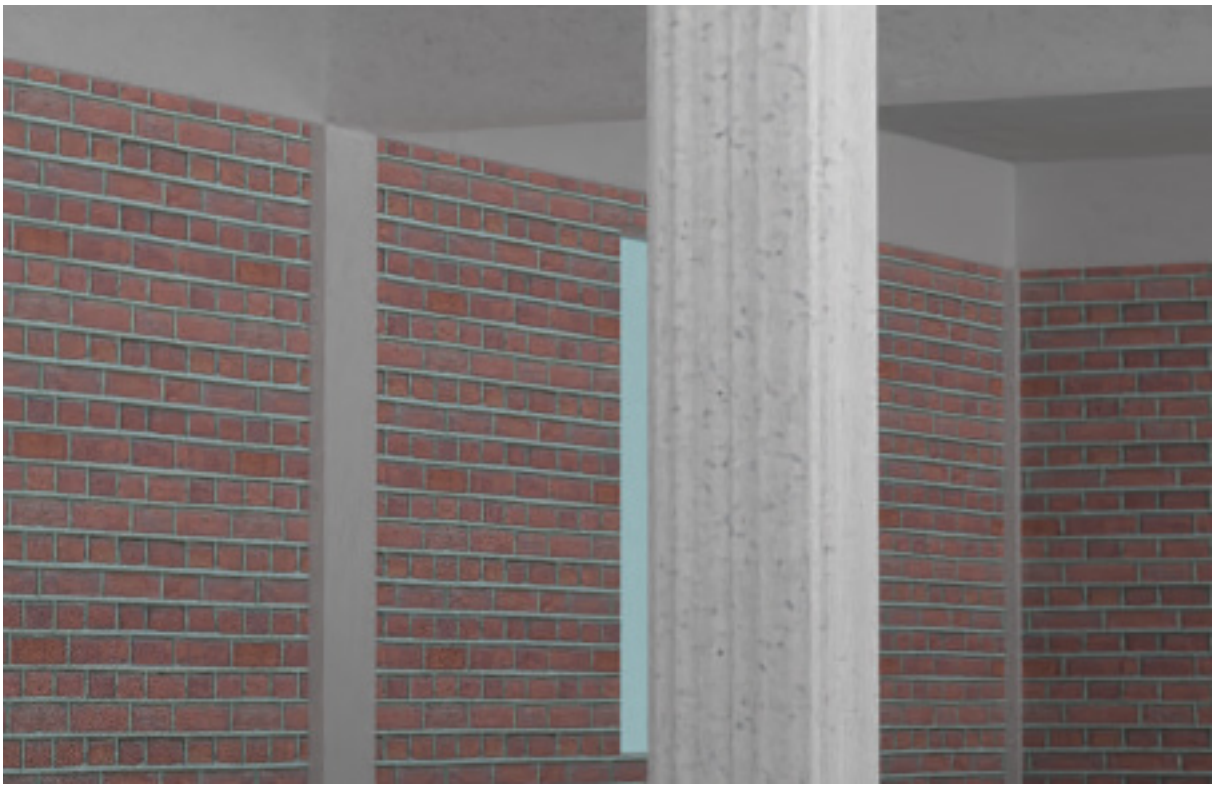

Figure I.2 - Step 2: In order to increase the bonding capacity between the current column and the new system, the columns are roughened to increase its contact area. This roughening can be done mechanically by sandblasting or using a light jackhammer.

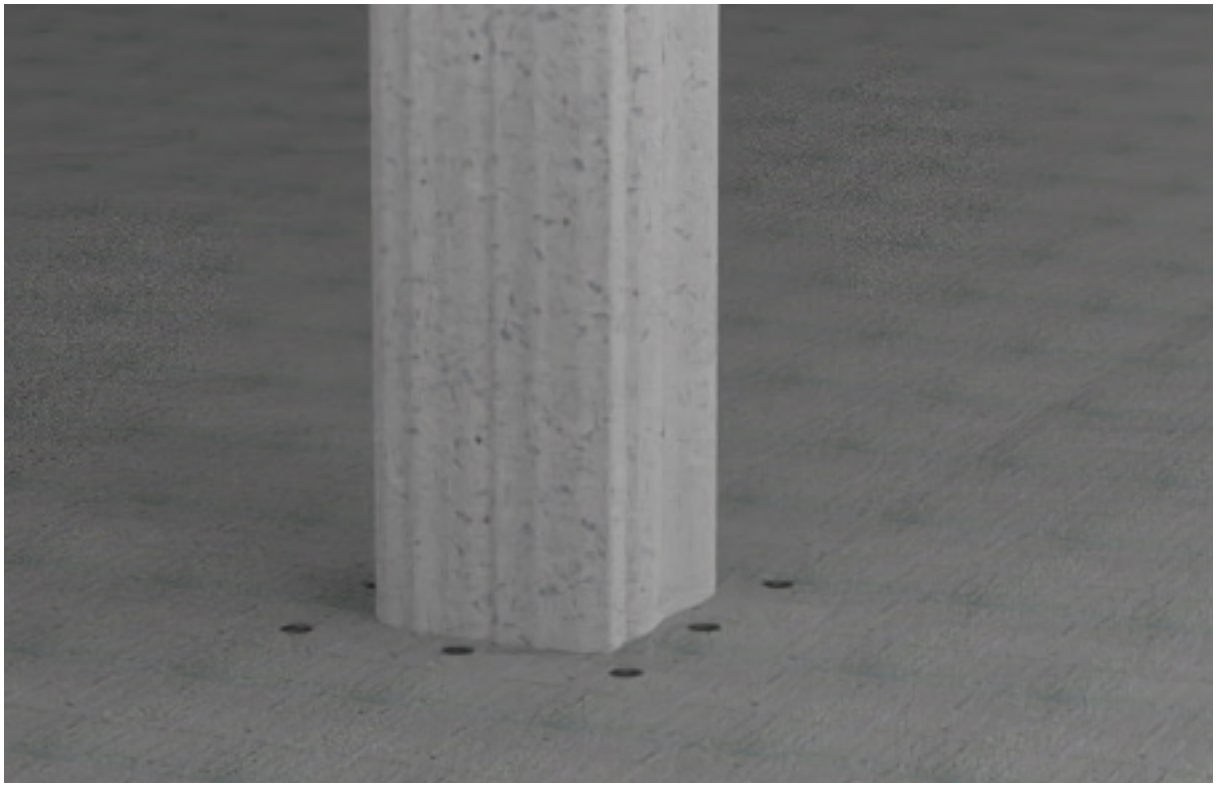

Figure I.3 - Step 3: In this step, holes are drilled in the existing slab in order to accommodate the longitudinal rebars. These holes are drilled with a larger diameter to ensure that concrete can flow in to solidy the connection.

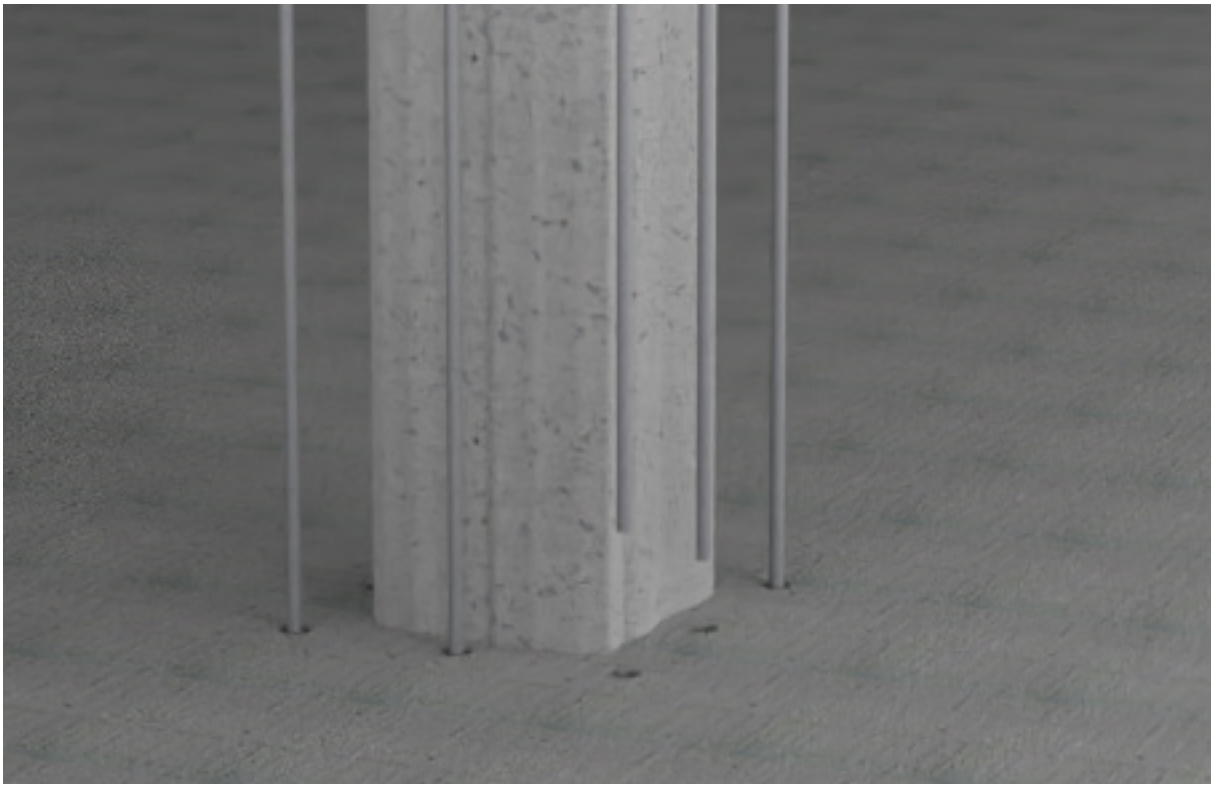

Figure I.4 - Step 4: Consequently, the first longitudinal rebars (with a length of 800 mm) can be placed inside these pre-drilled holes. Around these longitudinal rebars, the first stirrups and shear dowels can be placed to make the steel framework before pouring the cast-in-place concrete.

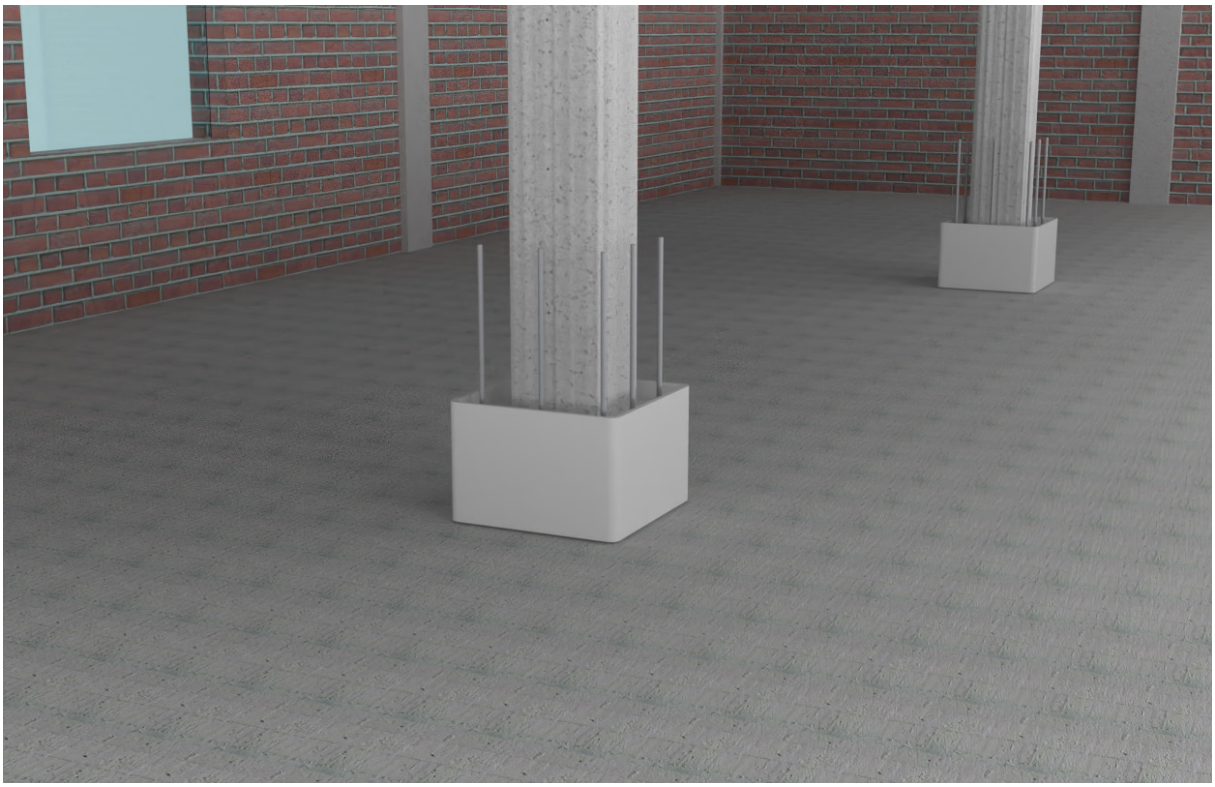

Figure I.5 - Step 5: In the next step, the bottom mould is placed around the column by fastening two identical halves of the steel together to form the formwork of the cast-in-place bottom. This provides the more reliable concrete bottom at the more stressed areas of the column, namely at its joints.

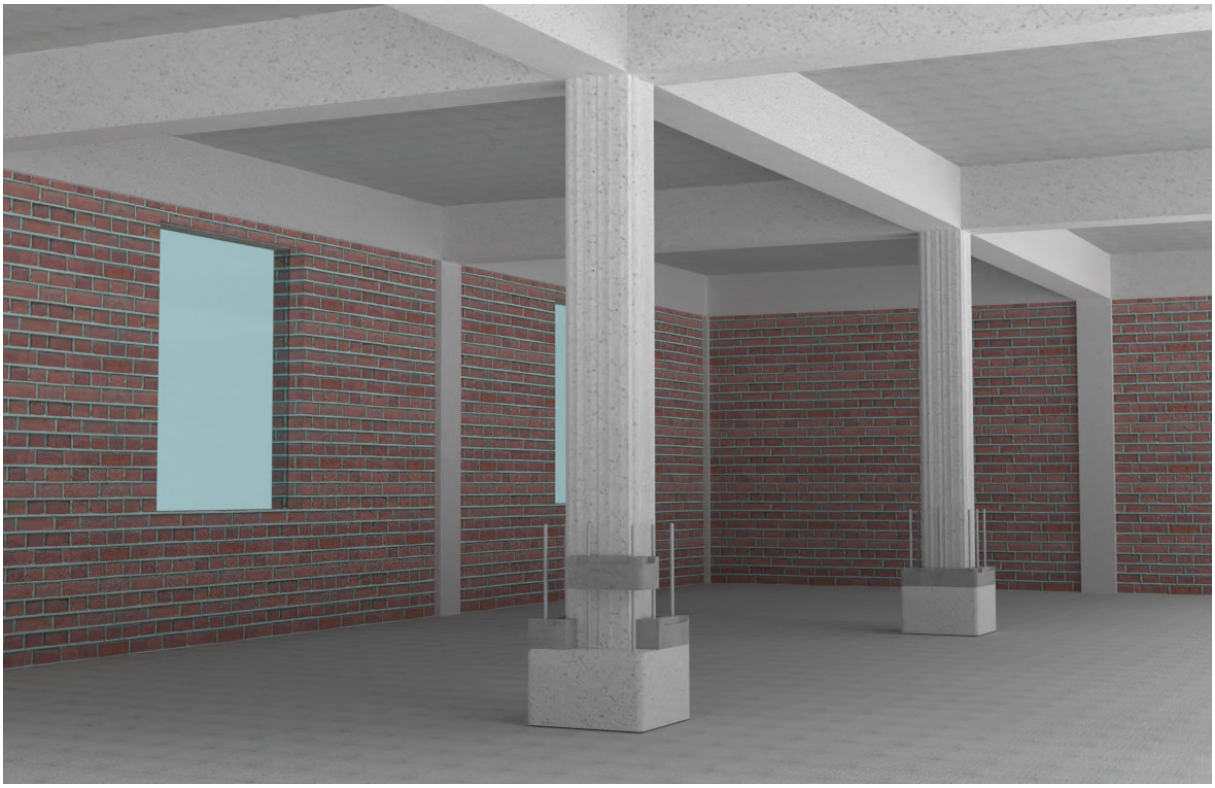

Figure I.6 - Step 6: After the casted concrete has hardened enough, the bottom layer of modular blocks can be placed. This bottom bricks have a flat bottom in contrast to the other bricks which contain the shear teeth. In order to solidify this connection, a bonding layer of cement is applied on the casted concrete.

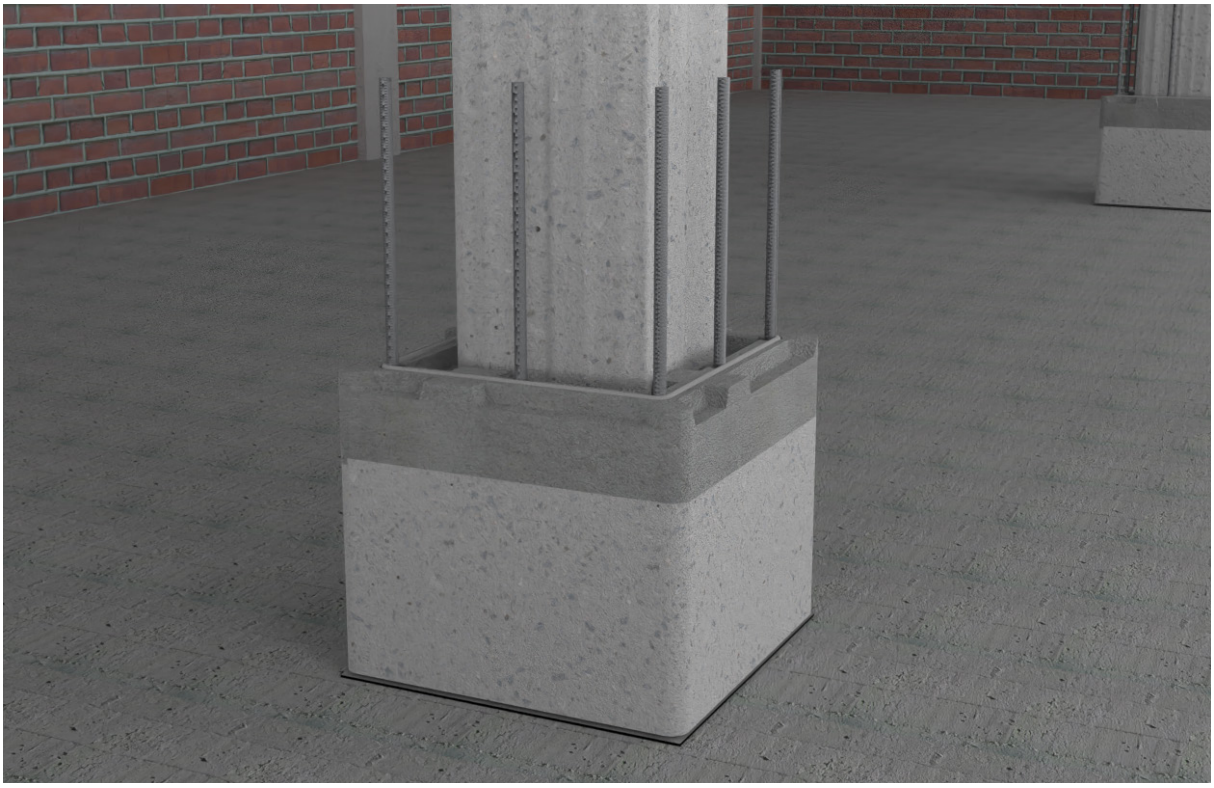

Figure I.7- Step 7: Once the bottom blocks are in place, the first stirrup element is placed in the horizontal grooves of theblock elements, in order to confine the system.

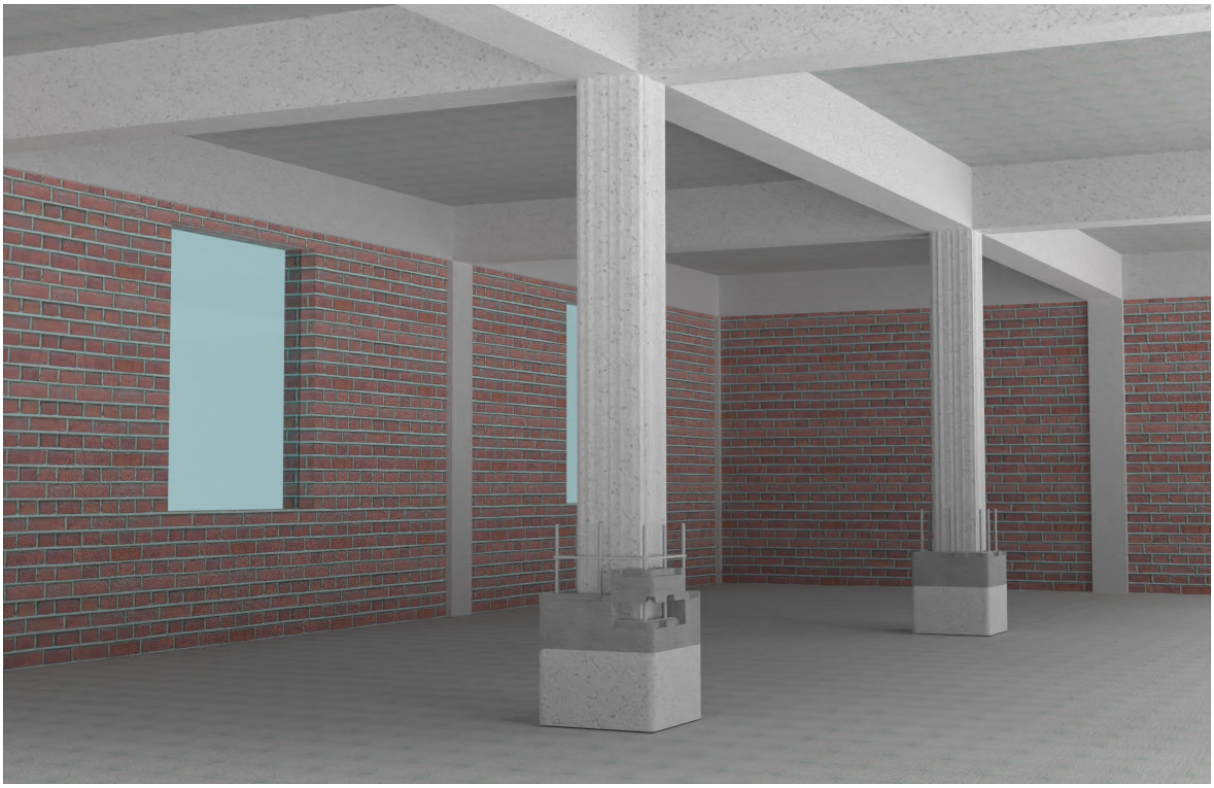

Figure I.8 - Step 8: Before placing the second layer of blocks, a layer of cement will be applied on top of the first block elements to provide the proper adhesion the system needs. After the mortar application, the next layer of bricks can be slid over the longitudinal rebars, followed by placing the stirrup element in the horizontal groove.

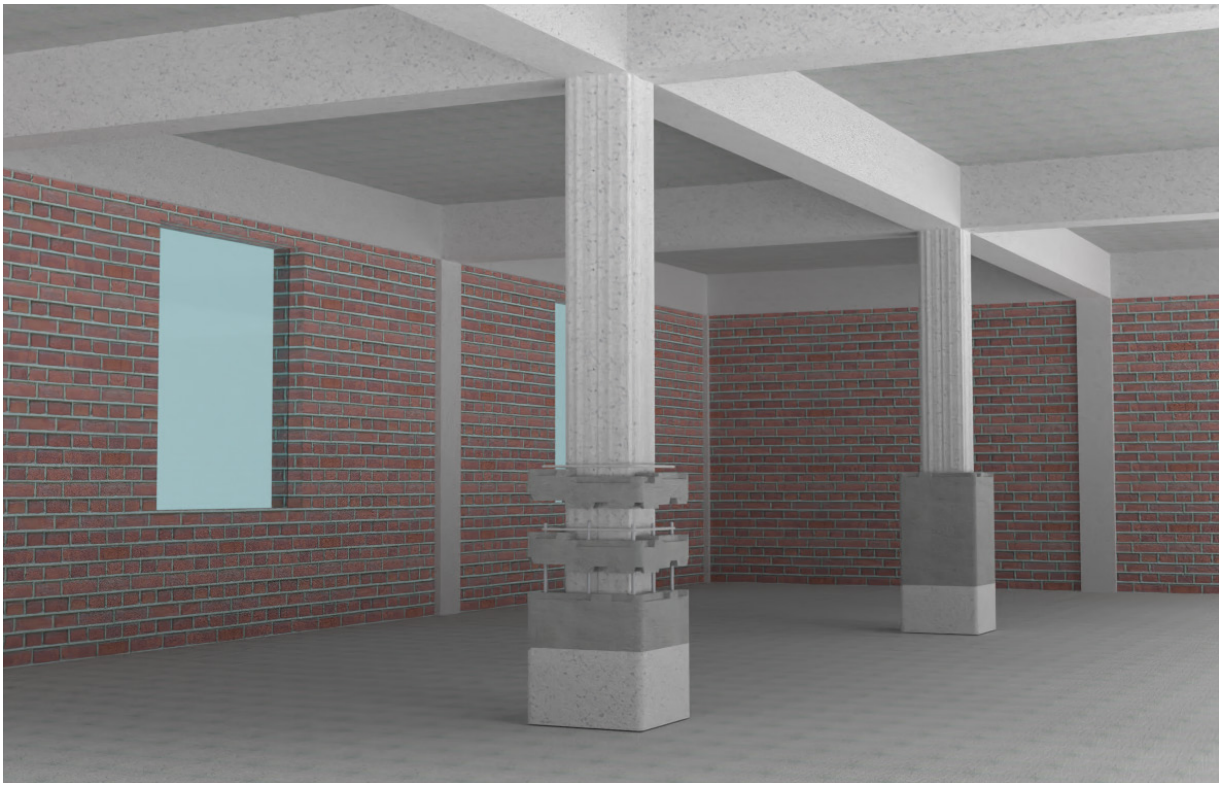

Figure I.9 - Step 9: The placement of the modular block and stirrup elements follow one another in combination with placing the shear dowel in the pre-drilled holes in the column and hooking these dowels around the longitudinal rebars. This process is repeated until the end of the longitudinal rebar is reached.

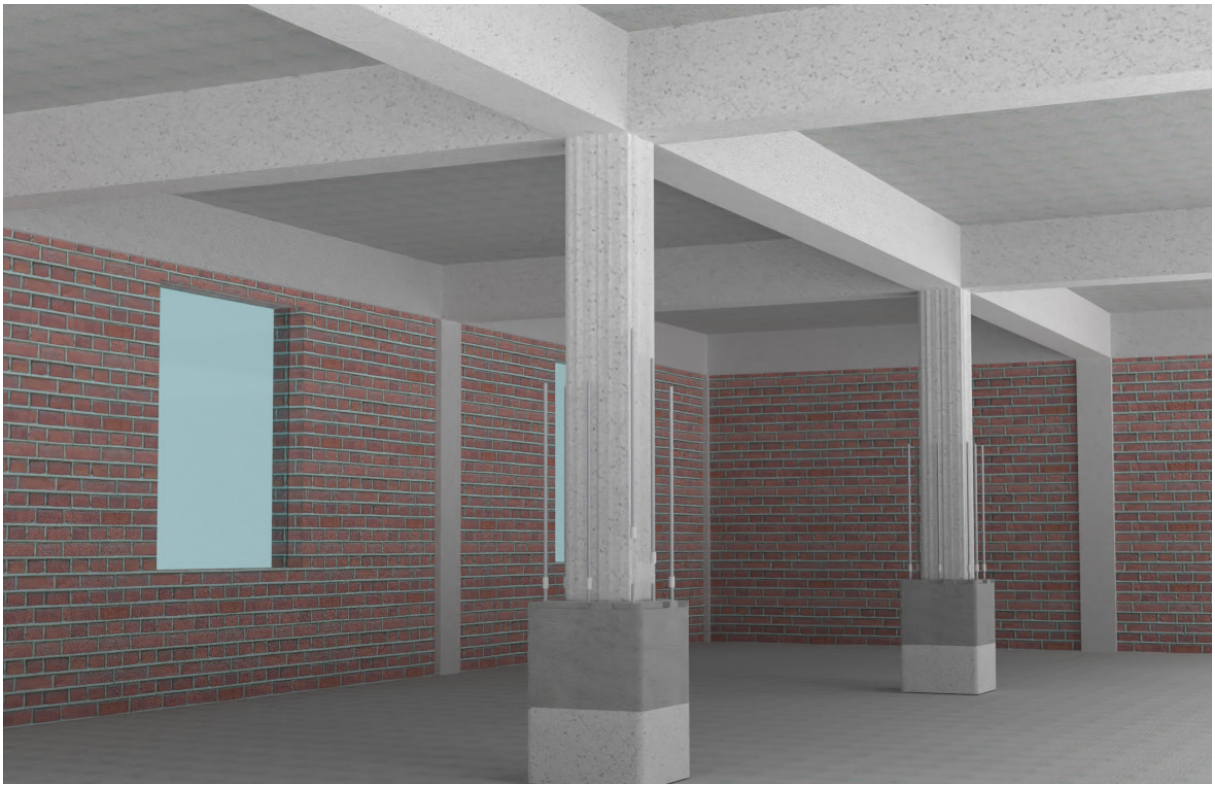

Figure I.10 - Step 10: In this step, the end of the longitudinal rebar is connected to a new rebar by using mechanical rebar couplers. This ensures that a new batch of modular blocks, stirrups and shear dowels can be placed to further build the retrofit system.

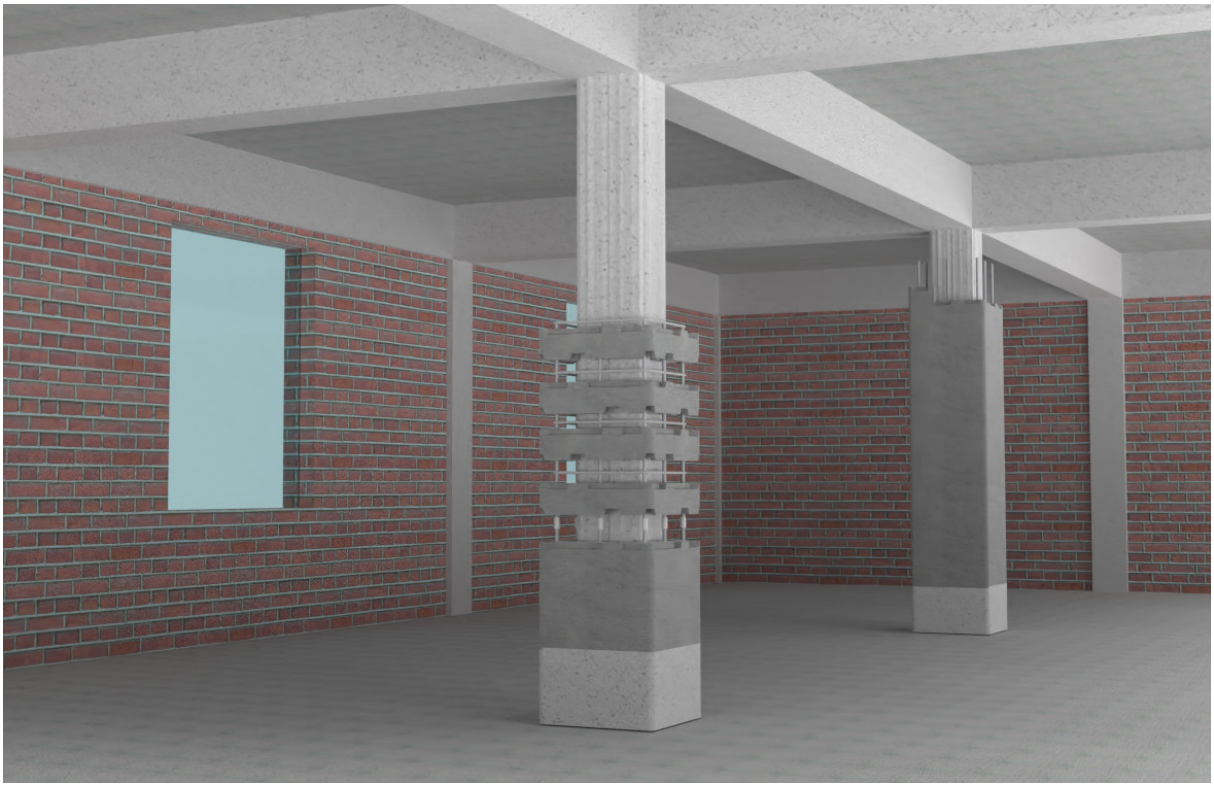

Figure I.11 - Step 11: Now, the same steps are repeated over and over until the top of the column is almost reached.

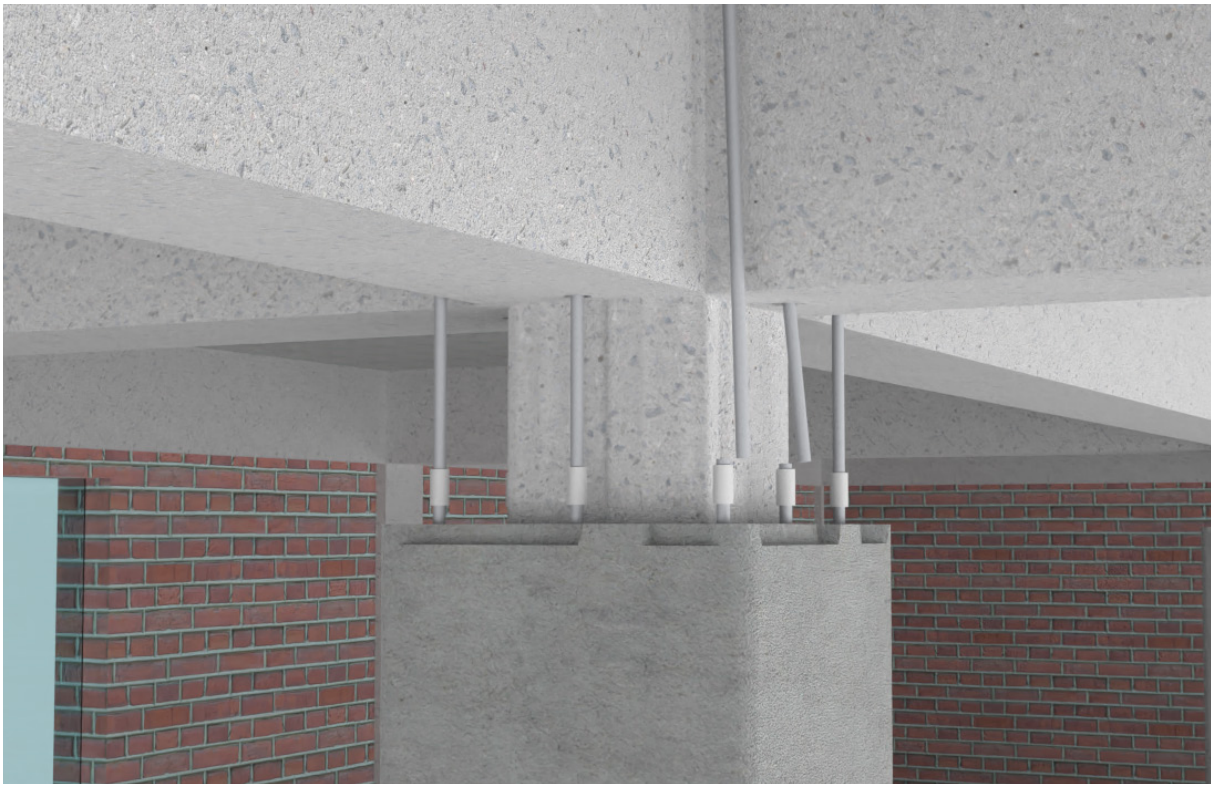

Figure I.12 - Step 12: The last rebars are fastened by sliding them into pre-drilled holes in the ceiling. In order to allow fastening in this relatively narrow space, couplers must temporarily be slid down to allow insertion of the final rebar segments.

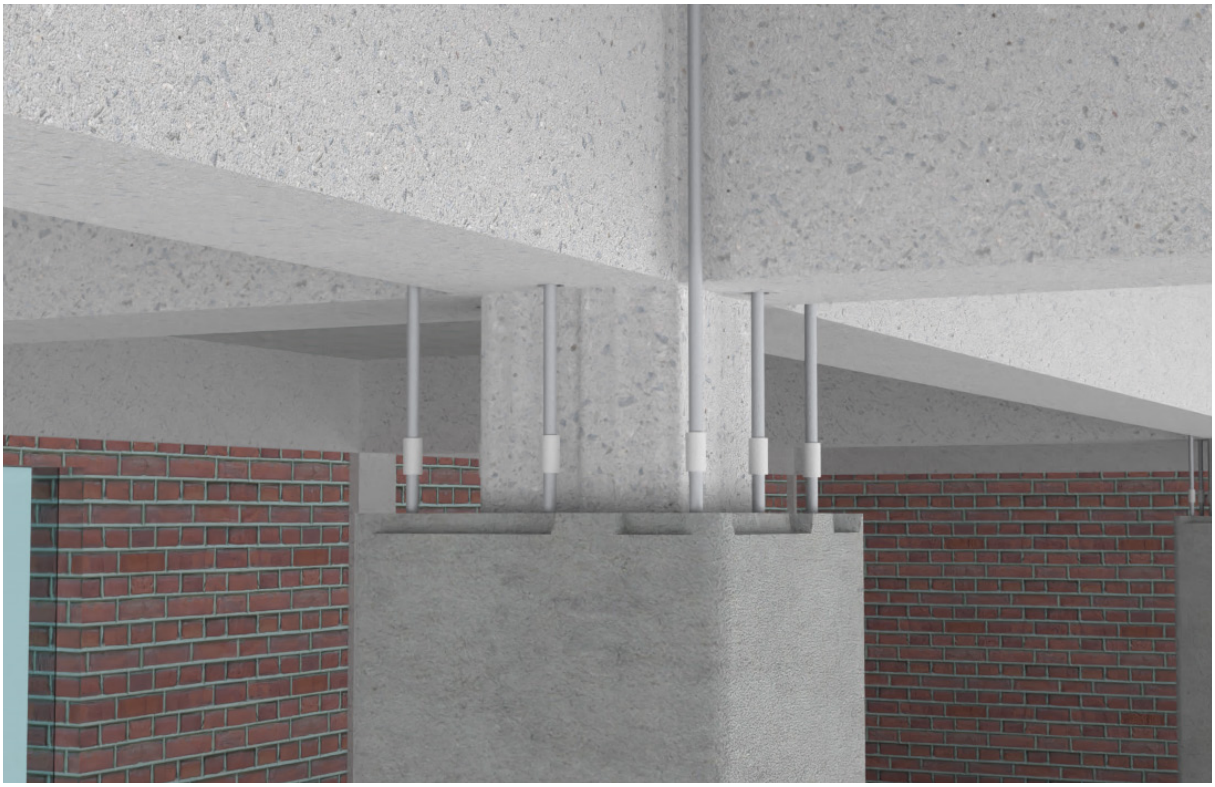

Figure I.13 - Step 13: After the longitudinal rebar is inserted, the couplers can be turned back into its intended place, connecting the longitudinal rebars into one continuous element.

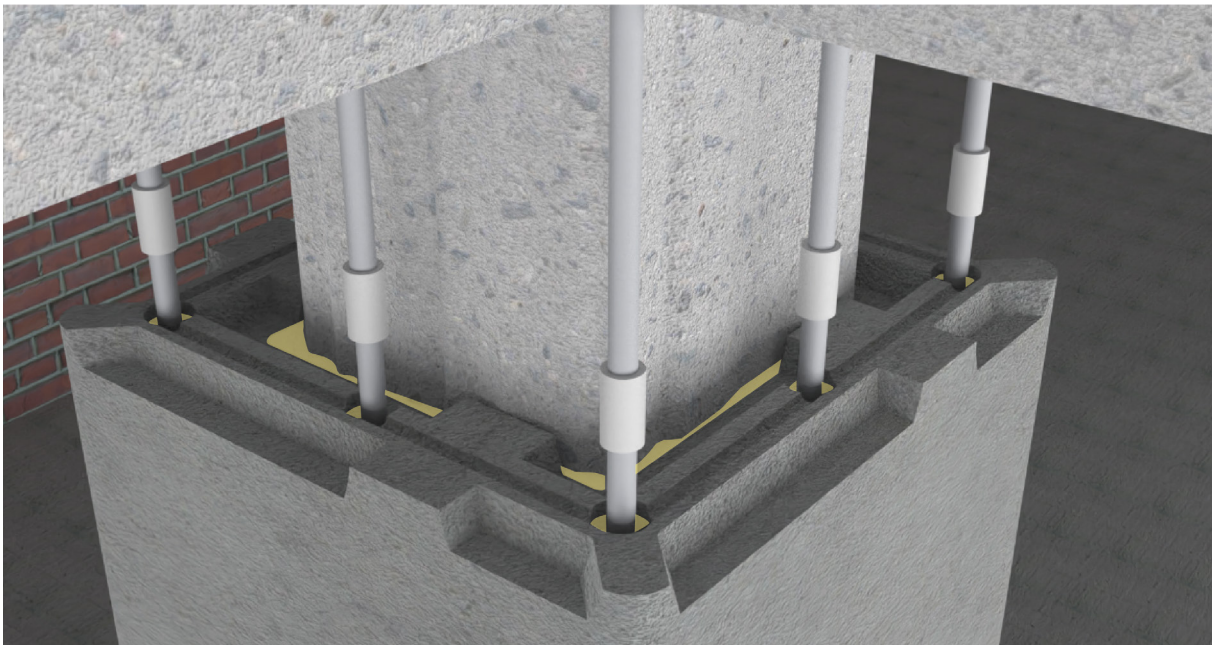

Figure I.14 - Step 14: After the modular block part of the retrofit element is done, the system is solidified by using a non-shrink cementitious injection grouts. This very flowable grout is injected in the longitudinal rebar holes which allows it to flow through the stirrup grooves to other parts of the system. This grout is also injected inbetween the current column and the new system ensuring proper transfer of shear forces between the old and new system.

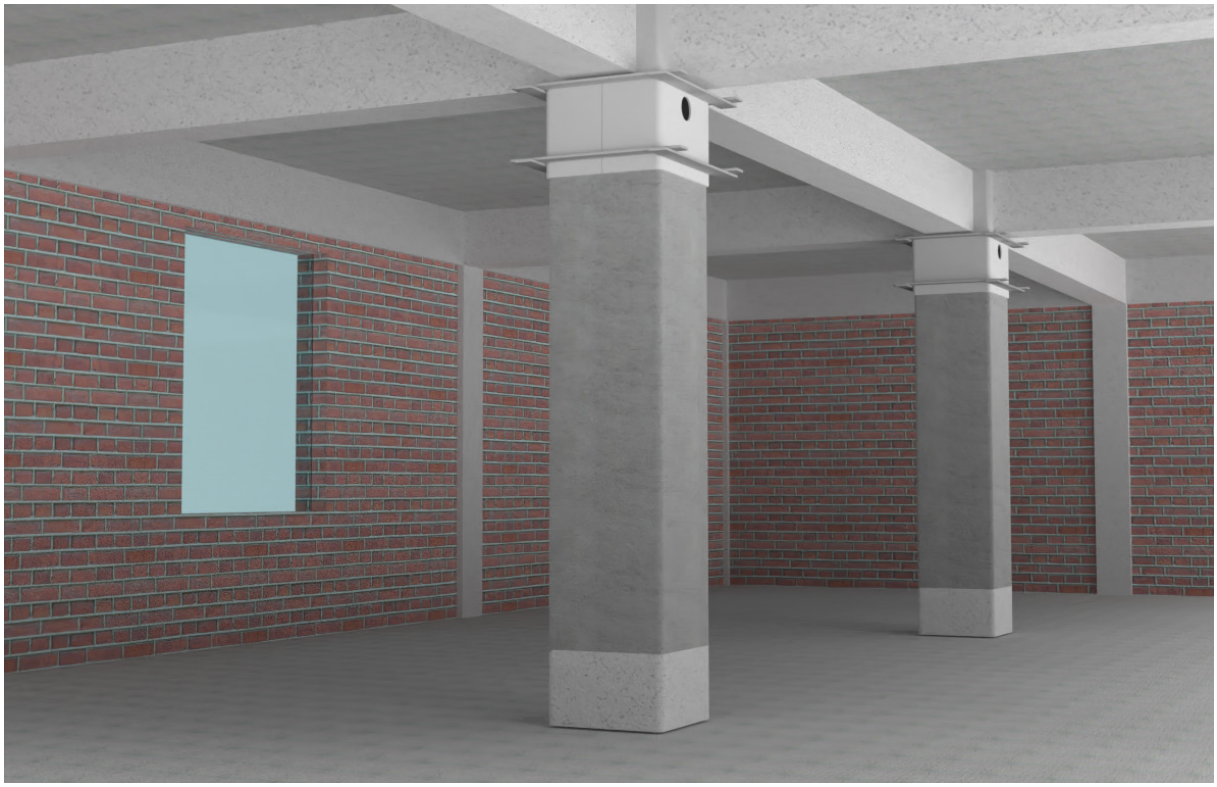

Figure I.15 - Step 15: At last, a steel formwork, consisting of two halves is applied and fastened at the top of the column. This formwork contains a Ø 100 mm gap for the insertion of the virgin concrete through a tube and two Ø 30 mm air vents at the other side, allowing trapped air to escape during pouring, preventing air pockets and incomplete filling of the formwork.

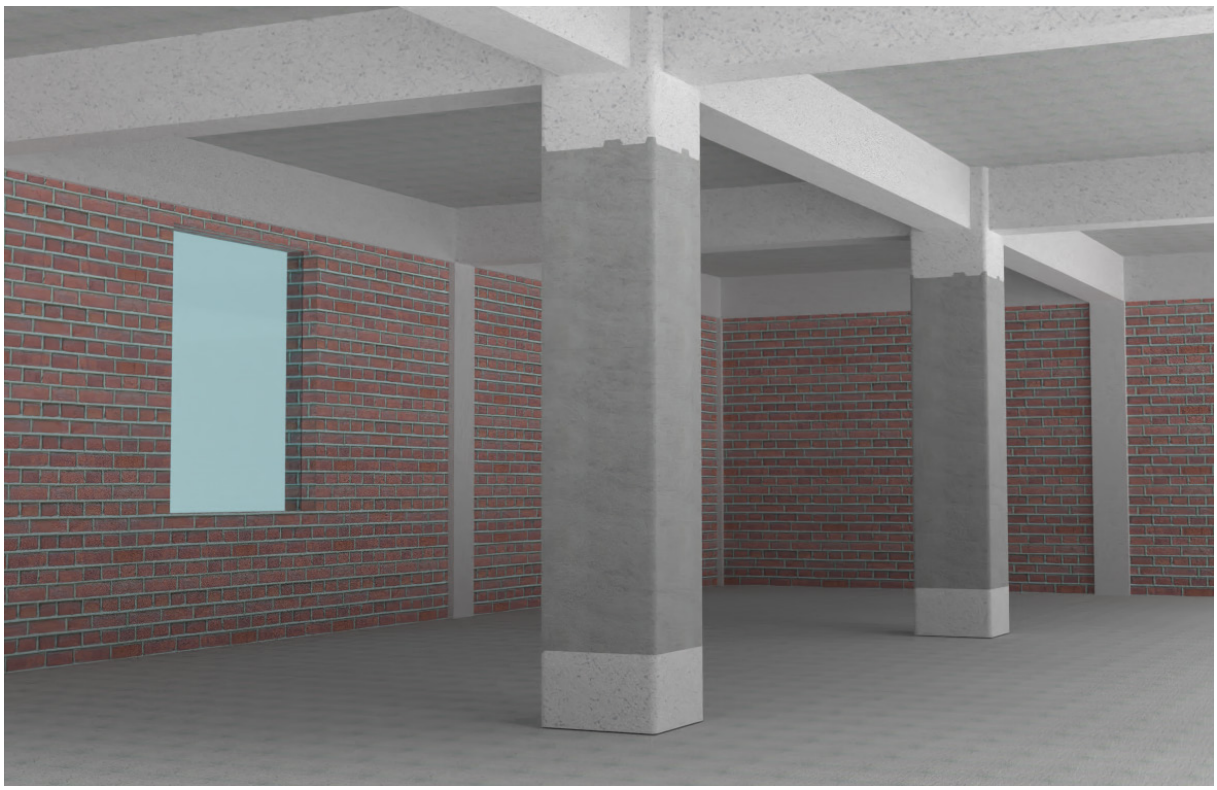

Figure I.16 - Step 16: After the cast-in-place concrete is applied at the top and is hardened, the formwork can be removed and the installation of the column jacketing is done.

Appendix J: Retrofit application of shear walls

In this appendix, the installation steps of shear wall retrofitting with the precast shear wall blocks is shown. What exactly is done per step is discussed in greater detail in this section in order to get a good understanding of the installation process.

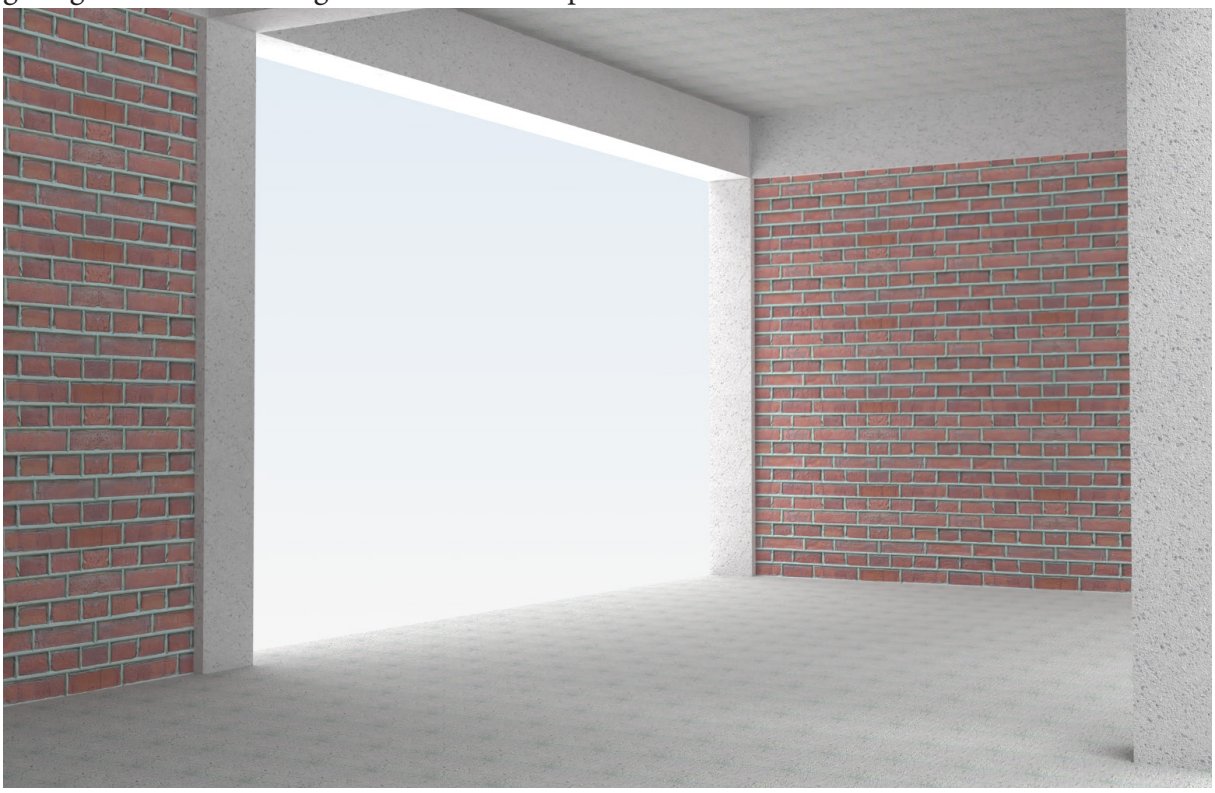

Figure J.1 - Step 1: In this step, the infill bricks of the wall are taken out to make space for the new retrofit shear wall system.

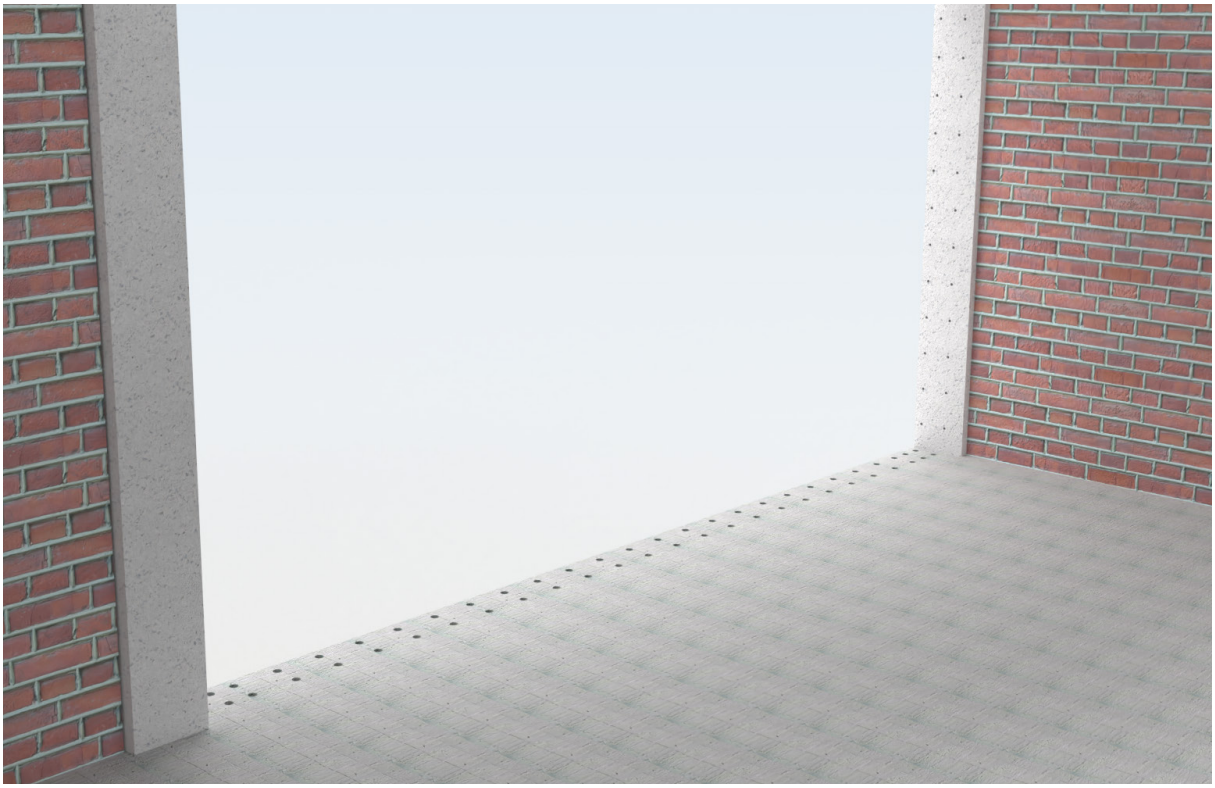

Figure J.2 - Step 2: Following up, holes are drilled in the existing concrete frame (column & slabs) at certain distances in order to accommodate the longitudinal rebars and the shear dowels.

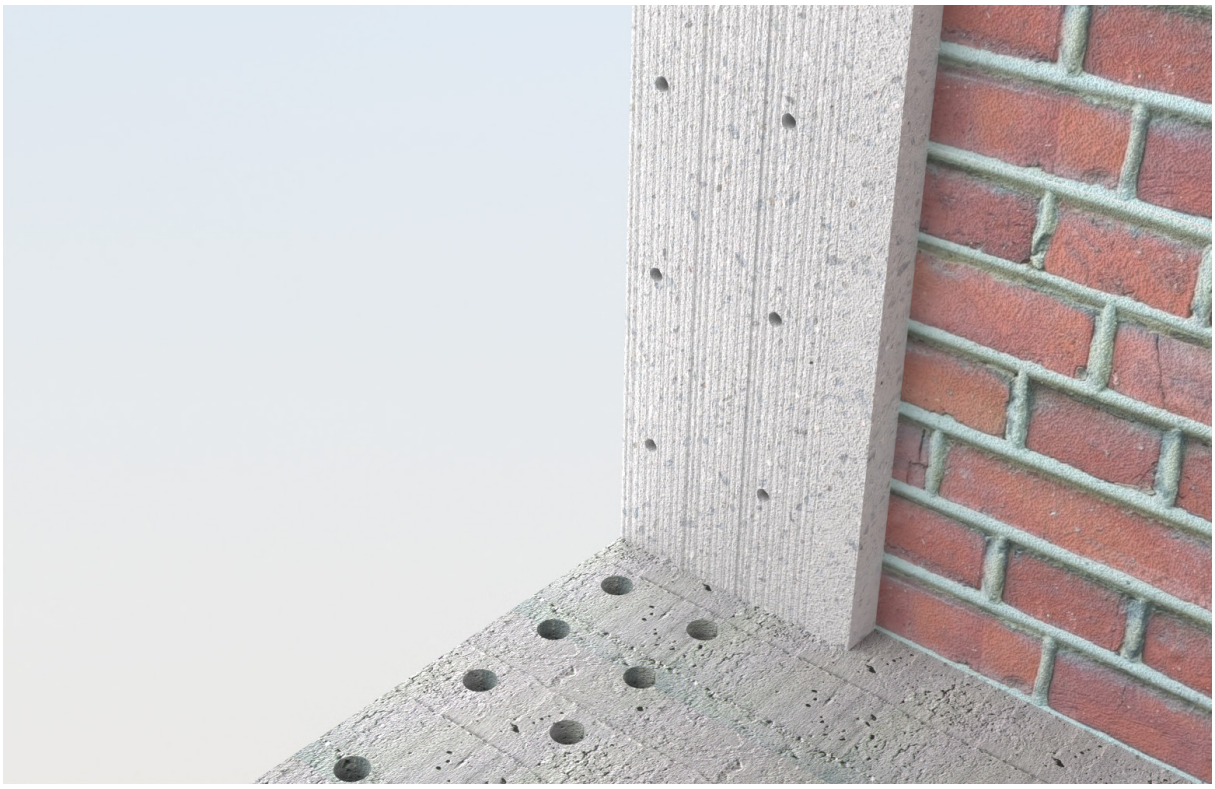

Figure J.3 - Step 3: Next, the columns of the frame are roughened in order to increase surface area and therefore the bond area of the connection.

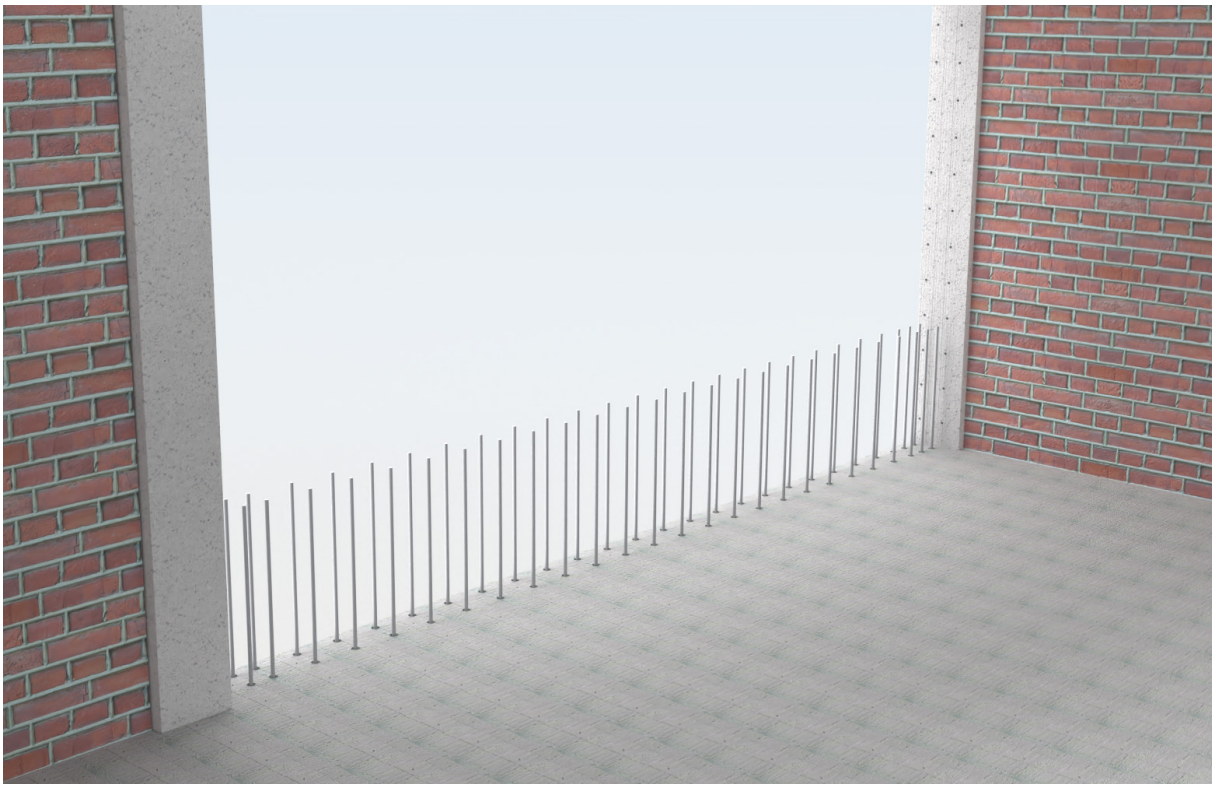

Figure J.4 - Step 4: Consequently, the first longitudinal rebars (with a length of 800 mm) can be placed inside these pre-drilled holes. Along these longitudinal rebars, stirrups and cross-ties should be placed to provide the steel framework before pouring the cast-in-place concrete.

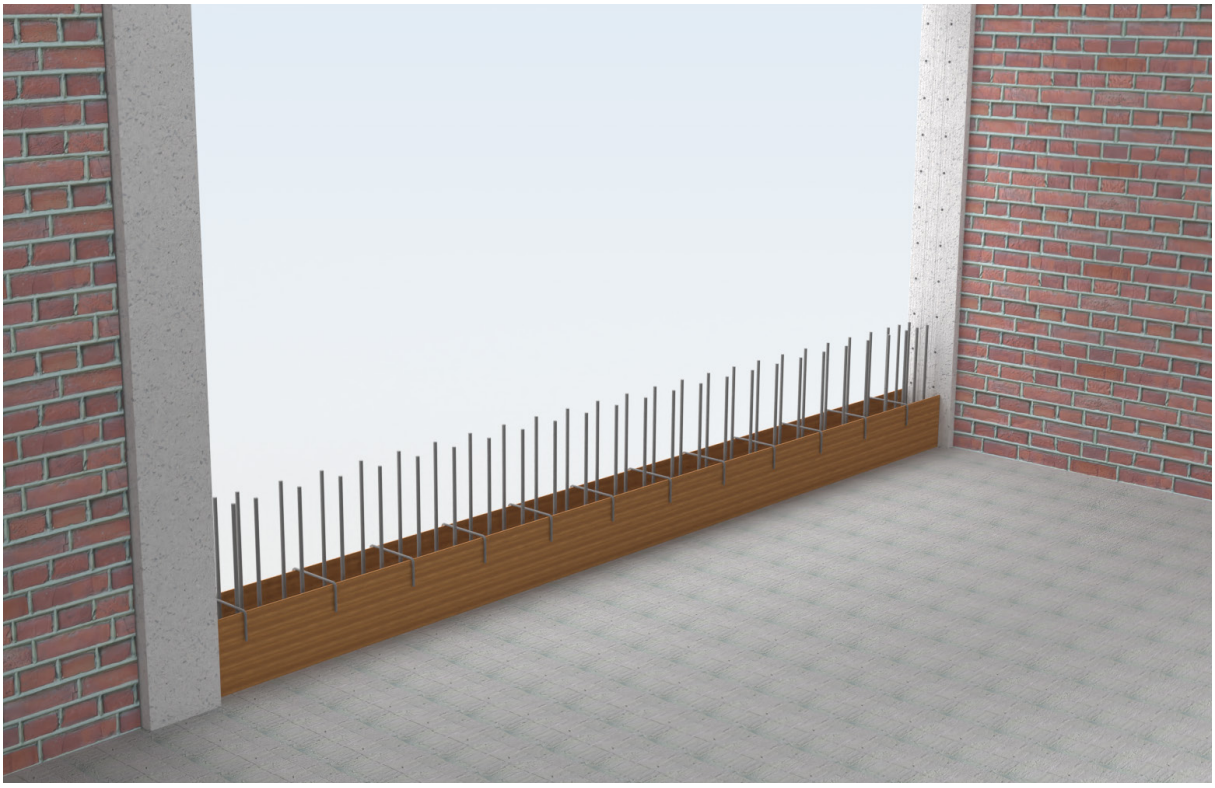

Figure J.5 - Step 5: After insertion of the longitudinal rebars, the timber formwork can be placed. It is deliberately chosen to use a timber formwork because of the larger and irregularity of the sizes of the formwork, making them out of steel would be less practical than just simply using timber ones.

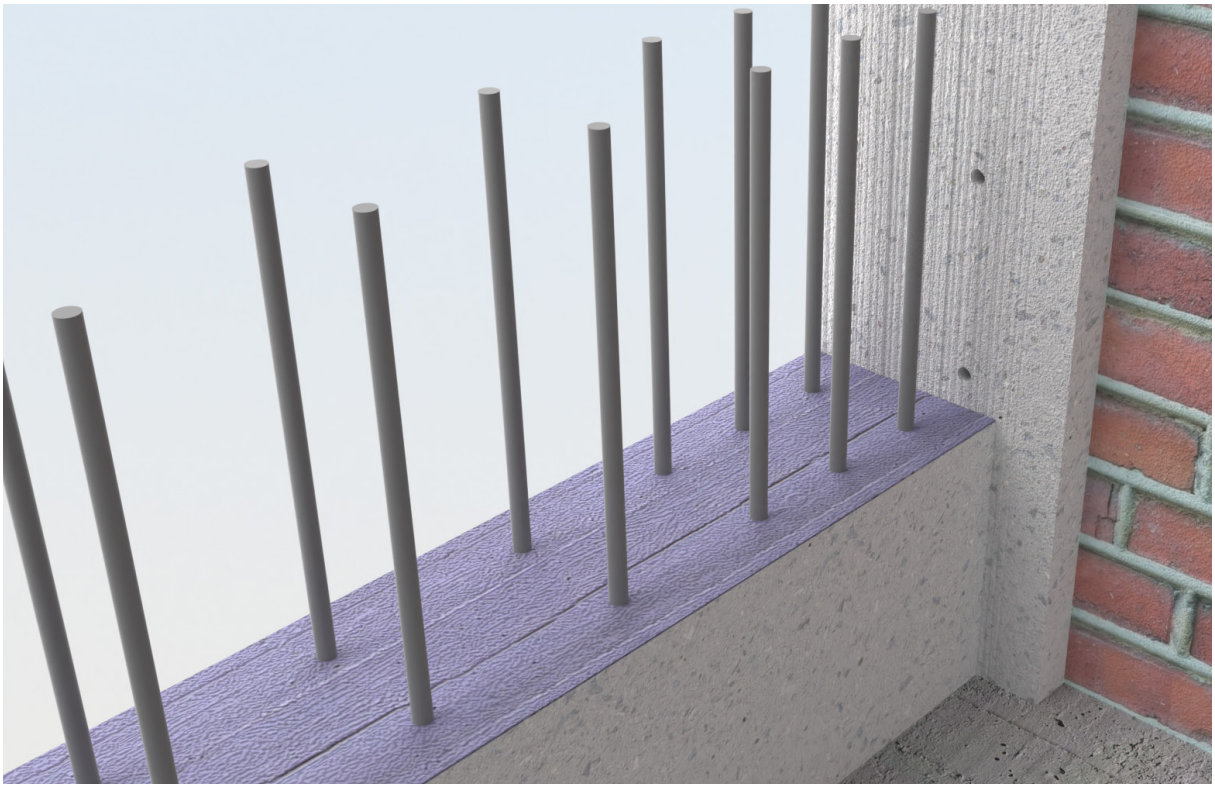

Figure J.6 - Step 6: When the cast-in-place bottom is done and hardened, an adhesion layer is applied to provide proper bonding between the cast-in-place bottom and the shear wall blocks that will follow.

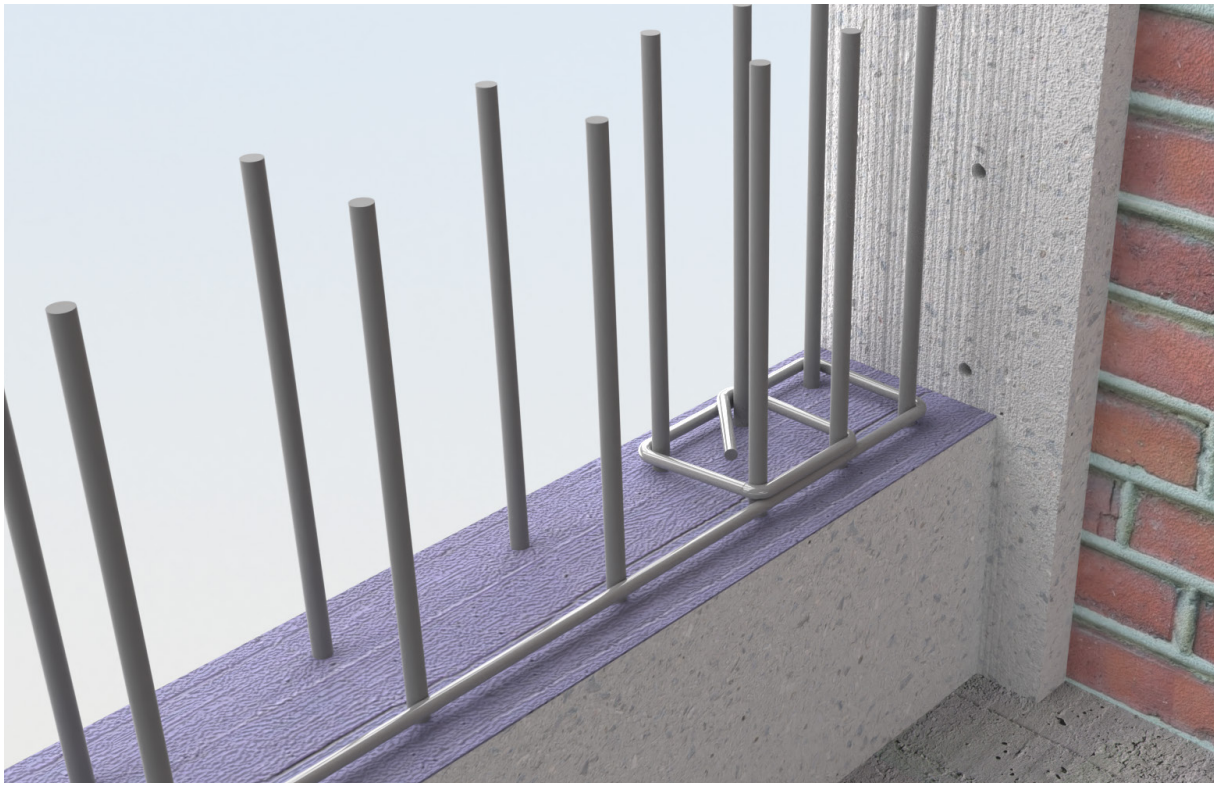

Figure J.7 - Step 7: Consequently, the first stirrup can be placed inside the adhesion. This stirrup element provides confinement around the longitudinal rebars and is looped around the edge vertical rebars multiple times finishing of with a 135° hook. This strong confinement should prevent the stirrup from getting loose during the cyclic seismic loading of an earthquake.

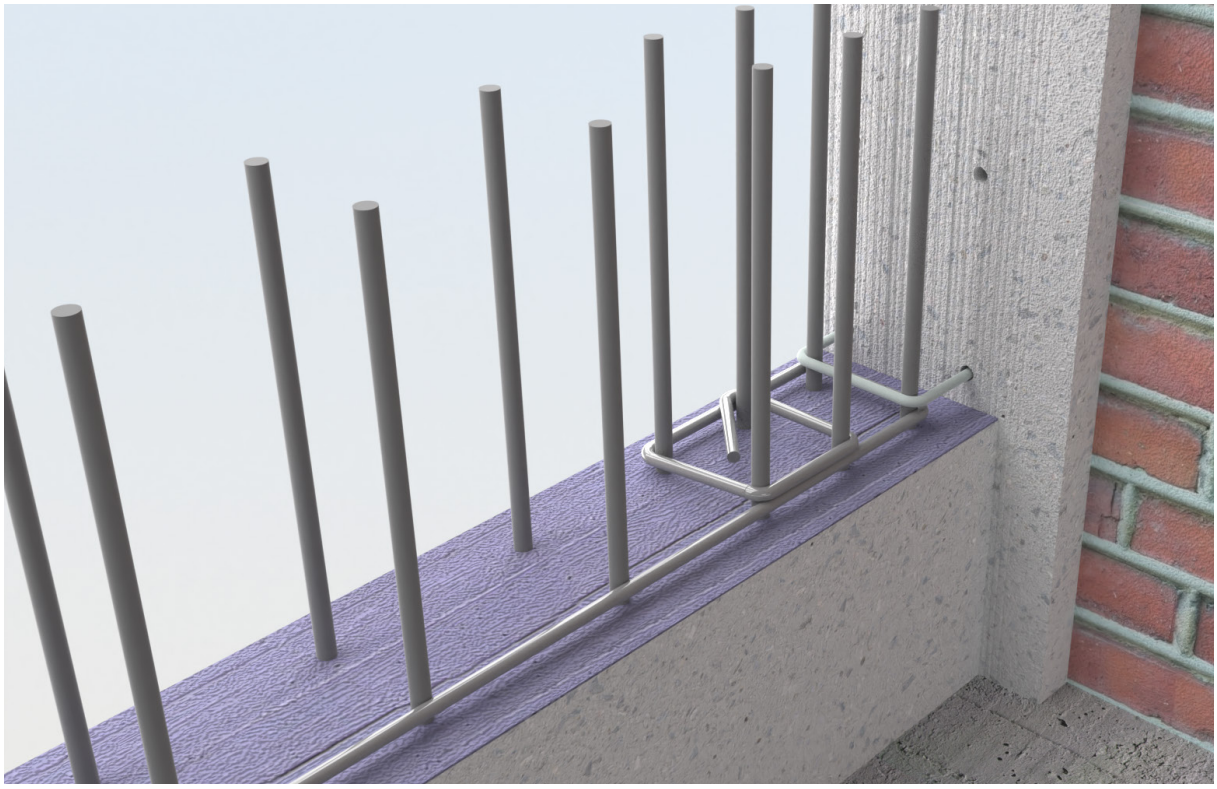

Figure J.8 - Step 8: On top of the stirrups, a shear dowel is placed, connecting the retrofit system to the old concrete frame. These shear dowels are placed on alternating sides at every 100 mm.

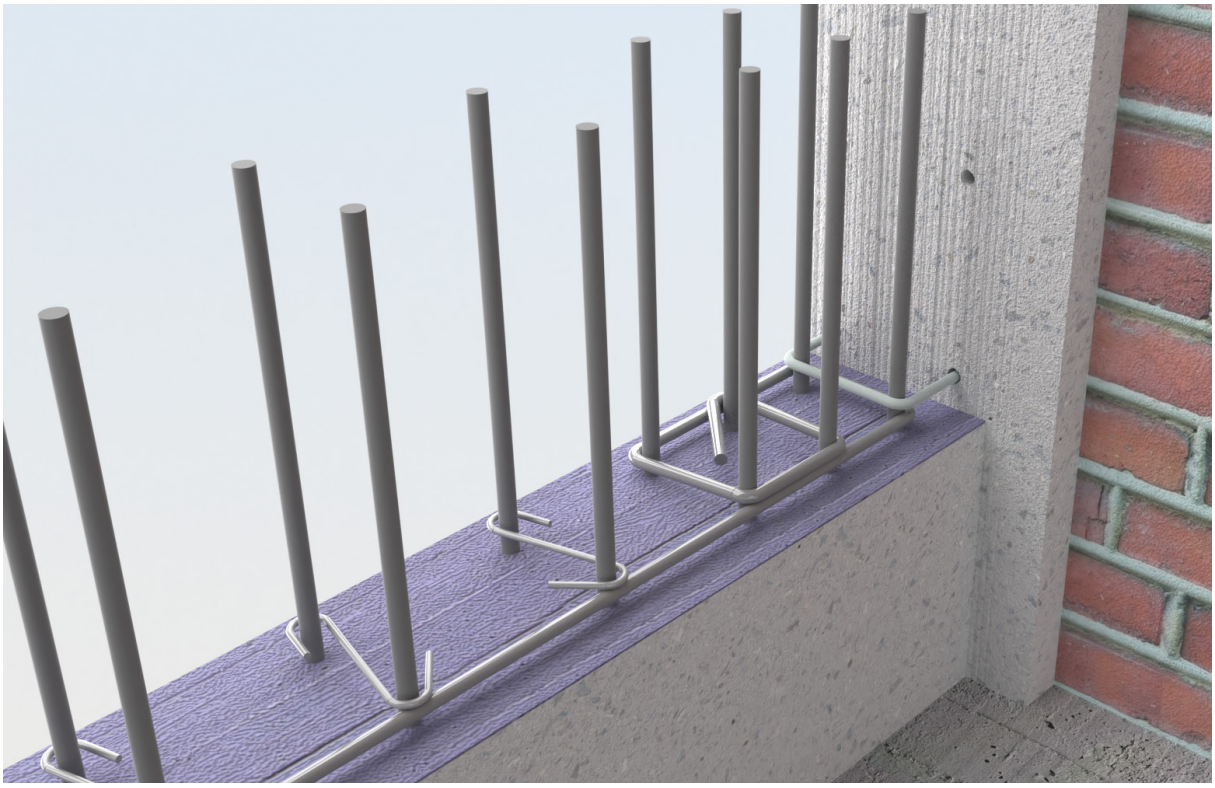

Figure J.9 - Step 9: The last rebar element that are placed are the cross-ties. These S-shaped elements connect to opposite longitudinal rebars and therefore provide the extra confinement necessary for the shear wall system.

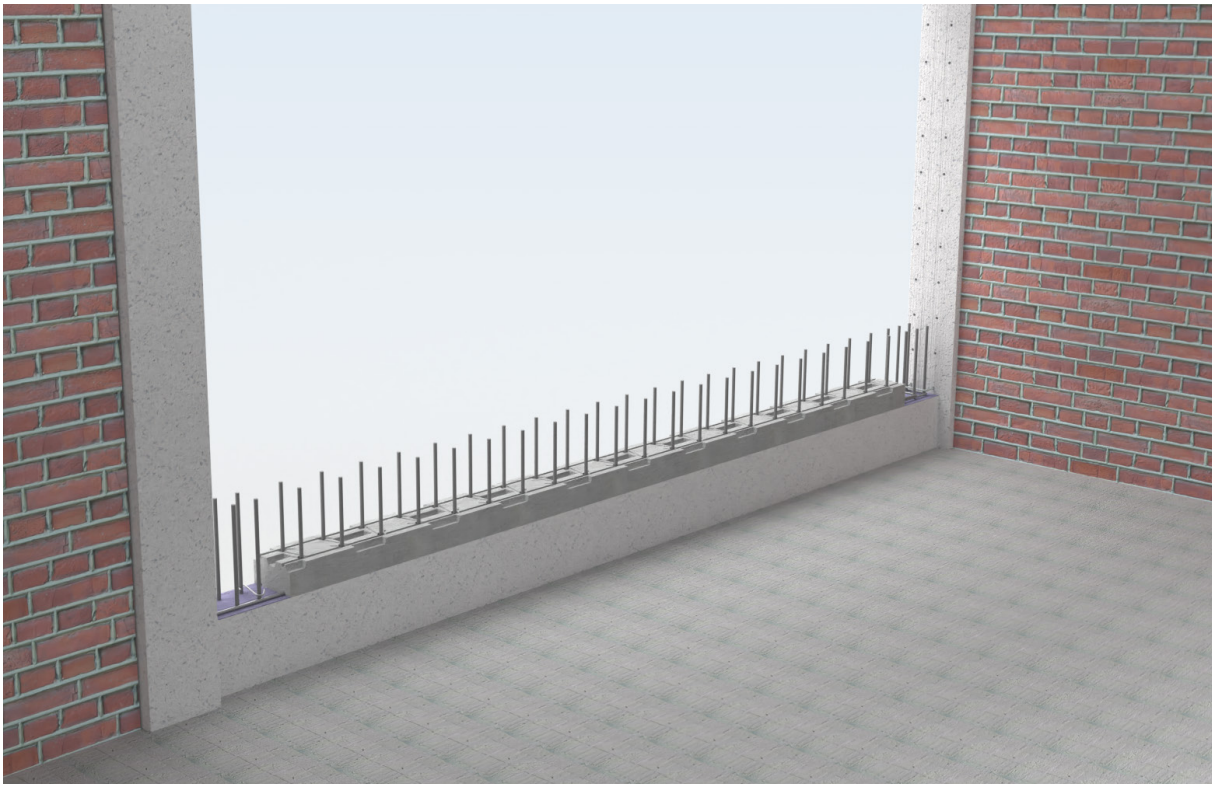

Figure J.10 - Step 10: After all the rebar elements are prepared and in place, the first row of the bottom bricks (without shear teeth on the bottom) can be slid over the longitudinal rebars.

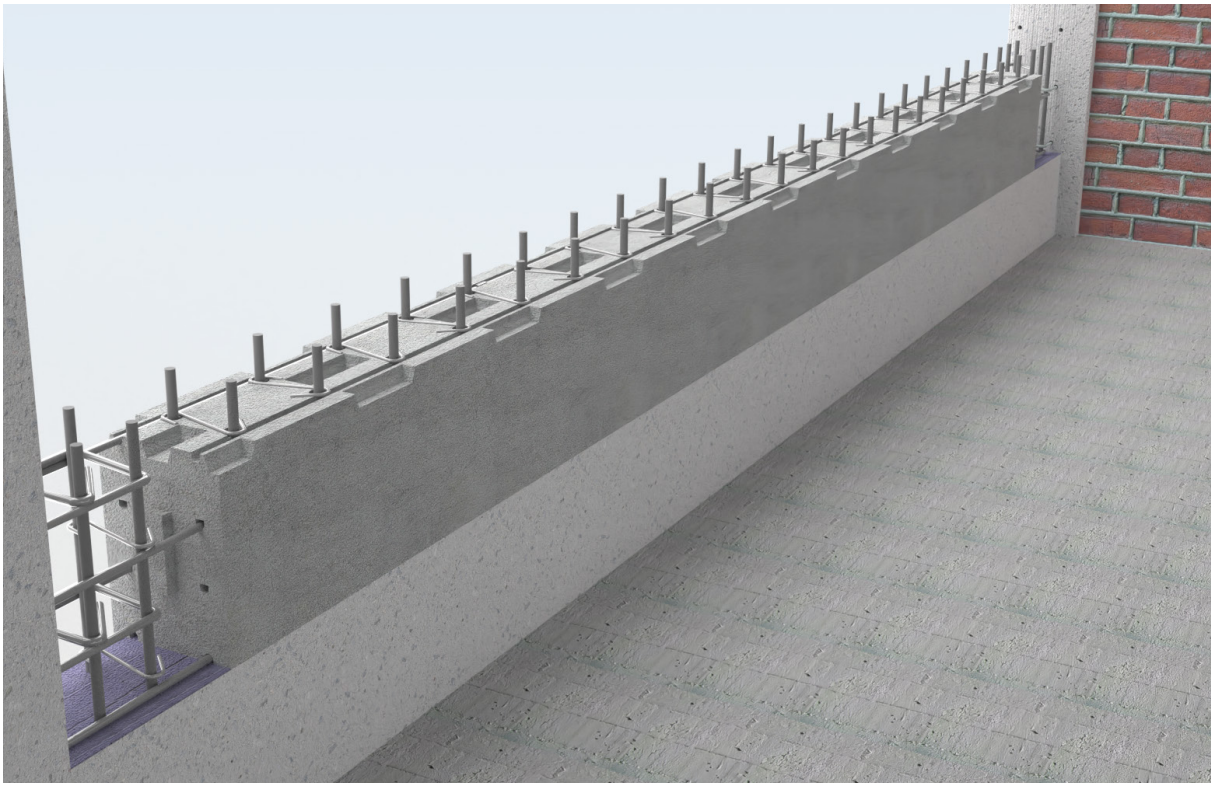

Figure J.11 - Step 11: Consequently step 7 to 10 are repeated to build up the system until the end of the longitudinal rebar is reached. Furthermore, as marked in the image on the side, some of the edge bricks contain an edge bump, this bump is deliberately made in order to provide extra mechanical interlock with the cast-in-place side of the frame (see Figure J.20).

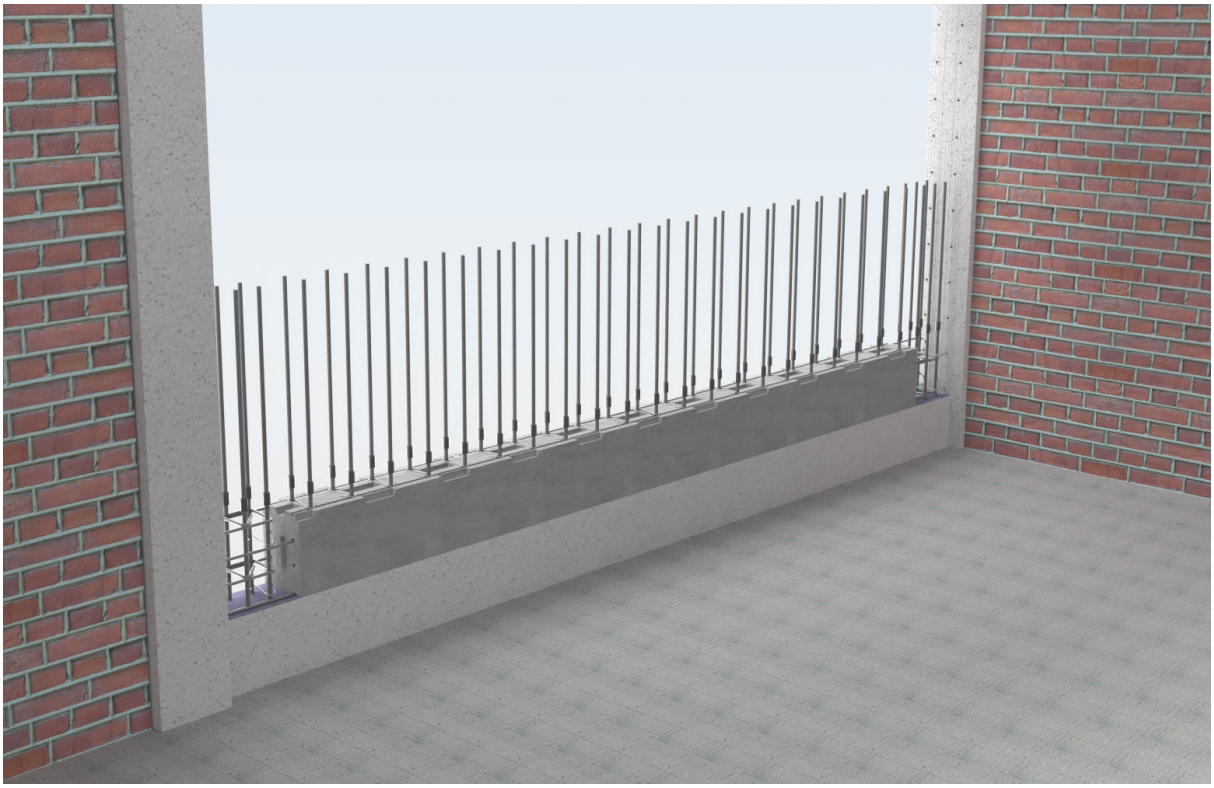

Figure J.12 - Step 12: In this step, the exposed end of the longitudinal rebar is extended using a mechanical rebar coupler, allowing the next rebar segment to be connected. his maintains reinforcement continuity between block layers and enables the next sequence of modular blocks, stirrups, and shear dowels to be installed.

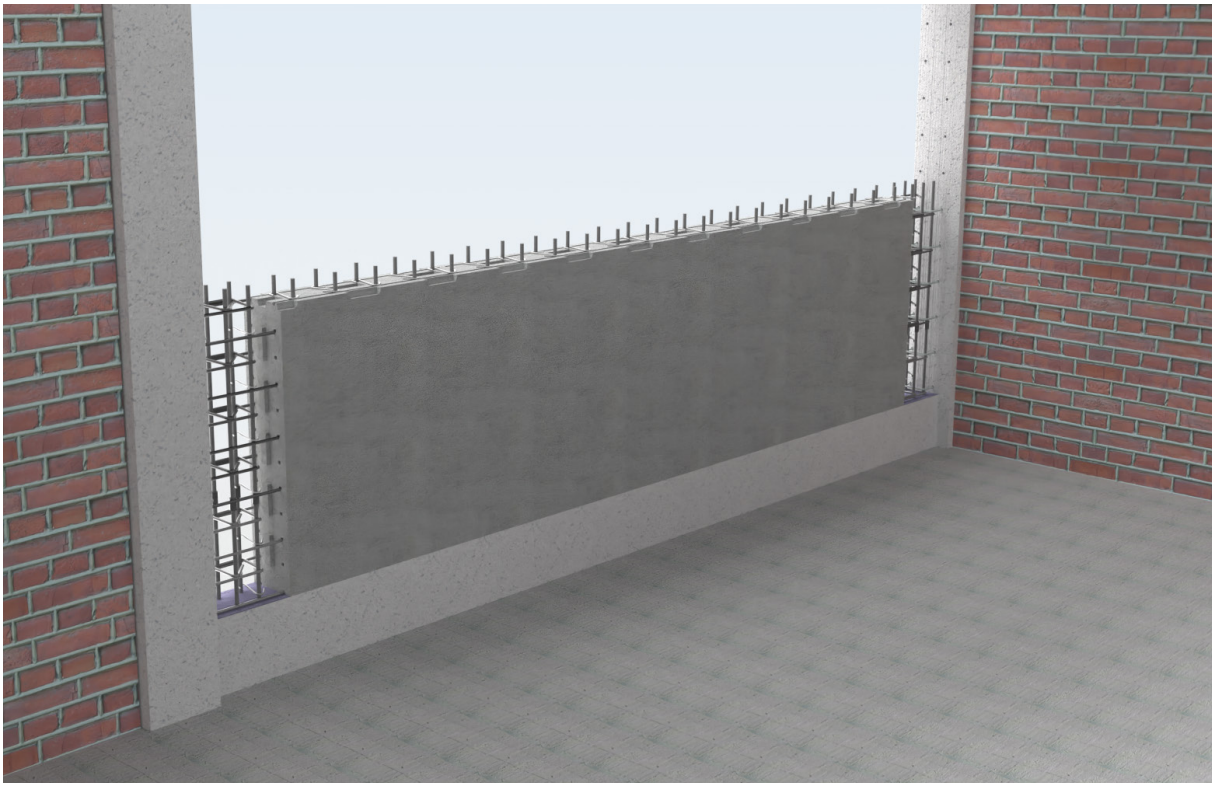

Figure J.13 - Step 13: Now, the same steps are repeated over and over until the top of the frame is almost reached.

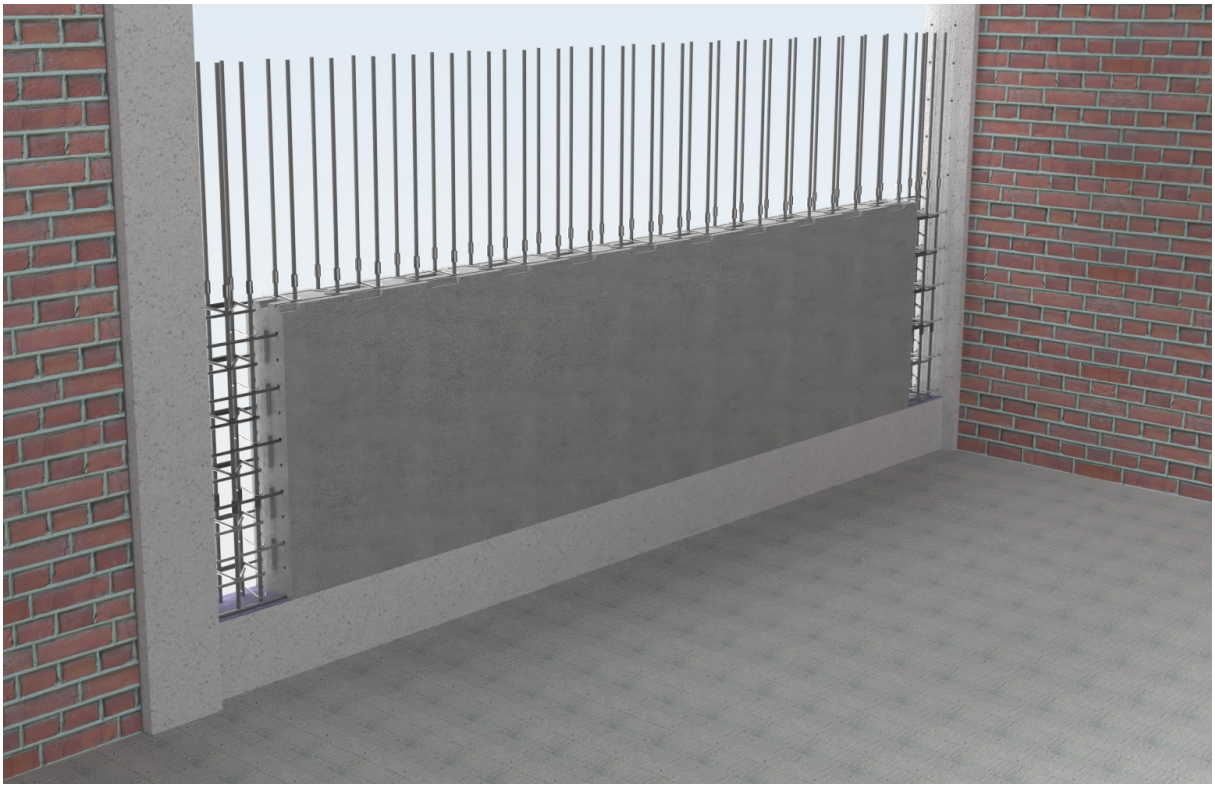

Figure J.14 - Step 14: After coupling the longitudinal rebars, the same steps are repeated over and over until the top of the frame is almost reached.

Figure J.15 - Step 15: The last rebars are fastened by sliding them into pre-drilled holes in the ceiling. In order to allow fastening in this relatively narrow space, couplers must temporarily be slid down to allow insertion of the final rebar segments.

Figure J.16 - Step 16: After the longitudinal rebar is inserted, the couplers can be turned back into its intended place, connecting the longitudinal rebars into one continuous element.

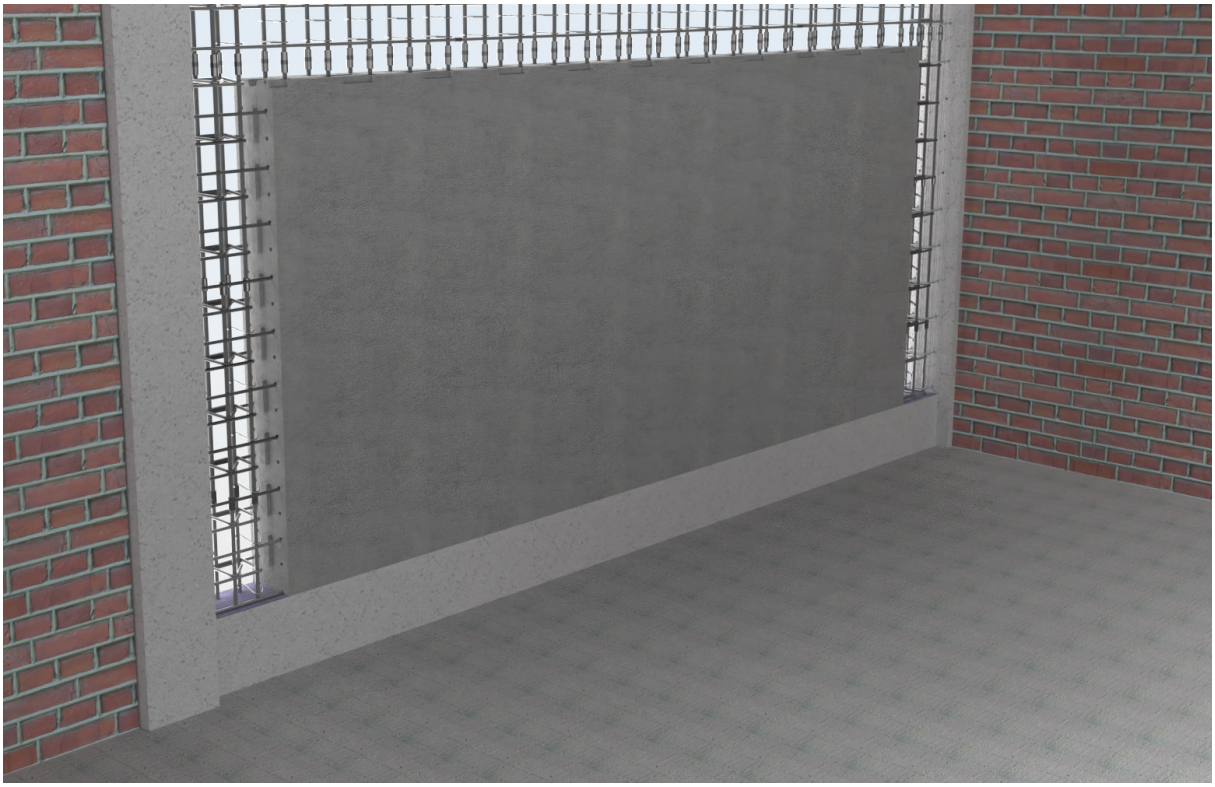

Figure J.17 - Step 17: After the whole rebar framework is finished, non-shrink injectable grout is used to be injected in the longitudinal rebar holes (while the stirrup grooves on the side need to be plugged), in order to solidify the connection between the stseel and precast concrete elements.

Figure J.18 - Step 18: This pouring is done by applying a timber framework which is stabilised by using adjustable push-pull props. Furthermore, three Ø100 mm holes are applied for the insertion of the cast-in-place concrete, while four smaller Ø30 mm air vents are also made to allow trapped air to escape during pouring, preventing air pockets and incomplete filling of the formwork.

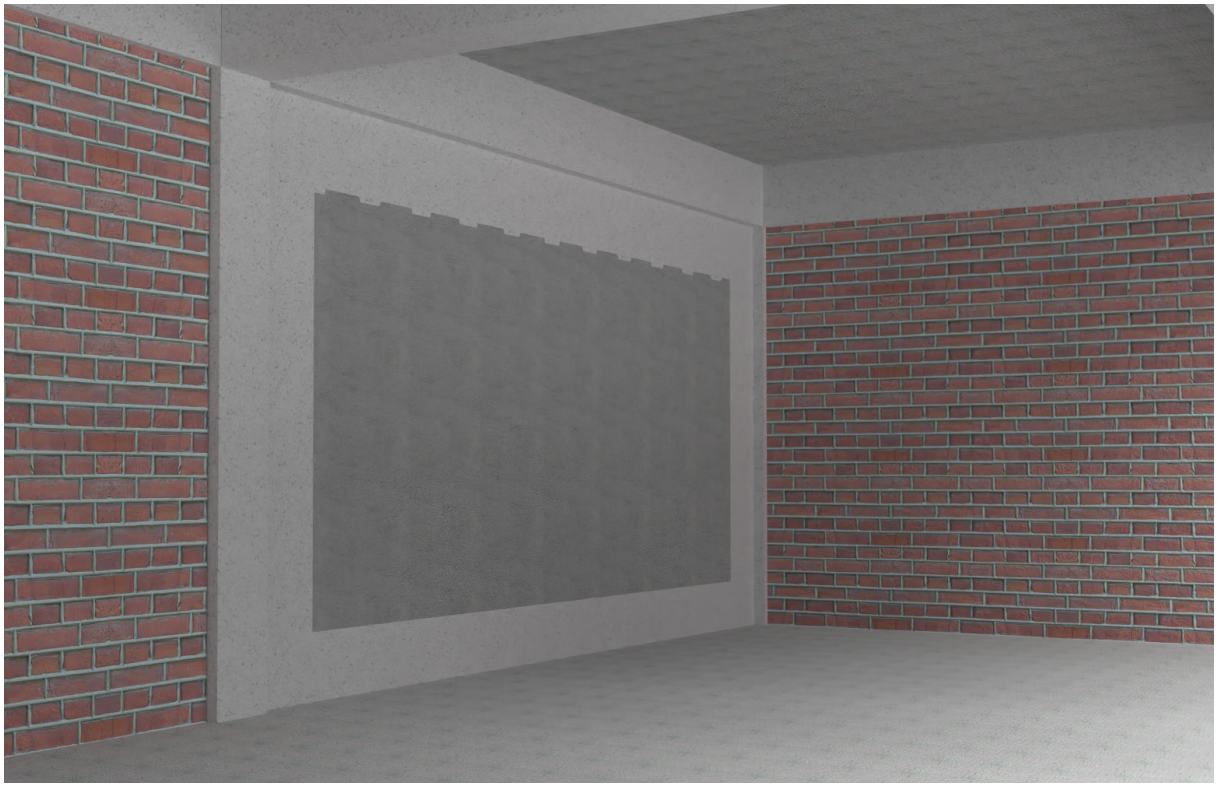

Figure J.19- Step 19: After the cast-in-place concrete is applied at the top and sides and this poured concrete is hardened, the formwork can be removed and the installation of the retrofitting shear wall element is done.

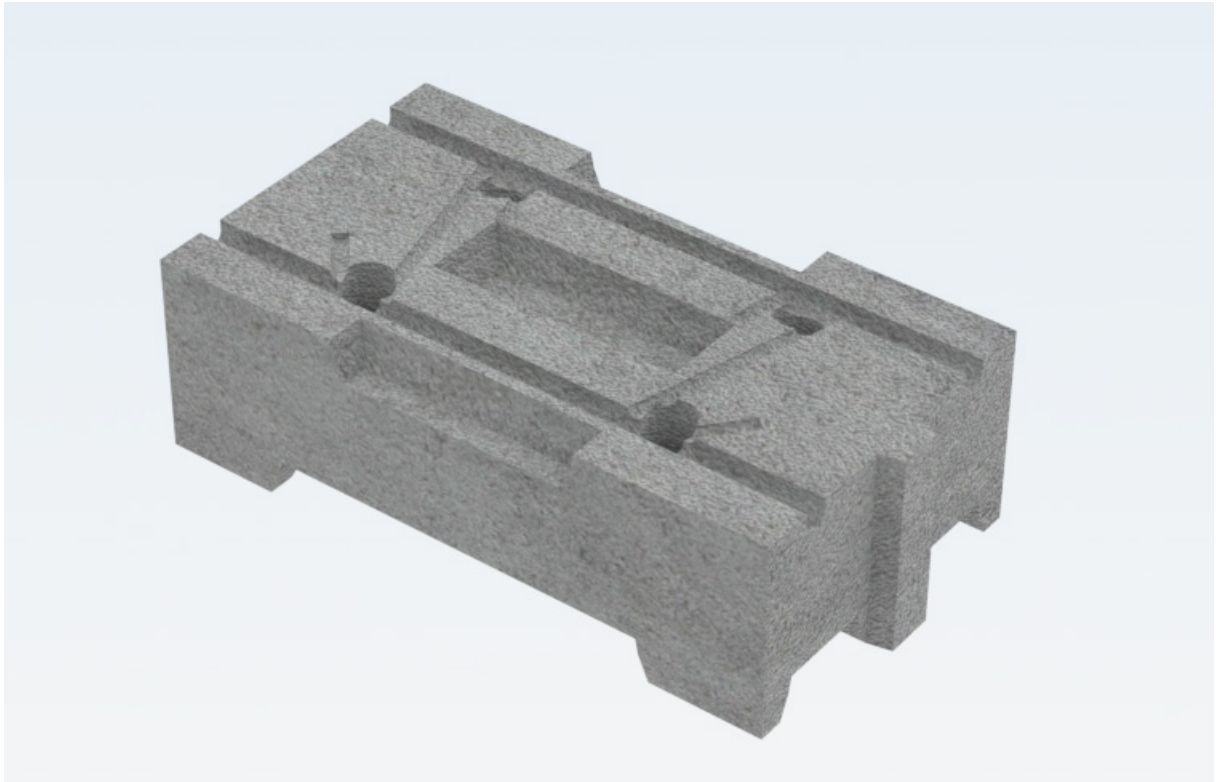

Figure J.20: This illustration shows one of the retrofit shear wall block types that is utilized at the side. The difference to a 'regular' shear wall block type is that this edge block comes with a shear tooth at its side (on the right side in this image), providing extra mechanical interlock with the cast-in-place concrete frame at the side.